



Application of ECC/FRC in connections of integral bridges

Master of Science thesis
C.J.A. van der Wilt





Application of Ecc/FRC in connections of integral bridges

Master of Science Thesis

For the degree of Master of Science at Delft University of Technology



Faculty of Civil Engineering and geosciences

Structural Engineering

Concrete Structures

Kees Jan (C.J.A.) van der Wilt

October 10, 2014





Thesis committee members TU Delft:

Prof. dr.ir. D.A. Hordijk

Department Design and Construction – Structural and Building Engineering – Concrete structures

Dr. Ir. C. van der Veen

Department Design and Construction – Structural and Building Engineering – Concrete structures

Dr. M.H. Kolstein

Department Design and Construction – Structural and Building Engineering – Steel structures

Ir. L.J.M. Houben

Department Structural Engineering – Road and Railway Engineering – Road Engineering

Thesis committee members Iv-infra b.v.:

Ir. H.C. Peerdeman c.i., RO

Consultant concrete structures

Dr.ir. H.W.M. van der Ham c.i.

Consultant concrete structures





Summary

The focus of this study is to research if ecc/frc is applicable for integral bridges. Integral bridge are bridges without or partly without intermediaries. A bridge normally consist of a substructure, superstructure and intermediaries. The superstructure comprises the bridge deck and the substructure consist of the abutments, piers and the foundation. The intermediaries are expansion joints and bearings which enables the bridge to deform and/ or to transfer the deformation and loading from the superstructure to the substructure. With or without intermediaries leads to different structural systems. A bridge with these intermediaries is called a 'conventional bridge' and a bridge without these intermediaries is called a 'fully integral bridge'. There are also structural systems in between a conventional bridge and a fully integral bridge. (see chapter 1)

Integral bridges have been built in the United States, Canada, Australia and several countries in Europe. The choice for an integral bridge over a conventional bridge depends strongly on the length of the bridge, the bridge location, the climate and the requirements of the bridge and the road. In some states of the U.S., integral bridges are preferred over conventional bridges. Hence, more than 1000 integral bridges have been built in the U.S. including the longest steel and concrete integral bridges. Some states in the U.S. prefer integral bridges over conventional bridges, because in their experience the elimination of expansion joints and bearings leads to a more durable structure and less maintenance. The maximum bridge length is disputed by the State engineers. Normally the allowable length is between 60 and 180 meter depending on the state limitations. (See section 3.1)

Integral bridges are not used as a common practice in the Netherlands. The preferred structural system is a conventional bridge. The integral bridges that have been built, seem to be a choice of the designer. Most of the integral bridge that have been built, are single span bridges. (See section 3.1)

All construction elements of an integral bridge are monolithically connected. This results in one integral system where there is interaction between the sub- and superstructure and between the bridge and the embankment soil. This is an important difference compared to a conventional bridge, where the sub- and superstructure function more like single structural systems. The structural system of an integral bridge can be schematized as a portal frame. In this case the beam of the portal frame is the superstructure and the columns comprise the substructure. In a portal frame, deformation in the beam will cause deformation in the columns. The deformation that occurs in the bridge deck of the integral bridge is caused by loading, temperature influences and time-related material effects. These loads and effects will cause the following rotations and displacements in the structure (see section 3.2):

- Vertical displacement and rotation (weight of the bridge, asphalt, traffic)
- Rotation (temperature gradient daily cycle)
- Contraction (shrinkage, creep, elastic shortening prestressing)
- Expansion (temperature yearly cycle)



An integral bridge is a durable structure due to the absence of expansion joints and bearings. However, without expansion joints and bearings the bridge deforms into the soil due to the deformation of the bridge deck. The deformation of the bridge deck is caused by the temperature influences and time-related material effects. The time-related material effects are shrinkage, creep and elastic shortening in case of a prestressed concrete element. These effects are responsible for deformation of the bridge deck in time. The temperature influences lead to a cyclic behaviour. This behaviour could be divided in two cycles, namely a yearly and a daily cycle. Both cycles causes cyclic deformation of the bridge deck. This deformation of the bridge deck is only possible if the bridge is able to deform into the soil. This may imply certain problems, because the soil is not rheological. These problems are (See also section 0 and chapter 4):

- Settlement of the soil close to the abutment 'bump in the road'
- Asphalt/pavement problem
- Foundation/piles
- Early age cracking
- Wing walls
- Cracking of the abutment stem or the bridge deck at the abutment

The major goal of this thesis is to investigate if the application of frc/ ecc in the connection of integral bridge has advantages. Fibre reinforced cementitious composites could be distinguished from conventional concrete due to the application of fibres. The application of fibres leads to some interesting properties, for example a higher strength, more ductility, more toughness, durability, higher stiffness and thermal resistance. FRC composites could be distinguished in 'hardening and 'softening'. An FRC composite has 'hardening' when the structural strength is equal to or greater than the cracking strength. This means that after the first 'crack' the tensile strength of the FRC composite is still increasing. This hardening can also occur under bending, and then the FRC composite is called 'deflection-hardening'. When this hardening occurs under tension then the FRC composite is called 'strain-hardening'. An FRC composites has 'strain-softening', when the tensile strength declines after the first crack. (see chapter 6)

There is chosen to apply the FRC composites in the connection. A major motivation is to reduce reinforcement in the connection between the sub- and superstructure. This is firstly investigated by constructing strut-and-tie-models (STM) and string-panel model (SPM). The STM and SPM showed that influence of foundation pile on the connection is decisive. Two mechanisms could describe for the structural behaviour of the foundation pile in the connection. The first mechanism is the transfer of forces and moments by friction between the foundation pile and the surrounded concrete (Figure 7-4A) and the second mechanism is the transfer of forces and moments by a coupling force (Figure 7-4b). Both mechanisms are analysed by using the STM and SPM. This provided a good image of the flow of the forces and stresses in the connection. (See chapter 7 and appendix A)



The 2D FEM is developed on basis of the results of the STM and the SPM and the building project 'bridge Schokkeringweg'. The forces, the moment, the boundary conditions and the dimensions are based on the calculations of the 'bridge Schokkeringweg'. The research focuses on the two mechanisms. Therefore, friction and cohesion between the foundation pile and the surrounded concrete and the horizontal reinforcement in this area are taken as variables. The results show that the strength of the connection depends mostly on the horizontal reinforcement and cohesion and friction have almost no influence. (More about the conclusions, see section 8.6)

The next step was to investigate the effect of the FRC composites on the 2D FEM. The FRC composites used in this research are classified on basis of tensile strength, strain and 'hardening or softening'. For this research, a 2D FEM with and without horizontal reinforcement in the area of the foundation pile is used. The results show that FRC composites leads to an improvement of the rotational stiffness of the connection and for 2D FEM without horizontal reinforcement also to a higher structural strength of the connection. However, the improvements are minor and therefore it is advised to not apply FRC composites in integral bridges. (see section 9.4)





Table of Contents

1	Introduction	1
1.1	Preface and the definition of integral bridges	1
1.2	Motivation of the study	2
1.3	Targets	3
1.4	Research process	4
1.5	Scope of the study	5
2	Conventional bridges	6
2.1	The structural system of a conventional bridge	6
2.2	Conventional bridge deck design	7
2.3	Abutment design	11
2.4	Design of intermediate connections	13
3	Integral bridges	16
3.1	Common practice of integral bridges	16
3.2	Structural system integral bridges	19
3.3	Abutment and pier design	21
3.4	Foundation design	26
3.5	Approach slabs	32
3.6	Problems and limitations with integral bridges	34
4	Deformation of integral bridges and their consequences	38
4.1	Overview	38
4.2	Temperature influences (cyclic deformation)	38
4.3	Time dependent material properties	41
4.4	Interaction between the substructure and the soil	43
4.5	The proposed model of the integral bridge and the soil	49
5	Fibre Reinforced Cementitious composites (FRC composites)	50
5.1	Introduction	50
5.2	Classification of fibre reinforced cementitious composites	50
5.3	The influence of fibres	52
5.4	Engineered cementitious composites (ECC)	54
5.5	Tailor made mixtures for structural applications in integral bridges	57
6	Structural applications of FRC composites in integral bridges	58
6.1	Introduction	58
6.2	Potential structural applications of FRC composites	59
6.3	Other parameters that are influencing the structural element of a FRC composite	63
6.4	The proposed structural application of integral bridge	64
6.5	Research approach	69
7	Analytical calculations of the connection	71
7.1	Analytical model of the connection according to the Eurocode	71
7.2	Introduction of the stringer-panel method and the strut-and-tie model	73
7.3	Stringer panel model of the bridge connection	74



7.4	Calculation of the stringer-panel models and the strut-and-tie models (SPM & STM)	75
7.5	Evaluation of the SPM an STM and recommendations for the detailed design connection	78
8	2D FEM of the bridge connection	81
8.1	Evolution of the 2D FEM	81
8.2	Input of the 2D FEM	86
8.3	Analysis procedure	95
8.4	Results	96
8.5	Comparison of the results with the strut-and tie models of chapters 7	114
8.6	Recommendations for the connection according to the results of the 2D FEM	118
9	2D FEM with FRC composites	120
9.1	The design of the 2D FEM with FRC composites	120
9.2	The mechanical properties of the FRC composites used in the 2D FEM	121
9.3	Results	123
9.4	Recommendations and Conclusions	143
10	Conclusion and recommendations	144
10.1	Conclusion	145
10.2	Recommendations	146
	References	147
	APPENDICES	150
A	The stringer-panel and the strut-and-tie models	150
B	Data input TNO DIANA	150
C	Potential improvements	150
D	3D FEM of the bridge connection	150



1 Introduction

1.1 Preface and the definition of integral bridges

Bridges are applied to structure span or provide passage over a river, chasm or road. A bridge consists of a substructure, superstructure and intermediaries. The superstructure comprises the bridge deck and the substructure consists of abutments, piers and the foundation. The expansion joints and the bearings are the intermediaries and their function is to enable the bridge deck to deform and/or to transfer the deformation and the loading of the superstructure to the substructure and the soil. With or without these intermediaries leads to different structural systems. A bridge with these intermediaries is called a 'conventional bridge' and a bridge without these intermediaries is called a 'fully integral bridge'. There are also structural systems in between a conventional bridge and a fully integral bridge. These structural systems are given in Figure 1-1.

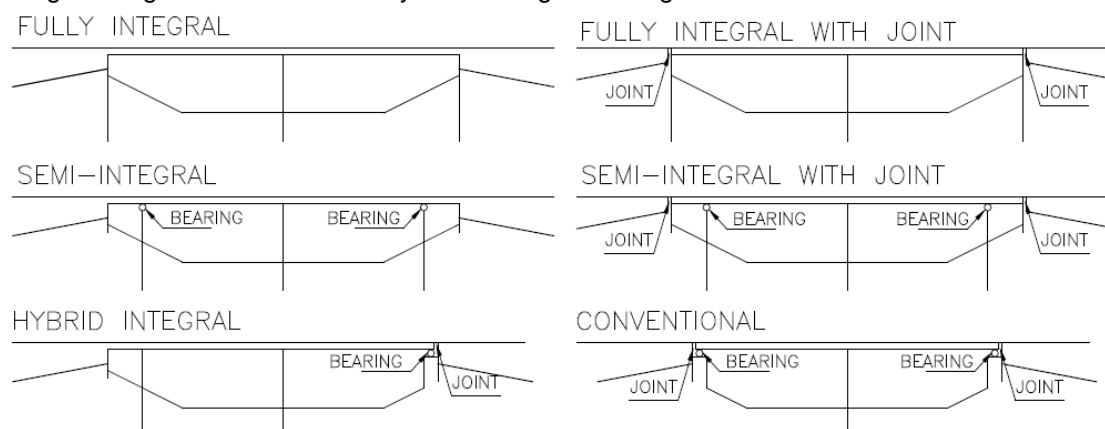


Figure 1-1 The different structural systems of bridges [1]

Without these intermediaries, the super- and substructure are monolithically connected what leads to a certain bridge rigidity. The bridge deck cannot deform freely and will interact via the substructure with the embankment soil. The degree of interaction between the bridge and embankment soil and the certain bridge rigidity is the basis of a structural classification. Figure 1-2 describes this proposed structural classification. The structure types in Figure 1-1 are based on the models in Figure 1-2.

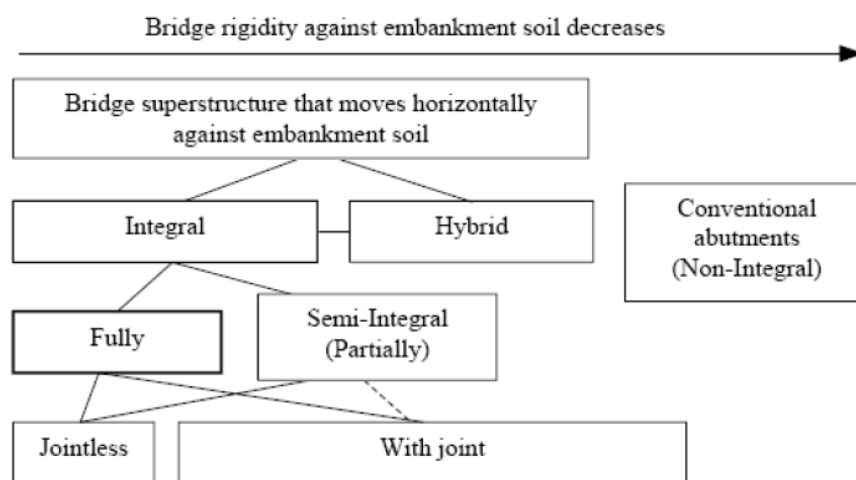


Figure 1-2 Proposed classification on the basis of abutment type of bridge moving horizontally against embankment soil. In this figure, a joint refers to an expansion joint [1].

So integral bridges could be distinguished from conventional bridges due to their rigid connections. The definition of integral bridges is therefore:

An integral bridge is designed without expansion joints between adjacent spans and/or without expansion joints and bearings between spans and abutments [16, p. 1].

Integral bridges are developed because of the problems with deck joints and bearings. Deck joints are expensive to buy, install, maintain and repair. Besides, they are responsible for a decrease of durability due to leaking deck joints and allowing de-icing chemicals to attack bridge ends, abutments and bearings. Bearings could also be expensive and demand a repair over time. If bearings need a replacement, the costs are even higher [2].

1.2 Motivation of the study

Integral bridges are economical and durable compared to conventional bridges. The maintenance and construction costs are lower compared to conventional bridges [1]. Still the use of these bridge types is minimal in comparison to conventional bridges. This is because of the problems and uncertainties related to the interaction between the integral bridge and the embankment soil [2].

Another complexity is that the connections have to resist moments and forces what often leads to a lot of reinforcement in the connections. Ecc/ fibre reinforced concrete have some mechanical properties that could be interesting to restrain these moments and forces in the connection.

The goal of this thesis is to research if the use of materials like ecc/ fibre reinforced concrete is an improvement compared to conventional concrete for connections of integral bridges.



1.3 Targets

In the graduation plan ('plan van aanpak') the research goal is already discussed. An important aspect to reach this goal is the overall research and the targets. The overall research question is:

Is engineered cementitious composite/ fibre reinforced concrete suitable to be applied in monolithic connections of integral bridges?

To answer this research question a few targets need to be accomplished. The first two targets depend on this 'Pre-study'. In total five targets are formulated. These targets are:

1. **A basic design:** the pre-study will be used to create a basic design. Important factors are the type of bridge deck, the type of abutments, the type of piles and the connection between substructure and superstructure.
2. **Material design:** For an integral bridge specific mechanical material properties are needed. The second target of this pre-study is to specify a few material mixtures that will be used in the design calculations.
3. **To construct a conventional concrete design:** After the basic design a more detailed design could be created. The target is to develop a conventional design that can be used as a comparison for ecc/frc designs.
4. **Ecc / frc designs:** With help of the material and basic design an ecc/ frc design can be generated. A selection of ecc/ frc designs with different mechanical material properties will be analysed.
5. **Comparison between the conventional concrete design and the ecc/frc designs:** After the calculations a comparison between the designs will be made.



1.4 Research process

The steps in this thesis are showed in Figure 1-3. The research is divided into four steps: step 1=plan, step 2=literature research, Step 3=design, Step 4=analysis. The pre-study plays an important role in the thesis. In the pre-study, the basis for the design process is founded. The design process comprises two sub steps. The first sub step is the design of a multi-span integral bridge made of conventional concrete. The second sub step is actually more than one sub step, because it consists of multiple designs. The number of designs in sub step 'ecc/ frc design' is not clear yet. At the end of this pre-study a number of designs are chosen based on the material composition of ecc/ frc. Step 4 also has two sub steps. The first one starts already when the first ecc /frc design is ready. The results of this comparison will be used for the following frc/ ecc designs. The last sub step requires no explanation.

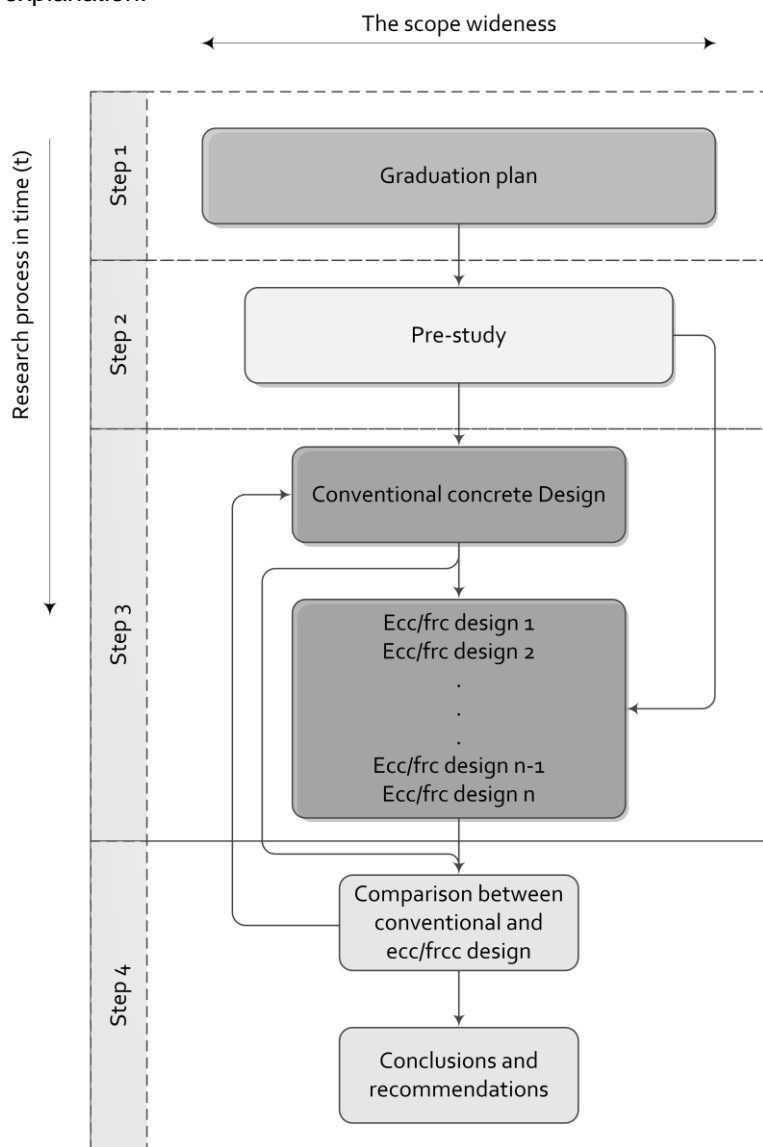


Figure 1-3 Research process



1.5 Scope of the study

The focus of this study is to research if ecc/frc is applicable for integral bridges. To reach applicability, it is important to limit the scope. Before the pre-study a few choices have been made:

- **Integral bridges:** This thesis focuses on fully integral bridges only. Other structural systems, for example semi-integral have been mentioned in the first section, but they will not be discussed further.
- **A standard project:** For the design of the integral bridge a project has already been chosen. This is the project 'de N236 aanleg faunapassages' and is located in a marshland. This is a bridge of 88 meters long and is a part of an expressway.
- **Multi-span bridges:** The focus will be on multi-span bridges. This type of bridges has both a connection between the superstructure and substructure and a connection between spans.
- **The skew:** Normally, the skew has an effect on the design length of an integral bridge. The skew is limited, because of non-uniform stresses. For the research the skew is limited to zero degrees. This is the equivalent of a 'kruisingshoek' of 100 gon.
- **The material:** Steel and steel-concrete integral bridges will be mentioned, but the focus is on concrete integral bridges only.

The goal of this pre-study is to limit the scope. After the pre-study it will be checked whether or not the first two targets have been accomplished and if all parameters for the basic design are set.



2 Conventional bridges

2.1 The structural system of a conventional bridge

The superstructure of a multi-span bridge is composed of a number of bridge decks and the substructure consists of abutments, supports and the foundation. As intermediary a conventional bridge has expansion joints and bearings. In Figure 2-1 a sketch of a multi-span bridge is given.

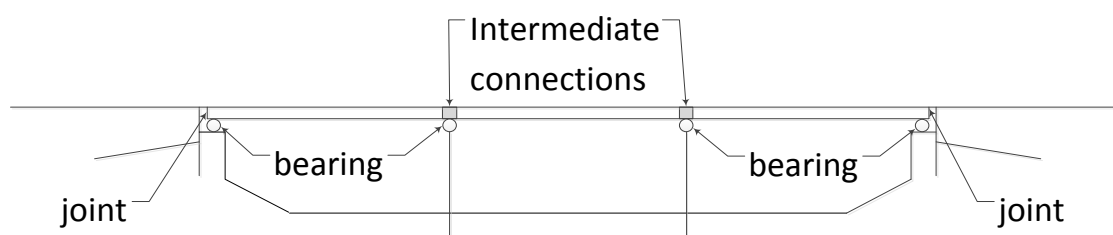


Figure 2-1 Sketch of a multi-span bridge

The intermediate connections could be monolithically and continuous or with an expansion joint. This leads to two different structural systems. If the spans are connected, negative bending moments occur at the supports and the moments in the middle of span will be smaller. With an expansion joint the spans will act separately. This leads to larger moments in the middle of the span and no moment distribution from one span to the other. Figure 2-2 shows the difference between the continuous spans and the separate spans and their moment distribution.

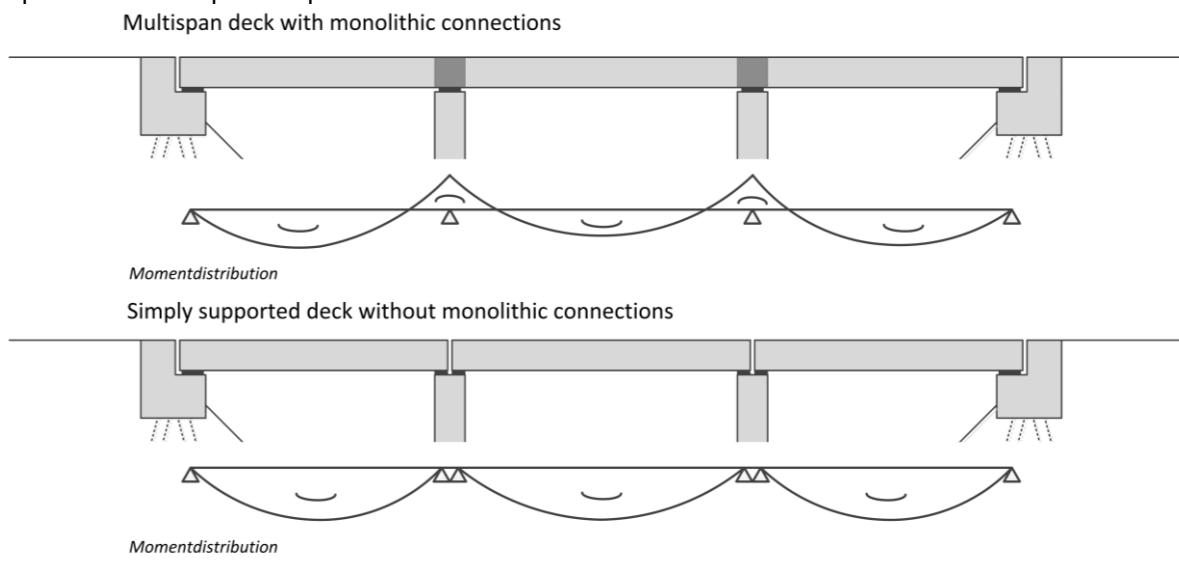


Figure 2-2 Difference in moment distribution with or without a monolithic connection

Due to the expansion joints and bearings, the superstructure can deform freely and the lateral forces from the superstructure to substructure are minor. The lateral forces that will occur have to be absorbed by the supports and the foundation. Therefore, braced foundation piles are used to create a rigid substructure. The loads that have influence on the substructure are illustrated in Figure 2-3

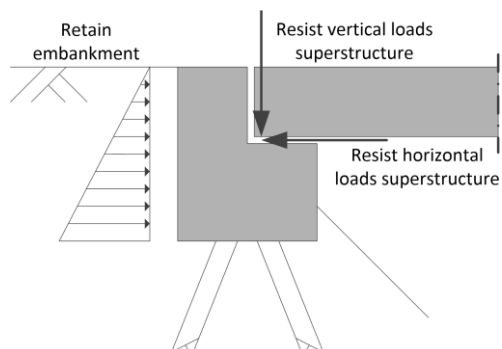


Figure 2-3 Visualization of the substructure under loading

In the next sections, the options for bridge decks (§2.2), abutments (§2.3) and intermediate connections (§2.4) will be discussed.

2.2 Conventional bridge deck design

The total length of the observed bridge is 88 meter, as was mentioned in §1.5. The bridge is divided in three spans (27 meter – 34 meter – 27 meter) to cross a ditch in the middle and two small roads at the side. There are several options to construct the bridge deck for lengths between 25 and 40 meter. Figure 2-4 gives an overview of these options, based on [3, 4, 5].

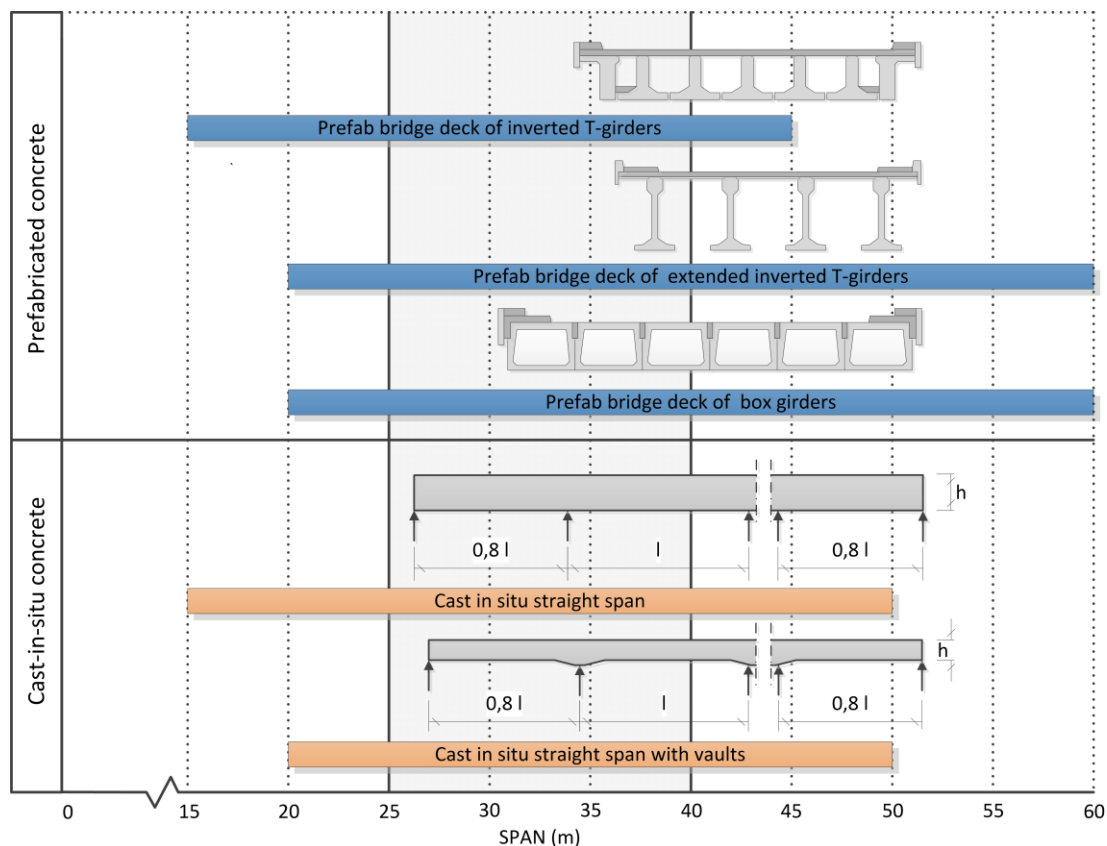


Figure 2-4 Cross-sections of different bridge decks and the possible span-to-span distance



The options for constructing a bridge deck could be divided in two groups:

- Cast-in-place concrete bridge deck (§2.2.1)
- Prefabricated concrete bridge deck (§2.2.2)

2.2.1 Cast-in-place concrete bridge deck

As showed in Figure 2-2, the construction of a continuous bridge deck on a bridge with multiple spans lead to negative bending moments at the supports and positive bending moments in the middle of the spans. With a cast-in-place deck it is possible to absorb these negative bending moments by the application of curved post-tensioned cables (Figure 2-5). The curved cables lead to a reversed moment distribution with positive bending moments at the supports and negative bending moments in the middle of the spans. If the curved cables are insufficient to carry the load, straight cables are also used. In order to comply with the crack width, reinforcement is applied at the supports and in the middle of the span. [6]



Figure 2-5 sketch of a cast in situ multi-span bridge with curved cables

The application of a continuous bridge deck on a bridge with multiple spans also leads to a smaller bridge deck height; because the moments are lower than in a single span bridge deck.

Building a bridge cast-in-situ is more flexible than building a bridge with prefab concrete. There is a variety of different types of bridge decks usually determined by the architect. The most common are given in Figure 2-6. The cross-sections d or e are only applied if the lengths are approximately between 35 and 50 meter. For shorter spans massive slabs are chosen. Cross-sections b or c are also possible with holes. These holes are applied to reduce the weight of the bridge deck.

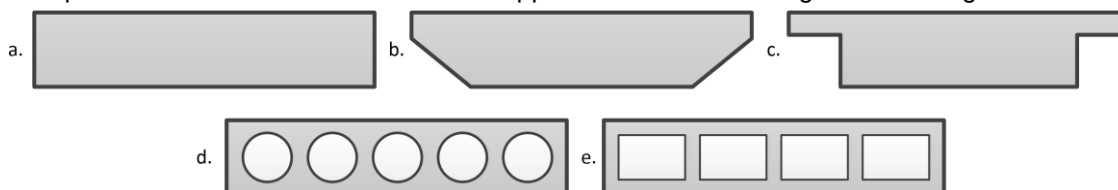


Figure 2-6 Various cross-sections of a cast-in-situ bridge deck

A cast-in-situ straight span with vaults is also constructed to reduce the weight of the structure. This method is applicable with the various construction details of Figure 2-6 and is economically interesting from 20 meter to 50 meter.

The construction of the bridge deck could be done, when the substructure is built and the bearings are in place. The construction process consist of a few steps:

- Constructing of the scaffolding and the formwork
- Reinforcing of the bridge deck and installation of the tendons
- Pouring of the concrete
- Prestressing of the cables after curing of the concrete
- Uninstalling of the scaffolding



It is not always possible to construct a cast-in-place concrete bridge deck. This depends on the location of the building project. It is not applicable, if the size of the building site is limited or the bridge has to span a highway or a railroad. Sometimes the construction of the bridge deck takes place alongside the location of the bridge and is later placed in position (Figure 2-7).



Figure 2-7 Horizontal jacking of a bridge deck

2.2.2 Prefabricated concrete bridge deck

The different types of prefab bridge decks are given in Figure 2-4. The options are:

- Prefab bridge deck of inverted T-girders
- Prefab bridge deck of extended inverted T-girders
- Prefab bridge deck of box girders

The different types of cross-sections are based on the girders that are common in the Netherlands. The prefabrication of bridge deck girders are also common in other countries, however the dimensions of the girders are different.

The girders are built in the factory. This construction process is described in detail in [4, 3] and will not be further discussed in this pre-study. It is important to mention that all the type of girders are standard concrete strength class C55/65 or higher. The girders are also pre-tensioned, before the concrete is poured.

A bridge deck with inverted T-girders (also the extended version) has a top layer of reinforced cast-in-place concrete, usually with a concrete strength of C30/37 or higher. This top layer is, together with the transverse beams, responsible for the connection between the girders. In case of box girders the connections are a part of transverse beam and are made of a concrete with a lower strength than the girders.



At the building site, the construction of the bridge deck consists of a few steps. This is done after the construction of the substructure:

- Placing of the girders
- Installation of the permanent formwork
- Reinforcing of the top layer /connections between the girders /transverse beams
- Pouring of the top layer /connections between the girders /transverse beams

The type of bridge deck construction depends strongly on the location of the project. Nowadays most of the construction projects are close to highways, railroads and/or urban areas. This has been resulted in the demand of concrete bridges with limited disturbance. Precast girders have an advantage during construction, because placing of the girder bridge deck only takes one night work. This shorten the construction time at building site too.

Another benefit of the girders is that scaffolding is not necessary. The completion of the bridge deck after placing of the girders takes place without disturbances for the traffic.

2.2.3 *Pros and cons of cast-in-place bridge deck and prefab bridge deck*

Both construction methods have their advantages and disadvantages. In the last two subsections a part of these advantages and disadvantages are already discussed. In this section an overview is given in Table 2-1.

<i>Cast-in-place concrete bridge deck</i>	
advantages + no limitation in the dimensions of the cross-section + limited deck height + no intermediate connections needed (continuous deck) + low construction cost + Design freedom + Less vulnerable for calamities + More robustness	disadvantages - Scaffolding + formwork needed - longer construction time - applicability depends on the location
<i>Precast concrete bridge deck</i>	
advantages + low traffic disturbance + no scaffolding needed + short construction time + better quality of the concrete due to pouring in the factory	disadvantages - limitations of the cross-section (transport, weight) - dependent on the planning of the prefab factory - complex connections, if the bridge is continuous - larger deck height in comparison to cast-in-place bridge deck

Table 2-1 Pros and cons of cast-in-place bridge deck and prefab bridge deck

Remark Table 2-1: The intermediate connections will be further discussed in section 2.4.



2.3 Abutment design

The substructure is the component that includes all construction elements that supports the superstructure. Its purpose is to transfer the loads from the superstructure to the foundation and embankment soil [7]. The construction elements of the substructure are the abutments, the piers and the foundation. The piers and the foundation will be discussed in sections 3.3 and 3.4. This section is about abutments. The other two construction elements are not discussed here, because there is not a significant difference between a pier and foundation in an integral bridge and a conventional bridge (Figure 2-8).

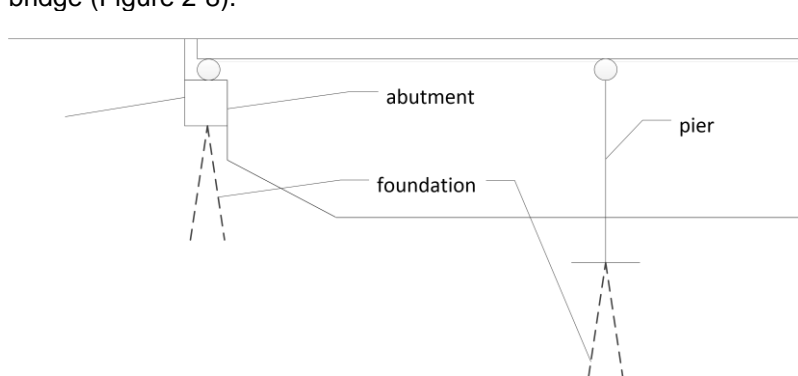


Figure 2-8 A sketch of the substructure of a conventional bridge

An abutment is a construction element of the substructure at the end of the bridge. Its function is to provide end support for the bridge superstructure and to retain the approach roadway embankment [7]. Sometimes wing walls are connected to the abutment. They are applied to retain the embankment soil and not to support the superstructure.

There are different options to construct a conventional abutment. The most common are:

- **Full retaining or wall abutment (Figure 2-9b):**
 - Cantilever
 - Counterfort
 - Mass Concrete or gravity
 - Stub-counterfort
- **Stub abutment (Figure 2-9a)**
- **Open or spill-through abutment**

An 'open or spill-through abutment' is not common in the Netherlands, but it is applied in the United States [8]. A wall and stub abutment are frequently applied in the Netherlands.

A full retaining or wall abutment is built over the total height and has to retain the embankment soil. This abutment type provides end support for the bridge and retains the entire roadway embankment (Figure 2-9b). A stub abutment is built at top of the embankment and retains only a minimum height of the embankment (Figure 2-9a).



A wall abutment is more expensive than a stub abutment, but in case of a wall abutment the costs for the superstructure are significantly lower. The span length of a bridge with stub abutments is larger due to the slopes (see Figure 2-9). Nevertheless, a stub abutment is used more often than a wall abutment in roads, because the sight for car drivers who are passing under the bridge is better which increases the safety [3]. Therefore, it is usually also a requirement of the Dutch Department of Transportation.



Figure 2-9 Common types of abutments

A standard abutment consists of certain elements (Figure 2-10). These elements are:

- Back wall
- Abutment stem
- Wing walls
- Footing
- Cheek wall
- Bridge seat

STUB ABUTMENT

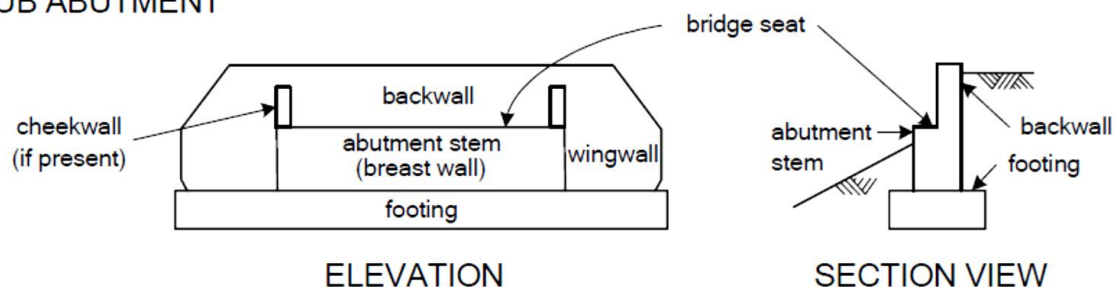


Figure 2-10 Elements of a standard abutment

The back wall and wing walls are applied to retain the embankment soil. Wing walls are not always a part of the abutment. Sometimes they are separated construction elements and attached to bridge by an expansion joint. The footing is connected to the foundation structure. If the soil is rigid, a spread footing is applied as the foundation.



2.4 Design of intermediate connections

The intermediate connections are applied between two adjacent spans. There are three options to connect the two adjacent spans (Figure 2-11):

- Full continuity
- Partial continuity
- Simply supported

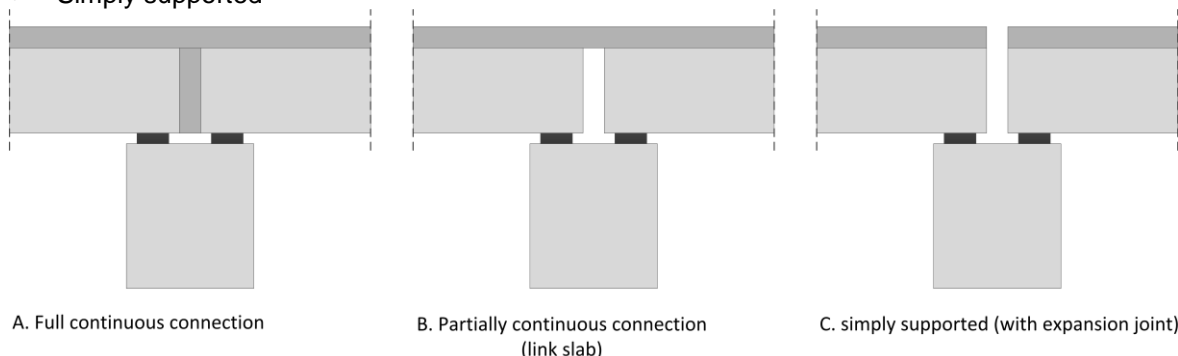


Figure 2-11 Different options for an intermediate connection

A multi-span bridge deck is created with the first option and the last option leads to a single span deck. In section 2.1, the difference between a simply supported deck and a multi-span deck has already been discussed. The middle option results in a continuous connection, but with rotational flexibility, so that the two single spans are still able to rotate independently. From a structural point of view, the girders are simply supported and coupled by a hinge.

A prefab deck with a simply supported connection is rather simple to construct and thus it is much applied. The simply supported connection is constructed with an expansion joint. The focus of this thesis is to eliminate expansion joints and to apply integral bridges. Therefore, the simply supported method is not further discussed here.

Full continuity is much applied with a cast-in-place concrete bridge deck, because it is simple to execute the bridge deck and it leads to a smaller bridge deck height. For these reasons a cast-in-place deck with full continuity is always preferred and will not further be discussed (see also subsection 2.2.1). If the bridge deck is made of prefab girders it is more complex to construct a full continuous connection, because a lot of reinforcement is required in a limited space. The reinforcement is needed to compensate the negative bending moment at the intermediate support. The negative bending moment at the intermediate support is caused by the additional dead load and the live load. It is not the full dead load, because the prefab girders are first simply supported and then connected to each other. The deformation due to dead load of the girders and time dependent behaviour of the structure has already occurred. A full continuous connection between prefab girders is also quite expensive due to the large amount of reinforcement and the labour intensive construction. Therefore, the combination of full continuity and prefab girders is not much applied.



2.4.1 Full continuity

A full continuous connection can be achieved by coupling the two adjacent spans with reinforcement in the top slab and diaphragm. Examples of this connection are given in Figure 2-12.

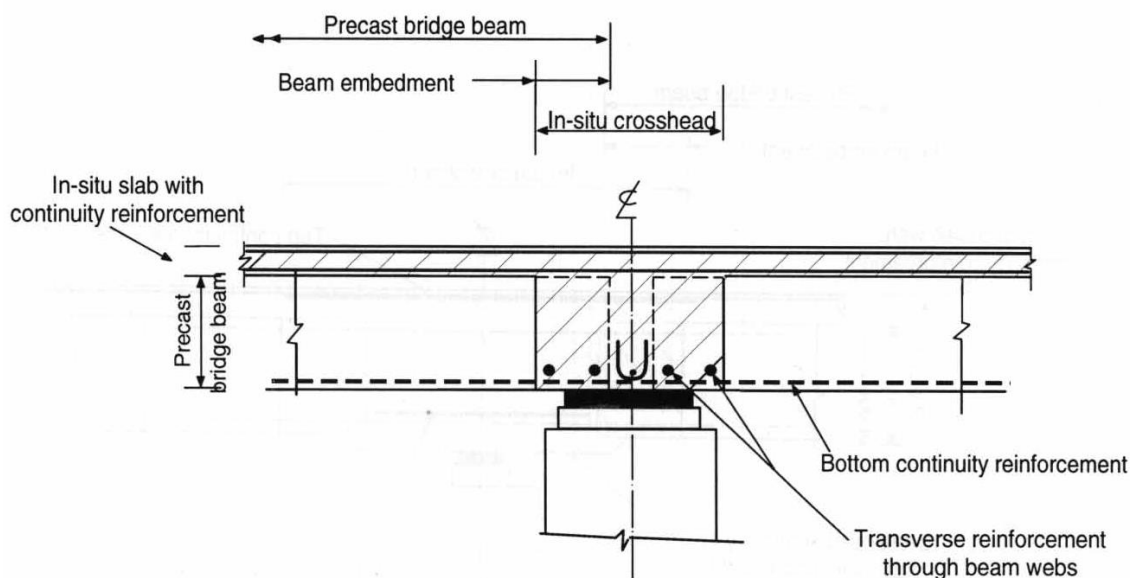


Figure 2-12 A standard construction detail of a full continuous connection

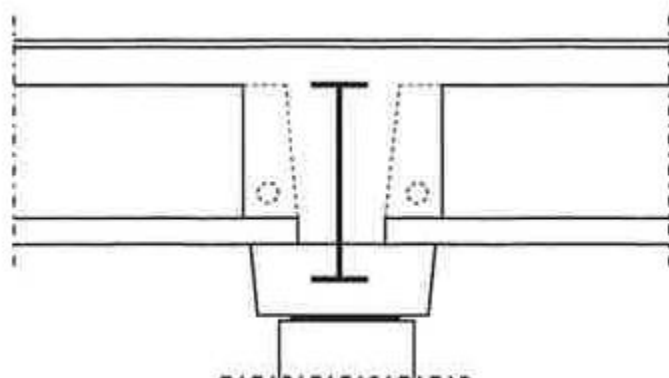


Figure 2-13 A construction detail of a full continuous connection with a Preflex beam

The first step of execution is to place the girders on the supports. Then the connection is reinforced and poured with concrete. Another common option to construct a full continuous connection is the application of a 'Preflex beam' (Figure 2-13). However, this method is not used anymore due to high labour cost and an expensive steel beam [9].

2.4.2 Partial continuity

A partial continuous connection is also called a 'link slab'. A standard solution for partial continuity is given in Figure 2-14. The link slab is applicable for different type of prefab beams, also for reversed T-beams, extended reversed T-beams and box-beams. The box beams do not have a deck slab and therefore a space is created in the box beam.

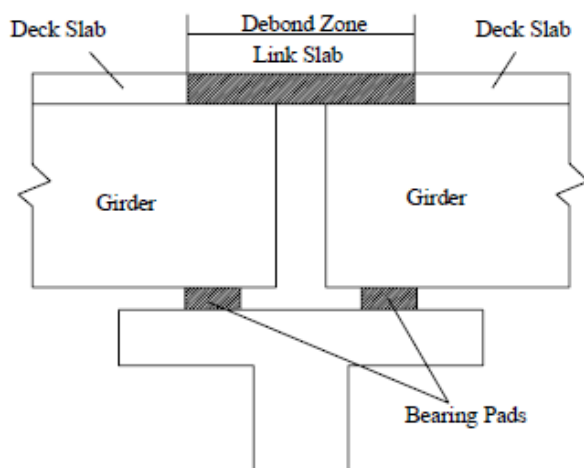


Figure 2-14 A standard detail for connection with a link slab

A link slab is a hinged connection and that is why negative bending moments cannot be absorbed. The link slab is called in Dutch 'een kraakplaat', what refers to a slab which is able to crack. The slab will crack, because it is 'the weakest link in the connection' and generally loaded with tension. The concrete in the slab will not resist tension and cracks. Hence, it is important that the crack width is limited to create a durable structure. In practice, a lot reinforcement of small diameter is applied to limit the crack width. The cracks are well distributed over the total width of the link slab. Figure 2-15 shows a detail of this reinforcement.

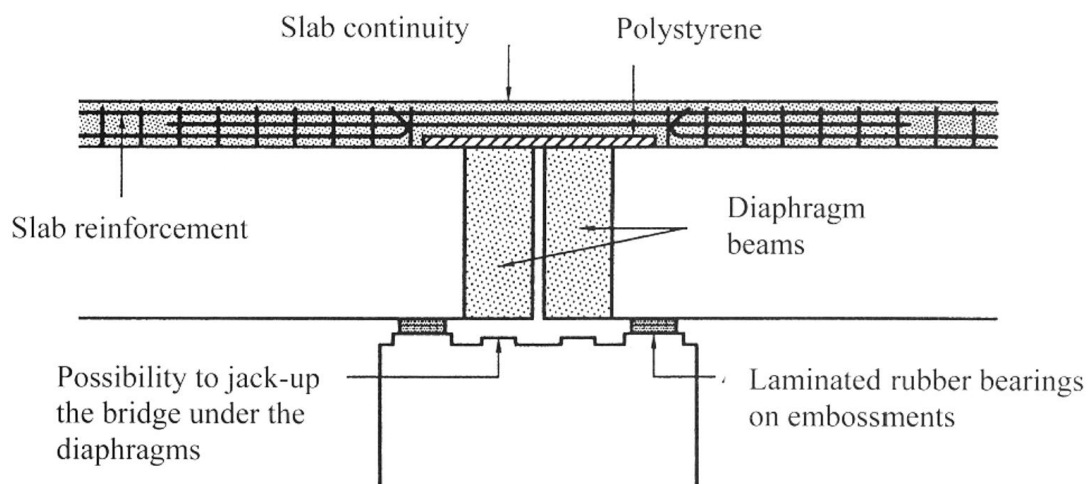


Figure 2-15 A standard detail of a link slab with reinforcement [4]

A link slab is cheaper compared to a full continuous connection and therefore it is an interesting alternative. The question is, if it is applicable for integral bridges as well. The answer is probably no, because the forces (tension and compression) due to the deformation of the bridge deck and the rigidity of the abutment and soil are much higher. However, integral bridges with prefab girders are never applied in the Netherlands.



3 Integral bridges

3.1 Common practice of integral bridges

Integral bridges have been built in Australia, Canada, Japan, the United States and several countries in Europe. The choice for an integral bridge over a conventional bridge depends strongly on [1]:

- the bridge length
- location of the future bridge
- the climate
- the requirements of the bridge and the road

In the next subsections the practice in the US and the Netherlands will be further discussed.

3.1.1 Common practice in the United States (U.S.)

A survey conducted by the University of Maryland indicates that 41 State Departments of transportation (DOT) are using integral bridges [2]. Only in 8 States more than 1000 integral bridges have been built. The longest integral bridge in concrete as well in steel has also been constructed in the U.S. The longest precast concrete integral bridge has been built by the state of Tennessee. It has a length of 358 meter (Figure 3-1).

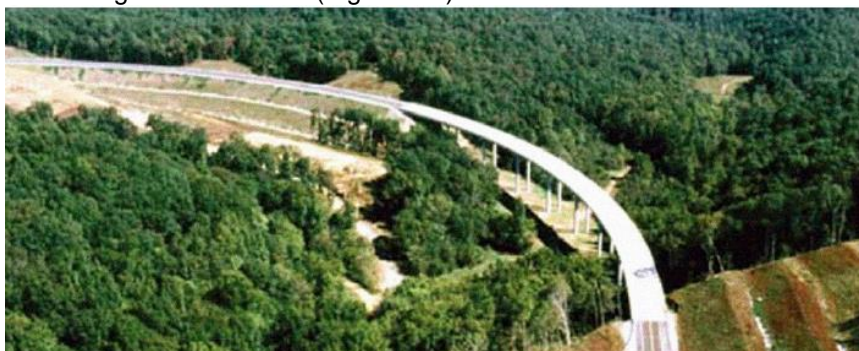


Figure 3-1 State 50 Happy Hollow Creek Tennessee, USA

The first integral bridge was built in the state of Colorado in 1920. In the next years other States followed. Their choice for integral bridges was made because of the limited durability of expansion joints and bearings. In their experience the elimination of expansion joints and bearings leads to a more durable structure and less maintenance [10]. The building costs are also lower than conventional bridges. The major reason for that is that earth pressure forces are transferred by the superstructure from one abutment to the other abutment. This leads to a less material use [1].

In 10 States, the use of integral bridges is preferred over conventional bridges, if the bridge length is not too long and soil conditions are not too complex [2]. The maximum bridge length is disputed by the State engineers. Normally the allowable length is between 60 and 180 meter depending on the state limitations. These bridge length limitations depends on the maximum allowed lateral pile displacement, the thermal conditions, the soil conditions, the skew and type of material [11, p. 7].



Most of the States have experience with steel, concrete and steel-concrete bridges [11]. The concrete bridges are designed with precast concrete girders, precast box beams and cast-in-place concrete. Figure 3-2 is a standard design for a multi-span precast concrete girder bridge.



Figure 3-2 Prefab prestressed concrete integral abutment bridge under construction

For steel and steel-concrete bridges (Figure 3-3) the length limitations are stricter due to thermal deformation. Steel is more affected by the cyclic temperature behaviour and therefore, there is more thermal deformation than in concrete. For that reason the longest steel bridge that was built, is shorter than the largest concrete bridge.



Figure 3-3 Steel-concrete integral bridge

3.1.2 Common practice in the Netherlands

In 2000, Maijenburg [12] investigated the integral bridges that were built in the Netherlands. Almost all the integral bridges are single span bridges with a length between 0 and 40 meter. Only one bridge which is also the longest bridge in the Netherlands has a length of 70 meter (Figure 3-4). This is a bridge with 3 spans and constructed of prestressed concrete.



Figure 3-4 Longest integral bridge in the Netherlands. It is located by Son and Breugel.

Nowadays more integral bridges have been built including some concrete multi-span bridges. A recent infrastructure project 'A2 Randweg Eindhoven' has five integral bridges with one two-span precast girder bridge of 39 meter [13]. Another recent infrastructure 'project A73 Zuid' consist of several single span cast-in-place concrete bridges with one multi-span cast-in-place concrete bridge [14]. Iv-Infra recently designed a multi-span bridge as well. This cast-in-place concrete bridge has a length of approximately 60 meter (Figure 3-5).



Figure 3-5 Bridge Schokkeringweg N50

In the Netherlands, integral bridges are not used as a standard practice. The preferred structural system is a conventional bridge. The integral bridges that have been built, seem to be a choice of the designer [12].



3.2 Structural system integral bridges

All construction elements of an integral bridge are monolithically connected. This results in one integral system where there is interaction between the sub- and superstructure and between the bridge and the embankment soil. This is an important difference compared to a conventional bridge, where the sub- and superstructure function more like single structural systems (Figure 3-6).

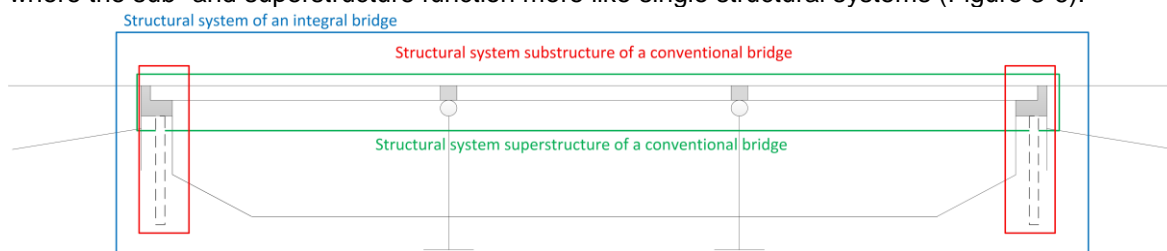


Figure 3-6 Structural systems of conventional and integral bridges [15].

The bridge deck deforms due to loading, temperature influences and time-related material effects. In one structural system these deformations have influence on the substructure too. The degree of influence depends on:

- The length of the bridge
- The bridge deck design
- The connections between the sub- and the superstructure
- The foundation design
- The embankment soil
- The abutment/ pier design

3.2.1 The connections between the sub- and superstructure

The continuous connection between the bridge deck and the abutment can allow or resist the deformation. This depends on the structural design of the connection, the sub- and superstructure. A connection that will not deform or resist the deformation is called rigid (Figure 3-7a). In this case, the rotation is equal to zero. When the connection allows the deformation, it is called 'a pinned connection' (Figure 3-7b). In this case, the moments are equal to zero. In reality the continuous connection behaves partly rigid and partly pinned. So the moments and rotations are both unequal to zero.

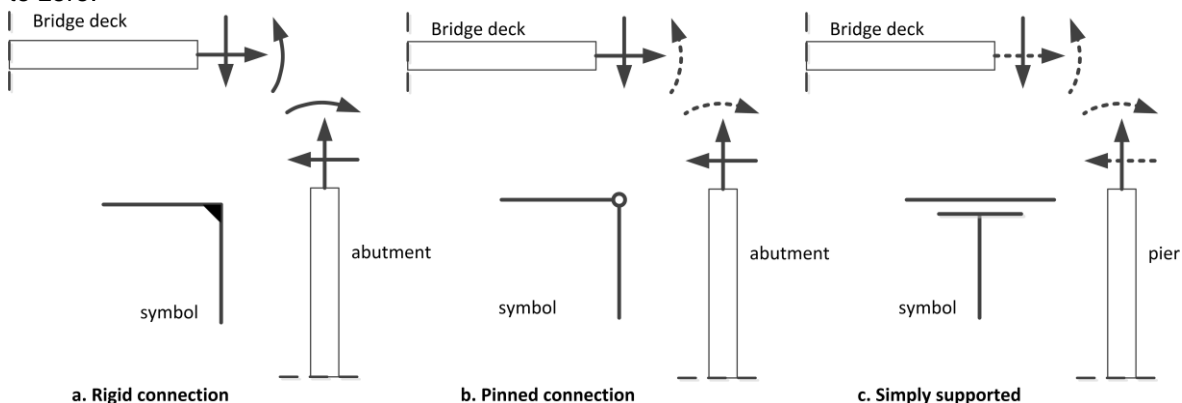


Figure 3-7 The degree of rigidity of the connection



The piers can be either integrated in the integral bridge or self-supported. [10] The integrated piers are monolithically connected with superstructure and the connection will not deform (Figure 3-7a). The self-supported piers are provided with bearings and allow deformations. The fixed bearings can be seen as pinned connections (Figure 3-7b). They allow rotations, but no displacements. If movable bearings are applied the construction can be seen as simply supported (Figure 3-7c). They allow rotations and displacements.

3.2.2 *The structural system integral bridges under loading and deformation*

An integral bridge is one structural system as mentioned before. The structural system of an integral bridge can be schematized as a portal frame. In this case the beam of the portal frame is the superstructure and the columns comprise the substructure. In a portal frame, deformation in the beam will cause deformation in the columns. The deformation that occurs in the bridge deck of the integral bridge is caused by loading, temperature influences and time-related material effects [12]. These loads and effects will cause the following rotations and displacements in the structure:

- Vertical displacement and rotation (weight of the bridge, asphalt, traffic)
- Rotation (temperature gradient daily cycle)
- Contraction (shrinkage, creep, elastic shortening prestressing)
- Expansion (temperature yearly cycle)

A visualization of these displacements and rotations are given in Figure 3-8. The intermediate supports are schematized as simply supported. In reality this means that the piers are single structural systems and not part of the structural system of the integral bridge. The foundation is schematized as a column with a rigid footing. This is a simplification for this visualization and will be further discussed in chapter 4. The load cases will also be further elaborated in chapter 4.

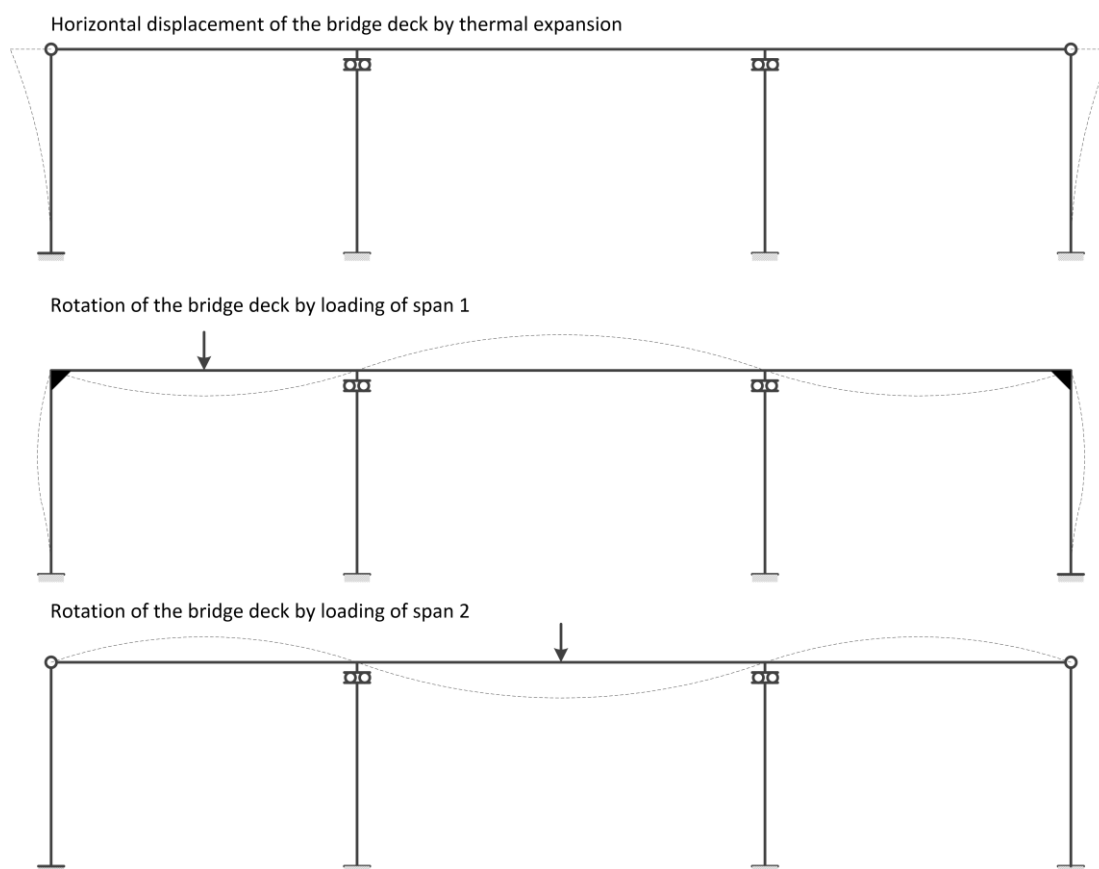


Figure 3-8 Visualization of the structural system under loading and thermal expansion

3.3 Abutment and pier design

The abutments and piers are both part of the substructure. The abutment of an integral bridge is integrated in the structural system. A pier is not always integrated in the structural system and sometimes separated by a bearing construction, as mentioned in section 3.2. Integral abutments and piers are further discussed in the next subsections.

3.3.1 Abutments

An integral abutment differs from other abutment configurations due to the monolithic connection with the superstructure. No bearings or expansion joints are applied at the bridge ends. According to the 'BA 42/96 design of integral bridges' [16] there are four different integral abutment configurations. These four different integral abutment configurations are given in Figure 3-9. The frame abutments (a and b) and the embedded abutment (c) are mainly used for single span integral bridges [1, 12]. The embedded abutment (c) is also applied for the longest integral bridge in the Netherlands (Figure 3-4). The bridge has been founded on a combination wall of shell- and sheet- piles and function as a retaining wall too. The bank pad abutment (d) has no foundation construction and is directly founded on the soil. This construction method is often used in the United Kingdom. The end-screen abutments (e and f) are both abutments in a semi-integral bridge and will be not further discussed in this pre-study.

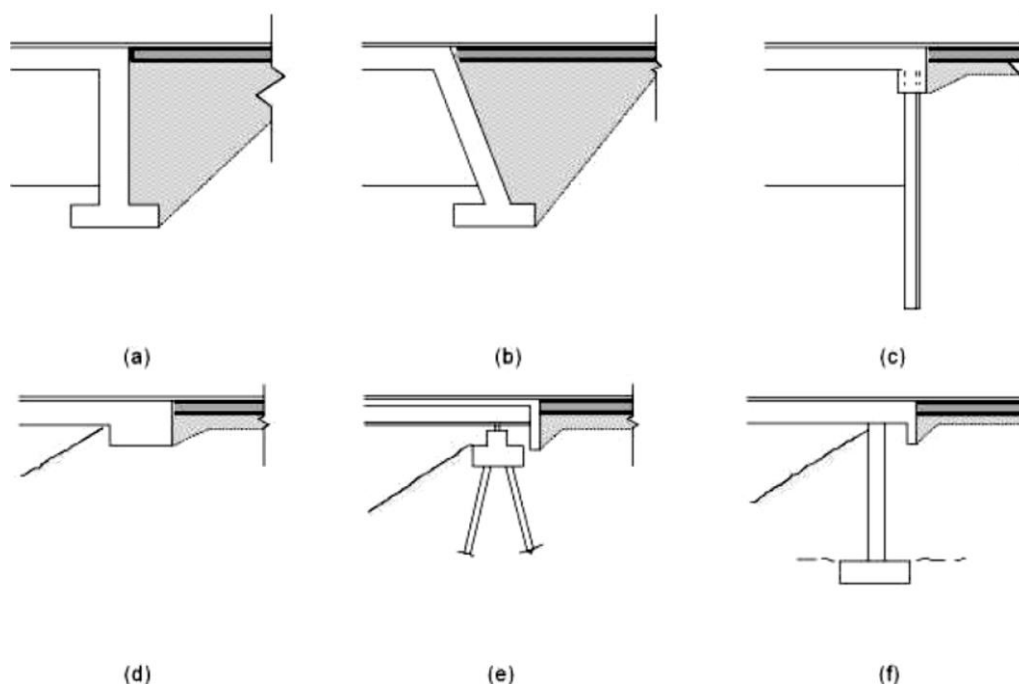


Figure 3-9 (a) & (b) frame abutments, (c) embedded abutment, (d) bank pad abutment, (e) & (f) end screen abutments. Integral bridge abutments according to [16].

In the U.S., an integral stub abutment is mainly applied. This is an abutment that is directly connected with the superstructure and founded on one row of vertical piles. The vertical piles are applied to allow the superstructure to deform in the lateral direction. The philosophy is that if braced piles are used the abutment cannot displace. The ability to displace is essential for abutments, because the forces and the moments as result of the deformation of the superstructure will be too large to resist [10]. The integral stub abutment is executed with a deck of cast in place concrete, prefab girders or steel girders. A construction detail of this integral stub abutment is given in Figure 3-11.

An integral stub abutment is mostly applied as a rigid connection, but there are other options, like a pinned-head and a hinge abutment (Figure 3-12 and Figure 3-13). In case of a pinned-head, urethane or poly-foam padding is wrapped around the pile head. The pile in Figure 3-12 is wrapped with a padding of 25 mm over a height of 1 m. In case of a hinge abutment, the substructure rest on a neoprene pad and the superstructure is doweled on the abutment. Researchers termed this abutment type as semi-integral, but others consider the hinge abutment as integral [17]. In both abutment configurations, the moments at the pile head are negligible. That is different in comparison to a rigid connection, where the moments could be very large.

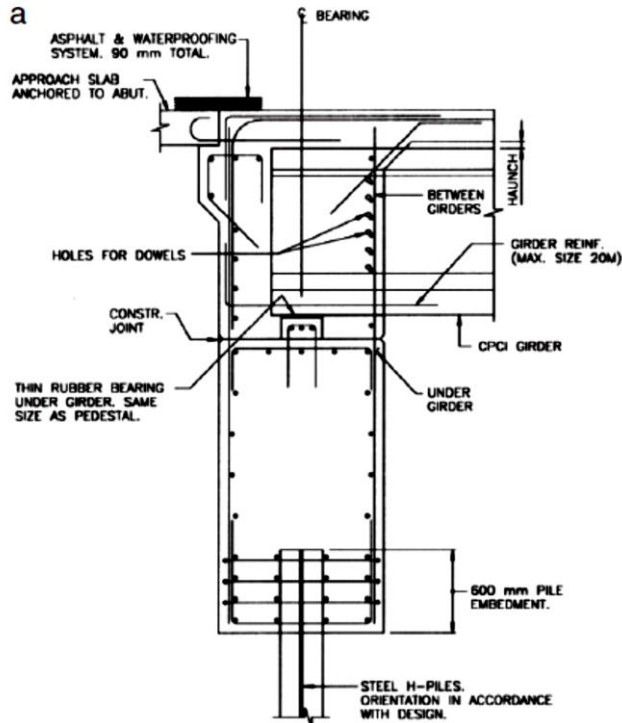


Figure 3-10 A standard construction detail of an integral stub abutment

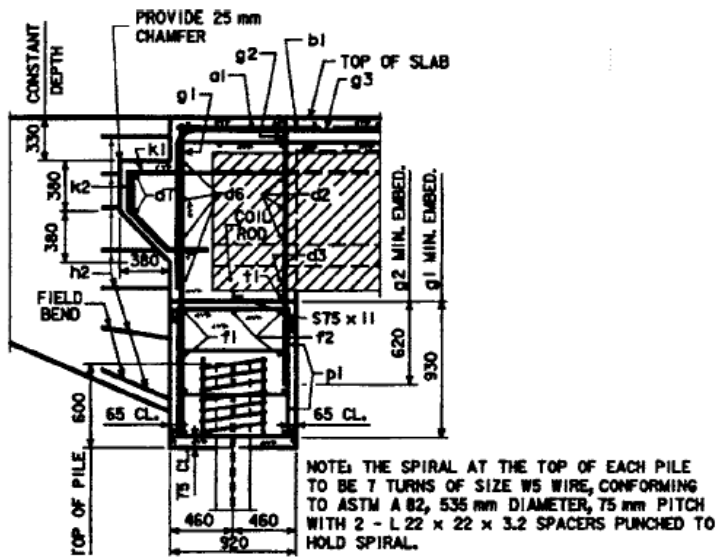


Figure 3-11 A standard construction detail of an integral stub abutment also called a fixed-head construction [17]

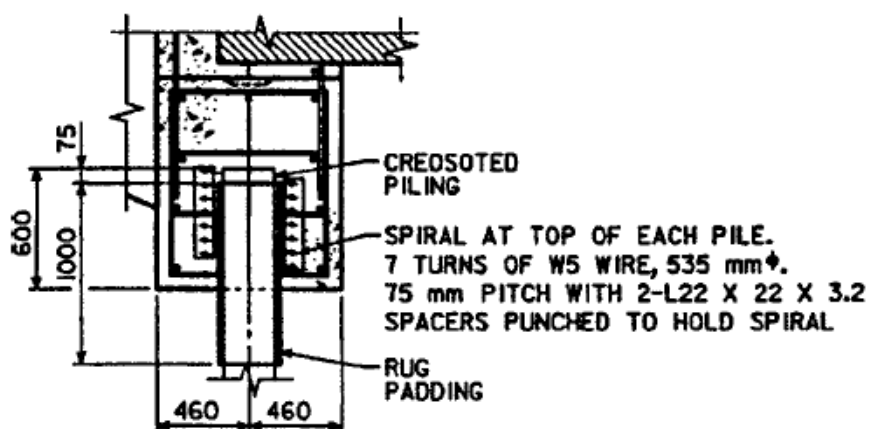


Figure 3-12 A pinned-head pile construction of a stub abutment [17]

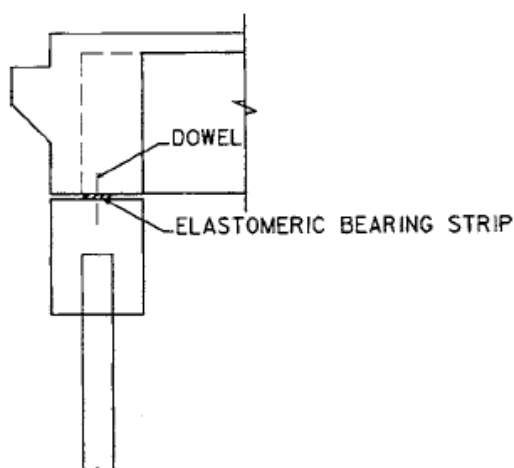


Figure 3-13 A hinged stub abutment [17]

Wing walls are also used in integral abutments. The most common method is that wing walls are rigidly cast to the integral abutment, so that they move into or out of the retained soil. There are no restrictions for the length of the wing walls, only it is not allowed in some states to locate piles beneath the wing walls. Having multiple rows of piles in the lateral direction provides a moment coupling force which will restrain the abutment to rotate and may induces forces in to the structure that were not accounted for. [18]

3.3.2 Piers

A pier is a construction element of the substructure and its basic function is to transfer the vertical loads from the superstructure to the foundation. Structurally, there are two options for a pier construction: A self-supported pier and a flexible integral pier. A self-supported pier is not continuous connected with the superstructure and is built on a rigid foundation. Only a relatively small part of the horizontal loads due to the deforming bridge deck are transferred to the self-supported pier. This is because of the bearings that are applied. The flexible integral piers are continuous connected with the superstructure and founded on vertical piles. Like the integral abutments, vertical piles are applied to allow the superstructure to deform in the lateral direction.

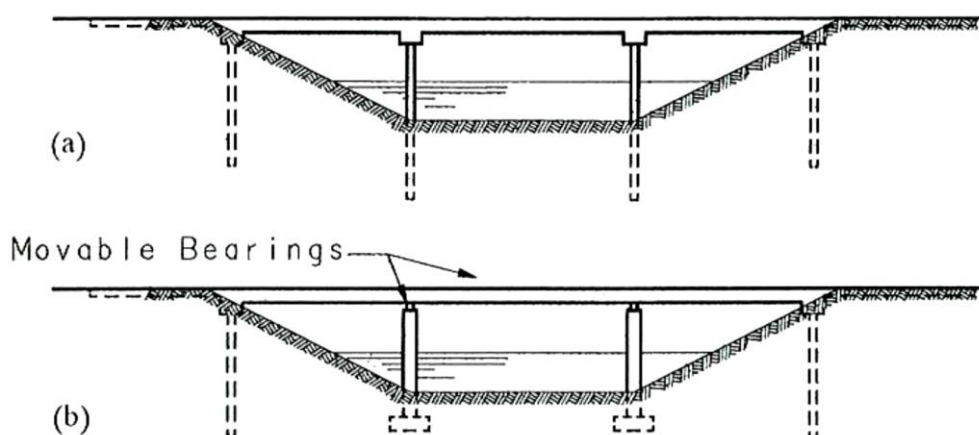


Figure 3-14 (a) integral bridge with integral flexible piers and (b) integral bridge with self-supported piers [10]

There are different options to construct a self-supported pier. Figure 3-15 gives the most common self-supported piers that are applied onshore in the Netherlands.

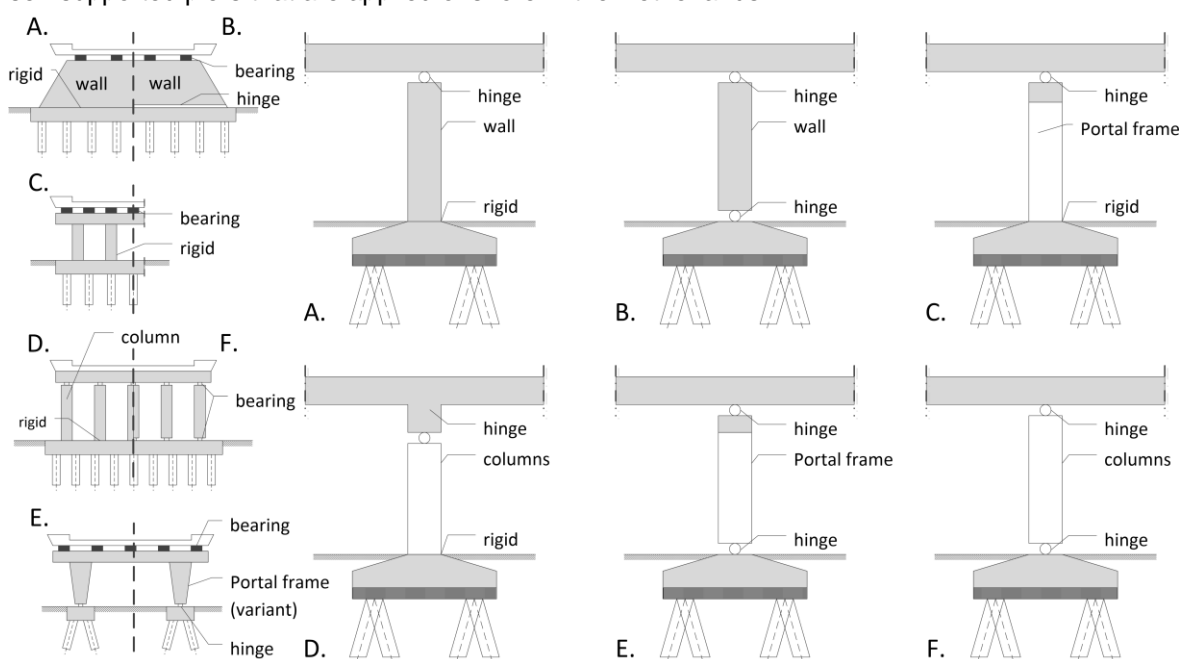


Figure 3-15 Different options for a self-supported pier

If piers are continuous connected, it is important that they are able to displace. The vertical piers consist of slender piles that are linked to each other by a cross beam (Figure 3-14a and Figure 3-16). This applies to multi-span bridges with more than two spans [10]. If an integral bridge has an odd number of spans, it is possible to execute the middle pier as rigid. As example, the bridge 'Schokkeringweg', is executed with a rigid integral middle pier (Figure 3-5). When an even-span integral bridge is constructed with integral piers, it is uncertain if the bridge deforms in the right or the left direction. This leads to uncertainties in the structural design which is not recommended.

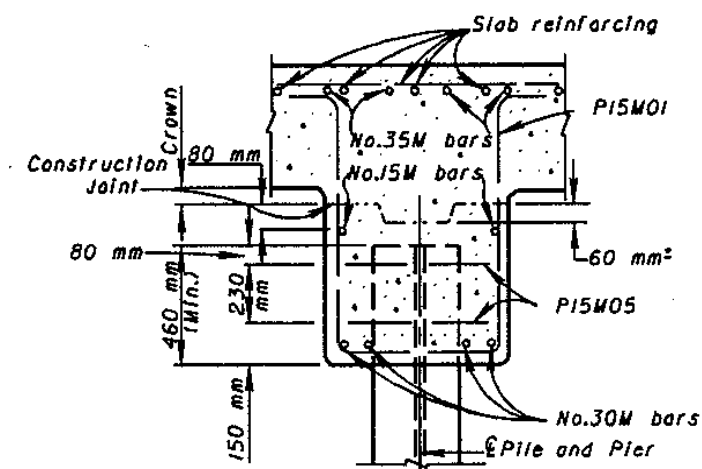


Figure 3-16 A full continuous connection between a pile and a cast-in-place bridge deck

3.4 Foundation design

The foundation is the lowest part of the substructure that transfers the loads from the bridge deck to the soil. There are several foundation configurations such as piles, sheet-piling and a spread footing or shallow foundation. Important for the foundation of an integral bridge is that it transfers not only the vertical loads, but also the deformation of the bridge deck to the soil.

3.4.1 Pile foundation

A pile foundation is applied, when the subsoil is not able to bear the bridge on a spread footing. In case of integral bridge, the pile foundation needs to deform in lateral direction as well. This leads to other requirements for the pile foundation compared to a pile foundation of a conventional bridge. Therefore, the pile foundation consists of one row of piles to allow the bridge deck to deform and require the piles a certain deformation capacity. In the U.S., steel H- or HP-piles are mostly used, but also steel shell-piles, cast-in-place concrete piles, prestressed concrete piles and wooden piles are applied. Figure 3-17 gives an overview of the piles that are used.

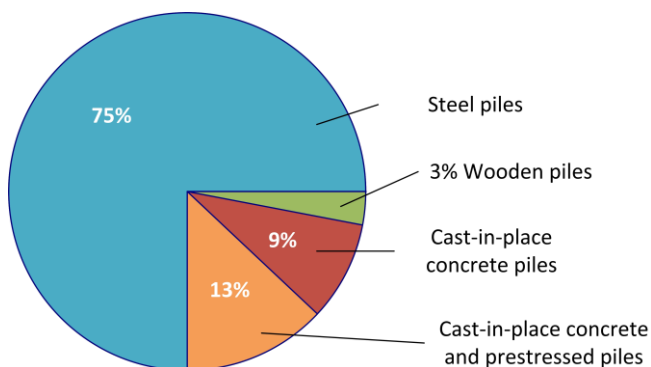


Figure 3-17 Type of piles used in the U. S. [12]



The deformation capacity of a pile is a limiting factor for the maximum length of an integral bridge. The total deformation depends on the total length of the bridge. When the total length increases, the total deformation also increases. A pile of an integral bridge is monolithically connected with the bridge deck and will deform as well. If the deformation capacity of the pile is not sufficient, the bridge is not executable. Therefore, the bridge length is limited in most of the states.

There are also options to increase the allowable deformation of the piles. These options are pre-bored holes or pile sleeves. Pre-bored holes are applied, if the soil is quite rigid and the pile cannot deflect. After the pile is brought in place, the hole is filled with a flexible material. Empty holes lead to long-term maintenance problems, so the holes are filled with a deformable material such as bentonite slurry, loose sand or pea gravel. The piles sleeves are made of corrugated steel and are placed over the pile head. The sleeves are filled with a deformable material too [17].

The abutment is fixed-, pinned-headed or hinged as mentioned in subsection 3.3.1. This has influence on the structural behaviour of a foundation pile. If the abutment is fixed-headed, the pile can also be modelled as rigidly connected. This applies for a pinned-headed and a hinge abutment too. Research suggests that the tip of the pile can be modelled as rigid, because the bottom part of the pile is rammed into the rigid soil. (Figure 3-18) [19]

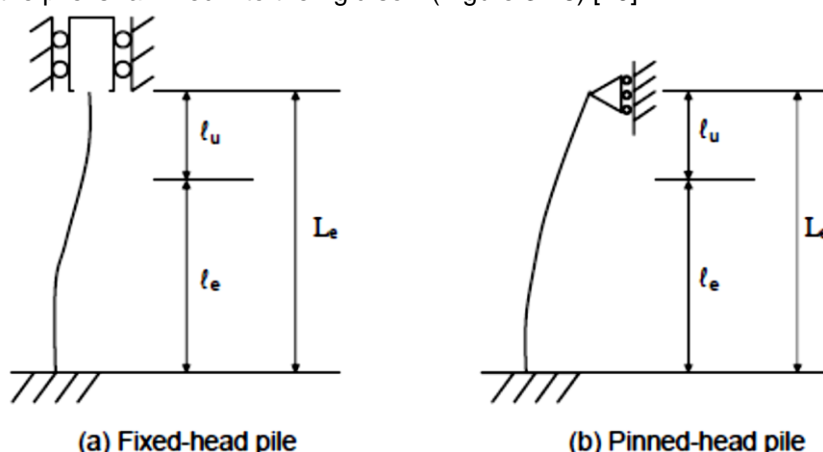


Figure 3-18 Structural models of a pile foundation

3.4.1.1 Steel piles

In the U.S., most of the piles in integral bridges are made of steel. Steel H- or HP-piles are preferred for integral bridges. The idea to use steel piles in favour of concrete piles is that they have more deformation capacity. The H- and HP-piles are single symmetric. This means that they have a strong and weak axis in case of stiffness [17]. There are two options: In line with the skew of the bridge or in line with the centreline (Figure 3-19).

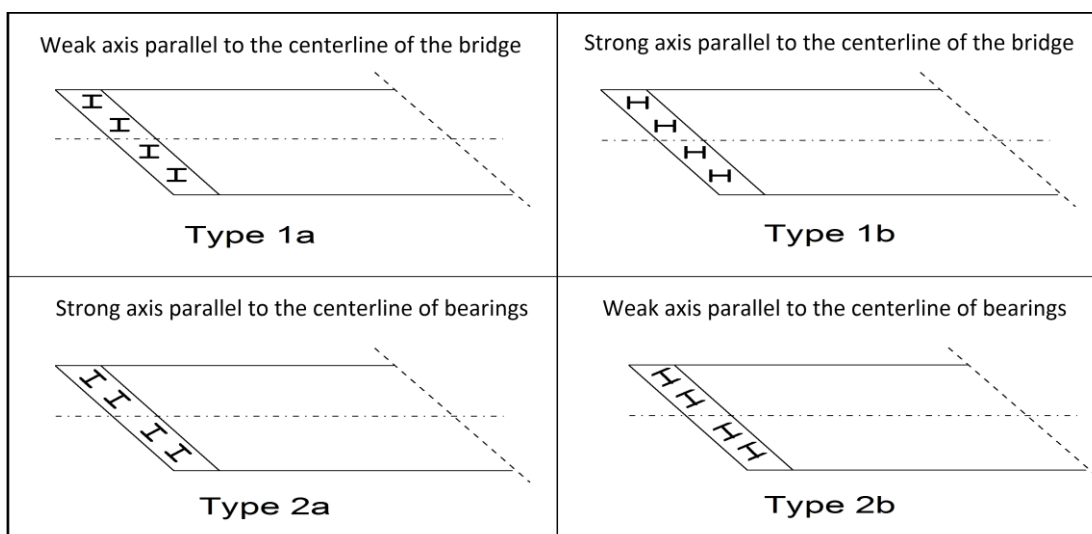


Figure 3-19 Possibilities of axis direction [12]

Steel shell piles are used too. The idea is that these piles have more stiffness than H- or HP-piles. Therefore, they are not able to deform as much. The top part of the piles is sometimes filled with concrete. With concrete, the pile is more resistant against buckling. A part of the multi span integral bridges that are built in the Netherlands is founded on steel shell piles filled with concrete. The bridges in Figure 3-4 and Figure 3-5 are founded on steel shell piles as well. This is the most common method for integral bridges in Europe. [18] Steel shell piles with concrete have more bearing capacity than steel H-piles. In the U.S. steel H-piles are mainly designed for the lateral deformation and not standard for the vertical loads. [18] Steel shell piles are therefore more suitable, when the bearing capacity of the pile is important.

Orientation of H- or HP-piles

The Federal Highway Agency (FHWA) did a survey in 2004 and 39 States responded. The conclusion in case of pile design is that there is no uniform approach for the pile orientation. Most of the States orient the piles in the weak axis, but others prefer the orientation in the strong axis. [20]

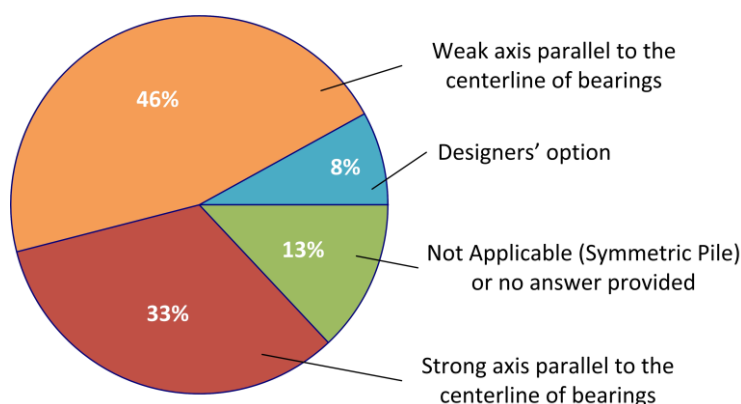


Figure 3-20 Typical pile use orientation for integral bridges



There is a concern for pile yield, if the pile is rigidly connected to the abutment. An argument for weak-axis orientation is that only the tips of flanges will yield under large bending stresses, leaving the basic core of the pile to carry vertical load. Other states note that H-piles are better able to resist flange buckling, if the piles are oriented in the strongest axis, although others disagree. [17]

3.4.1.2 Concrete piles

Most of the bridges in the Netherlands are founded on precast prestressed concrete piles. Some small integral bridges are founded on precast prestressed concrete piles too. The precast prestressed concrete piles are cheaper than steel piles and they do not corrode. The bearing capacity of a concrete pile is also higher than a steel pile, because the friction between concrete and soil is higher than between steel and the soil. The cross-section of a concrete pile is larger, what leads to a higher bearing capacity too. Still, concrete piles are not usual in the U.S., where more than 9000 integral bridges are built. The common belief is that precast prestressed concrete piles are not able to deform enough and starts to crack when deformation of the bridge deck is too much. The research that is done about precast prestressed concrete piles also points in this direction. [21, 12] In the research, the pile was covered with a carpet wrap to create a hinge. Still, cracks occur in the lateral direction.

Tennessee regularly uses precast concrete piles in Western Tennessee, because of the soil. This different from Central and Eastern Tennessee where steel H-piles are applied. Tennessee limits the pile displacement in the lateral direction to 25 mm. This is the equivalent of integral bridge of 140 m. European countries also use precast prestressed concrete piles for integral bridges, but they mainly use them for single span bridges. [18]

3.4.1.3 Wooden piles

At this time Iowa is the only state that permits wooden piles. The wooden piles may be used without padding for bridge lengths up to 46 meters. Padding is required for bridge lengths between 46 and 61 meter. For bridge lengths less or equal to 40 meter pre-bored holes are not necessary. If the length is more than 40 meter, pre-bored holes of 3,5 meter filled with bentonite slurry are required. [17]

3.4.1.4 Combination of drilled shaft and pile

Another technique is applicable, when adjacent structures are sensitive to vibrations or driven piles are not possible. This is a drilled shaft in combination with a pile. First the shaft is fully or partially drilled. Then a pile is embedded in the shaft. This method is also called 'stabbed shaft' or 'stabbed pile' and can provide the flexibility that is needed for an integral abutment. [17] The construction process is given in Figure 3-21.

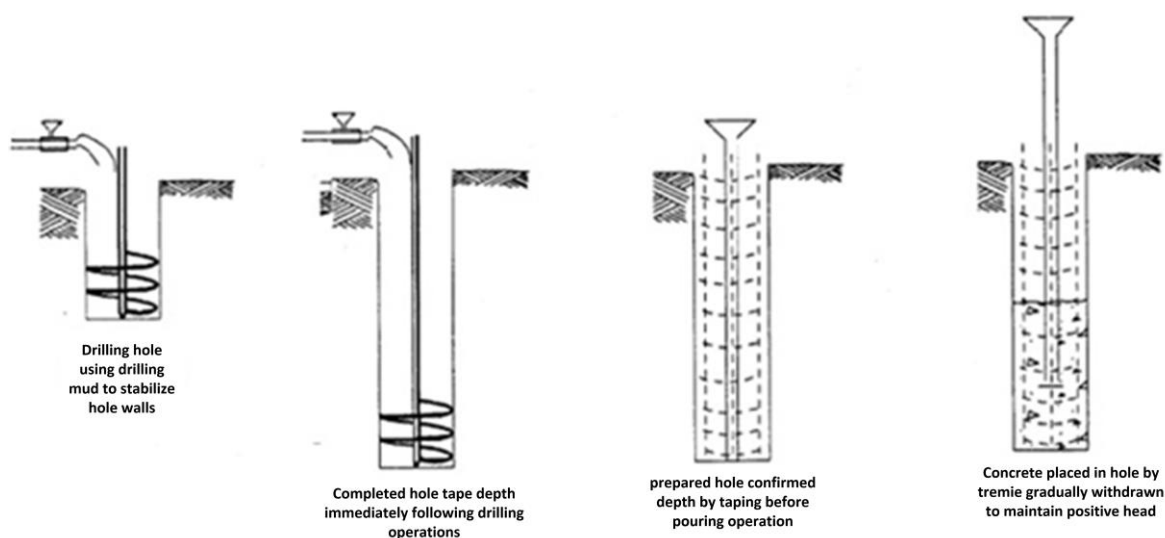


Figure 3-21 Construction process of the drilled shaft method

3.4.2 Wall foundation

A wall foundation has not only bearing capacity, but is able to retain the embankment soil as well. Therefore, slopes are not demanded which lead to a shorter bridge deck. This makes a wall foundation a cheaper option compares to a stub abutment. Only this foundation is not always applicable because of traffic safety (§2.3).

A wall foundation is made of steel sheet piles, a combination of steel sheet and shell piles, a monolithic concrete wall or concrete sheet piles. The wall foundation is applicable in combination with a frame abutment or an embedded abutment. The frame abutment consists of a monolithic concrete wall, which is founded on a spread footing or a pile foundation. It is not clear if this is a wall foundation or an abutment, because it has the same function as a wall foundation and an integral abutment. An example of a monolithic concrete wall is given in Figure 3-22.

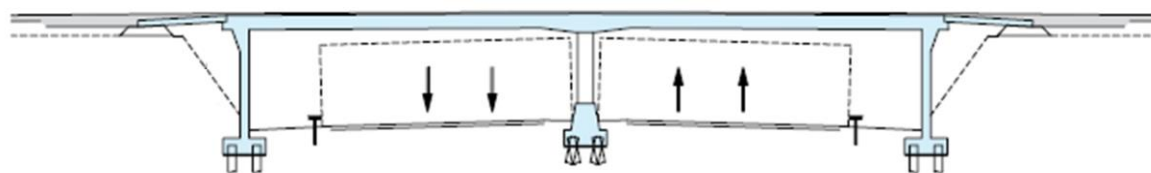


Figure 3-22 Integral bridge design A73: A combination of a frame abutment and a wall foundation [14]

The concrete sheet piles are presumably never applied with integral bridges. Whether it is possible, it is also never been studied. Probably the flexibility of the concrete sheet pile is insufficient and this is quite important for foundations of integral bridges.



3.4.2.1 Steel sheet piles and wall/pile combination

A retaining wall of steel sheet piles is used in combination of an embedded abutment. Especially in England, but also in other European countries this method is common. There are different types of sheet pile walls or combinations with other steel sections. The most frequent used sections are given in Figure 3-23. The choice for a type of section depends on the length and weight of the bridge deck and the soil conditions. The lighter profiles (type A and B) are used for short and light bridges. Heavier and longer span bridges needs heavier profiles (type C, D and E). Type D is commonly used in the United Kingdom. This is the equivalent to type E, which is standard in the Netherlands. Type C is a combination of two sheet piles or a sheet pile and a steel plate welded to each other.

Disadvantageous for steel sheet piles that steel corrodes. The sheet piles require a sufficient lifetime. Options to increase the lifetime are:

- Coating to protect the sheet pile
- Use of high strength steel
- Cathodic protection below the water level
- Concrete protection below the water level
- Metallisation of the sheet pile
- Structural design

Another option is to design a sheet pile with a sacrificial thickness. In principle, a thickness of 1 mm extra should be enough in a normal environment (CUR166) [22].

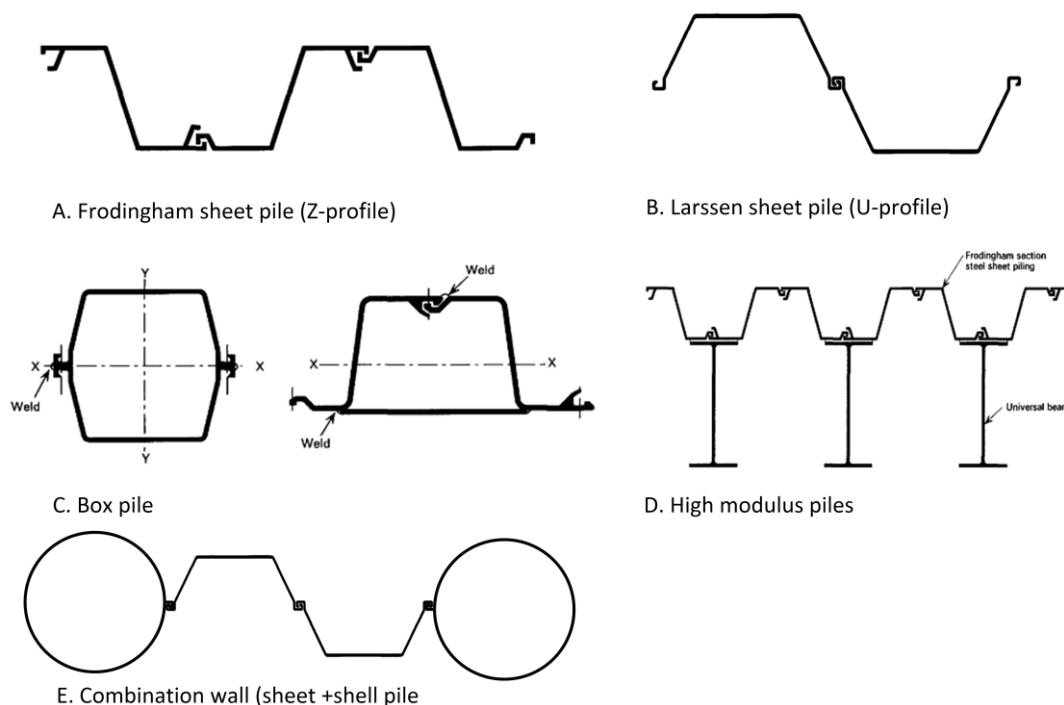


Figure 3-23 The most frequent used sections for an integral abutment [22, 12]



3.4.3 Spread footing

A foundation on spread footing is only applicable, when the soil is rigid enough. In the United Kingdom, a spread footing is used a lot for single span bridges with frame abutments. In some states in the U.S. and in some provinces in Canada, a spread footing is applied as well. Figure 3-24 is an example of an integral stub abutment in Alberta, Canada. Some of the integral bridges in the Netherlands are founded on a spread footing too. Just as in the U.K. the bridges have frame abutments. Generally this is not possible in the Netherlands due to the soft soil. [17]

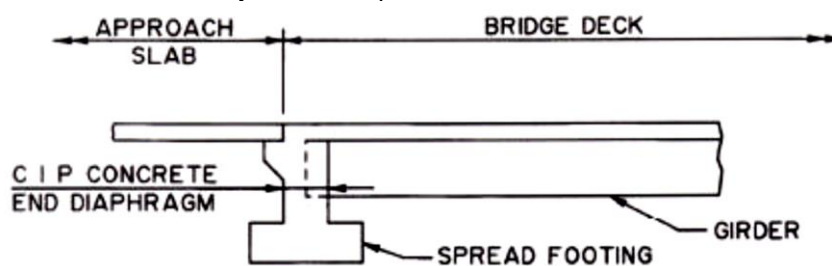


Figure 3-24 Integral bridge on a spread footing

Spread footings are not always applicable or desired. For example, a spread footing in rocky soil is not recommended. Spread footings also settle more than another type of foundation and they will compress the soil faster. [12]

3.5 Approach slabs

In general, the road settles after time and the bridge will not settle due to the foundation structure. The approach slab is applied as a transition structure between the bridge and the soil and to avoid that a gap will occur in the pavement structure. In the Netherlands, approach slabs are common for both conventional and integral bridges. The approach slabs are recommended in other European countries too. In the U.S., it varies by state. In some states it is a requirement, others do not apply them. [18]

The approach slabs of a conventional bridge are free-floating. This means that they are not connected with the bridge structure. The slabs will only displace in the vertical direction, because a conventional bridge will not displace in the horizontal direction. This is different for integral bridges, which will displace in the horizontal direction as well. Therefore, approach slabs are mostly connected with the bridge and will also displace in the horizontal direction. This connection between the approach slab and bridge can be rigid, hinged or pinned. In the U.S., the method differs by state [11]. The most common connection detail is Figure 3-25.

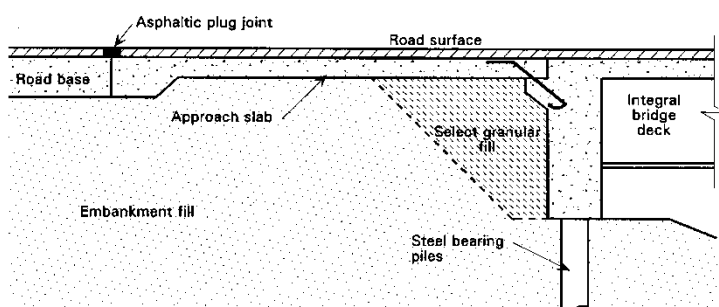


Figure 3-25 A common detail connection between bridge and approach slab

In the Netherlands, approach slabs are mainly prefabricated at the building site and brought later in position. The DOTs of the U.S. pour the approach slab cast-in-place. Problems could arise in the connection detail between the bridge and the approach slab, because the slab is constructed against a moving bridge. Therefore, the time of concreting is quite important. In Tennessee the requirement of a slab is to pour the concrete early in the morning or at the end of the day, when the sun has less influence on the lateral deformation of the bridge deck. [12]

It is essential that construction elements of an integral bridge can take over the deformation. This also applies for the approach slabs. Normally the friction between the soil and slab is very low. So the slab displaces very smoothly. But sometimes the soil resists the slab to displace. Then it is important that the soil below the slab is removed and replaced by frictionless soil.

In some countries a buried approach slab, also called 'a drag plate', is used. The belief of the users is that this method is easier, if the soil structure between the pavement and slab needs repairing. The difficulty is that it is hard to do maintenance on the approach slab connection. [18]

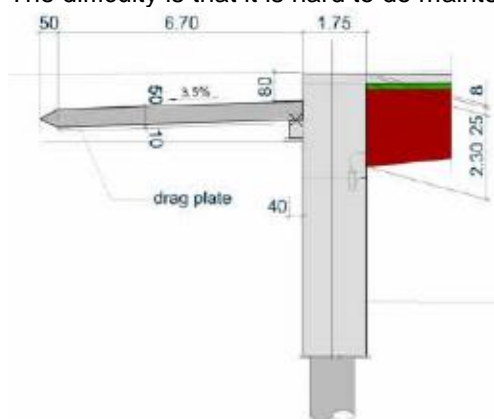


Figure 3-26 Example of a buried approach slab



3.6 Problems and limitations with integral bridges

An integral bridge is a durable structure due to the absence of expansion joints and bearings. However, without expansion joints and bearings the bridge deforms into the soil due to the deformation of the bridge deck. The deformation of the bridge deck is caused by the temperature influences and time-related material effects. The time-related material effects are shrinkage, creep and elastic shortening in case of a prestressed concrete element. These effects are responsible for deformation of the bridge deck in time. The temperature influences lead to a cyclic behaviour. This behaviour could be divided in two cycles, namely a yearly and a daily cycle. Both cycles causes cyclic deformation of the bridge deck. This deformation of the bridge deck is only possible if the bridge is able to deform into the soil. This may imply certain problems, because the soil is not rheological. These problems are [10, 20]:

- Settlement of the soil close to the abutment 'bump in the road'
- Asphalt/pavement problem
- Foundation/piles
- Early age cracking
- Wing walls
- Cracking of the abutment stem or the bridge deck at the abutment

In the next subsections the current problems will be further discussed and the temperature influences and time-related material effects are further discussed in chapter 4.

3.6.1 *Settlement of the soil close to the abutment 'bump in the road'*

Settlement of the soil due to traffic is common, especially in the Netherlands with weak soil top layers. At bridge approaches this phenomenon leads to uneven settlement, because the bridge is unable to settle too much due to the resistance of the foundation. Uneven settlement is reduced by the application of the approach slab at bridge end, but overtime maintenance at the bridge end is still necessary.

Uneven settlement at the bridge end of an integral bridge is even larger than a conventional bridge. An integral bridge deforms during the year, because of the seasonal temperature changes. This deformation is also imposed on the soil, however the behaviour of the soil on this deformation is different. The deformation of the soil is unlike the bridge permanent. The effect of this permanent deformation is a void between the bridge and the backfill. The consequences of this void depend on whether or not an approach slab is constructed as part of the bridge [23]. With an approach slab, this void leads not instantly to problems, but after a certain time it will. The approach slab is forced to span over the void, a function for which the slabs are not typically designed. This leads to slab failure when the void becomes too large to span. Note that a void does not have to be deep to damage the approach slab. The slab only needs to loose contact with the ground surface. Without an approach slab this void creates instantly a 'bump in the road at the end of bridge' (Figure 3-27). This causes discomfort to vehicle drivers and possible damage to both pavement and vehicle. Therefore, periodic maintenance is usually required. A survey, published by the University of Maryland, also indicates that settlement of the soil at the bridge end is a common problem. [2] In addition, the settlement occurs already after a few years.

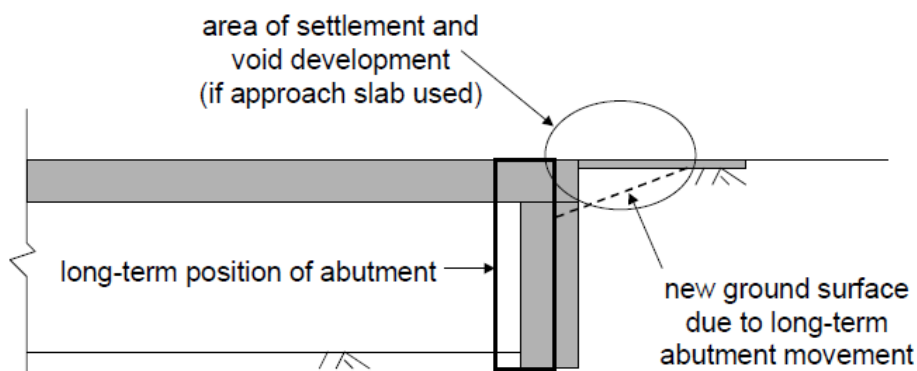


Figure 3-27 Settlement development of an integral bridge abutment

Other factors besides temperature and soil conditions which affect the settlement are [15]:

- Poor construction practices
- Length of the bridge
- Erosion
- Inefficient drainage system
- High traffic loads

Poor construction practices are for example: A poor connection between the abutment and the approach slab and settlement of the back fill material due to insufficiently compacted soil. Erosion and poor drainage are two factors which appear together. The drainage of a bridge is often insufficient, what leads to erosion of the soil at the bridge ends. The length of the bridge is important, because the longer the bridge, the more deformation occurs. An increase of the deformation leads to a larger void between the bridge abutment and the back fill.

In the U.S., some states require a compressible backfill material to minimize the influence of the cyclic deformation of the integral bridge on the uneven settlement of the bridge approach. The most common material is expanded polystyrene (EPS), but also other lightweight materials are applied. [20] The past few years some research is done to improve the material. The problem is to find a good backfill material, because the cyclic deformation of the integral bridge demands a compressible material, but the settlement behaviour demands a dense material. [23]

3.6.2 Asphalt/ pavement problem

Problems with the pavement occur due to the settlement of the soil and the cyclic deformation of the integral bridge. Settlement of the soil leads to cracking and damage of the pavement. Especially integral bridges without approach slabs needs periodic pavement maintenance. The asphalt/ pavement problem also occurs at conventional bridges, but due to the larger settlements the consequences are worse.



Like the backfill material, the pavement is also imposed by the cyclic deformation of the integral bridges. The pavement is usually unable to take over this deformation, because it is not a rheological material. Due to friction between the pavement and the integral bridge, the pavement does not contract to its original length after expanding. This residual expansion increases after repeated cycles and results in pavement growth. The pavement growth is responsible for longitudinal stresses in bridge structure and sometimes damage to the abutment. Besides pavement growth, pavement cracking occurs. After contraction, the pavement will not expand to its original length due to friction between the pavement and the bridge surface. These processes can be prevented by the application of relief joints. Relief joints are strips of bituminous material and are widely used in U.S [15]. Despite the positive experiences, relief joints are not applicable for long integral bridges. The cycle deformation of a long integral bridge are simply too large for the application of relief joints. A suitable solution for longer integral bridges is to apply pavement reinforcement at the approach slab (Figure 3-28). Two materials are commonly applied, which are glass fibre and polypropylene. [12]

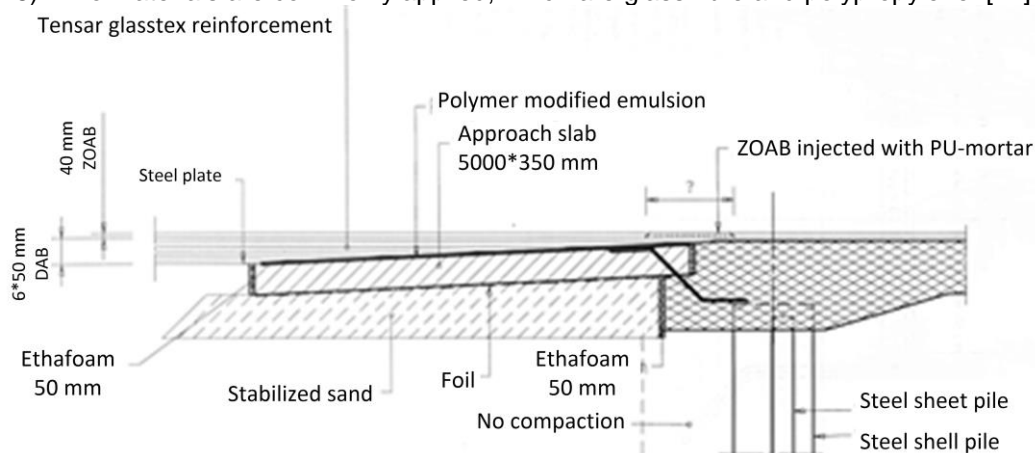


Figure 3-28 Approach slab with glass fibre reinforcement

3.6.3 Foundation/piles

Integral bridges need piles with sufficient deformation capacity, as mentioned before in subsection 3.4.1. Steel piles have the best deformation capacity and therefore they are common for integral bridges. In some states, concrete piles are also used for integral bridges, but only in combination with shorter bridge lengths. Concrete piles are used less due to the lower deformation capacity. Hence, the deformation capacity of the pile is a limiting factor for the total bridge length. [15] An option to allow more deformation is to execute the piles in predrilled holes (Figure 3-29). Predrilled holes are applied in the U.S., when the integral bridge is built in rigid soil. Then the pile is able to deform more, but the bearing capacity of the pile decreases. [18]



Figure 3-29 Steel H-piles in combination with predrilled holes and sleeves

The cyclic deformation is a limiting factor for the type of pile and indirectly for the allowable bridge deck length too. The low cycle behaviour due to seasonal temperature changes has influence on the pile yield and may consider as a risk. However it has not been established that fatigue leads to failure of the pile. [1]

3.6.4 *Early age cracking*

Early age cracking can be a significant problem in concrete. Early age cracking could occur when a new element is poured against an existing element. In this case, deformations of the concrete are restrained due to the friction with the existing element. Integral bridges have the preconditions which could lead to early age cracking, because the superstructure is poured on the substructure. Therefore in some states it is not permitted to pour the superstructure directly on the substructure. [2].

3.6.5 *Cracking of the wing walls*

It is common practice to connect the wing walls monolithically to the abutment stem. If the wing walls are also founded on piles, it is possible that the wing walls restrain the lateral deformation of the integral bridge. In this case the cracking of the wing walls could occur. [2]

3.6.6 *Cracking of the abutment stem or the bridge deck at the abutment*

In the past some states have noticed cracks in the abutment stem or in the bridge deck close to the abutment. These cracks occur, because the integral bridge is restricted to deform. Hence the length of the bridge is limited to a certain length, but also other factors are restricted, like the skew, the type of pile and type of backfill. [2]



4 Deformation of integral bridges and their consequences

4.1 Overview

Unique in integral bridges is that the deformation of the bridge deck has influence on the total structure. This deformation is caused by the temperature influences and the time-dependent material properties. In the next sections the temperature influences and the time-dependent material properties are further discussed.

4.2 Temperature influences (cyclic deformation)

Temperature changes cause cyclic deformation of the bridge deck. These temperature changes itself are caused by environmental factors (Figure 4-1).

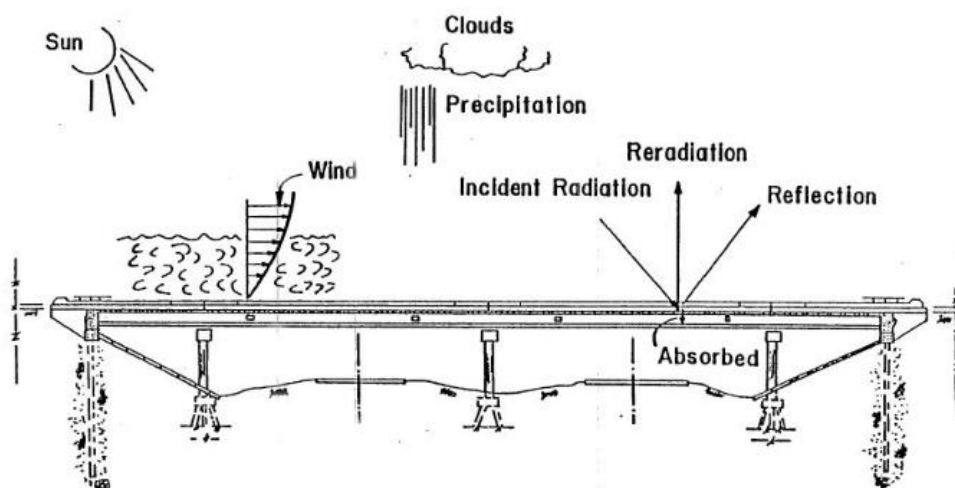


Figure 4-1 The environmental factors that are responsible for temperature influence on the bridge deck [1]

These environmental factors have influence on the bridge temperature. Another important factor is the material of the bridge deck. For example a steel deck is more affected by the temperature change than a concrete deck; because steel is more thermal-sensitive and the geometry of a steel bridge deck is generally smaller than a concrete bridge deck. Based on theoretical and practical research a parameter for the bridge temperature has been defined, 'the effective bridge temperature' (EBT) [24]. In Figure 4-2 the EBT is given. The EBT consists of two temperature changes, the seasonal and daily temperature change. These changes cause cyclic behaviour. In the next subsection this behaviour will be further discussed.

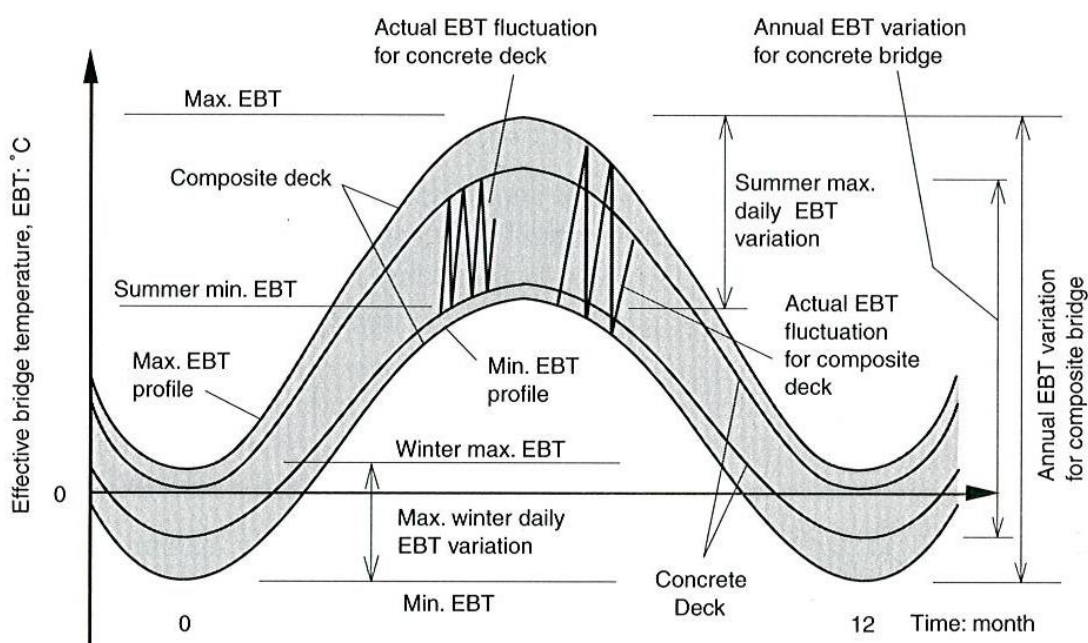


Figure 4-2 The effective bridge temperature showing the comparison between a concrete and a composite deck

4.2.1 Cyclic temperature behaviour

Fluctuations in the temperature lead to cyclic deformation of the bridge deck. As mentioned before there are two temperature changes, the daily and seasonal temperature change. The daily temperature change is responsible for a high cycle deformation with small fluctuations. The influence of these fluctuations is relatively small and therefore insignificant for the design of the integral bridge. [12] The seasonal temperature change causes a low cycle deformation with the greatest contraction of the bridge deck in the winter nights and the greatest expansion during the summer days.

Cyclic deformation could cause damage to the integral bridge and is responsible for plasticization of the soil. The cyclic deformation affects the connection between the super- and substructure in particular. The bridge deck wants to deform and substructure and the adjacent soil are responsible for a certain degree of restraining. Dicleli [25] investigated the effect of thermal loading on the performance of steel H-piles in integral bridges. He concluded that the cyclic deformation capacity of the H-pile decreases when the soil becomes stiffer. The cyclic deformation is, together with the span length, the limitation for the total length that is executable. For long bridges (more than 100 meter) low cyclic behaviour could lead to fatigue, but this is not been established yet. [26] However it is clear that large deformation leads to plasticization and a flow of granular material. [27]

4.2.2 Temperature components

According to the Eurocode [28] the temperature could be divided in four parts. The most important components are the mean bridge temperature and the gradient bridge temperature across the bridge deck depth, which are called 'uniform temperature component' (ΔT_u) and 'the vertical temperature difference component' (ΔT_{Mz}).

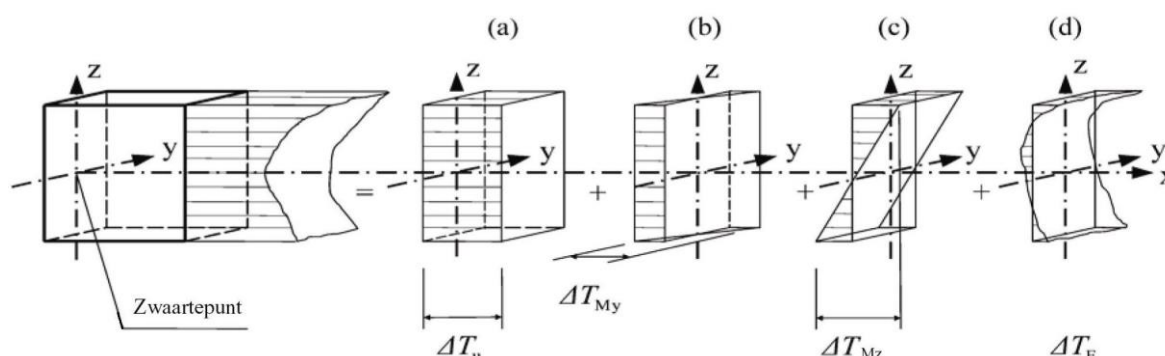


Figure 4-3 Graphic representation of the temperature components in the superstructure

In a bridge deck, two uniform temperature components could be distinguished the maximum temperature and minimum temperature. The maximum effective bridge temperature causes the maximum expansion of the bridge deck and the minimum effective bridge temperature creates the maximum contraction of the bridge deck. According to the Eurocode the following formulas are applicable:

$$\Delta T_{u;con} = T_0 - T_{e,min}$$

$$\Delta T_{u;exp} = T_{e,max} - T_0$$

The vertical temperature component causes a curvature in the bridge deck. Like the uniform temperature components the curvature could be positive or negative. In the Eurocode, the vertical temperature component could be considered by using an equivalent linear difference component with $\Delta T_{M;Cool}$ and $\Delta T_{M;Heat}$ which should be applied between the top and the bottom of the bridge deck.

The other components according to the Eurocode are 'the Eigen-temperature' of the bridge deck and the gradient bridge temperature across the bridge deck width. The Eigen-temperature is a non-linear temperature component what results in a system of self-equilibrated stresses which do not have a net-load effect on the bridge deck. The gradient bridge temperature across the bridge deck width is equal to zero, because the temperature difference between the left- and the right-hand side of the bridge deck is negligible.

If the 'uniform temperature component' (ΔT_u) and the 'vertical temperature component' (ΔT_M) are taking into account, the following equations could be used according to the Eurocode:

$$\Delta T_{M;cool}(\Delta T_{M;heat}) + \omega_u \Delta T_{u;con}(\Delta T_{u;exp})$$

$$\omega_M \Delta T_{M;cool}(\Delta T_{M;heat}) + \Delta T_{u;con}(\Delta T_{u;exp})$$

Where the recommend values of ω_u and ω_M are 0,35 and 0,75 respectively. The largest contraction and largest expansion are decisive.



4.3 Time dependent material properties

The time-dependent material properties that occur in concrete, are shrinkage and creep. Due to the prestressing elastic shortening of the beam occurs as well. These time-dependent material properties lead to a deformation of the superstructure and indirectly a deformation in the pile head.

In the U.S. not all the states are taking the time-dependent material properties into account. Only 33% of the responding states account for creep effects and only 44% take shrinkage into account. [20] However some states see shrinkage and creep as a problem. The reason why they do not take time-dependent material properties into account, is not completely clear. Some possible reasons will be discussed further in the subsections.

4.3.1 Shrinkage

Shrinkage is contraction of the concrete that occurs without the influence of any load which is caused by the drying of the material and the volume change due to the hydration of the cement (the chemical shrinkage of the material during the hydration process is not taken into account). In case of an integral bridge shrinkage is an important factor, because contraction of the superstructure also affects the substructure and the adjacent soil.

According to the Eurocode [29] two shrinkage processes are responsible for the contraction of a concrete member. These types of shrinkage are:

- *Autogenous shrinkage*: Autogenous shrinkage of cement paste and concrete is defined as the macroscopic volume change occurring with no moisture transferred to the exterior surrounding environment. It is the external shrinkage as result of the hydration of cement particles. [30]
- *Drying shrinkage*: Drying shrinkage is caused by drying of the concrete member. Drying shrinkage is a process that goes on over a longer time.

Another shrinkage process that occurs, is thermal shrinkage due to hardening. After the hardening process, the temperature of the concrete member decreases until the ambient temperature is reached. Enduring this process the concrete member will shrink.

In case of a bridge deck with prefab girders shrinkage could also lead to a rotational deformation of the bridge deck. The prefab girders are poured in the factor and therefore a part of the total shrinkage already occurred before the girders arrive at the building site. The top layer of the bridge deck is not poured yet, so the shrinkage has not been occurred. This leads to a differential shrinkage which results in deformation of the bridge deck. [31] (Figure 4-4)

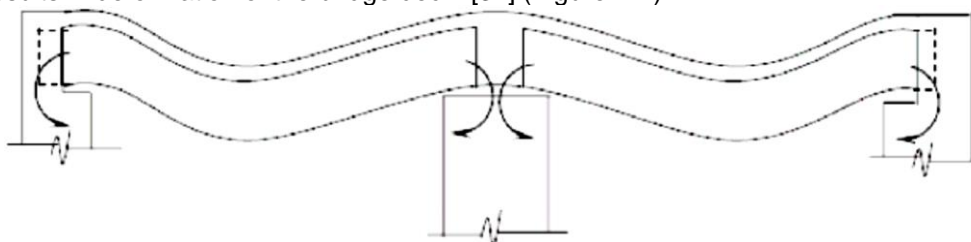


Figure 4-4 Deformation in a continuous composite joint less construction due to differential shrinkage, sustained dead load of the girder and deck slab



The deformation of the integral bridge due to shrinkage could be reduced. This depends on some factors. These factors are:

- The way of execution of the integral bridge
- The type of bridge deck
- The material composition of the concrete mixture

The way of execution of the integral bridge is important for the deformation due to shrinkage. Most of the shrinkage occurs in the first months after construction; therefore, sometimes the bridge deck is first poured and posttensioned. After time, the connection between the sub- and the superstructure is constructed. The same holds for prefabricated prestressed girders. When the girders arrived at the building site most of the shrinkage has already occurred; hence, when building time is limited and shrinkage is an influential factor, a precast bridge deck is preferred.

The concrete composition can be modified to decrease the amount of shrinkage. Important factors that have influence on the amount of shrinkage, are:

- The water content
- The type and content of aggregates
- The cement composition
- The water-cement ratio
- The additives

For example: More water leads to a larger drying shrinkage and a higher strength concrete has a lower degree of hydration, what leads to more autogenous shrinkage in time.

4.3.2 Creep

'Creep' can be defined as an increase of deformation in time under a sustained constant load. Creep of concrete is caused by the deformation of the gel structure and the chemical non-bonded water. Some factors that do have influence on the total deformation due to creep, are:

- The climate in which the structure is situated: Important factors are the relative humidity and the temperature.
- The development of the degree of hydration: In particular the degree of hydration under loading. This depends on the age of the concrete member, the type of cement and the curing conditions.
- The strength class of the concrete
- The dimensions of the cross-section
- The load duration

In practice, this means that all concrete members will creep, especially prestressed concrete members; prestressing can be seen as a constant load. Therefore, the deformation due to creep leads not only to a deformation, but also to a contraction of the concrete member. Like shrinkage, creep in an integral bridge leads not only to a deformation of the bridge deck, but indirectly also to a deformation of the substructure. However, unlike shrinkage the deformation of the bridge deck could be in the positive direction as well. A prestressed concrete girder for instance undergoes due to an eccentric prestressing a positive deformation. (Figure 4-5)

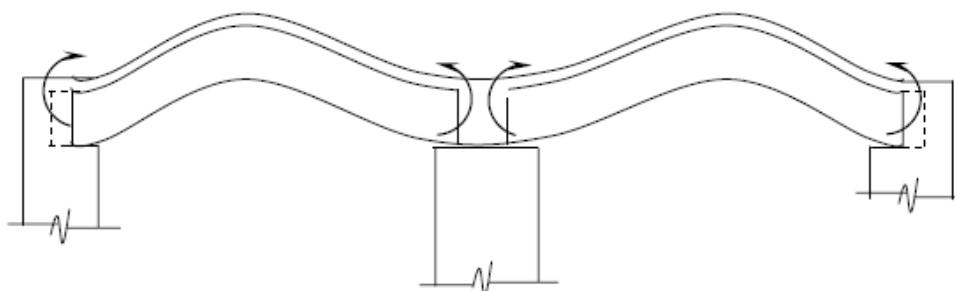


Figure 4-5 Creep deformation in a continuous composite jointless construction due to an eccentric prestressing force

4.3.3 *Combination of the time-dependent material properties*

Shrinkage, creep and elastic shortening lead all to a contraction and/or deformation of the superstructure. In integral bridges, this contraction has a major influence on the total structure; therefore, the time-dependent material properties have influence on the design of the total structure, especially the connection between the sub- and superstructure. [31]

4.4 **Interaction between the substructure and the soil**

In integral bridges, deformation of the superstructure leads to a deformation of the substructure into the soil. The interaction between the substructure and the soil is therefore critical. Thereby a distinction could be made between the pile-soil interaction and the abutment-soil interaction. According to Arsoy [15] 74-88% of the bridge deformation of an integral stub abutment in dense sand is absorbed by the abutment-soil interaction. Only 12-26% of the deformation is transmitted by shear force interaction between the abutment and foundation. Obviously other soil conditions and a different integral bridge design leads to another substructure-soil interaction. Therefore, it is important to understand the substructure-soil interaction to give a good representation of the forces and deformations in the structural system of the integral bridge.

In the next subsections, the pile-soil and the abutment-soil interaction will be further explained.

4.4.1 *Interaction between the abutment and the soil*

Soil is rheological material. This means that a deformation of the material could lead to the modification of the soil properties. Over time multiple methods are developed to give a good representation of the soil behaviour. Some of these methods will be discussed in this subsection. A distinction could be made between the analytical and the empirical theories.



4.4.1.1 Classical theories of the soil behaviour

A lateral earth pressure coefficient (K) is used to describe the lateral earth pressure a soil will exert. [27] This coefficient K depends on the vertical earth pressure ($K=\sigma_h/\sigma_v$). This means that the lateral earth pressure is related to the vertical pressure at any location in the soil profile. K depends also on the soil conditions and history of the soil modification. In principle, three categories are distinguished: the neutral or at rest (K_0), the active (K_a) and the passive (K_p) coefficient (Figure 4-6). There are different theories both analytical and empirical that determine the value of the K coefficients. These common theories are:

- Rankine theory (1857)
- Coulomb theory (1776)
- Caquot and Kerisel Theory (1948)
- Terzaghi and Peck's empirical charts (1948)
- Bell's relation

In the U.S., where most of the integral bridges are built, the Rankine theory is mostly used to calculate the lateral pressure coefficient. Rankine assumes that soil is cohesion less, the wall is frictionless, the soil-wall face vertical and the failure surface on which the soil moves is planar. This theory is applied together with Bell's relation which takes the cohesion into account. Most of the states apply the passive soil pressure for the design of integral bridges. Others use passive soil pressure in case of expansion and active soil pressure in case of contraction of the integral bridge. [11] If only the passive soil pressure is used, some do not take into account the passive soil pressure for single span bridges and short two-or three-span bridges. For modest bridges, only two-third of the maximum value of the total passive earth pressure is applied. [10]

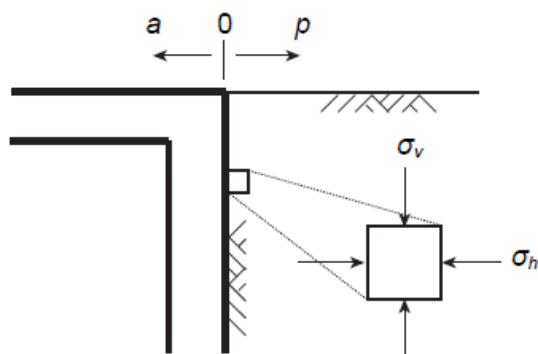


Figure 4-6 The lateral earth pressure adjacent to structure

The temperature change of passive soil pressure is based on the fact that the earth pressure depends on the displacement of the integral bridge. The total displacement of the integral bridge is defined by total length of the bridge, the time-dependent material properties and temperature influences. If the total displacement increases, the lateral soil pressure also increases. For a good estimation of the occurring lateral soil pressure a resultant is used. Important to understand is that a conservative estimation of the occurring lateral soil pressure does not lead to a conservative design, but to an incorrect design. The substructure is considered too rigid, if the lateral soil pressure is estimated too conservative. This leads to underestimated moments in the middle of the span and overestimated moments at supports of the bridge deck.



England et al. [24] developed a coefficient K^* from experiments into the cyclic stress of the backfill soil adjacent to a wall abutment on a spread footing. This coefficient K^* is a modification of the standard K coefficient for lateral earth pressure. The coefficient has been included in de BA42A 'The design of integral bridges' [16] (Figure 4-7). The K -coefficient varies over the height of the wall. The formula of K^* is given below. The value d and H stand respectively for the thermal displacement at the top of the abutment and the height of the wall abutment.

$$K^* = K_0 + \left(\frac{d}{0,03H} \right)^{0,6} K_p$$

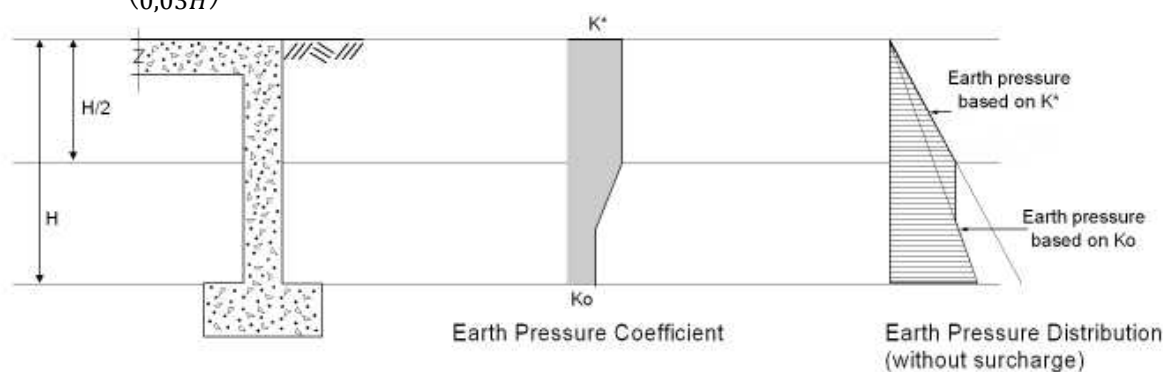


Figure 4-7 Modified lateral earth pressure coefficient according to England et al.

4.4.1.2 Spring stiffness model

Another method to model the soil behaviour is to define the soil as a series of uncoupled 'Winkler springs', where the deflection at one level of the abutment is not presumed to affect the value of the reaction force at another level of the abutment. [27] The 'Winkler springs' are dependent of the force-displacement relation. This force-displacement relation could be defined both linear and nonlinear (Figure 4-8).

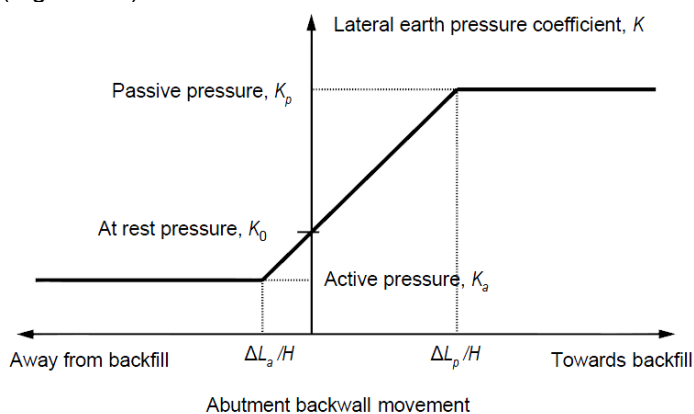


Figure 4-8 Elasto-plastic diagram of non-linear springs restraining abutment back wall



A lot of research on integral bridges focuses on the interaction between the soil and substructure. Generally, the behaviour of the soil is modelled as nonlinear. The idea is that the soil stiffness increases in time due to the cyclic deformation of the superstructure. This behaviour is particularly noticeable at very long integral bridges [25, 27]. An increasing stiffness of the soil occurs due to a combination of cyclic deformation and traffic that crosses the bridge. When the bridge contracts after expansion, a gap arises between the substructure and the adjacent soil. This gap closes because of erosion of adjacent soil due to crossing traffic. When the bridge expands again more soil needs to be displaced, what leads to increase of the soil stiffness.

Different design manuals submitted curves that describe the active and passive deformation to design the Winkler springs, (Figure 4-8). These curves are designed for loose, medium and dense cohesion less granular materials and are based on the finite element analysis conducted by Clough and Duncan (1971). An example of a curve is given in Figure 4-9 . This curve is attached to the manual for design of bridge foundations (NCHRP) [32].

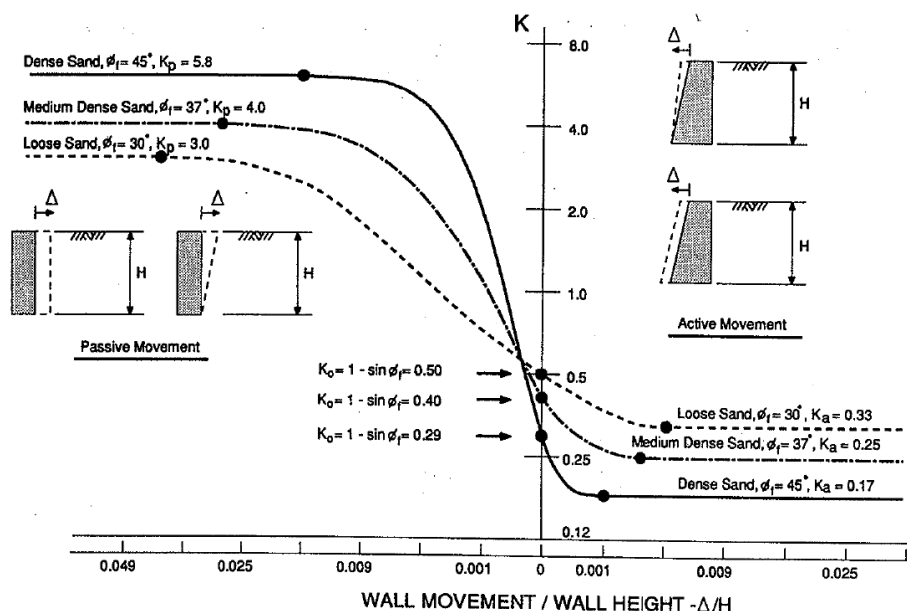


Figure 4-9 Relationship between wall displacement and earth pressure (NCHRP, sand) [32]

4.4.2 Interaction between the pile and the soil

For the analysis of the interaction between the pile and soil, generally the 'Winkler soil model' (Figure 4-11) is used. This model assumes that the pile soil interaction could be described as a couple of lateral and vertical springs. According to Greimann et al. [33] three curves could be distinguished:

- **The p-y curves:** Represents the relationship between lateral soil pressure against the pile and the corresponding lateral pile displacement.
- **The f-z curves:** Describes the relationship between the skin friction and the relative vertical displacement between the piles and the surrounding soils.
- **The q-z curves:** Describes the relationship between the bearing stress at the pile tip and the pile-tip settlement. The total pile tip force is calculated by the product of q.

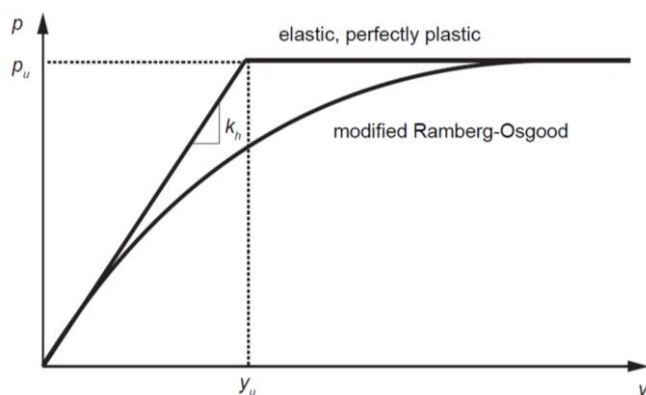


Figure 4-10 Typical elasto-plastic p-y curves

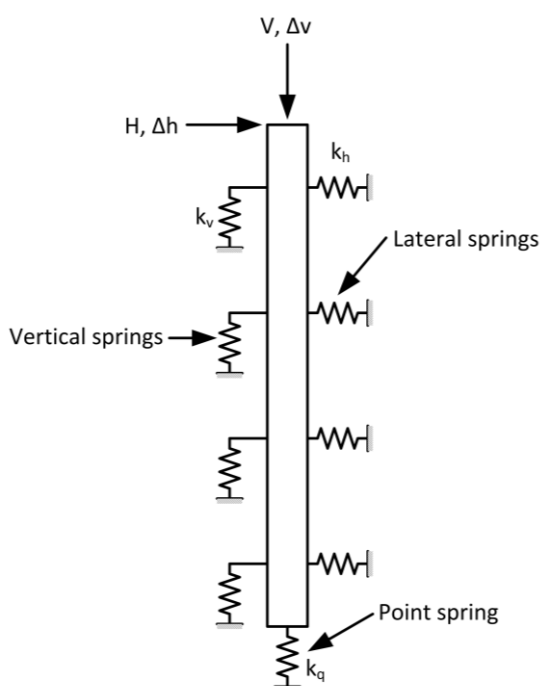


Figure 4-11 Winkler Soil model

Of these three load-displacement interaction curves, the p-y curves (Figure 4-10) are the most accurate for piles subjected to lateral deformation. These curves were first designed by Matlock (1970). Later, other p-y curves were developed to describe the lateral nonlinear force-displacement behaviour of the soil. Some examples of these methods are Reese, Bushan et al. and the API method. The API method is used nowadays to determine the lateral nonlinear force-displacement behaviour and gives a good indication of the actual behaviour. [27] Software applications, like D-Pile, are based on this method.



According to Greimann, embedded long piles with a small diameter could be computed with the equivalent cantilever method. This method assumes that the lowest part will not displace; therefore, it is considered as rigid. If the lowest part could not displace, the only failure modes are due to buckling of the pile (Figure 4-12). Otherwise, the pile will fail due to the vertical load (slip mechanism, Figure 4.4–8) or the deformation of the pile (failure of the soil, Figure 4-14).

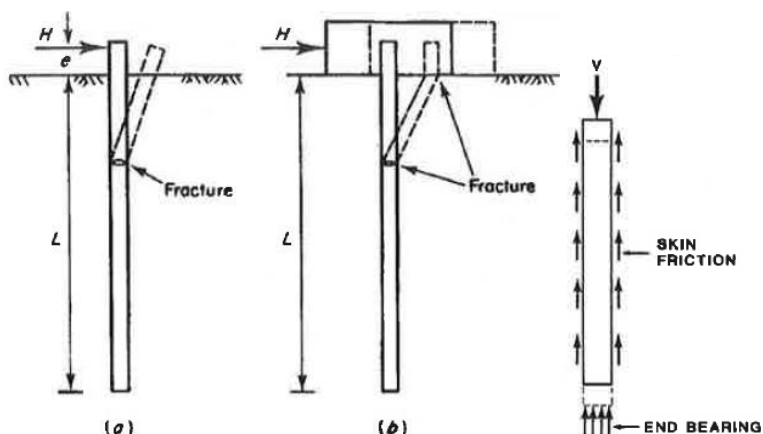


Figure 4-12 Failure mechanisms for long piles

Figure 4-13 The pile displaces when tip load and wall friction is not sufficient (slip mechanism)

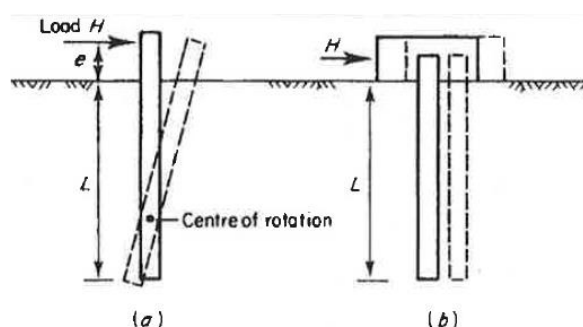


Figure 4-14 Failure mechanisms for short piles (failure of the soil)

According to Greimann [33] lateral group effects for a pile foundation could be ignored, if the spacing of the piles perpendicular to the direction of loading is greater than 2.5 to 3 times the pile diameter or width. Normally the group effect of piles is included in the design, because a single pile behaves differently than a group of piles. The total lateral capacity of a group of piles for instance is less than a sum of single piles. The same applies for the vertical capacity. [12]

A single pile has influence on a larger width than the pile diameter. To take this effective width into account, the later earth pressure coefficient K is multiplied by a factor ('schelfactor'). This factor depends on the friction angle of the soil. For cohesion less soil like sand the effective width is larger than for clay or peat.



4.5 The proposed model of the integral bridge and the soil

Based on the last section (§4.4) a structural model could be designed for the soil-substructure interaction. The Winkler springs in **Error! Reference source not found.** are an adjustment to the structural model of section 3.2. This is the structural model where the deformation due to temperature influence and time-dependent material properties is taken into account. There are also load combinations possible, where the pile is subjected to a settlement. Then springs at the tip and the shaft are attached to the structural model (Figure 4-11).

The Winkler springs in the model have linear force-displacement behaviour. The assumption is that it concerns a medium size bridge; therefore, the deformation of the bridge deck does not lead to a plasticization of the soil (see subsection 4.2.1). Further, there will be varied with spring stiffness to get a clear view of the structural behaviour of the integral bridge. In the design phase, this will be discussed more in detail.

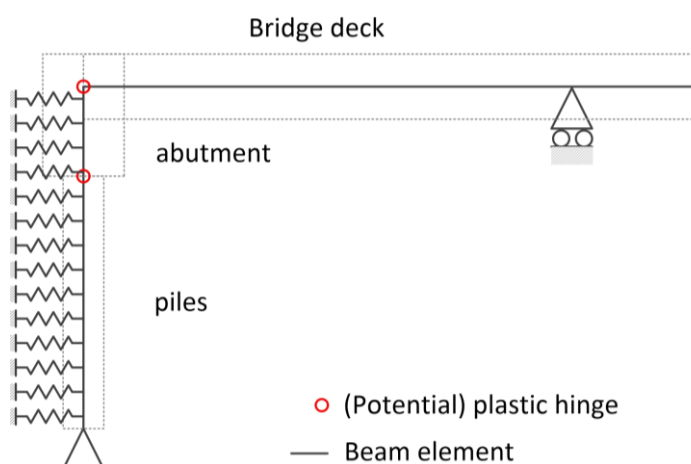


Figure 4-15 Proposed model soil-substructure interaction

In Figure 4-15, the potential hinges are indicated. This concerns the connections between the piles and the abutment and between the abutment and the superstructure. In accordance with fail mechanisms (4.4), the largest moments and forces will probably occur at these positions. In the design phase it will be further examined whether this is the case.



5 Fibre Reinforced Cementitious composites (FRC composites)

5.1 Introduction

Fibre reinforced cementitious composites could be distinguished from conventional concrete due to the application of fibres. The application of fibres leads to some interesting properties, for example strength, ductility, toughness, durability, stiffness and thermal resistance. At the moment FRC composites are still more expensive, but with the wide opportunities, it is possible to save expenses on the total structure and therefore the material is also economically interesting. [34]

The major goal of this thesis is to investigate if the application of frc/ ecc in the connection of integral bridge has advantages. This chapter will discuss the possible mechanical properties of FRC composites. Within FRC composites a variety of cementitious composites are possible. The next section will go deeper into the variety of FRC composites (§5.2). Further the influence of fibres (§5.3) and the structural applications (§5.5) will be discussed. In section 5.4, the possibilities and properties of the material engineered cementitious composites (ECC) will be explained.

5.2 Classification of fibre reinforced cementitious composites

Within FRC composites a variety of cementitious composites are applicable. Besides, there is also an overlap in the properties of the different fibre reinforced cementitious composites; therefore, the FRC composites could be classified on different ways. A common approach to classify the various FRC composites is given in Figure 5-1.

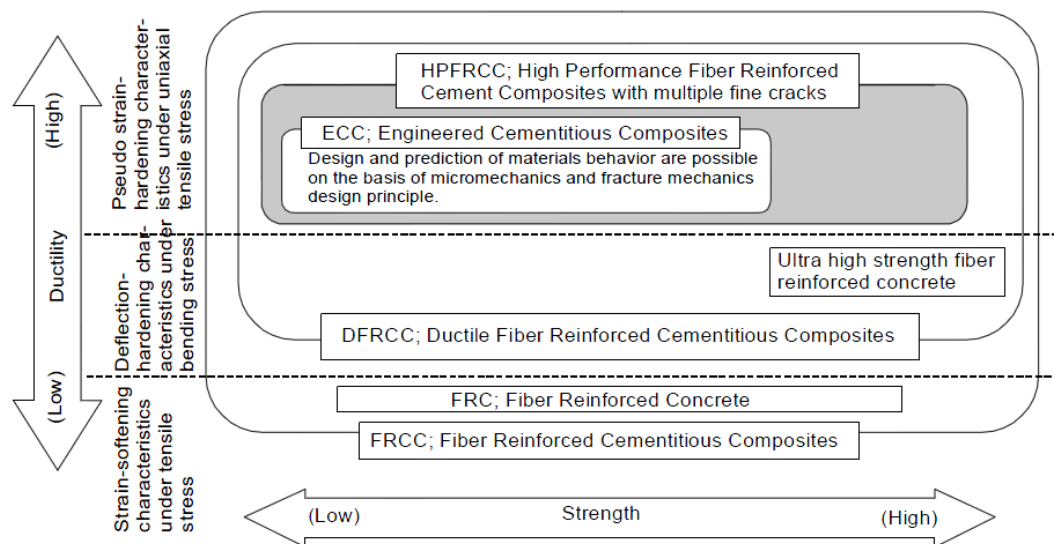


Figure 5-1 Classification of fibre reinforced cementitious composites [35]

This classification of FRC composites depends on the strength and the ductility of the FRC composites. On the y-axis, the ductility is given. The ductility is divided in 'strain-softening under tensile stresses', 'deflection-hardening under bending stresses' and 'strain-hardening under tensile stresses'. This ductility division is based on the material behaviour of various FRC composites under bending and uniaxial tensile stresses. Naaman and Reinhardt [36] clarified this by an illustration of



the tensile-strain and load-deflection behaviour (Figure 5-2). A distinction in this figure is made between ‘hardening’ and ‘softening’. An FRC composite has ‘hardening’ when the structural strength is equal to or greater than the cracking strength. This means that after the first ‘crack’ the tensile strength of the FRC composite is still increasing. This hardening can also occur under bending, and then the FRC composite is called ‘deflection-hardening’. When this hardening occurs under tension then the FRC composite is called ‘strain-hardening’. In general only a relative low content of fibres is needed to acquire deflection-hardening behaviour. For obtaining strain-hardening behaviour, a higher content of fibres is required. Therefore, also according to Naaman and Reinhardt, a FRC composite with strain-hardening behaviour has also deflection-behaviour, but not vice-versa. The FRC composites with deflection-hardening are called ‘Ductile Fibre Reinforced Cementitious Composites’ (DFRCC). A subgroup of DFRCC is the ‘High Performance Fibre Reinforced Cement Composites with multiple fine cracks’ (HPFRCC). HPFRCC have both deflection-hardening and strain-hardening behaviour, in accordance with Naaman and Reinhardt. Examples of DFRCC are given in Figure 5-3. It is clearly visible that the flexural tensile stresses of DFRCC are still increasing during the deflection hardening stage. Another example of a composite with strain-hardening behaviour is Engineered Cementitious Composite (ECC). ECC is a cementitious composite with similar mechanical properties as conventional concrete, but with different stress-strain behaviour. More about ECC will be discussed in section 5.4.

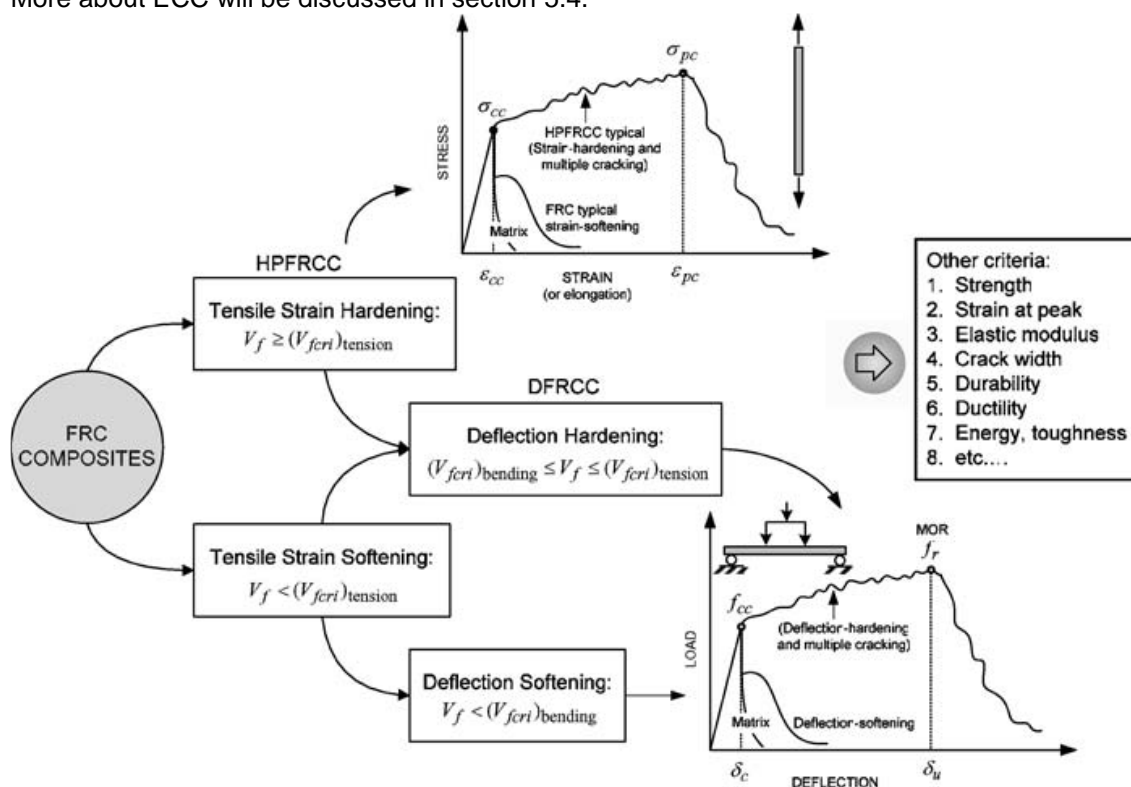


Figure 5-2 Classification of FRC composites based on their tensile stress-strain response

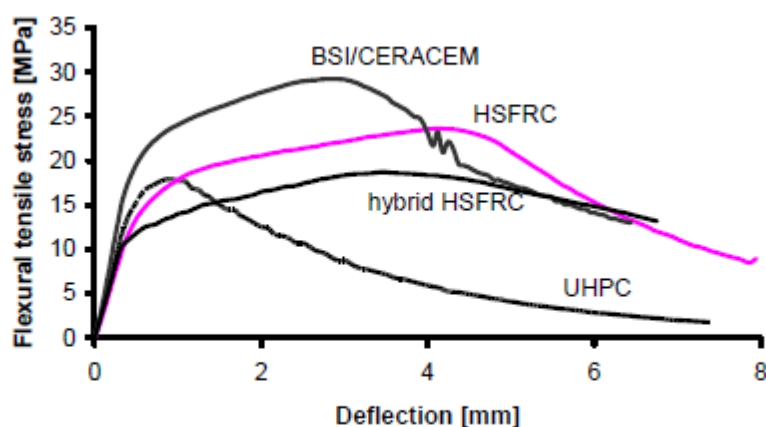


Figure 5-3 Average static stress-deflection curves of beams made of DFRCC mixtures [37]

5.3 The influence of fibres

Fibres have a major influence on the stress-strain/ load-deflection behaviour as mentioned in section 5.3; in fact, fibres are responsible for the hardening of the material and a still increasing strength after the first crack has occurred. According to Markovic [38] the hardening stage corresponds with the cracking of the concrete. Thereby Markovic distinguish two types of cracks, the micro- and the macro cracks. The micro cracks originate in the strain hardening stage and the macro cracks develop due to connecting micro cracks. This process is given in Figure 5-4.

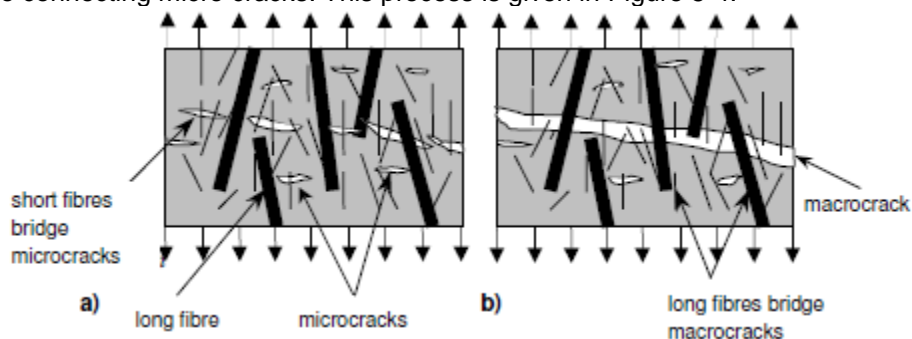


Figure 5-4 The two types of cracks; a) micro cracks and b) macro cracks, according to Markovic

In Figure 5-4a, it is clearly visible that in particular the short thin fibres are bridging the micro cracks and the long thick fibres are decisive when the macro crack originates (see Figure 5-4b). An important remark to Figure 5-4 is that at certain point the short thin fibres are not able to bridge the crack anymore; therefore, long fibres are decisive when it comes to macro cracks and the phase when the crack pattern is fully developed ('the strain-softening stage'). This coincides with Figure 5-5, where the 'strain-hardening' and 'strain-softening' phase are described.

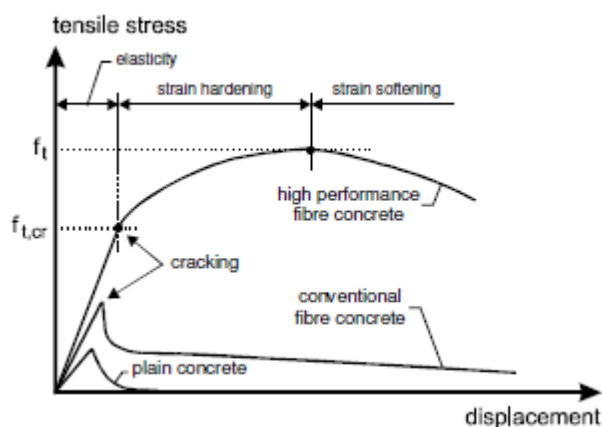


Figure 5-5 Tensile stress-displacement relation of a ductile fibre reinforced cementitious composite

The range of a stage, as described in Figure 5-5, depends strongly on:

- The fibre content
- The geometry of the fibre
- The angle of the fibre with respect to the loading direction
- The roughness of the fibre surface
- The mechanical properties of the fibre (strength, stiffness, etc.)

The factors that are given above are connected to each other and are in coherence with a good fibre and concrete mixture distribution responsible for the stress-displacement behaviour of the DFRCC. This stress-displacement behaviour can be adjusted by adapting the factors. Some examples to acquire specific stress-displacement behaviour are:

- *To obtain a high tensile strength?*
 - A large quantity of fibres that bridges the cracks: The most effective method to acquire a large quantity of fibres is to apply a high content of short thin fibres.
 - A good resistance toward pull out behaviour of the fibre: This means a rough fibre surface and a fibre which has a small angle (between 0 and 20 degrees) with the tensile forces.
- *To obtain a strain-hardening behaviour?*
 - A large quantity of fibres that bridges the cracks: The most effective method to acquire a large quantity of fibres is to apply a high content of short thin fibres.
 - A relative low resistance toward pull out behaviour of the fibre: This means a smooth fibre surface and a fibre which is aligned with the tensile forces.
- *To obtain a strain-softening behaviour?*
 - A good resistance toward pull out behaviour of the fibre: This means a rough fibre surface and a fibre which has a small angle (between 0 and 20 degrees) with the tensile forces.
 - Long fibres: The long fibres are able to bridge the macro cracks which lead to a good behaviour in the strain-softening stage.



Higher fibre content does not explicitly lead to better stress-displacement behaviour. When too many fibres are applied, the compaction of the mixture decreases and therefore the stress-displacement performance decreases. The fibre content that is applicable for self-compacting concrete depends on the length and diameter of the fibre. For more than 1% (79 kg/m³ of steel) fibres, with a length of 60 mm, of the total volume of the mixture leads already to a low workability. In case of short fibres (max. 13 mm) a content of 4 to 5% (314 to 393 kg/m³ of steel) fibres is still applicable to obtain a good workability. [38]

As mentioned before, short fibres are mostly responsible to bridge the micro cracks and long fibres are decisive when comes to macro cracks. Markovic introduced a hybrid High Strength Fibre Reinforced Concrete (Hybrid HSFRC) with a composition of short straight fibres (6-13 mm) and long hooked fibres (30-60 mm). The research showed that a combination of short and long hooked fibres have a better performance than only short or long fibres. Long fibres for instance have a 20-30% better tensile strength behaviour when short fibres are also present in the concrete.

The presence of fibres in the concrete leads evidently to better stress-displacement behaviour. This is not the case when it comes to fatigue behaviour. Lappa studied the fatigue behaviour of the DFRCC under bending given in Figure 5-3. The result is that the DFRCC have the same fatigue performance as conventional unreinforced concrete. Only one DFRCC had higher fatigue strength than conventional unreinforced concrete. This was also the DFRCC with the most homogenous mixture and the most stable results in static stress-displacement performance. [37]

5.4 Engineered cementitious composites (ECC)

ECC has a unique strain-hardening behaviour as noted before. This strain-hardening behaviour depends as well as the other mechanical properties on the composition of ECC. In the next subsections the composition of ECC and its mechanical properties are discussed.

5.4.1 Composition of ECC

The ECC mixture has, other than conventional concrete, a large amount of cement and only small aggregates. A standard ECC mixture is composed of:

- Sand: Fine sand with an average grain size of 110 µm and a maximum grain size of 250 µm.
- Fly ash: This is mainly fly ash with a low grain size, like silica fume.
- Water
- Cement
- Chemical additives
- Fibres

The water/cement (w/c) ratio of ECC is in comparison with conventional plain concrete very low. A w/c ratio of about 0,3 is standard for an ECC mixture. Still ECC has a good workability due to the application of plasticizers. Unlike conventional plain concrete, the amount of aggregates is very low for a concrete mixture (~30% for ECC / ~75% for conventional plain concrete).



Various types of fibres can be used in ECC, like steel, polyvinyl alcohol (PVA) or polyethylene (PE). Most of the research concentrates on PVA and PE fibres due to their good behaviour in the mixture composition. [39] The surface of the fibres in ECC are coated with a hydrophobic material to decrease the frictional bond of the fibre. Hereby the strain capacity of the ECC increases enormously (see Figure 5-6). This increase in strain capacity all occurs in the strain hardening stage. In correspondence with section 5.3 the strain hardening behaviour is entirely due to a large quantity of short thin fibres with a relatively low resistance toward pull-out behaviour.

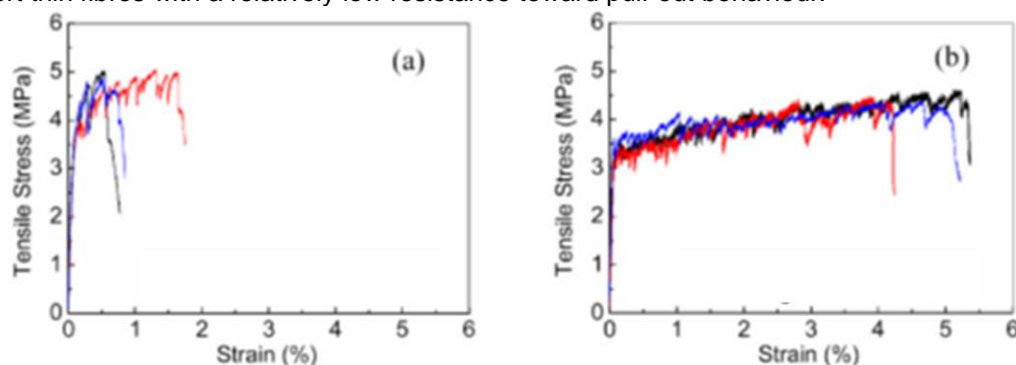


Figure 5-6 (a) ECC without coated fibres and (b) ECC with coated fibres [40]

As mentioned before in section 5.3, the direction of the fibres in the mixture is also important to acquire a good strain-hardening behaviour. A good strain-hardening behaviour is obtained when the fibres are aligned with the direction of the main tensile stresses. [38] A good alignment of the fibre depends on the length of the fibre, the size of the aggregate and the mixing- and pouring-procedure. It appears that the short fibres are more aligned with the direction of the main tensile stresses. This is because short fibres are less distort due to the aggregates, when the concrete is poured in concrete layers in the lateral direction.

The durability of ECC is also examined. The research shows that ECC has a more durable performance than conventional concrete. In the strain hardening stage, ECC has only micro cracks. These micro cracks are rather small, so self-healing of the mixture is still possible. In addition, micro cracks have almost no intrusion of water and de-icing chemicals what leads to an improvement of the durability too. [41]

The drying shrinkage of ECC is much larger than conventional structural concrete due to the absence of coarse aggregates. [42] The autogenous shrinkage of ECC is larger, because of the high cement content and the low W/C ratio. In the material itself autogenous shrinkage does lead to cracking, but due to the fibres, the cracks are considerably small. The effect of autogenous shrinkage is larger, when ecc is poured against another concrete element. [43]

5.4.2 Mechanical properties

Most of the mechanical properties of ECC are comparable with conventional concrete. For example the compression strength of ECC is approximately between 30 and 70 MPa. Also the tensile strength of ECC is low (maximum 5 MPa). As mentioned before the strain-hardening behaviour of ECC is unique. This strain-hardening behaviour leads to a strain capacity of 3-8%. Still the crack width is



relatively small (maximum of 80 μm). The stress-strain behaviour and the crack width are given in Figure 5-7. [40]

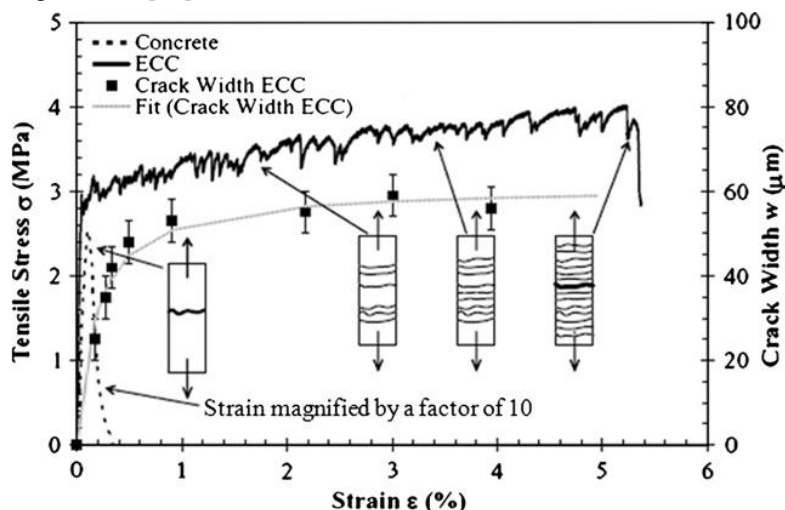


Figure 5-7 Stress-strain behaviour and the crack width of ECC

The high strain capacity leads also to good stress-deflection behaviour. In Figure 5-8, an ECC plate in a four point bending test is given. As showed, the ECC plate is deflected, but the micro cracks are hardly visible. Therefore ECC is more suitable than conventional concrete for structural applications where cracking or ductile behaviour are decisive. An example of a suitable structural application is a link slab between two prefab bridge spans (Figure 2-14), where the conventional concrete is replaced by ECC. [44]



Figure 5-8 ECC plate in four-point bending test

Tests were done to investigate the shear behaviour of ECC. It turns out that a normal reinforced ECC (R/ECC) beam has a better shear performance than a conventional reinforced concrete beam with stirrups. Under shear ECC develops multiple cracking and shows a ductile behaviour. [45] The conventional concrete beam on the other hand experiences spalling of the concrete cover. Under cyclic loading, the R/ECC beam also shows a better performance than the conventional concrete beam with stirrups; therefore, the fatigue behaviour of an R/ECC can be seen as promising. [40, 46]



5.5 Tailor made mixtures for structural applications in integral bridges

In this research, the mechanical properties will be used to define a mixture for structural applications in integral bridges. The concrete mixture composition, including the fibres, have influence on the mechanical properties. The most important mechanical properties of FRC composites are:

- A high strength (in tension, compression and bending)
- A strain-hardening response (Figure 5-9a)
- A strain-softening response (Figure 5-9b)

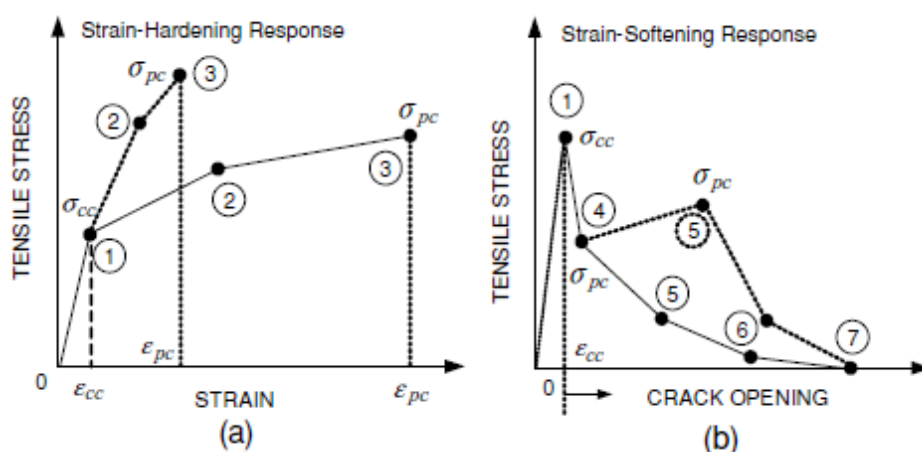


Figure 5-9 (a) a typical stress strain response for a strain-hardening FRC composite and (b) a typical stress strain response for strain-softening FRC composite

The strength capacity and the strain behaviour are the two most important aspects which could be adjusted to create the perfect mechanical properties. Thereby two extremes can be defined: These extremes are:

- A high strain capacity versus a high strength capacity (Figure 5-1)
- Strain-hardening behaviour versus strain-softening behaviour (Figure 5-9)

A high strain capacity lead to a lower strength capacity and a low strain capacity lead to a higher strength capacity. This is applicable for all FRC composites. An example is ECC, which has a normal strength capacity, but has extraordinary strain behaviour.

The type of strain behaviour is important for the cracking behaviour. The strain-hardening response leads to more cracks with a small width and the strain-softening response has one crack which become larger when the strain increases. So, if the crack width is decisive for the structural application, the strain-hardening response is the preferred behaviour.

It depends on the structural application of the integral bridge which mechanical properties are needed. In the next chapter (chapter 6), different structural applications are given. Also one of these structural applications will be further designed and researched in chapter 6 and 7. An important notification is that integral bridges demands deflection capacity which is possible for a strain-hardening and a strain softening response. Besides it is not clear yet, whether a high strength is favourable or a high strain capacity.



6 Structural applications of FRC composites in integral bridges

6.1 Introduction

In the first section (§1.1), the definition of integral bridges is presented. This definition is given below:

An integral bridge is designed without expansion joints between adjacent spans and/or without expansion joints and bearings between spans and abutments [16, p. 1].

The sub- and superstructure and adjacent bridge decks are monolithically connected due to the absence of expansion joints and bearings in the integral bridge; therefore, the structural system of the integral bridge differs from a conventional bridge. Loads, time dependent material properties and temperature influences have effect on the total structural system of the integral bridge and lead to deformations and eventually to problems. Figure 6-1 shows this relation between the loads, the deformations and the resulting problems and limitations and how they are connected to each other. The relation, between the loads, the deformation and the problems and limitations, is based on chapters 3 and 4.

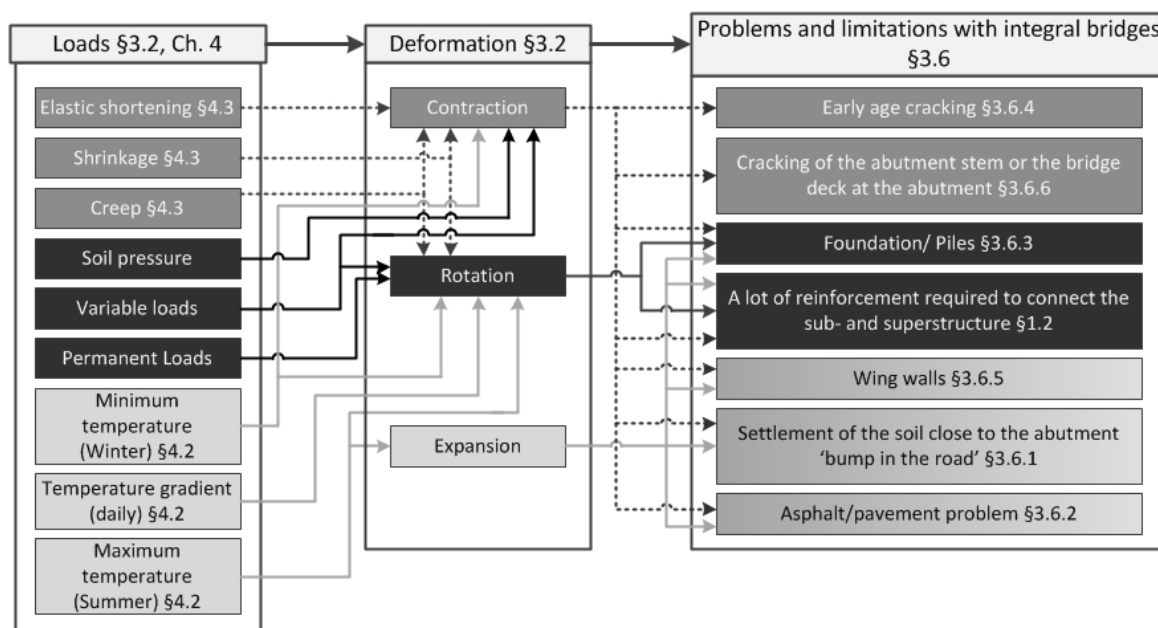


Figure 6-1 The relation between the loads, the deformations and the problems and limitations

In principle, a reduction of the first step 'the loads' is not possible, but their influence can be reduced. This leads to a reduction of the deformations and eventually to a decrease of the problems; therefore, the focus is on the deformations of Figure 6-1. The quest for a reduction of the deformations is sought in the application of FRC composites in the integral bridge. Thereby, it is important to mention that it is too complex to reduce all the deformations in once; hence, a choice is made to reduce not all deformations in once, but to focus on the lateral deformation (contraction and expansion) or the



rotation. Therefore several structural applications of FRC composites will be discussed in section 6.2. The main aspects of a specific structural application of FRC composites will be examined in this section too.

Besides the relation of Figure 6-1, there are other parameters that influence the design of the structural application of FRC composites. These parameters are given in Figure 6-2. On the left of Figure 6-2, the soil resistance is given. As mentioned in section 4.4, the stiffness of the soil has a major effect on the deformations and moments in the structural system of an integral bridge. As also mentioned, the stiffness of the soil depends on the soil conditions of the building site. This soil conditions will be discussed in subsection 6.3.2 and are decisive for the design of the structural application of FRC composites. On the right of Figure 6-2, the structural design of the integral bridge is presented. The structural design of the integral bridge has consequences for the design of the structural application of FRC composites as well. The 'design choice' for certain structural components in the right encirclement of Figure 6-2 is described in subsection 6.3.1.

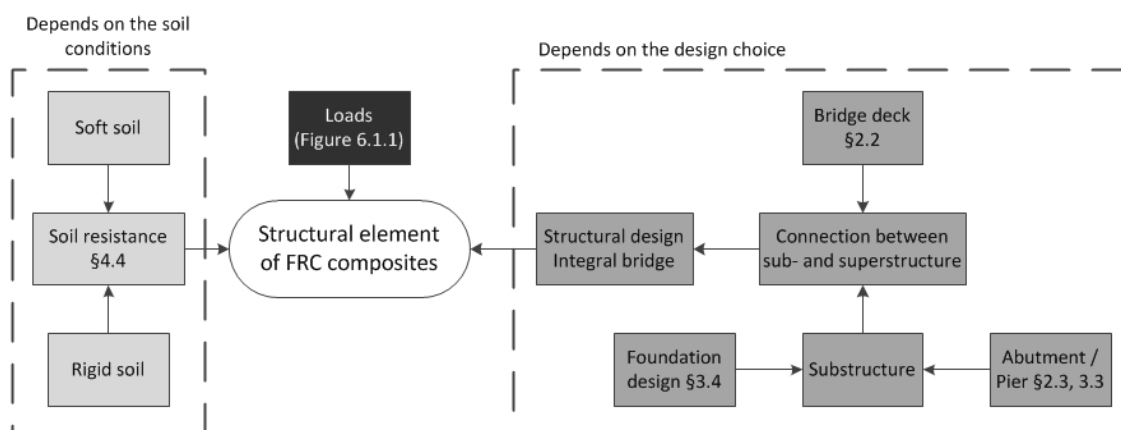


Figure 6-2 The parameters that influence the structural application of FRC composites

In the last two sections of chapter 6, the final choice for a specific structural application of FRC composites (§6.4) is made and the 'Research approach' (§6.5) will be discussed.

6.2 Potential structural applications of FRC composites

The deformation can be split up in a rotation and a lateral deformation. To reduce exclusively the rotation or the lateral deformation demands a different structural application. For example: A structural application that reduces the lateral deformation only requires an FRC composite which is able to absorb the cyclic deformation. This is possible when the FRC composite has a sufficient strain capacity in the lateral direction. The position of the structural application is also important to successfully absorb the lateral deformation. In this section, the different positions of the structural application will be examined and the FRC composite that is needed for that structural application. The complexities for the different positions will be examined as well.



In total four potential structural applications are presented. The first two structural applications are given in Figure 6-3. Figure 6-3A shows a structural application in the connection between sub- and superstructure. Figure 6-3A is in comparison with the other structural applications a complex application, because it is uncertain how this connection will behave under loading. This means that Figure 6-3A could be flexible under rotation, but also flexible under lateral deformation. In what extent, it is more flexible under rotation or under lateral deformation is totally uncertain. Besides, it is difficult to examine which FRC composite is needed and if the results of the calculation are a good representation of the structural behaviour of the FRC composite. Another disadvantage of this structural application is the difficult executability.

Figure 6-3b shows a structural application of FRC composite in the bridge deck. This position has been chosen to absorb only the effects of the lateral deformation in the bridge deck. The rotations due to the loads of Figure 6-1 are absorbed by a connection of conventional concrete between the sub- and superstructure. It is important that the structural application is completely separated from the substructure-superstructure connection to absorb the lateral deformation successfully. The requirements for the FRC composite are a good strain capacity in the lateral direction and a structural behaviour as conventional concrete in the vertical direction. This requires a FRC composite with mechanical properties that are comparable with ECC (§5.4). A complexity of Figure 6-3b is that the prestressing is present in the structural application. This prestressing will probably malfunction the strain behaviour of the structural application.

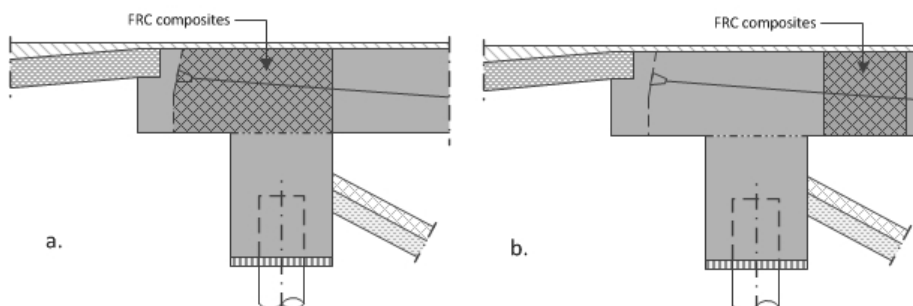


Figure 6-3 Structural application of FRC composites: A.in the sub- and superstructure connection and B. in the bridge deck close to the abutment.

The last two structural applications are given in Figure 6-4. Figure 6-4c shows a structural application in the abutment-pile connection. There has been chosen for this position, because a lot of reinforcement is needed in this area. This one of the problems described in Figure 6-1 and section 1.2. A connection with more deflection capacity or a stronger material could lead to a reduction of the amount of reinforcement; therefore, a FRC composite is acquired with sufficient deflection capacity and which is able to transfer the shear forces and the moments from the superstructure to the substructure. This could be a FRC composite with 'strain softening' or 'strain hardening' behaviour or with a high tensile strength. The disadvantage of an FRC composite with 'strain hardening' behaviour is that the strain is not divided over a number of cracks, but concentrated in only one discrete crack, like unreinforced conventional concrete; however, the crack width of the FRC composite is decisive for this structural application.

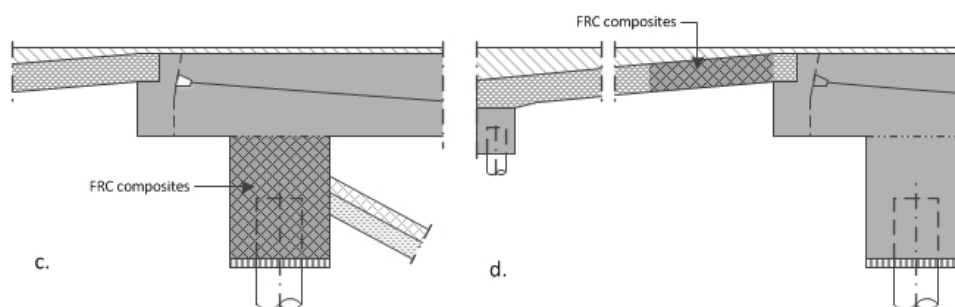


Figure 6-4 Structural application of FRC composites: C.at the pile-abutment connection and D. in the approach slab.

Figure 6-4D shows a structural application in the approach slab. This structural application is like Figure 6-3B to reduce the problems due to the lateral deformation; therefore, the structural application of Figure 6-4D needs sufficient strain capacity. To apply the structural application in the approach slab, the effects of the problems related to the soil could be minimized. For example less maintenance of the embankment soil is needed. An important notification is that the problems are not solved, but the effects are less. This means that under the approach slab, the soil is still able to settle. This is consistent with subsection 3.6.1, which describes the growth of a gap under the approach slab due to the lateral deformation and the related problems; therefore the structural requirements for the approach slab of integral bridges are higher than for conventional bridges. These requirements are also applicable for the structural application of Figure 6-4D and the FRC composite of this structural application. For example, the FRC composite requires to have enough strength and bending capacity in the vertical direction. The approach slab in Figure 6-4D has a foundation under the approach slab too. This foundation is situated in Figure 6-4D, because it is expected that the structural application will not work when the approach slab can deforms freely in the lateral direction.

In summary, all structural applications of Figure 6-3 and Figure 6-4 are focusing on different problems. The structural applications, their focus, their disadvantages and their requirements are given in Figure 6-5.



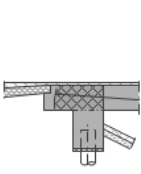
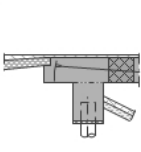
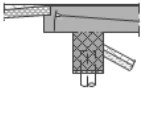
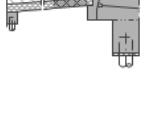
	The Focus of the structural application on the problems
	The disadvantages of the structural application
	The requirements of the FRC composite
 <p>Figure 6.2-1a</p>	<ul style="list-style-type: none"> ✓ All problems of Figure 6.1-1 - Design is rather complex - Complex executability - The structural behaviour of this structural application is uncertain • Strain capacity in lateral direction • A sufficient deflection capacity • Sufficient crack width control • Adhesion between the FRC composite and the conventional concrete • Enough strength capacity
 <p>Figure 6.2-1b</p>	<ul style="list-style-type: none"> ✓ Problems related to the lateral deformation of Figure 6.1-1 - Complex executability - The structural behaviour of this structural application is uncertain • Strain capacity in the lateral direction • Sufficient crack width control • Adhesion between the FRC composite and the conventional concrete • Comparable structural behaviour in the vertical direction as conventional concrete
 <p>Figure 6.2-2c</p>	<ul style="list-style-type: none"> ✓ Too much reinforcement required in the connection between sub- and superstructure §1.2 ✓ Reduction of the pile head loads - A combination of shear force and moment in the structural application due to the interaction between the sub- and superstructure • A sufficient deflection capacity • Sufficient crack width control • Adhesion between the FRC composite and the conventional concrete • Comparable structural behaviour in the vertical direction as conventional concrete
 <p>Figure 6.2-2d</p>	<ul style="list-style-type: none"> ✓ Reduce the effects of the settlement of the soil close to the abutment ✓ Minimize the asphalt/pavement problem - Extra foundation costs - Problems are not solved, but the effects are less • Strain capacity in lateral direction • Sufficient crack width control • Adhesion between the FRC composite and the conventional concrete • Comparable structural behaviour in the vertical direction as conventional concrete

Figure 6-5 The focus of the structural application on the problems, the disadvantages of the structural application and the requirements of the FRC composite

Besides these structural applications, there are options for the design of the structural application which could reduce the problems as well. Only these structural applications are not a structural element of the integral bridge. Some examples are:

- A structural element of a FRC composite in the concrete pavement on top of the approach slab. The goal with this structural element is to reduce the pavement problem, mentioned in subsection 3.6.2.
- A structural element next to the abutment which is able to deform in the lateral direction, but which does not settle. This requires a material with a low contraction coefficient in the lateral direction and no deformation in the vertical direction.



6.3 Other parameters that are influencing the structural element of a FRC composite

There are other parameters that have influence on the structural element of FRC composites (Figure 6-2) besides the loads, The parameters, which depend on the design choice, are discussed in subsection 6.3.1 and the parameters, related to the soil conditions, are discussed in subsection 6.3.2.

6.3.1 *Parameters that depend on the design choice.*

The parameters that depend on the design choice are the structural elements of the integral bridge. These elements are:

- The bridge deck (superstructure)
- The abutments (substructure)
- The piers (substructure)
- The foundation (substructure)

In the next subsections, the choice for each structural element is systematically explained. The design choices are based on project ‘the Schokkeringweg’.

6.3.1.1 The bridge deck (superstructure)

The choice is to apply a prestressed cast-in-place bridge deck of conventional concrete. The prestressing consists of curved cables and the conventional concrete is in strength class C60/67. Further, the bridge deck is a straight span with a massive slab (**Error! Reference source not found.b**). These choices are based on section 2.2. According to this section a cast-in-place concrete bridge is in advantage when the building site has sufficient space. The building site is situated in an area with a low population density. Also a cast-in-place bridge is in advantage, when it comes to design freedom.

6.3.1.2 The abutments (substructure)

As an abutment, an integral stub abutment has been chosen for the design of the integral bridge. A conventional stub abutment is common for road bridges in the Netherlands. Besides, all structural applications discussed in section 6.2 are based on the integral stub abutment. The integral stub abutment will consist of a structural strength of C28/35.

6.3.1.3 The piers (substructure)

A middle pier shall be designed as an integrated pier and the remaining piers shall be designed as self-supported piers. This is standard for piers, as mentioned in subsection 3.3.2. A self-supported pier is divided by bearings from the superstructure and therefore not a part of the structural system of an integral bridge. The middle pier is an integrated and hence a part of the integral bridge. The focus of this thesis is on the connection at the abutment; therefore, the piers will not further discussed in this thesis.



6.3.1.4 The foundation (substructure)

Commonly, a foundation of an integral bridge consists of a single row of piles to allow the superstructure to deform laterally. For the design of this integral bridge, the same foundation is used. There has been chosen for steel shell piles as foundation piles. These piles are common for moderate integral bridges in Europe, as discussed in section 3.4. Steel shell piles have a certain flexibility in the lateral direction and bearing capacity in the vertical direction; therefore, they perform well in soft conditions, which is common in the Netherlands.

6.3.2 *Parameters that depend on the soil conditions*

The soil conditions are quite important for the design of an integral bridge. For instance the total bridge length depends on the soil conditions and the soil conditions affect the rotations and moments in the connection between the sub- and superstructure.

The soil structure at the building location is, according to the 'soil investigation report', uniform for the total area. The first soil layer is composed of peat (from ground surface -1.0 m + N.A.P. to -2.0 a -3.0 m + N.A.P.). The layers below this peat layer contain sand. The first layers are silt sand and the lower layers are composed of dense sand. Common for a flat country like the Netherlands, bridges do need embankments. These embankments are ordinary constructed of sand. So in general, the soil structure is composed of sand layers and has ideal soft soil conditions. The soil conditions are ideal, because the resistance of the soil in the lateral direction is relative low and sand next to the abutment does not settle that much. The soil structure will settle more, when the soil consists of large peat layers.

A more detailed soil structure will be presented in the 'Design phase'.

6.4 **The proposed structural application of integral bridge**

The structural application that is further investigated is.

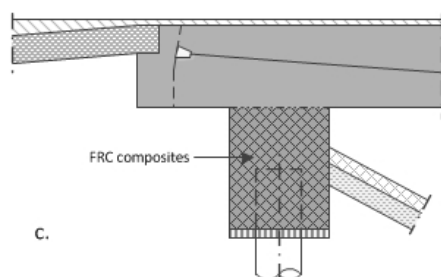


Figure 6-6C Structural application of FRC composites at the pile-abutment connection



The structural application of Figure 6-4C has been chosen, because of:

- A major motivation of the study (§1.2) is to reduce reinforcement in the connection between the sub- and superstructure. This structural application focuses on this problem.
- The structural applications of Figure 6-3 are rather complex in comparison with Figure 6-4C, because prestressing is present in the structural application. Also, the drying shrinkage of an FRC composite is much larger than a conventional concrete, which lead probably to cracks in the interface between the FRC composite and the conventional concrete.
- This structural application of Figure 6-4d focuses on the problems related to the settlement of the soil. There are better structural applications to eliminate or reduce the settlement of the soil. These structural applications are all located in the soil adjacent to the integral bridge and without the use of concrete. An example is the use of a backfill material (§3.6.1). The pavement problem can be eliminated by other applications as well. For example an elastic material or reinforcement in the pavement (§3.6.2).

6.4.1 *The required mechanical properties due to forces, moments and deformations in the structural application*

As mentioned before in section 6.2, the structural application of Figure 6-4c has to function as hinge construction. This means that the structural application should be able to:

- Rotate due to the deformations of the bridge deck
- Transfer shear forces from the superstructure to the substructure
- Absorb the moments (Smaller moments are still present in a plastic hinge)
- Transfer the vertical forces due to permanent and variable loads, to the foundation

The deformations, forces and moments require certain mechanical properties. Most of properties are already discussed in previous sections. A list of these required mechanical properties are:

- Deflection capacity
- Shear capacity
- Tension and compression strength in the vertical direction

Furthermore the crack width is sometimes decisive in the structural design of conventional concrete integral bridges. Another requirement is that the crack width is not decisive for the structural application.

6.4.2 *The proposed mechanical properties*

As discussed in chapter 5, the main mechanical properties of an FRC composite are the strain capacity and the strength capacity. Both mechanical properties are required for the structural application, but a high strain capacity leads to a low strength capacity and vice versa. Therefore the research will focus on the two mechanical properties: the strain capacity and the tensile strength. Besides, the research will focus on the strain behaviour and therefore compositions with both strain-hardening and strain-softening behaviour will be investigated. For the other mechanical properties (compression strength, shear capacity) of subsection 6.4.1 is assumed that they are equal to or greater than the mechanical properties of conventional concrete.

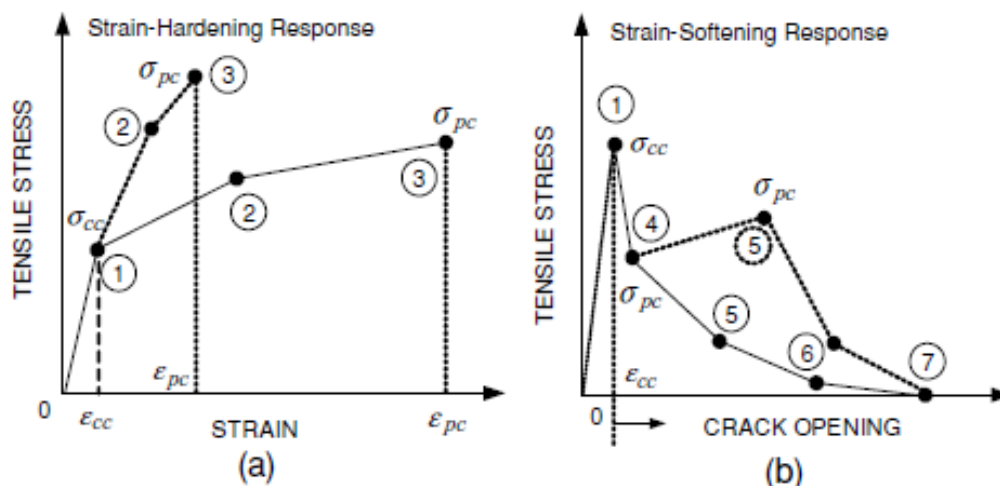


Figure 6-7 (a) a typical stress strain response for a strain-hardening FRC composite and (b) a typical stress strain response for strain-softening FRC composite

The two mechanical properties, tensile strength and strain capacity are related. In several figures of previous sections, the tensile strength-strain relations of FRC composites were given. The most representative ones for this research are from Naaman and Reinhardt [36] (Figure 5-9/Figure 6-7). These figures show the strain-hardening and strain-softening response of the compositions used in this research. Furthermore, the compositions of this research represent the two extremes, a maximum tensile strength or a high strain capacity. This is given in the validation grids (Figure 6-8)

		Tensile Strength in N/mm ²		
		2,5	5,0	10
Strain in % and H and S = Hardening and Softening	1S			x
	1H		x	x
	3S		x	x
	3H	x	x	
	5S	x	x	
	5H	x		

		Tensile Strength in N/mm ²		
		2,5	5,0	10
Strain in % and H and S = Hardening and Softening	1S			x
	1H	0		x
	3S			
	3H			
	5S	x		0
	5H	x		

A.

B.

Figure 6-8 A. Validation grid with 10 compositions and B. validation grid with 4 or 6 compositions



The 'validation grids' are developed to investigate what mechanical properties (strain capacity or tensile strength) acquire the greatest benefits in comparison with conventional concrete. These two validation grids are divided in tensile strength (horizontal direction) and strain capacity (vertical direction). Also the strain capacity is divided in compositions with strain-hardening and strain-softening response. These validation grids represent the correlation between two extremes: the strain and the tensile strength. Validation grid Figure 6-8A is the larger grid with 10 compositions, which acquire a 'finer mesh' of the results and validation grid Figure 6-8B is the smaller grid with 4 or 6 compositions. Validation grid Figure 6-8A is developed is to investigate a large number of compositions, but due to the time frame, Figure 6-8B is perhaps more realistic.

The tensile strength is divided in 2.5, 5 and 10 N/mm². These values are representative for already developed FRC composites. The strain is divided in 1, 3 and 5 % and strain-hardening and strain-softening response. The values of the strain are based on investigated literature of ECC and Fibre reinforced concrete. Both strain-hardening and strain-softening response will be researched, because compositions with both strain-hardening and strain-softening response have 'deflections capacity'. The strain-hardening response is favourable, when it comes to 'crack width control', but strain-softening response is more common for FRC composites. Especially when the structural element with FRC composites is executed in less ideal conditions, for instance at a building site.

The compositions, presented in the validation grids of Figure 6-8, are standing for a tensile stress-strain relation. Figure 5-9/Figure 6-7 and Naaman and Reinhardt [36] are used as inspiration to create Figure 6-9 and Figure 6-10.

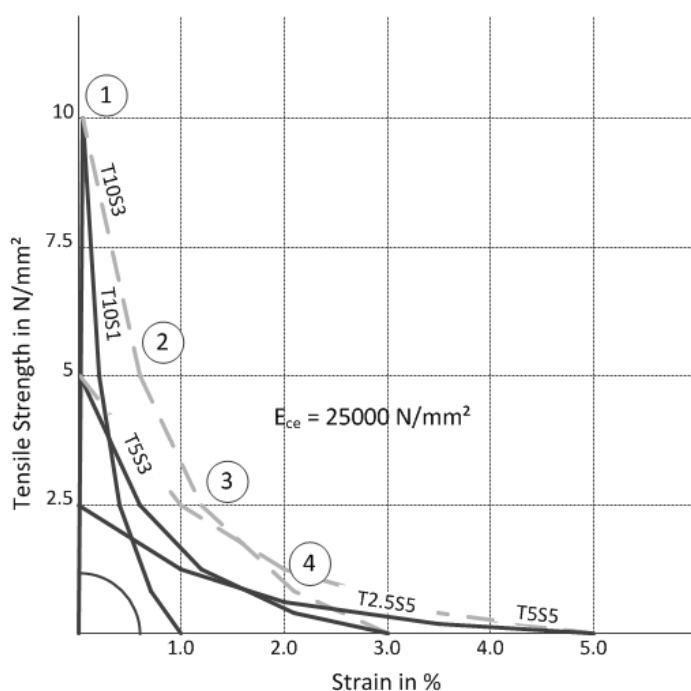


Figure 6-9 Tensile stress-strain relation graphs of the validation grids: The strain-hardening response. Remark T= Tensile strength and S= Softening

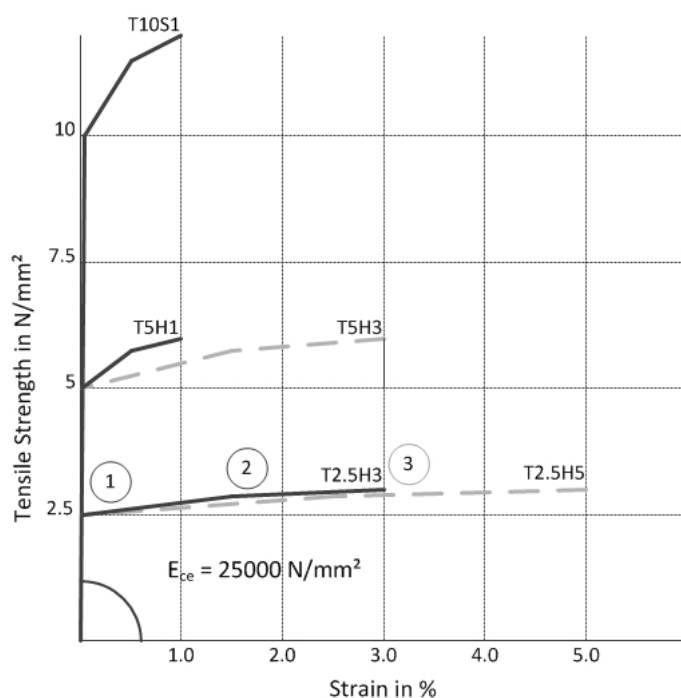


Figure 6-10 Tensile stress-strain relation graphs of the validation grids: The strain softening response. Remark T= Tensile strength and H=Hardening

The Elastic modulus is the same for each composition. This is set on 25000 N/mm². The points for the strain-hardening response are set on:

1. The tensile strength of the validation grid
2. 1/2 of the tensile strength and 0.2 of the strain
3. 1/4 of the tensile strength and 0.4 of the strain
4. 1/12 of the tensile strength and 0.7 of the strain

The points for the strain-softening response are set on:

1. The tensile strength of the validation grid
2. 1.15 of the tensile strength and 0.5 of the strain
3. 1.2 of the tensile strength and 1.0 of the strain

A table with the specific points shall be attached to the report of 'the design phase'.



6.5 Research approach

The next section of this thesis is the research approach. This section discusses the research steps. The research consists of four research steps. These steps are:

- Input
- Calculation by hand
- The detailed design: connection
- The research of FRC composites

In chapter 1, the project 'N206 Faunapassage' has been chosen for the conventional design. This has changed due to an alteration in the research process. This chapter and a calculation by hand are developed instead of the conventional design; therefore, the data of project 'schokkeringweg' is applied in 'the design process'. This data consist of the bridge design, as discussed in section 6.3, and the overall calculation. The calculations that are done in this research process are all calculations of the connection detail. These calculations will be used to create a model for the research to FRC composites in the connection between the sub- and superstructure. An overview of the research steps that has to be taken after the pre-study are given in Figure 6-11.

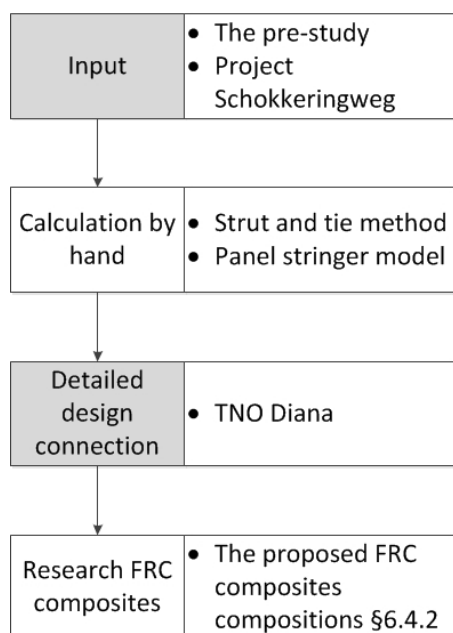


Figure 6-11 The research approach



The research approach consist of four steps: Input, calculation by hand, detailed design connection and the research FRC composites. The input of the research approach consist of the pre-study and the project 'Schokkeringweg'. The data of the project 'Schokkeringweg' is used for the calculation by hand and the detailed design connection; thereby, consideration should be given to the forces and moments of the overall calculation and the specific design choices, like the dimensions, the location and the amount of reinforcement, the concrete strength and properties of the foundation. This data is also used to create a detailed design connection. The detailed design is used for the research of FRC composites. A structural model for the detailed design is given in Figure 6-12. This structural model shall be imported in the software program 'TNO Diana'. The correctness of the structural model could be tested by a comparison between the calculation by hand and the structural model in TNO Diana. When the structural model is correct, the research to FRC composites could start.

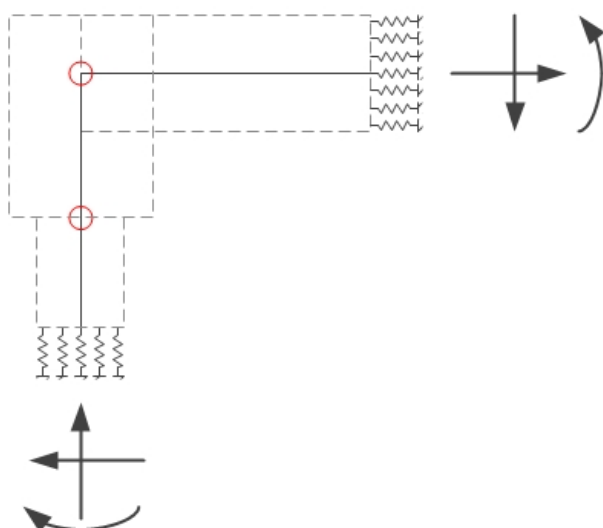


Figure 6-12 Structural model of the connection

Points of interest of this structural model are:

- the boundary conditions
- the forces and moments in the structure from the calculation by hand
- integration of the reinforcement in the structural model from the calculation by hand

The motivation of the research is to reduce reinforcement in the connection between the sub- and superstructure by applying FRC composites in the abutment. If FRC composites will be useful to reduce reinforcement is demonstrated in this research step. First the proposed FRC composite compositions of subsection 6.4.2 are imported in the structural model of the connection. Then the calculations shall be done. The output of the structural models with FRC composite compositions are compared to the structural model with conventional reinforced concrete.



7 Analytical calculations of the connection

The analytical calculations of the connection are an important step in the research of FRC composites. These calculations are done to acquire a better understanding of the structural behaviour of the connection due to the forces and moments. So far, the knowledge about the structural behaviour of the connection is limited. In particular, the structural behaviour of the foundation pile in the connection is uncertain. Therefore, more knowledge is needed to get a better understanding about the structural behaviour and how FRC composites could be beneficial for a bridge connection. In the next section, the approach and results according to the Eurocode [29] are described. This is followed by sections about stringer panel models and its results.

7.1 Analytical model of the connection according to the Eurocode

A model of a prefab column footing is given in subsection 10.9.6.3 of the Eurocode [29]. This model is given in Figure 7-1A and describes a prefab column-floor connection. This model could also be used for a bridge connection, because it describes a similar structural behaviour. In both models the forces and moments are transferred by friction and a coupling force. Figure 7-1B shows a model for the bridge connection which is constructed according to Figure 7-1A. The dimensions, forces and moments are based on the stringer panel models which are explained in the next sections.

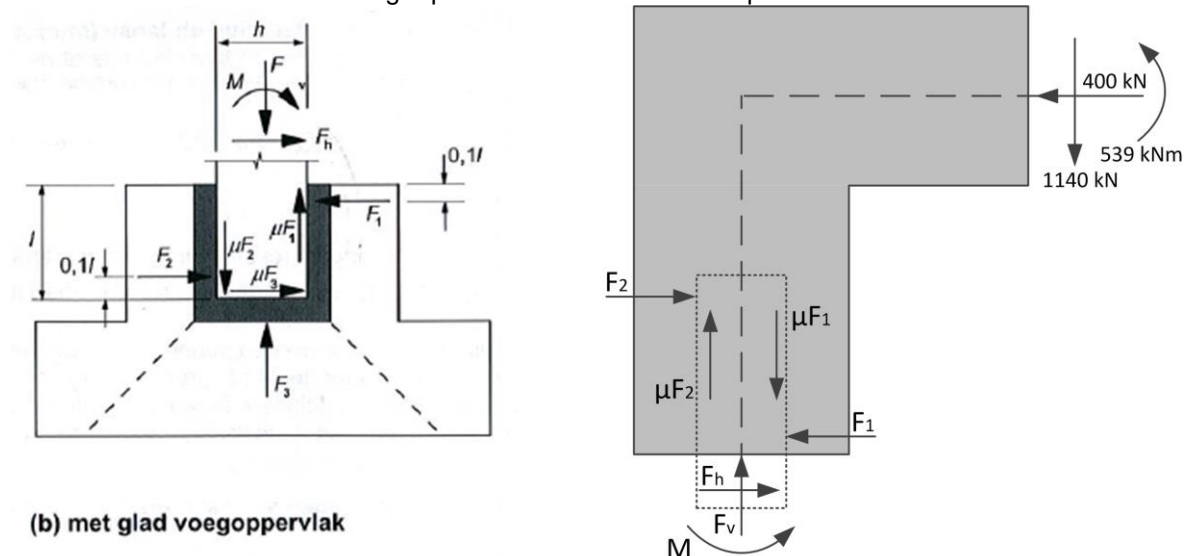


Figure 7-1 A. Analytical model of a column-floor connection B. Analytical model of a bridge connection

According to subsection 10.9.6.3 of the Eurocode [29], special attention is needed for:

- The detailing of the reinforcement at the top of the notch (close to F_1)
- The transfer of F_1 to the walls of the notch
- The reinforcement embedded in the column and walls of the notch
- The shear resistance of the column



As showed in Figure 7-1A, a part of the forces and moments are transferred by is a combination of the horizontal forces F_1 and F_2 in the column. This combination of forces is the coupling force. The force F_1 is important, because this force could lead to failure of the right wall of the notch. Therefore horizontal reinforcement is applied to improve the structural capacity of the notch. This structural behaviour corresponds with the first bullet: the detailing of the reinforcement at the top of the notch (close to F_1).

Figure 7-1A also shows the shear forces in the column. The shear forces depend on the frictional behaviour of the column with the walls. This depends on the friction coefficient μ . This friction coefficient is maximized by 0,3 for a prefab column-floor connection. However this does not apply for the bridge connection of Figure 7-1B, because the materials and the joints are slightly different. The bridge connection consist of a steel foundation pile in a concrete abutment. Then friction occurs between steel and concrete which is less than friction between concrete elements.

The column-floor connection is a good example for the bridge connection, but there are also two important differences. These difference are:

- The bridge connection is an asymmetric connection where the column-floor connection is symmetrical.
- The forces and moments of the bridge connection have a different point of engagement than the column-floor connection.

These differences could lead to another structural behaviour for the bridge connection. Therefore, analytical calculations are performed to acquire more knowledge about the structural behaviour of the bridge connection. These analytical calculations consist of the stringer-panel-method and the strut-and-tie models. The stringer-panel-method and the strut-and-tie model will be explained in section 7.2. The analytical calculations are described in section 7.4.



7.2 Introduction of the stringer-panel method and the strut-and-tie model

The stringer-panel method is developed as a tool for the design of structural concrete walls. Figure 7-2 shows an example of a model that is divided in panels and stringers. The idea is that the stringers are carrying the normal forces and the panels the shear forces and sometimes the normal forces. The stringers represent the reinforcement, the tension stiffening and the compressed concrete and the panels represent distributed reinforcement and concrete with shear stresses. The interaction of a panel and a stringer is a constant shear stress on the interface. [47] More about: its function and how to apply the stringer-panel method could be found in [48, 49, 50].

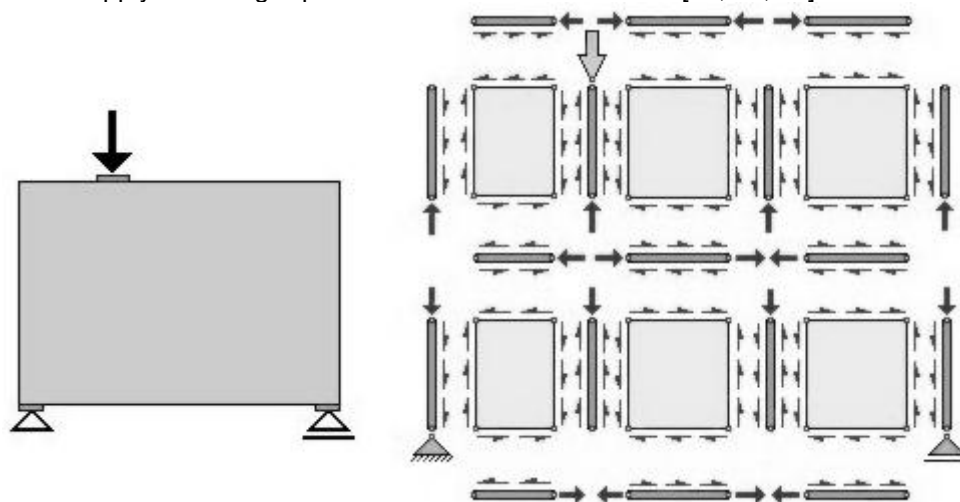


Figure 7-2 On the left: a reinforced concrete beam with a respectively large height and on the right: a figure of a stringer-panel model of the reinforced concrete beam. The stringers are the dark grey bars and the panels are the light grey squares.

The next step after the division of the model in panels and stringers is to calculate the shear forces in the panels and the normal and shear forces in the stringers. The results could be used to create a strut-and-tie model. The strut-and-tie model is a model which consist of members and nodes and corresponds with the stringer-panel model. These similarities are:

- The nodes of the strut-and-tie model are also the nodes of the stringer-panel-model
- The straight members of the strut-and-tie model are stringers in the stringer-panel model
- The diagonal members of the strut-and-tie model cross the panels of the stringer-panel model diagonally.

An example of a strut-and-tie model could be found in [48].



7.3 Stringer panel model of the bridge connection

The stringer-panel method is used to acquire a better understanding of the structural behaviour of the connection. The forces and the moments are obtained from calculations of bridge 'Schokkeringweg'. The forces and the moments represent the normal force, shear force and the moment in the superstructure. Like Figure 7-2, a stringer-panel model is constructed of the connection (Figure 7-3).

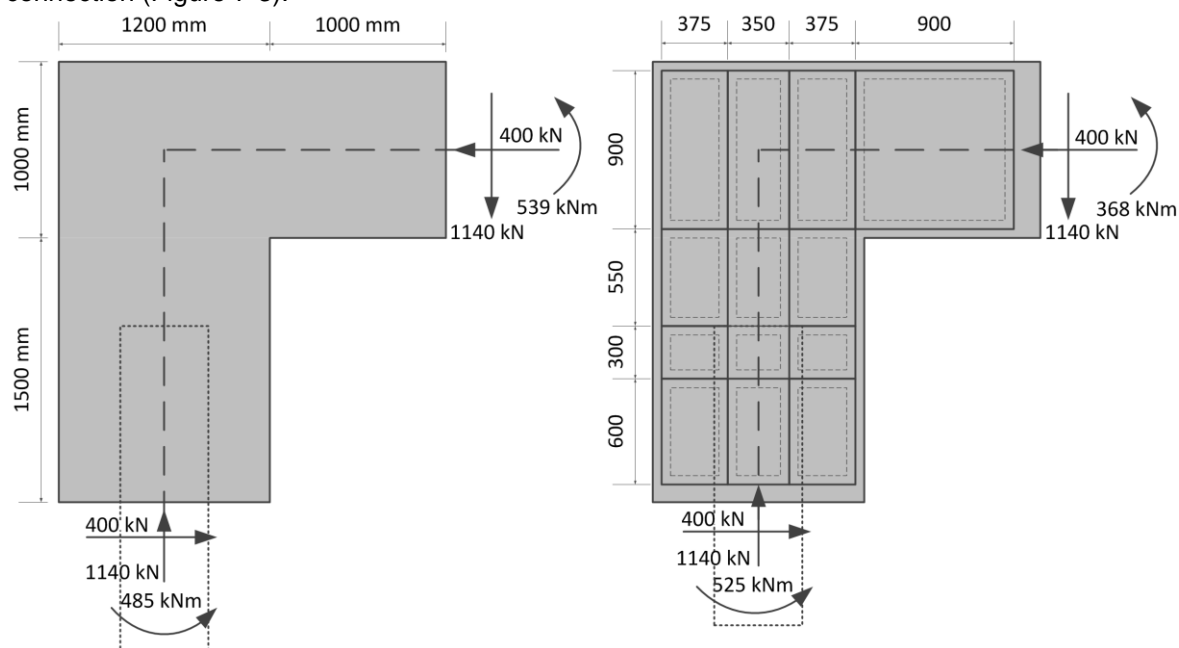


Figure 7-3: On the left: a detail of the connection between the sub- and superstructure and on the right: the stringer-panel model of the connection. The black lines stand for the stringers in the model and the dotted lines are the panels of the model

The dashed lines, both in the detail and the stringer-panel model of Figure 7-3, stand for the pile foundation. The pile foundation consists of a steel shell pile of 500 mm. The top layer of the steel shell pile is filled with concrete. The lower middle panels represent the pile in the stringer-panel model. The width of these panels is set on 350 mm, because this is a resultant width between the pile diameter of 500 mm and the reinforcement in the concrete top layer of the pile.

The moments in the connection and the string-panel model in Figure 7-3 differ from each other. The reason is that the geometry of the model is different from the detail of the connection. At the bottom of the connection, the geometry is changed due to the distribution of the moments and the forces in the pile head. This is further discussed in the next section. The geometry at the top is changed as well, because it is assumed that the stringer has width of 50 mm.



7.4 Calculation of the stringer-panel models and the strut-and-tie models (SPM & STM)

Analytical calculations of the bridge connection are performed to acquire more knowledge about the structural behaviour of the connection, as mentioned before in section 7.1. These analytical calculations consist of the stringer-panel models and the strut-and-tie models. These analytical calculations are described in this section.

The structural behaviour of the bridge connection depends on the structural behaviour of the foundation pile and the reinforced concrete of the lower part of the abutment, according to the model of Figure 7-1B. Two mechanisms occur in this particular area to transfer the loads to the foundation pile: The first mechanism is the transfer of forces and moments by friction between the foundation pile and the surrounded concrete (Figure 7-4A) and the second mechanism is the transfer of forces and moments by a coupling force (Figure 7-4b).

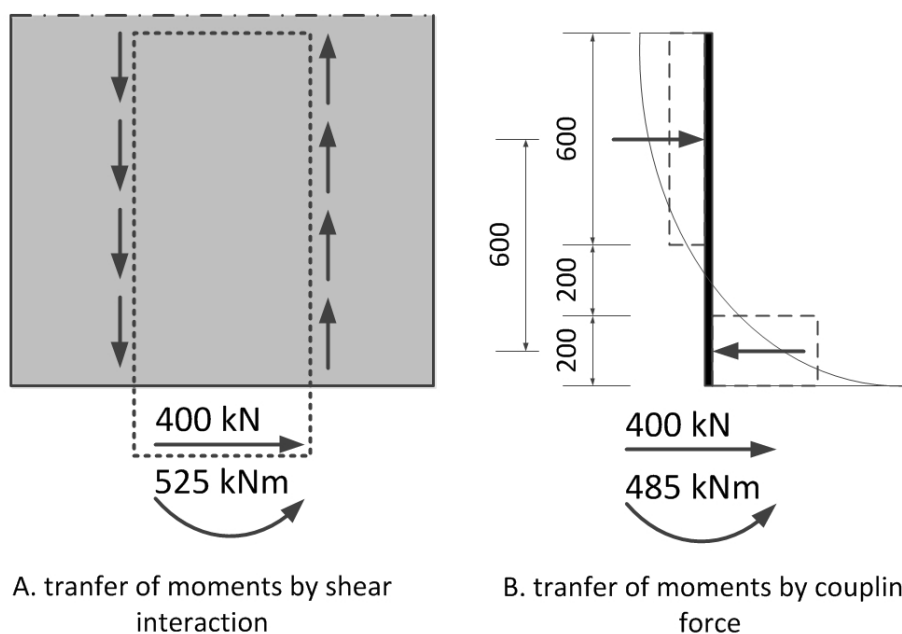
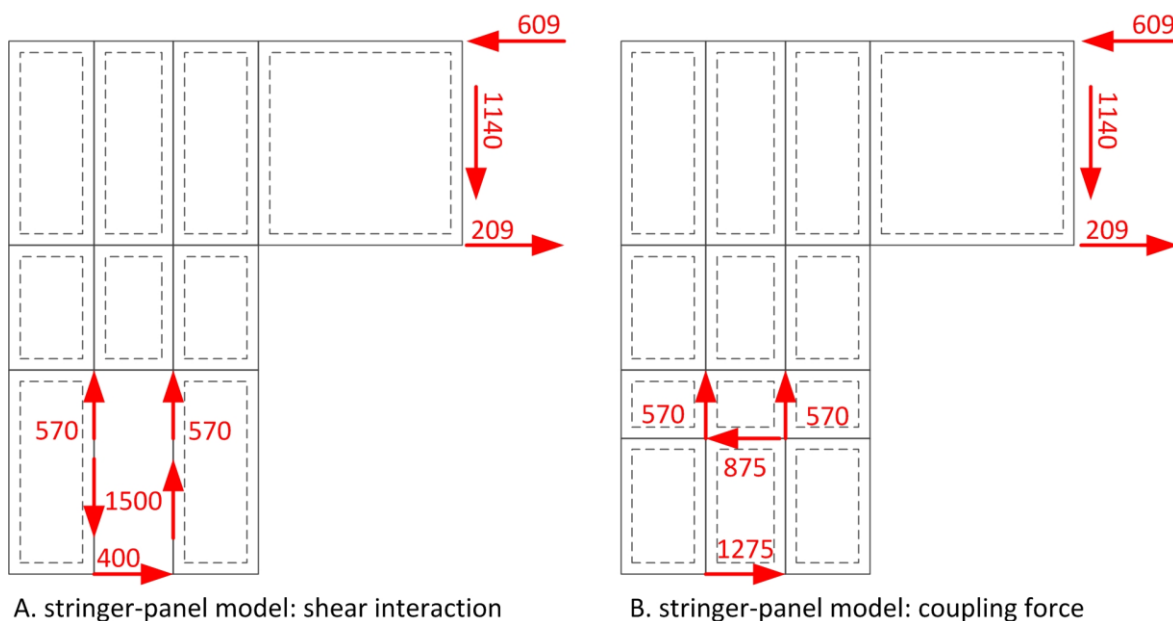


Figure 7-4 A. Transfer of moments from the super- to substructure by coupling force and B. transfer of moments from the super- to substructure by shear interaction

During the design process of the 'Bridge Schokkeringweg', two stringer-panel models were proposed by ir. H. Peerdeman (Figure 7-4A) and professor Blauwendraad ((Figure 7-4B) for the structural behaviour of the bridge connection. There are two stringer-panel models developed, because it is uncertain which mechanism has the major influence on the structural behaviour the bridge connection. This was the main discussion during the design process of the bridge connection of the 'bridge Schokkeringweg'.



A. stringer-panel model: shear interaction B. stringer-panel model: coupling force
Figure 7-5A. The stringer-panel model where the moments are transferred from the super- to the substructure by a coupling force and B. The stringer-panel model where the moments are transferred from the super- to the substructure by shear interaction

Figure 7-5 shows the two stringer-panel models when the mechanism are included in the stringer-panel model of Figure 7-3. The vertical force at the bottom of the connection is divided in two forces which are engaged on the top of the pile head. Further, the moments and the horizontal forces are split up in two forces which are engaged on the element at the right corner. The moment in the pile in stringer-panel model of Figure 7-5B is divided in two coupling forces according to Figure 7-4B. The sum of the shear interaction stresses of Figure 7-4A are forces engaged on the pile shaft (See Figure 7-5A).

The next step, in the stringer-panel method, is to determine the forces in the stringers and the panels. For stringer-panel model of Figure 7-5A, this is proposed by ir. H Peerdeman and stringer-panel model of Figure 7-5B is proposed by professor Blauwendraad. The results of the stringer-panel models of Figure 7-5 can be found in appendix A. With the stringer-panel models, the normal forces in the stringers and the shear stresses in the panels could be distinguished.

The last step in the stringer-panel method is, to use the determined stringer-panel models, the normal forces and shear stresses, to create the strut-and-tie models. A strut-and-tie model gives a good impression of the force distribution in the connection. For both stringer-panel models, this is done. These results can also be found in appendix A.



As mentioned in section 0, the structural behaviour or the force distribution in the connection was unclear. On the basis of the stringer-panel and the strut-and-tie model, it can be concluded that:

- When the moment, shear force and normal force are acting in this direction: Tension occurs in the stringers on the left side and at the top of the bridge deck and compression occurs on the right side and at the bottom of the bridge deck. This applies for both models of Figure 7-5.
- The panel in the right corner, where the forces and moment engaging, experiences the highest shear stresses. This applies for both models of Figure 7-5.
- In model A of Figure 7-5, high shear stresses occur in the panel above the pile.
- In model B of Figure 7-5, high shear stresses occur in the panels at the bottom of the connection and the panel in the left corner.

Where the maximum forces occur, the largest amount of reinforcement is required. On the basis of the forces, a lot of shear reinforcement is needed in the panel at the right corner and the stringers in tension also require reinforcement. Still it is not clear, whether model A or B of Figure 7-5 is decisive for the connection. In addition, it is not clear as well, what the influence is of the normal force, shear force or moment only on the connection. This is important, because if the forces change, the dimensions of the bridge change. A long bridge, for example, experiences a larger normal force and a bridge with large spans has a larger moment and shear force in the bridge deck; therefore, the next step in calculation is to create stringer-panel models with a normal force, a shear force or a moment only for model A of Figure 7-5 are given in Figure 7-6.

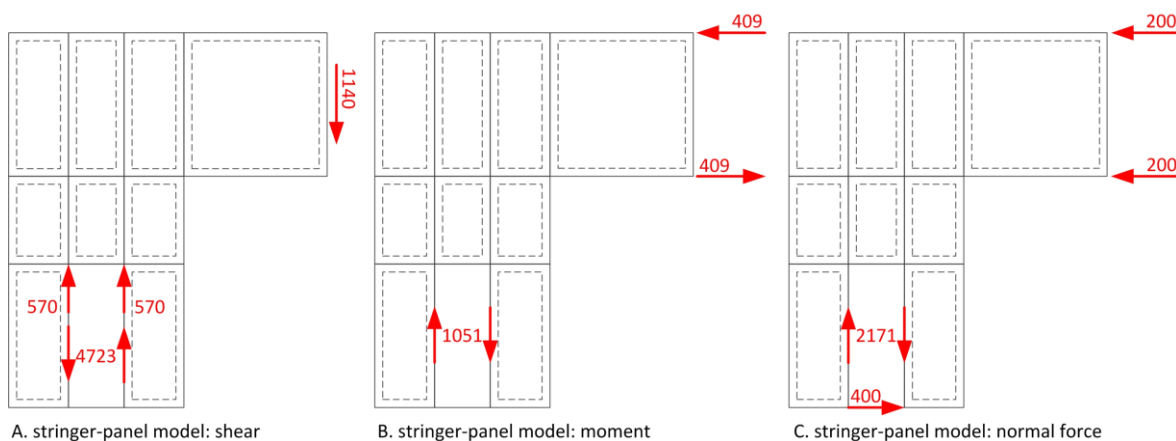


Figure 7-6 A. Stringer-panel model with the influence of shear only, B. stringer-panel model with a moment only and C. stringer-panel model with a normal force only. The stringer-panel models are based on model Figure 7-5A.



It is important to mention that it concerns a normal force, a shear force or a moment in the bridge deck. At the bottom of the connection, a moment is also applied to acquire equilibrium (requirement: $\sum M=0$, $\sum V=0$ and $\sum H=0$) in the connection; for Figure 7-5A, this moment is divided in two coupling forces which are engaged at pile shaft. This is showed in Figure 7-6 as well. The stringer-panel models of Figure 7-5B can be found in appendix A. In this case, the moment at the bottom of the connection is split up in two forces, like Figure 7-5B. Further, the stringer-panel models, with normal forces, shear forces or moments only, are used to define the shear stresses in the panels and the normal forces in the stringers. Like, the models of Figure 7-5, the stringer-panel models, the normal forces and the shear stresses are used to create strut-and-tie models. The strut-and-tie models can be found in appendix A as well.

On the basis of the stringer-panel and strut-and-tie models, new findings can be drawn. These new findings will be discussed in the next section.

7.5 Evaluation of the SPM an STM and recommendations for the detailed design connection

The new stringer-panel and strut-and-tie models, with a normal force, shear force or moment only, provide new findings into the structural behaviour of the connection. In this section, the new findings will be discussed. On basis of these new findings, first the models of Figure 7-5 will be evaluated and then the recommendations for the detailed design connection will follow. First the models based on Figure 7-5A are discussed and then the models of Figure 7-5B.

First step: The new findings resulting from the stringer-panel and strut-and-tie models

The models based on Figure 7-5A show some important findings. These findings are listed below:

- Only the normal forces have influence on the lower panels. This means that the shear force and the moment are not absorbed by friction between the pile shaft and the surrounding concrete, as was assumed according to Figure 7-4A.
- In most panels, the effects of the moment and the shear force are opposite; therefore, the normal force is decisive in the centre panels and the upper left panel. However, the shear stress in these panels is relatively low. This means that the influence of the normal force (and so the lateral deformation) is lower than expected.
- Only the shear force has influence on the upper right panel. This is also the panel with the highest shear stress.
- The upper centre panel experiences a high shear stress due to a combination of the moment, the shear force and the normal force.
- As established in section 7.4, the stringers on the left side and the top of the bridge deck are in tension and the stringers on the right side and the bottom of the bridge deck are in compression. The stringer-panel models show that the shear force and the moment due to the shear force are mostly responsible. The normal force and moment are responsible for a counter reaction.



The same list that is made for the models of Figure 7-5A can be created for the models of Figure 7-5B. The list with findings of Figure 7-5B is given below:

- The lower panels and the left upper panel experience the highest shear stress. This is caused by the moment due to the shear force. The moment and the normal force are responsible for a counter reaction.
- The upper right panel experiences a high shear stress. Like the models of Figure 7-5A, this is all due to the shear force.
- The centre panels are only under influence of the normal force. The moment and shear force are not responsible for a shear stress in these panels. The shear stress in the centre panels is however relatively low. This means that the influence of the normal force (and so the lateral deformation) is minor in comparison with the shear force.
- Like the models of Figure 7-5A, the stringers on the left side and the top of the bridge deck are loaded in tension and the stringers on the right side and the bottom of the bridge deck are in compression.

Second step: Evaluation after the list of findings

By taking the normal force, the shear force or the moment apart, new aspects become clear. The most important aspect, of the models of Figure 7-5A, is that the forces in the pile shaft are not transferred by friction between the pile shaft and the surrounding concrete, but due to an elastic deformation of the pile head, as the high shear stress in the upper centre panel shows. It is highly unlikely that the pile deforms elastically when the stiffness of the pile is taken into account; therefore, the transfer of forces by a coupling force in the pile is more logical (Figure 7-4B).

The focus will further be on the models of Figure 7-5B, because the transfer of forces by a coupling force in the pile is more logical. As mentioned in 'the list of findings' the highest shear stress is in the lower panels and the upper left and right panel. On basis of this findings, most of the shear reinforcement needs to be applied surround the steel pile and in the bridge deck. The concrete part between the pile and the bridge deck is less loaded than expected. The major reason is that the bridge 'Schokkeringweg' is a medium ranged bridge (58 meter) and therefore the influence of the normal force and indirectly the lateral deformation is minor. Other causes are the low stiffness of the soil and the flexible behaviour of the steel pile. Hence, it is expected when the bridge length and the soil stiffness increases and flexible behaviour decreases, the influence of the normal force on the connection increases.

As also established in the 'list of findings', the highest tension stress is in the stringer on the left side and the top the bridge deck; therefore, this area needs relatively a lot of reinforcement. This area is in case of crack width control the focus area of the connection as well.

The last important aspect of the 'list of findings' is that shear force has the largest influence on the connection, in particular on the lower part of the connection. This is specifically for the bridge 'the Schokkeringweg'. Like the bridge length, the soil stiffness and the pile choice have a major influence on the normal force, the span length is decisive when the shear force is taken into consideration. If the span length increases, the shear forces increases as well.



Third step: Recommendations for the detailed design of the connection

The stringer-panel and strut-and-tie models give a good representation of the force distribution in the connection. However, the mechanical properties of the material are not taken into account and the stringer-panel method is based on linear structural behaviour which is not in correspondence with reality. The mechanical properties of the material have normally influence on the structural behaviour of the connection. Therefore, it is important that the mechanical properties are adopted in further design and calculations. For the further design and calculations 'TNO Diana' is used. 'TNO Diana' is a software program which is based on the finite element method. TNO Diana is used, because the mechanical properties of the material can be adapted and changed in favour of the design. During the next design, it is interesting to see if the calculation models in TNO Diana show the same force distribution as the stringer-panel and strut-and-tie models, only with the mechanical properties adapted in design.

The stringer-panel and strut-and-tie models are based on linear structural behaviour, as mentioned before. In reality the material will behave plastically. This will have influence on the force distribution, because when a material like concrete fail, it is not able to absorb the forces. Beside, when plastic structural behaviour is taken into account, the material will crack, when the connection is heavily loaded. As mentioned before, exceeding of the maximum crack width could lead to more reinforcement. Hence, a point of focus for further design is crack width control.

The next step is to implement the recommendations into further design. This design is a detailed design to investigate if FRC composites are useful in reducing reinforcement in the connection.



8 2D FEM of the bridge connection

In this chapter, the 2D FEM of the bridge connection is described. The 2D FEM is developed in the computer program 'TNO Diana' [51]. The model is based on the strut-and-tie models and the bridge 'Schokkeringweg'. This means that the same dimensions and loads are implemented in the 2D FEM as applied on the stringer-panel models. Further, the material properties, the reinforcement design and the design of the foundation pile are a part of the design of the bridge 'Schokkeringweg'.

8.1 Evolution of the 2D FEM

At the start of the design of the 2D FEM, a simple model is created which is extended and developed over time. This evolution of the 2D FEM is discussed in this section. In total 7 models are developed with small improvements with respect to the previous models. This is discussed in the next subsections.

8.1.1 The first 2D FEM: Basic model

The basic model what is first developed is given in Figure 8-1. The basic model is developed as validation model for the boundary conditions and to simulate the results of the stringer-panel models of chapter 7. Therefore, the 2D FEM of Figure 8-1 has the same dimensions and loads as the stringer-panel models. The only difference is that linear elastic material properties are included in this 2D FEM.

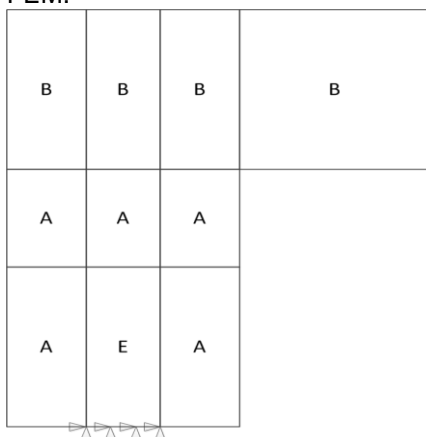


Figure 8-1 The first 2D FEM: A = structural abutment elements, B = structural bridge elements, E = structural elastic foundation pile element



After analysing the results of the 2D FEM, it came out that this model shows most similarities with stringer panel model of Figure 7-5A. This means that the total forces and moments in the connection are absorbed by the friction between the foundation pile and surrounded concrete. Figure 8-2B shows the stresses in the vertical direction of the connection. The vertical compression is on the right side and vertical tension is on left side of the connection. There is no difference between the stresses in the foundation pile and the surrounded concrete. This means that the foundation pile is fully embedded in the concrete abutment (100% friction). Besides of the friction, Figure 8-2B shows that the shear force is decisive in the structural behaviour. Because the shear force is responsible for tension at the left side and compression at the right side as presented in the results of chapter 7 and appendix A.

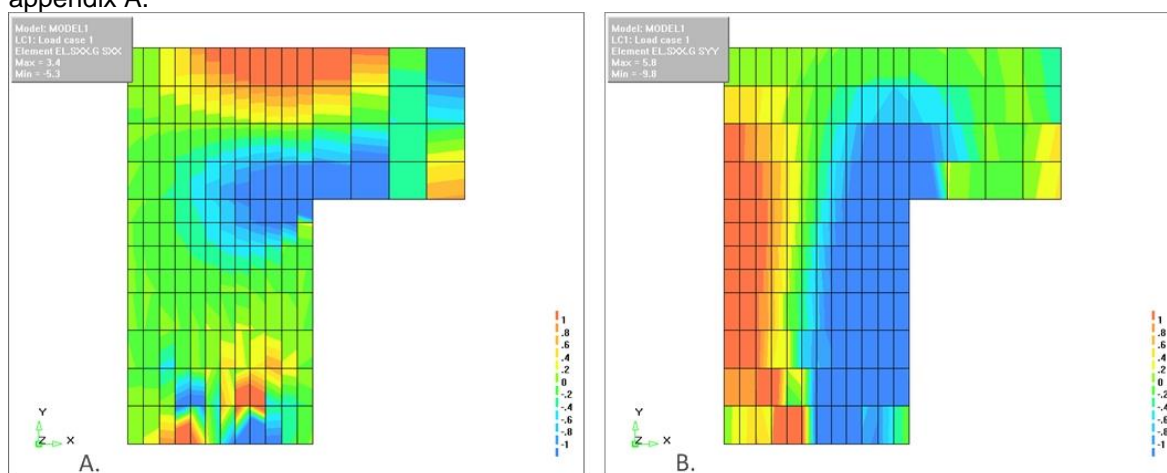


Figure 8-2 The first 2D FEM: A. stresses in x-direction and B. stresses in y-direction

8.1.2 The second 2D FEM: Implementing interface elements

The model of the Eurocode (Figure 7-1A) shows that not only the frictional behaviour is responsible for the transfer of the forces and the moments in the foundation pile, but also the coupling force plays an important role. Therefore, the second model was developed (Figure 8-3). This model is different from model 1 by implementing interface elements between the elastic foundation pile element and the elastic concrete elements.

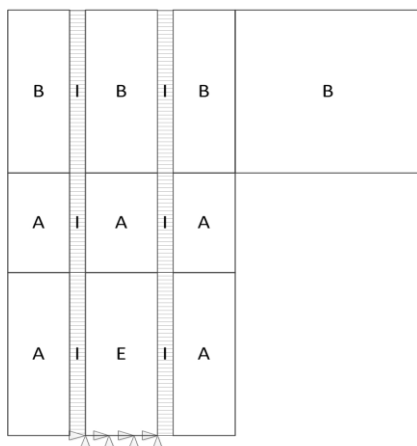


Figure 8-3 Second 2D FEM interfaces applied: A = structural abutment elements, B = structural bridge elements, E = structural elastic foundation pile element, I = interface elements

The interface elements are influencing the structural behaviour, because the friction between the elastic foundation pile element and the concrete elements is variable in this 2D FEM. Figure 8-4 shows the stresses in the x- and y-direction in the second 2D FEM with a shear modulus of the bottom interface elements equal to zero. The difference between the first and the second 2D FEM is that the stresses in the foundation pile differs from the surrounded concrete. A shear modulus equal to zero leads to a decrease of friction between the foundation pile and surrounded concrete and to an increase of the coupling force in this area. The increase of the coupling force can be seen by comparing Figure 8-2 and Figure 8-4A.

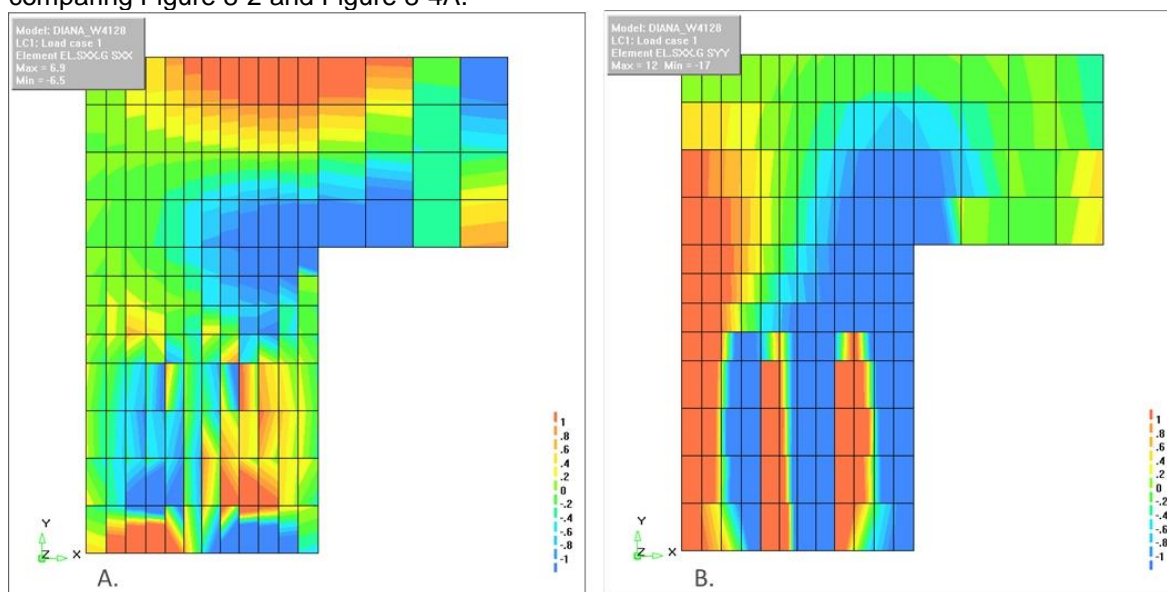


Figure 8-4 Second 2D FEM: A. stresses in x-direction and B. stresses in y-direction

8.1.3 The third 2D FEM: the reinforcement attached to the model

The next step in the modelling process was to include the reinforcement in the 2D FEM and to switch from linear to nonlinear analysis. This model is presented in Figure 8-5A. This model has embedded reinforcement in concrete elements and interface elements with elastic properties. The results of the calculation show that the elastic foundation pile element is dominant in the structural behaviour of the model. This is presented in Figure 8-5B. The major cracks develop around the foundation pile. This is found in all the 2D FEMs with different shear moduli. Therefore the elastic foundation pile element is replaced by the elements as showed in Figure 8-6A.

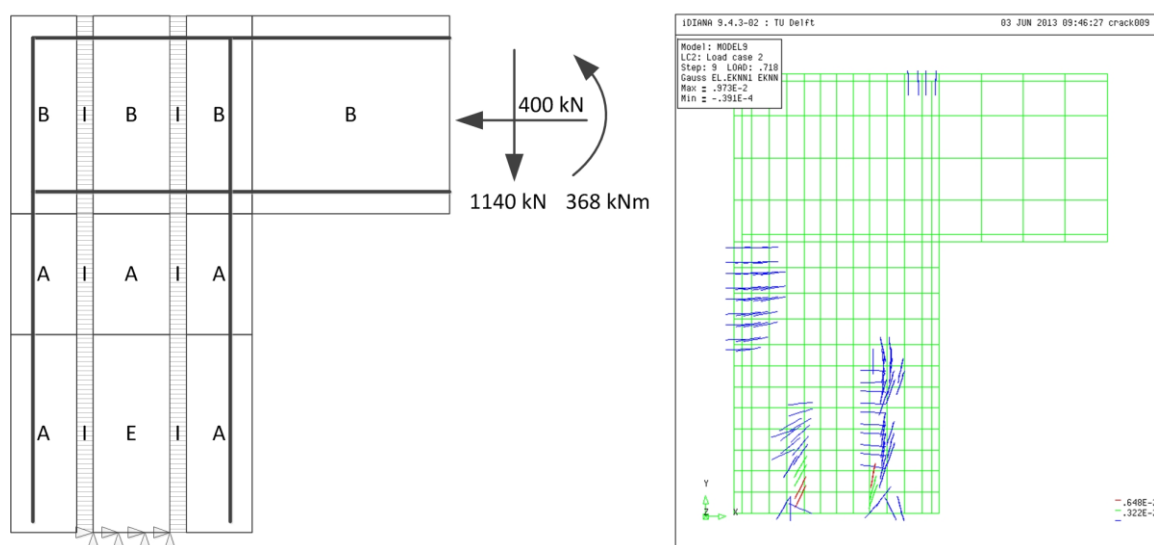


Figure 8-5 A. Third 2D FEM both reinforcement and interfaces applied: A = structural abutment elements, B = structural bridge elements, E = structural elastic foundation pile element and I = interface elements and B. third 2D FEM: Crack pattern of the connection

8.1.4 Fourth 2D FEM: the foundation pile adjusted

The foundation pile in the model of Figure 8-6A consists of steel line elements enclosed by two interface elements. The steel line elements represent a round steel pile and the interface element on the outside stands for the frictional behaviour between the steel line elements and the structural concrete elements. The interface element on the inside represents the friction between the steel line element and the concrete element inside the round pile. This model shows, like the previous 2D FEMs, that the behaviour of the foundation pile in the surrounded concrete is decisive for the structural behaviour of the connection (Figure 8-6B). The crack pattern of Figure 8-6B is also a result of 2D FEM with a shear modulus equal to zero. A decrease of the shear modulus leads in the 2D FEM of Figure 8-6A also to a decrease of the bearing capacity of the connection. This is however only based on the linear properties for the interface elements. This means in the connection that the interface elements are not able to transfer a part of the forces and moments, but the foundation pile is still connected with the surrounded concrete. Therefore, interface elements with nonlinear properties are introduced in the 2D FEM of Figure 8-6A. This leads to further reduction of the bearing capacity of the connection. This corresponds with the model of the Eurocode (Figure 7-1A), because of the absence of horizontal reinforcement only a small part of the forces and moments can be taken



over by a coupling moment in the foundation pile. Also, the friction is very low between a smooth steel pile and a concrete element. Therefore, the total bearing capacity is low.

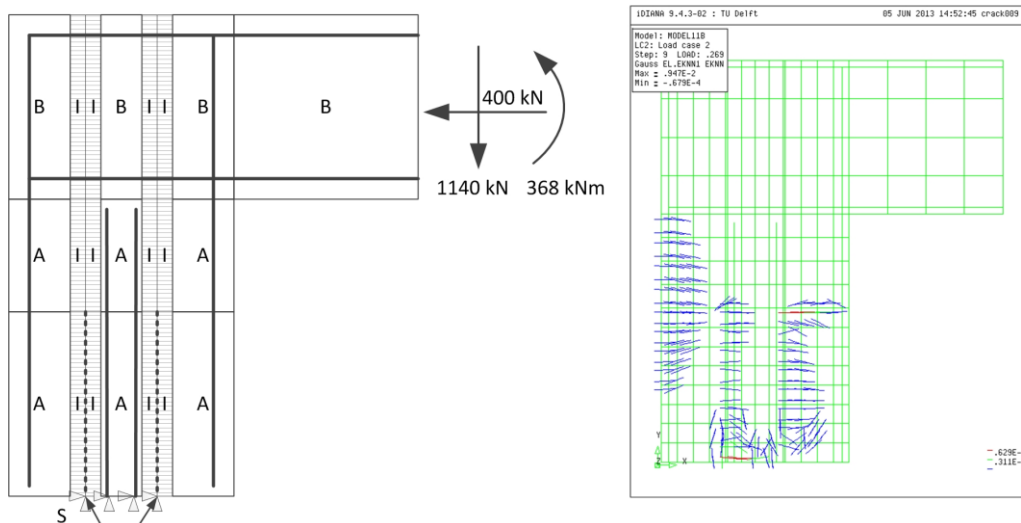


Figure 8-6 A. Fourth 2D FEM optimization of the foundation pile: A = structural abutment elements, B = structural bridge elements, E = structural elastic foundation pile element, I = interface elements, S = steel pile line elements and B. Fourth 2D FEM: crack pattern of the connection

8.1.5 The fifth 2D FEM: attachment of the horizontal reinforcement

The fifth 2D FEM includes horizontal reinforcement in the pile foundation (Figure 8-7) to increase the total bearing capacity of the connection and to show a more realistic behaviour of the structure. This is the last 2D FEM in 'the evolution of the 2D model'. The results will be discussed in section 8.4.

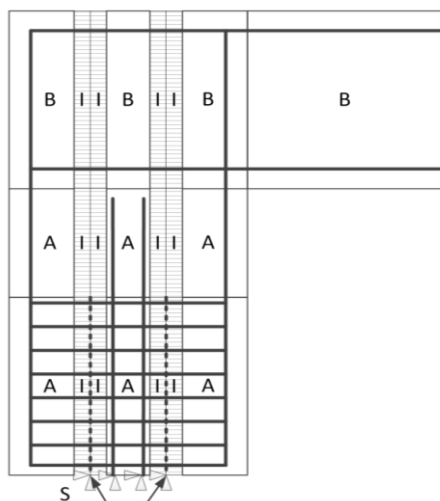


Figure 8-7 Fifth 2D FEM horizontal pile reinforcement and nonlinear mechanical properties for interface elements: A = structural abutment elements, B = structural bridge elements, E = structural elastic foundation pile element, I = interface elements, S = steel pile line elements



8.2 Input of the 2D FEM

The 2D FEM is composed of a physical structure, material properties, FEM elements/mesh and the boundary conditions. In the next subsections, each part of the input is further discussed. A major part of the data-input described in this section could be found in appendix B.

8.2.1 Physical structure

The physical structure of the 2D FEM is prescribed by the dimensions of the connection, the applied reinforcement and the applied foundation pile. Figure 8-8 shows the dimensions of the physical structure of the connection. The width of the physical structure is set on 1500 mm. This is the 'centre-to-centre distance' of the foundation piles.

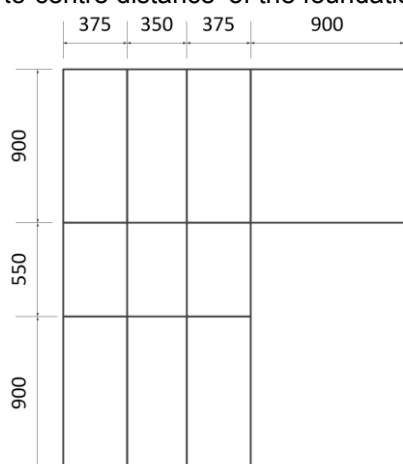


Figure 8-8 A basic physical structure with the dimensions

The applied foundation pile in the 2D FEMs is based on Figure 8-9A. In the more simple models, the cross-section of Figure 8-9B is applied. Figure 8-9B has the same width as the other plates of the physical structure of Figure 8-8. The applied foundation pile in the more complex 2D FEMs consist of a concrete plate enclosed by two steel line elements. The cross-section of this foundation pile is presented in Figure 8-9C. The steel line elements have a thickness of 12,5 mm and a width of 410 mm. The dimensions of the steel line elements have the same area and moment of inertia as the steel pile of Figure 8-9A.

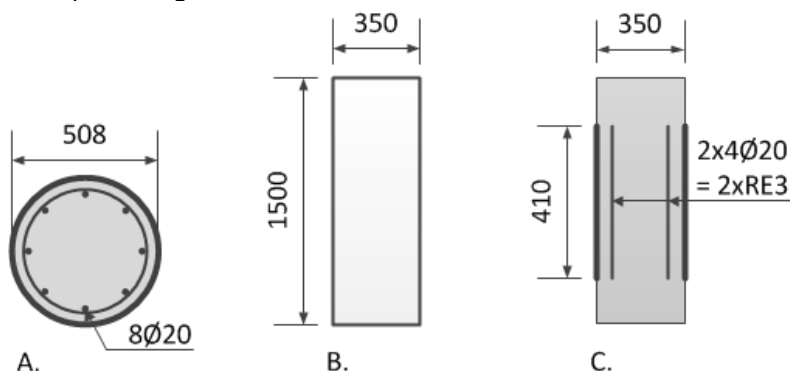


Figure 8-9 A. Cross-section of the bridge 'Schokkeringweg'; B. Elastic foundation pile; complex design foundation pile



The applied reinforcement is given in Figure 8-10 and Table 8-1. The reinforcement RE1 and RE2 are applied over a width of 1500mm. RE3 is the reinforcement in the foundation pile: Like the steel line elements, RE3 has the same area and moment of inertia as the pile reinforcement of Figure 8-9A. RE4 is the reinforcement next to the foundation pile and in this 2D FEM as reinforcement in the foundation pile. RE5 consists of 2 reinforcement loops around the foundation pile: Therefore, RE4 is modelled with the same amount as 4 bars in the foundation pile.

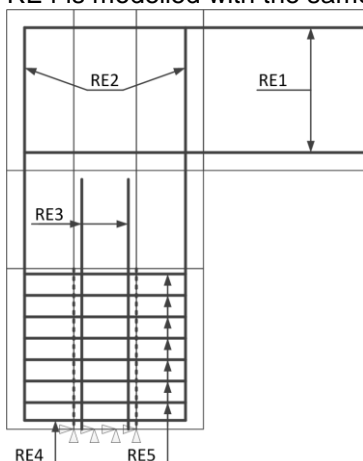


Figure 8-10 2D FEM with reinforcement

Reinforcement name	Amount	Area (A)
RE1	Ø16-100	3016 mm ²
RE2	Ø25-100	7363 mm ²
RE3	4Ø20	1250 mm ²
RE4	7Ø25	3436 mm ²
RE5	4Ø25	1963 mm ²

Table 8-1 Reinforcement in the 2D FEM

8.2.2 Material properties

The connection is composed of parts with different material properties. Basically, it consists of the concrete abutment, a part of the bridge deck and a steel pile filled with concrete as the foundation pile. This is showed in Figure 8-1. As discussed in subsection 8.1, the more advanced models have a more complex pile structure and interface elements between the steel pile and the surrounding concrete. First the concrete mixture will be explained.

8.2.2.1 Concrete (the bridge deck and the abutment)

The specifications of the materials are given in Table 8-2. These mechanical properties are based on the table 3.1 of the Eurocode [29].

Structural part	Concrete Class	E_{cm} (N/mm ²)	poisson ratio (ν)	$f_{ck;cube}$ (N/mm ²)	f_{ctm} (N/mm ²)	ϵ_u (%)
Bridge deck	C60/67	38500	0,15	67	4,2	0,2175
Abutment	C30/37	31000	0,15	37	2,9	0,2175

Table 8-2 Mechanical properties of concrete [29]



Beside the mechanical properties, the structural behaviour of the material is important. In the computer program 'TNO Diana', the compression and tension function are modelled. The selected compression and tension functions for the 2D FEM are given in Figure 8-11.

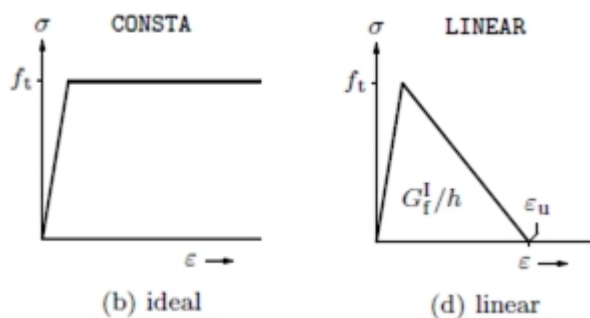


Figure 8-11 (b) predefined compression curve: Consta (d) Pre defined tension curve: Linear

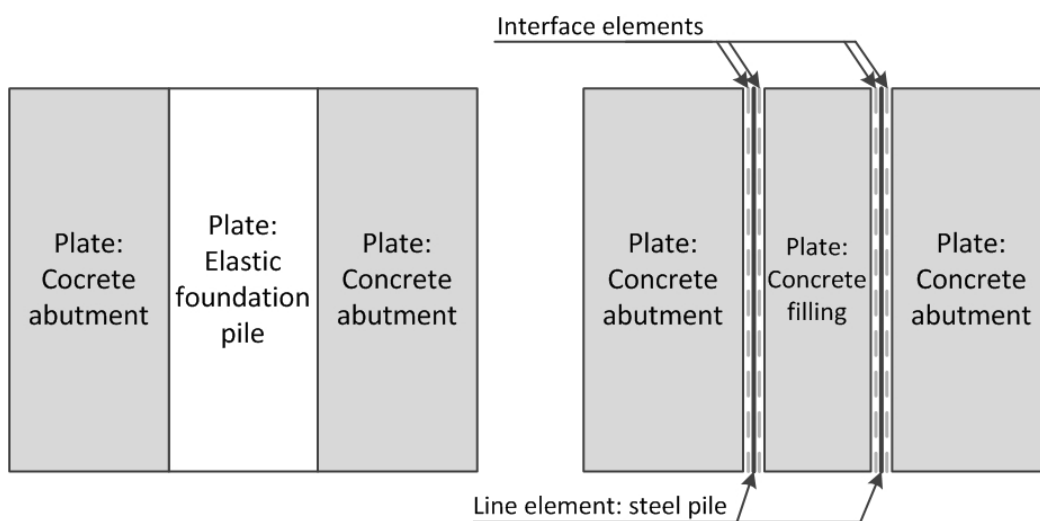
Concrete is a brittle material and will show therefore cracking behaviour. The cracking behaviour of the connection is important, because it is a decisive factor for the capacity of the connection. 'Smearred cracking' with 'a total strain rotating crack model' has been chosen for the 2D FEM. This crack model is selected, because it is well suited for cracking behaviour of reinforced concrete structures. Smearred cracking means in practice that many small cracks arise in the structural elements of the 2D FEM. This in total leads to a TNO Diana data input as shown in Figure 8-12.

1	YOUNG	3.100000E+04	2	YOUNG	3.850000E+04
	POISON	1.500000E-01		POISON	1.500000E-01
	TOTCRK	ROTATE		TOTCRK	ROTATE
	TENCRV	LINEAR		TENCRV	LINEAR
	TENSTR	2.900000E+00		TENSTR	4.200000E+00
	EPSULT	2.175000E-03		EPSULT	2.175000E-03
	COMCRV	CONSTA		COMCRV	CONSTA
	COMSTR	3.700000E+01		COMSTR	6.700000E+01

Figure 8-12 1. TNO Diana data file of the abutment (C30/37) and 2. TNO Diana data file of the bridge deck (C60/67)

8.2.2.2 The foundation pile

As discussed in subsection 8.1, the foundation pile is developed to optimize the structural behaviour of the connection. First the foundation pile is modelled as a plate with elastic material properties (Figure 8-13a) and afterwards the steel pile is defined as a plate enclosed by line elements (Figure 8-13b). The elastic material properties are a combination of the steel and concrete properties. The line elements stand for the steel pile and the plate is the concrete filling. The concrete filling has the mechanical properties of concrete C30/37 (Table 8-2). For the mechanical properties of the steel pile, see Table 8-3.



A. Model with an elastic foundation pile B. Model with plate and line elements

Figure 8-13 The two different models of the foundation pile: A. The start model with the foundation pile defined as an elastic plate element. B. The end model with the foundation pile as a concrete plate element enclosed by to steel line elements

Structural element	E_{cm} (N/mm ²)	Poisson ratio (ν)	σ - ϵ diagram
Elastic foundation pile (Figure 8-13a)	27730	0,3	x
Steel line elements (Figure 8-13b)	210000	0,3	Figure 8-14

Table 8-3 Mechanical properties of the foundation pile

The Young modulus of the elastic foundation pile is the summation Young modulus of the steel pile, the enclosed concrete element and the reinforcement. The steel line elements are applied for nonlinear structural behaviour; therefore also an σ - ϵ diagram is designed. The σ - ϵ diagram is based on section 7.1.3 of [52].

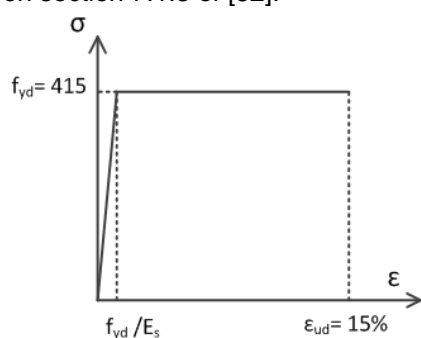


Figure 8-14 Stress-strain diagram for steel grade x60



Figure 8-15 shows the TNO Diana data for the steel line elements of Figure 8-13b.

```

3 YOUNG      2.100000E+05
  POISON     3.000000E-01
  YIELD      VMISES
  HARDIA     415. 0.002175 415. 0.15 0. 0.1501 0. 100.
  HARDEN     WORK
  
```

Figure 8-15 TNO Diana data input of the steel line elements Figure 8-13b

8.2.2.3 Interface behaviour

The interface elements are implemented in the 2D model to represent the friction between the foundation pile and the surrounded concrete elements. On both sides of the steel line elements interface elements are applied (Figure 8-6a and Figure 8-13b). The nonlinear mechanical properties of these interface elements are based on the Coulomb friction model (Figure 8-16). In the Coulomb friction model the c stands for the cohesion between concrete and steel and $\tan\phi = \mu$ is the friction between concrete and steel. The parameters for c and μ are based on the behaviour between concrete and steel scaffolding according to section 6.2.5 of the Eurocode [29]. These parameters are given in Table 8-4:

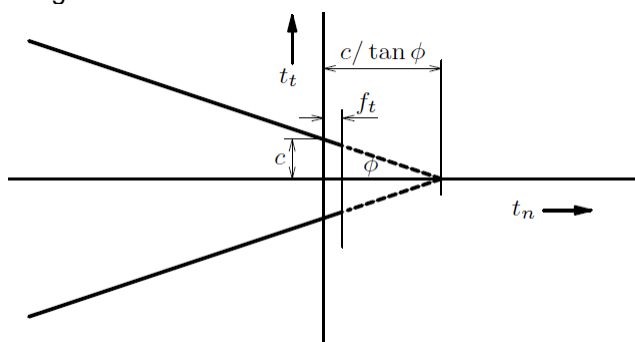


Figure 8-16 Coulomb friction model

Degree of roughness	Cohesion (c)	Friction (μ)
Very smooth	0,035	0,5
Very smooth	0,133	0,5
Smooth	0,266	0,6
Rough	0,532	0,7
Profiled	0,667	0,9

Table 8-4 Classification of the roughness of the scaffolding surface [29]



The TNO Diana data input for the interface elements with nonlinear elastic behaviour is given in Figure 8-17. The Frcval in Figure 8-17 are variables and the values of Table 8-4.

```

4 DSTIF      3.100000E+04    1.347800E+04
  FRICTI
  FRCVAL     3.500000E-02    5.000000E-01    1.000000E-05
  GAP
  GAPVAL     1.000000E-05
  MODE2      0

```

Figure 8-17 TNO Diana data input of the interface behaviour

The linear mechanical properties of interface elements are also adapted in the model. The Young modulus is the same as the concrete elements. Based on the Young modulus, the Shear modulus is determined. This is the standard equation for the Shear modulus:

$$G = \frac{E}{2(1 + \nu)}$$

8.2.2.4 Reinforcement

The material properties of the reinforcement are based on section 3.2.7 of the Eurocode [29] and section 3.2.2 of the ROK [53]. This leads to the σ - ϵ diagram of Figure 8-18 and $E_s = 210000 \text{ N/mm}^2$.

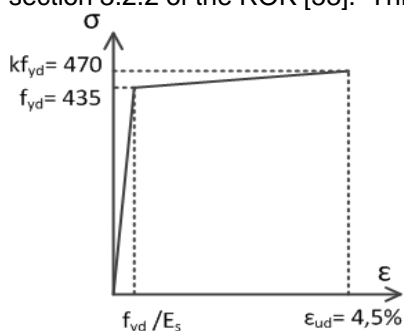


Figure 8-18 Stress-strain diagram for reinforcement steel B500B

The TNO Diana data input of the reinforcement is given in Figure 8-19.

```

7 YOUNG      2.100000E+05
  YIELD      VMISES
  HARDEN     WORK
  HARDIA     435. 0.002175 470. 0.045 0. 0.0451 0. 100.

```

Figure 8-19 TNO Diana data input of the reinforcement



8.2.3 Element types and mesh

To construct a 2D FEM, a variety of FEM elements are required. The 2D FEM consists of the regular plate elements (Figure 8-20), interface elements (Figure 8-21), regular beam elements (Figure 8-22) and embedded reinforcement elements (Figure 8-23).

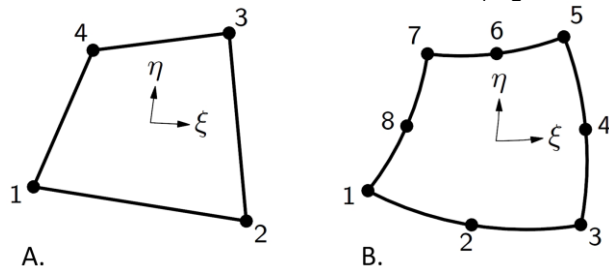


Figure 8-20 Regular plate elements A. Q8MEM and B. CQ16M

There are two types of regular plate elements applied in the first 2D FEM (Figure 8-1). The Q8MEM elements are used to calculate linear shear stresses. This is acquired for a comparison with the stringer-panel models. The CQ16MEM elements are 8 nodes elements which are used in all other 2D FEMs. These elements are based on quadratic interpolation and Gauss integration. The standard Gauss integration scheme is 2×2 , which is also applied in the 2D FEMs. The regular plate elements are used for the concrete abutment and bridge elements and the elastic pile foundation element.

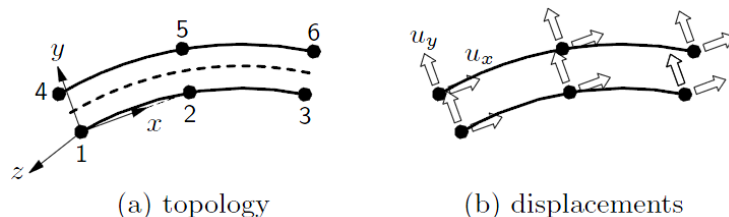


Figure 8-21 Interface element CL12I

The interface elements are applied for the frictional behaviour between the foundation pile and the concrete elements. The CL12I element is a two line element which is used in combination with 8-node regular plate elements (CQ16M).

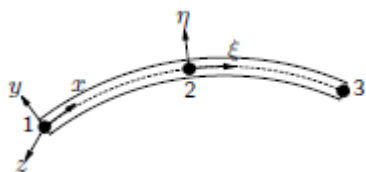


Figure 8-22 Regular beam element CL9BE

The regular beam element is used for the steel line elements of the foundation pile (Figure 8-22). This is a 3 nodes line element, which are applied in a 2D configuration. This could be in combination with an 8 node regular plate element (CQ16M) and a 3+3 node interface element (CL12I).

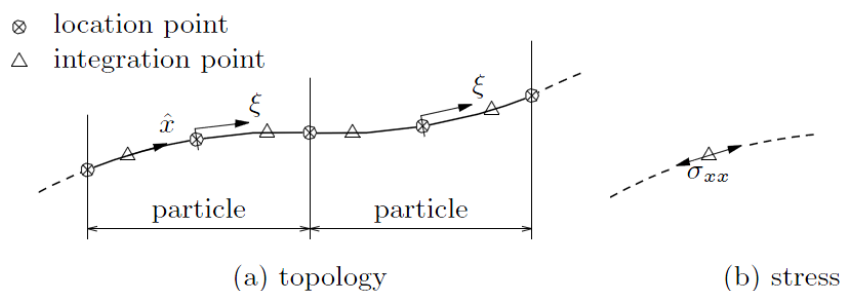


Figure 8-23 Reinforcement bar element

The reinforcement bar element is used for the reinforcement in the structural concrete elements. This means that a bar element is embedded in another element, in this case the regular plate elements.

In order to investigate which mesh size is optimal for the 2D FEM different mesh sizes are implemented. Eventually a mesh division of 4 is selected for the regular plate elements. Figure 8-24 shows the selected mesh of the 2D FEM included the reinforcement elements.

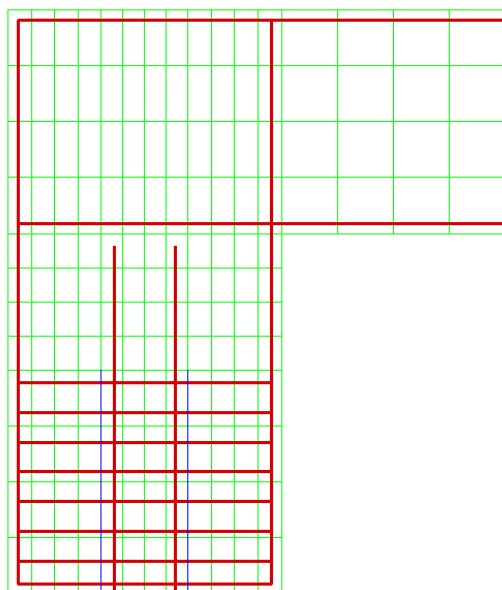


Figure 8-24 Mesh of the 2D FEM



8.2.4 Boundary conditions and loads

The loads and boundary conditions in the 2D FEM are based on the stringer-panel models of chapter 7 (Figure 8-25). The only difference between the stringer panel models of chapter 7 and the 2D FEM is that the loads are divided over the total height of the bridge structure. This is presented in Figure 8-26. The loads are divided over the total height of the bridge structure to avoid stress concentrations in the top part of the 2D FEM.

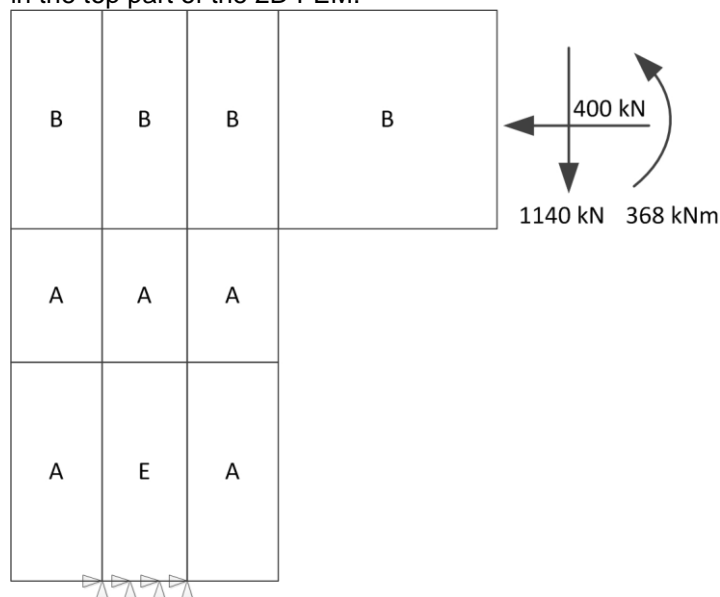


Figure 8-25 2D FEM with loads and boundary conditions

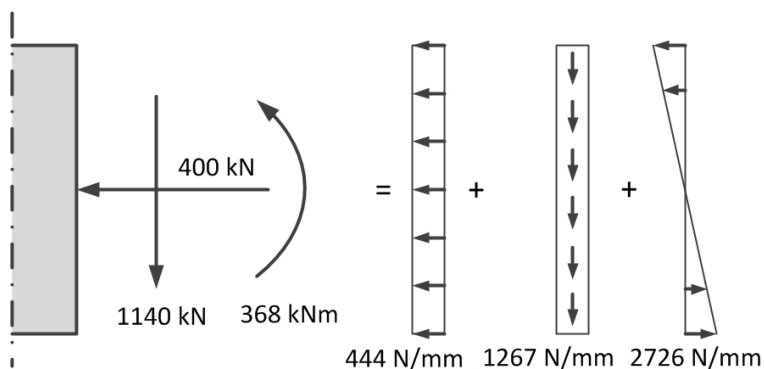


Figure 8-26 Loads implemented in the 2D FEM

The boundary conditions are set to avoid instability of the connection. This can be achieved when the sum of forces and moments are zero. In case of the connection, the forces and moments on both sides have to be in balance. Therefore, the boundary conditions at the pile foundation are set on zero for the translation in the vertical and horizontal direction (see Figure 8-25).



8.3 Analysis procedure

The analysis procedure of the 2D FEM starts when the data of section 8.2 is inputted. There are two different analyse procedures used for the connection: The linear static analysis and the nonlinear static analysis. First in subsection 8.3.1, the linear static analysis will be discussed. Followed by the nonlinear static analysis follows in subsection 8.3.2.

8.3.1 *Linear static analysis procedure*

The linear static analysis is used for the primitive 2D FEMs of section 8.1. This analysis is applied to check the boundary conditions, loads and the basic force distribution in the connection. From the results the model is further developed and evolved.

8.3.2 *Nonlinear static analysis procedure*

The nonlinear static analysis is used to analyse the complex 2D FEMs of subsection 8.1. The type of analyse procedure is developed during the first steps of the design process. The analysis procedure that is used includes force control with the arc length method and both discrete step sizes and iterative or automatic step sizes.

The arc length method is called 'indirect displacement control'. This method is used in combination with force control and gives the possibility to analyse the snap back behaviour of the connection under loading. During the snap back behaviour a part of the crack pattern of the connection develops. The information about the crack behaviour is important for the application of the FRC composites in the connection.

Force control is chosen over displacement control, because it gives better opportunities to compare the 2D FEMs with the stringer-panel models. Considering that the stringer-panel and the 2D FEMs both are loaded by forces and moments at the right side of the connection.

The analysis procedure is executed with two load cases. The first load case includes the horizontal force, the vertical force and the moment of Figure 8-26. The second load case consists only of the vertical force and the moment of Figure 8-26. The 2D FEM is first loaded with the first load case (1,0x) and then loaded with an increasing second load case until the connection fails. The second load case is executed without the horizontal force, because the horizontal force works in the opposite direction of the vertical force. This leads to a disruption in the structural behaviour of the connection in the ultimate limit state (ULS). A second load case with only a horizontal force is also possible, but a horizontal force in this 2D FEM has less influence on the structural behaviour. This changes when parameters as length or the soil condition are different. Other parameters are described in chapter 4.



As mentioned before, three different load step sizes are used: Discrete, iterative and automatic step sizes. The discrete step size is an explicitly specified step size and is only used for the first load case. The iterative and automatic step size causes both automatic adaptive load increments. The advantage of these automatic load increments is that a load step is automatically decreased if the iterative procedure fails convergence. Arc length control is adapted to the iterative and automatic step size. Arc length control is not possible in combination with the discrete step size. The automatic step size is also used for the first load case if the discrete step size fails convergence. The iterative step size is explicitly applied for the second load case.

8.3.3 Validation of the 2D FEM

The validation of the 2D FEM is an important check if the 2D FEM is correctly built. The validation consists of some important steps. These steps are:

- To check if the reaction forces at the boundary conditions were in correspondence with the loads. This is checked for all 2D FEMs.
- During the design process also stresses at significant points in the structure were checked. The model was modified when this was incorrect with the expectations of the results. As shown in section 8.1.
- A comparison of the results of the analysis with the stringer panels of chapter 7. This will be done in section 8.5

8.4 Results

As discussed in chapter 7, the moments and forces from the superstructure to the pile foundation are transferred by a coupling force in the foundation pile and by shear interaction between the foundation pile and the surrounding concrete. Both mechanisms are affected by the structural design of the connection; the shear interaction depends strongly on friction between steel and concrete and the coupling force is in large extent only possible when there is sufficient horizontal reinforcement at the bottom of the connection. The friction between steel and concrete and the reinforcement are both variables of the 2D FEM of Figure 8-7. In this subsection, these variables are researched due to deviation of the 2D FEMs. In total 4 variations of the standard 2D FEMs of Figure 8-7 are developed. These 2D FEMs have all only one variable. These models are:

	<i>Amount of horizontal loop reinforcement bars</i>	<i>Cohesion (c) and friction (μ)</i>	<i>Amount of reinforcement of the lowest bar</i>
Model 1	variable	Standard ($c=0.035$ and $\mu=0.5$)	Standard (3436 mm ²)
Model 2	8 loop reinforcement bars	variable	Standard
Model 3	1 loop reinforcement bar	Standard	Variable
Model 4	No reinforcement	variable	Standard

Table 8-5 the variation models of 2D FEM of Figure 8-7

Table 8-5 shows 4 models with 3 variables. These variables are the amount of loop reinforcement bars, cohesion and friction and the amount of reinforcement in the lowest bar. The amount of loop reinforcement bars are the horizontal reinforcement bars which are located near the foundation pile. This is shown in Figure 8-27. The lowest bar is loop reinforcement bar 1 and the upper bar is loop reinforcement bar 8. For example, model 3 has 3 loop reinforcement bars which are the lowest 3



reinforcement bars of Figure 8-27. The second variable which is the variable for model 2 and model 4 is cohesion and friction. In these two models, the cohesion and friction changes for the interface elements outside of the foundation pile. This is showed in Figure 8-27. The last variable is the amount of reinforcement of the lowest bar. The reinforcement in the lowest bar is normally 3436 mm^2 , but variable for model 3.

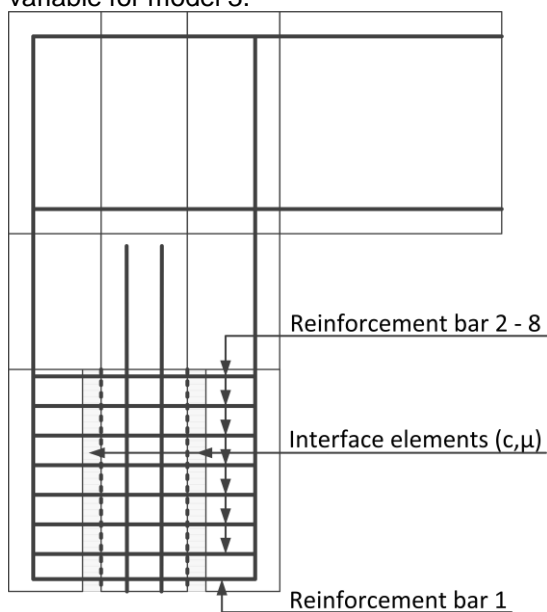


Figure 8-27 The variables of the different models based on the 2D FEM of Figure 8-7

The influence of the variables will be discussed in the next subsections. Also, the results will be presented in the subsections. Two important aspects that are analysed are: the total bearing capacity and the cracking behaviour of the connection.

8.4.1 Model 1: Influence of the loop reinforcement over the pile length

The first model varies in the number of horizontal loop reinforcement bars over the total pile length. There are in total 8 reinforcement bars in the 2D FEM of Figure 8-27 (7 loop reinforcement bars and 1 horizontal reinforcement bar at the bottom of the connection). In this subsection, the number of horizontal reinforcement bars is reduced in order to research its effect on the structural behaviour of the connection. Therefore, 7 sub models are developed with a different amount of horizontal reinforcement bars. These sub models have respectively 8, 6, 4, 3, 2, 1 or no reinforcement bars. These sub models are analysed and the results are presented in this subsection. The first part of the results is plotted in the force-displacement diagram of Figure 8-28. The force-displacement diagram shows the strength of the connection of each sub model. The models with more than 1 reinforcement bar have a similar force-displacement ratio in the first branch (until 1140kN). This changes in the second branch (after 1140 kN). Then the strength of the connection is less for models with a lower number of reinforcement bars. The model with only 1 reinforcement has a lower structural strength than the models with more reinforcement bars. Also, the displacement of the model with 1 reinforcement bar is significantly larger after 600 kN. The force-displacement also shows that the model with no reinforcement has much lower structural strength and the displacement increases



more. This means that horizontal reinforcement in the area of the foundation pile has major contribution to the structural strength of the connection.

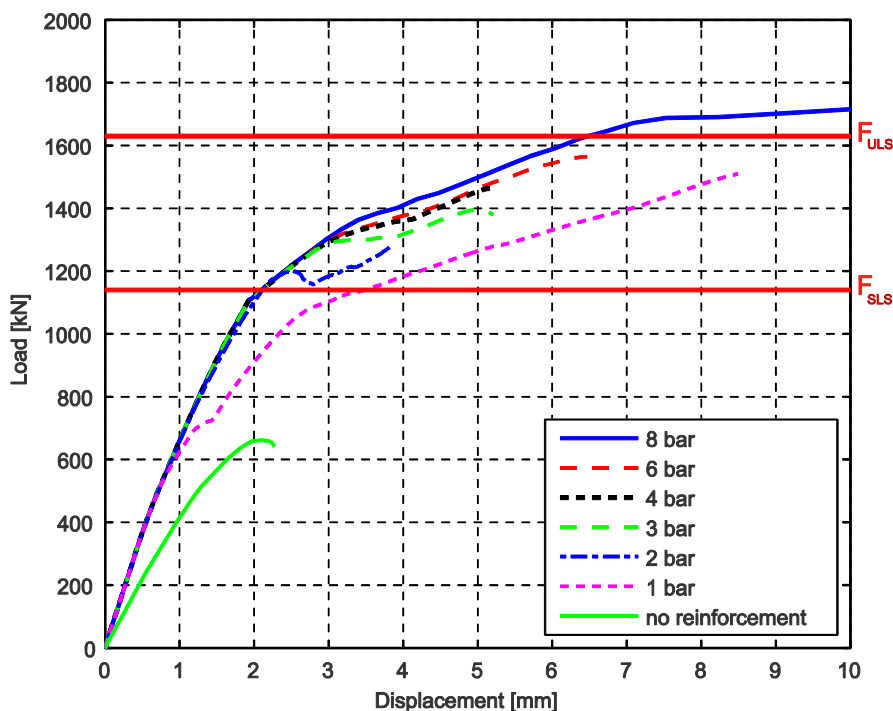


Figure 8-28 Force-displacement diagram: Influence of the horizontal reinforcement bars

Table 8-6 shows the critical values of Figure 8-28. The crack width at the service limit state (SLS) shows that a lower number of bars than the standard amount has no influence on the crack width. This is not applicable for the models with 1 bar and no reinforcement. The values of the ultimate limit state (ULS) for the crack width and the force show that the structural strength of the connection is less for a lower number of bars.

Number of bars	w_{SLS}	w_{ULS} at $F=1373$ kN	F_{ULS}
8 bars	0,22 mm	0,24 mm	1795 kN
6 bars	0,21 mm	0,24 mm	1564 kN
4 bars	0,20 mm	0,24 mm	1463 kN
3 bars	0,20 mm	0,28 mm	1396 kN
2 bars	0,22 mm	0,45 mm	1373 kN
1 bar	0,34 mm	0,53 mm	1510 kN
No reinforcement	x	∞	661 kN

Table 8-6 Critical values of Figure 8-28

The next step of the results is to analyse the cracking and structural behaviour. The cracking behaviour of the sub model with 8 reinforcement bars is presented in Figure 8-29. Cracks occur at two locations: the first crack is a vertical crack at the left side next to foundation pile (Figure 8-29A)



and the second crack is a horizontal crack at the right concrete section (Figure 8-29B). This cracking behaviour is the same for the other sub models.

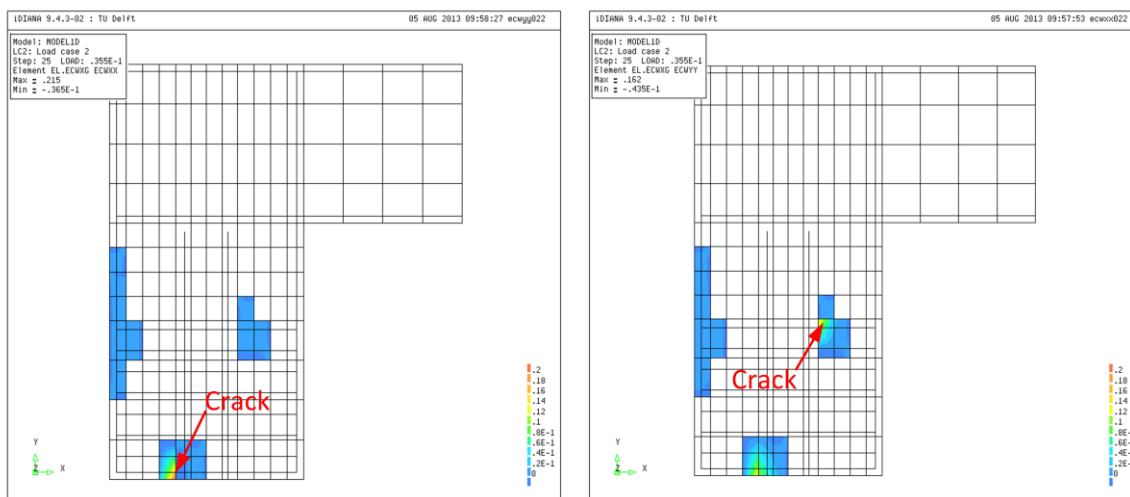


Figure 8-29 A. Crack width in x-direction and B. Crack width in y-direction ($F=1140$ And max. crack width = 0.2)

Figure 8-30 shows the cracking behaviour at the moment of failure for the sub models with 8 or 3 reinforcement bars. The sub model with 8 bars has a horizontal crack at the foundation pile. This is location where failure occurs. The sub models with 6 and 4 bars shows the same cracking behaviour. A vertical crack next to the foundation pile is decisive when the number bars is further reduced. This applies for the sub models with 1, 2 or 3 bars. The vertical crack occurs due to failure of the horizontal reinforcement bars. This means that sub models with a small number of bars fail due to failure of horizontal reinforcement and the sub models with a large number bars show failure of the concrete at the top of the foundation pile.

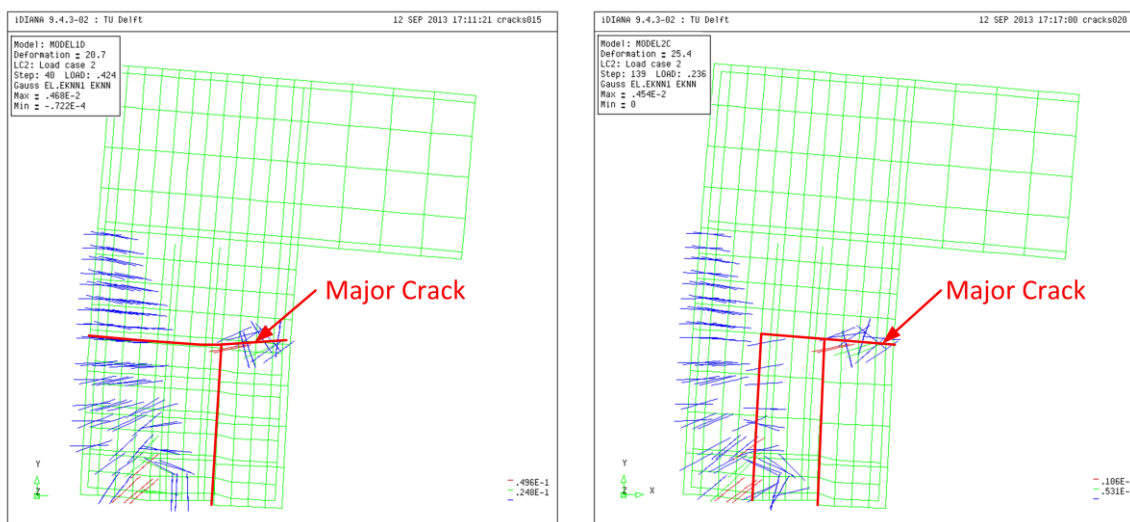


Figure 8-30 Crack patterns at moment of failure for: A. sub model with 8 reinforcement bars and B. sub model with 3 reinforcement bars



As mentioned before, the displacement of the sub model with 1 reinforcement is significantly larger than for sub models with a larger number of bars. Figure 8-31 shows the crack width in the x-direction for the sub models with 3 and 1 bars. In the connection, this leads to larger vertical crack at the right side of the foundation pile.

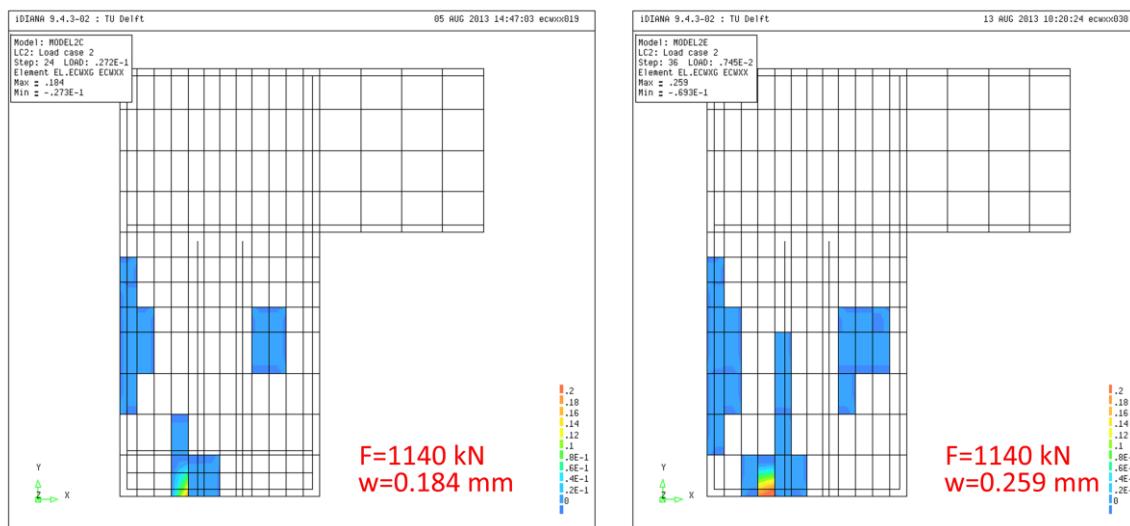


Figure 8-31 Crack width in y-direction at $F=1140$ kN for A. sub model with 3 reinforcement bars (max crack width of 0.184 mm) and B. sub model with 1 reinforcement bar (max. crack width of 0.259 mm)

The force-displacement diagram Figure 8-28 also shows a sub model without reinforcement. The strength of the connection of the sub model without reinforcement is small in comparison with the sub models with reinforcement. Figure 8-32 shows the sub model with no reinforcement. The connection fails due to large vertical crack at right side of the foundation pile. This vertical crack is much larger than for the sub models with horizontal reinforcement. So, the application of horizontal reinforcement leads to increase of the strength of the connection and to significantly smaller cracks.

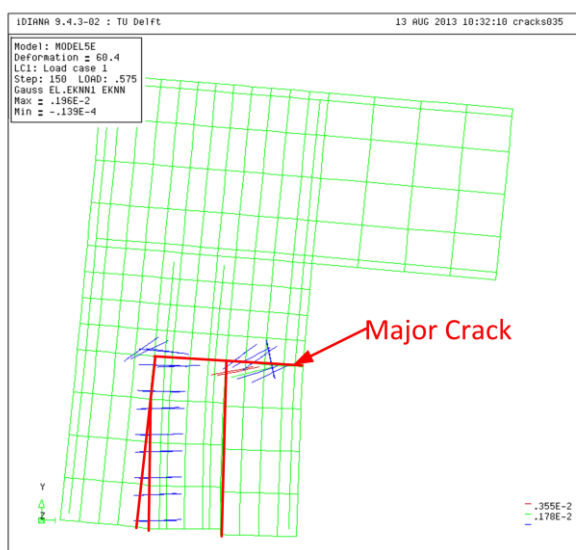


Figure 8-32 Crack pattern for sub model without reinforcement



Figure 8-33 shows the stresses in the reinforcement for x- and y- direction at moment of failure. The red- and yellow-coloured areas represent tension in the reinforcement. The tension in x-direction is located in the lowest bars of the horizontal reinforcement at the left side of the foundation pile. This means that tension occurs at the left side of the foundation pile. The same results occurred in the other 2D FEMs with horizontal reinforcement. A vertical crack arises when no reinforcement was applied. The figure at the right shows that the tension is concentrated in the reinforcement of the foundation pile: In particular at the left side of the foundation pile. Tension also occurs in the vertical bar at left side of the connection. However, these tensile stresses are comparably low.

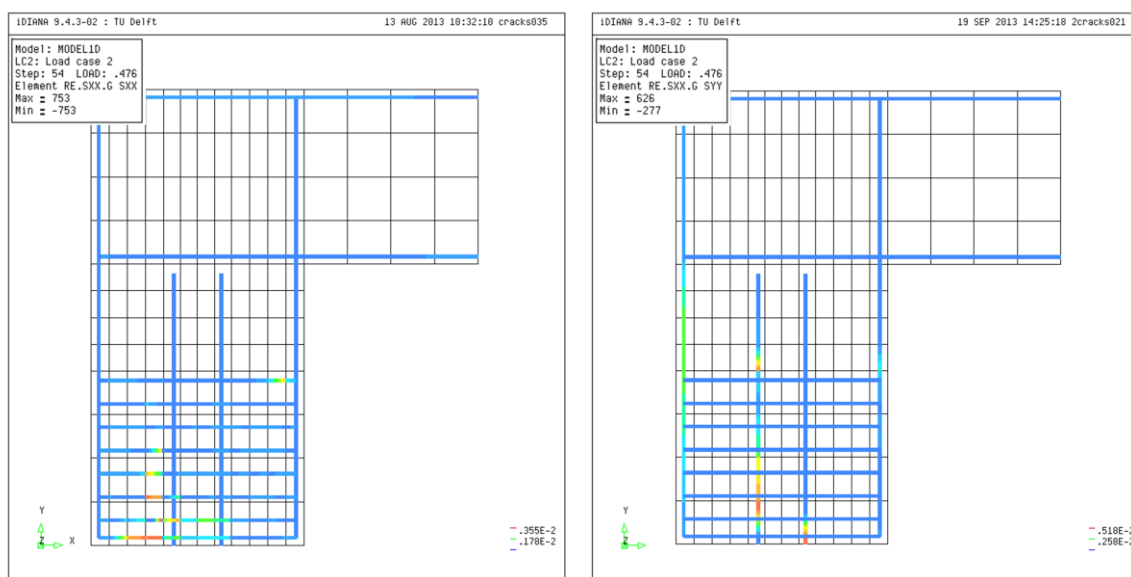


Figure 8-33 Stresses in reinforcement at moment of failure: A. in x-direction and B.in y-direction

8.4.2 Model 2: Influence of the cohesion and friction of a 2D FEM with reinforcement

The variables of model 2 are cohesion and friction of the interface elements between the foundation pile and the surrounded concrete elements. The horizontal loop bars are applied over the total height of the foundation pile. This means in total 8 reinforcement bars with a standard amount for the lowest bar (Figure 8-27). In total 6 sub models are developed to analyse the effect of cohesion and friction of the interface elements on the structural behaviour of the connection. The values of cohesion and friction are based on Table 8-4. The values are given in Figure 8-34.

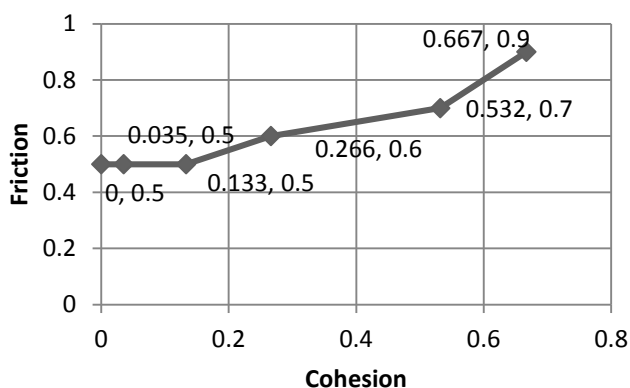


Figure 8-34 Chart of model 2 with cohesion and friction as variable

Figure 8-35 shows the force-displacement diagram for sub models with cohesion and friction as variable. As displayed, the structural behaviour is similar for different sub models. This means that the influence of cohesion and friction on the structural strength of the connection is insignificant.

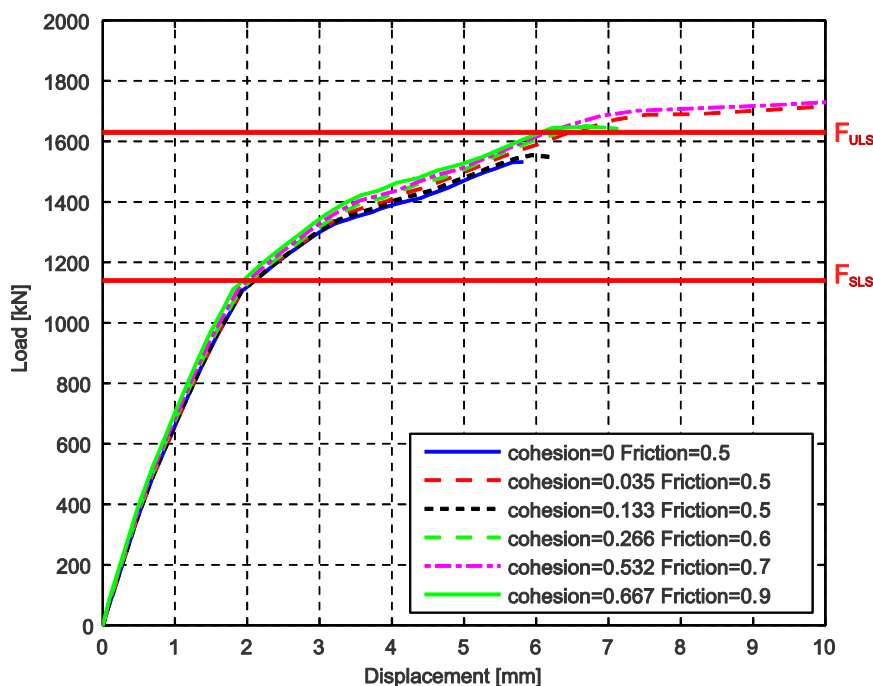


Figure 8-35 Force-displacement diagram: Influence cohesion and friction; with reinforcement

Table 8-7 shows the critical values of Figure 8-35. The structural behaviour for sub models with a higher cohesion and friction coefficients are the same as for the sub models with lower cohesion and friction coefficients. This means that according to Table 8-7 the cohesion and friction coefficients have no influence on the structural behaviour. Some sub models have a higher value for w_{ULS} and F_{ULS} . This is however for sub models with a low and high coefficients and is therefore not depending on cohesion and friction.



<i>Cohesion and Friction</i>	W_{SLS}	W_{ULS}	F_{ULS}
c=0 and $\mu=0,5$	0,21 mm	0,34 mm	1532 kN
c=0,035 and $\mu=0,5$	0,22 mm	6,17 mm	1795 kN
c=0,133 and $\mu=0,5$	0,21 mm	0,35 mm	1548 kN
c=0,266 and $\mu=0,6$	0,21 mm	0,41 mm	1642 kN
c=0,532 and $\mu=0,7$	0,21 mm	5,96 mm	1779 kN
c=0,667 and $\mu=0,9$	0,20 mm	0,40 mm	1646 kN

Table 8-7 Critical values of Figure 8-35

The next step is to analyse the cracking and structural behaviour of the connection. Figure 8-36 shows the crack width in the y-direction before failure of the connection of the sub model with cohesion of 0 and friction of 0.5 and the sub model with cohesion coefficient of 0.666 and a friction coefficient of 0.9. Both sub models show the same cracks in the y-direction: A major horizontal crack located above the foundation pile and a concentration of cracks at left side of the foundation pile. The major horizontal crack is eventually decisive for all the sub models with cohesion and friction as variables.

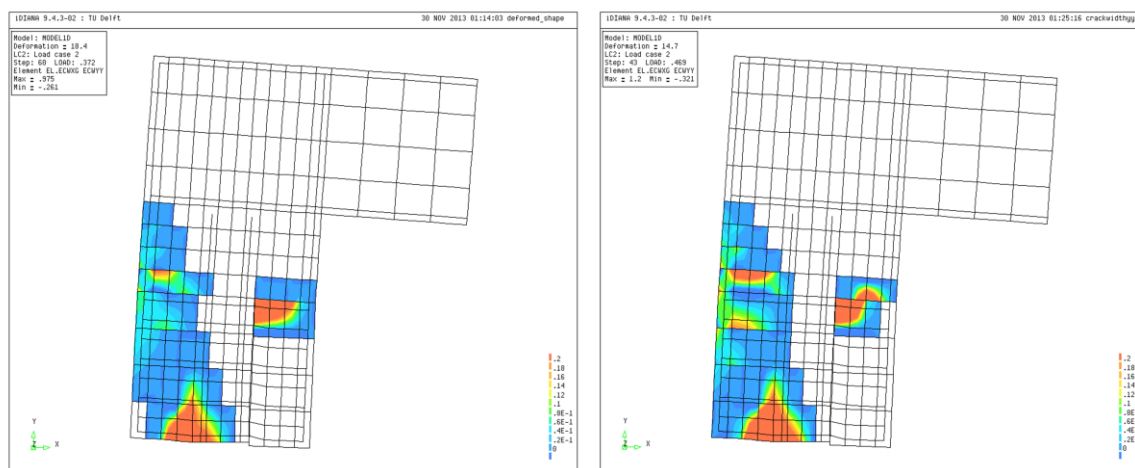


Figure 8-36 Crack width in y-direction for A. sub model with cohesion=0 and friction=0.5 and B. sub model with cohesion=0.667 and friction=0.9

Figure 8-37 shows the crack width in x-direction for the sub model with cohesion of 0 and friction of 0.5 and for the sub model with cohesion of 0.667 and friction of 0.9. The figure is taken at a force of 1140 kN which is the end point of the first branch of the force-displacement diagram of Figure 8-35. As showed in Figure 8-37, the crack width in x-direction is smaller for the sub model with cohesion of 0.667 and friction of 0.9. This is however very small and therefore negligible.

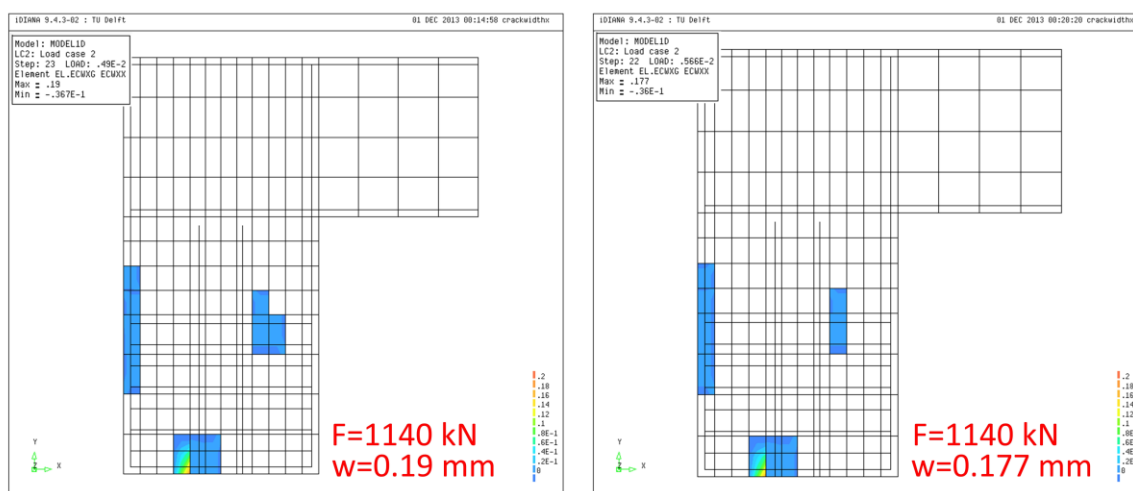


Figure 8-37 Crack width in x-direction at $F=1140$ kN for A. sub model with cohesion=0 and friction=0.5 (max. crack width=0.19 mm) and B. sub model with cohesion=0.667 and friction=0.9 (max. crack width=0.177 mm)

In summary, a higher value for cohesion or friction does not lead to a major improvement of the strength or structural behaviour of the connection. This is also applicable for the cracking behaviour of the connection which is similar for the different sub models.

8.4.3 Model 3: Influence of the horizontal reinforcement at the bottom of the connection

Model 3 is the 2D FEM of Figure 8-27 with only the 1 horizontal reinforcement bar at the bottom of the connection. Model 3 is developed to analyse the influence of the lowest horizontal reinforcement bar. As discussed before in section 7.1, the horizontal reinforcement at the bottom is important, because it controls the crack width and it improves the structural strength of the connection. This subsection focuses on the influence of the horizontal reinforcement by adapting the amount of the reinforcement. In total 5 sub models are developed with a different amount of reinforcement. The reinforcement amounts are respectively 0, 1000, 2000, 3436 and 5000 mm².

Figure 8-38 shows the force-displacement diagram of model 3. The 2D FEM based on the 'Schokkeringweg' has a reinforcement amount of 3436 mm². The force-displacement diagram shows that the strength of the connection is not significantly improved by applying a larger amount of reinforcement. Also, a small reduction of the reinforcement (sub model 2000 mm²) does not decrease the strength of the connection a lot. When the reinforcement amount is further reduced, the strength of the connection decreases too.

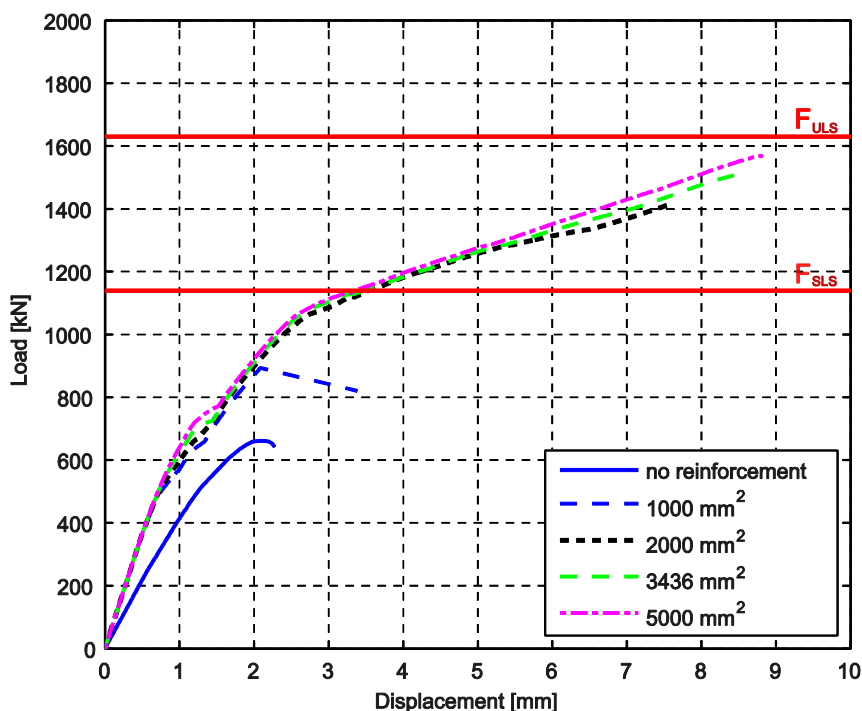


Figure 8-38 Force-displacement diagram: Amount of horizontal reinforcement at the bottom of the connection

Table 8-8 shows the crack width and force of the different sub models in SLS and ULS. This table shows that the crack width in the SLS decreases when the amount of reinforcement increases. Also, F_{ULS} increases when the amount of reinforcement increases. This means that the amount of reinforcement has a significant influence on the both the crack width and the structural strength of the connection.

Number of bars	w_{SLS}	w_{ULS}	F_{ULS}
No reinforcement	x	∞	661 kN
1000 mm²	x	0,44 mm	893 kN
2000 mm²	0,37 mm	0,67 mm	1417 kN
3436 mm²	0,34 mm	0,67 mm	1510 kN
5000 mm²	0,27 mm	0,66 mm	1568 kN

Table 8-8 Critical values of Figure 8-38

The next is to analyse the cracking and the structural behaviour of the sub models. Figure 8-39 shows the crack patterns at moment of failure for the sub models with 1000 and 3436 mm² reinforcement in the lower horizontal bar. Both models have a vertical crack at the right side of the foundation pile and a horizontal crack at the top of the foundation pile. The vertical crack arises, when the horizontal reinforcement starts yielding. This process starts earlier for the sub model with 1000 mm². Therefore, the strength of the connection for the sub model with 1000 mm² is lower than the sub models with more reinforcement. This behaviour is also visible in the force-displacement diagram of Figure 8-38.

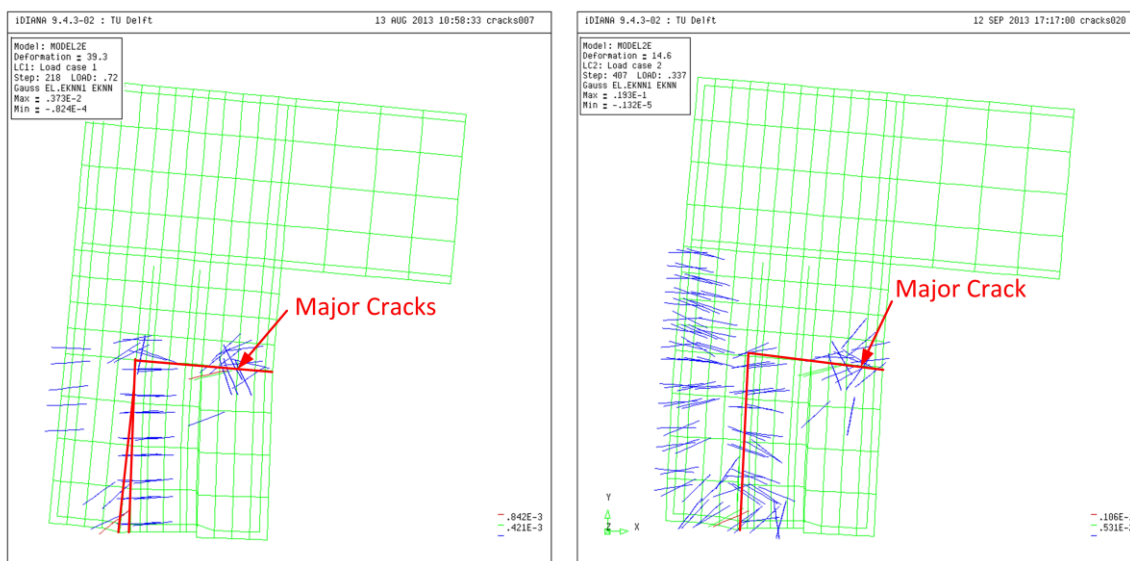


Figure 8-39 Crack patterns for A. sub model with 1000 mm² reinforcement and B. sub model with 3436 mm² reinforcement

The crack width in y-direction for the sub models with 1000 and 3436 mm² is presented in Figure 8-39. The force-displacement diagram of Figure 8-38 showed that an increase of the amount of reinforcement in the horizontal bar does lead to an improvement of the strength of the connection in the final stage. The two figures show similar cracking behaviour at the moment of failure. This is a large horizontal crack above the foundation pile and vertical crack at the left side of the foundation pile. The horizontal cracks in Figure 8-40B of the sub model with 3436 mm² are the main difference between the two sub models. This means that more reinforcement leads to an improvement of the strength, but also increases the tension at the left side of the connection. Therefore, more cracking occurs at the left side of the connection.

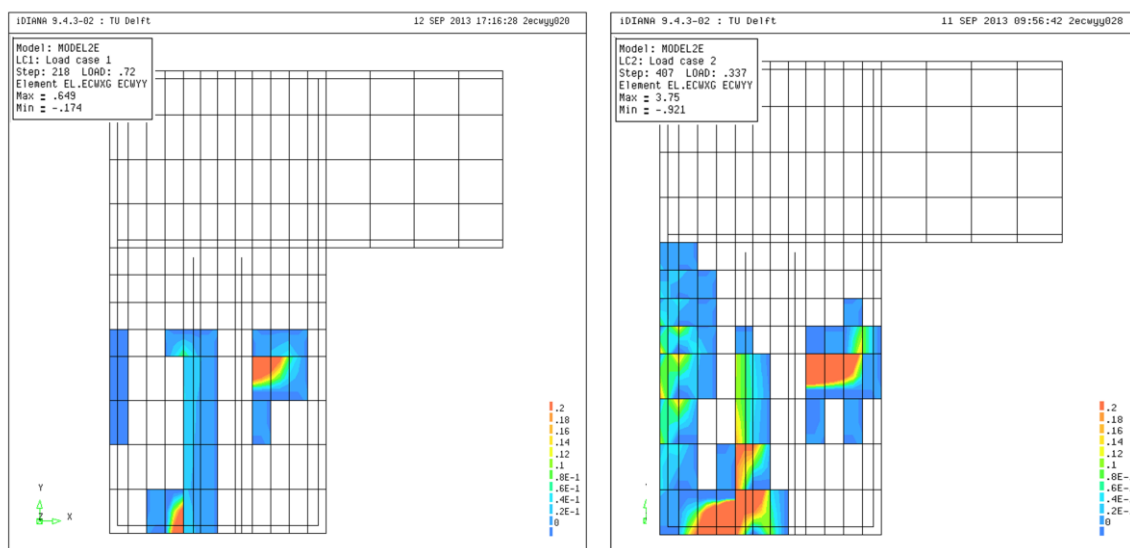


Figure 8-40 Crack width in y-direction for A. sub model with 1000 mm² reinforcement and B. sub model with 3436 mm² reinforcement



As mentioned before, a major vertical crack arises at the left side of the foundation pile. This crack decreases when the amount of reinforcement increases. The crack width in x-direction is given in Figure 8-40. Figure 8-41 shows the crack width for the sub models with 2000 and 5000 mm². The largest decrease of crack width occurs when the amount of reinforcement is upgraded from 2000 to 3436 mm². A further increase of the amount of reinforcement does lead to further a decrease of the crack width. However, a lot of extra reinforcement is needed for only a small improvement.

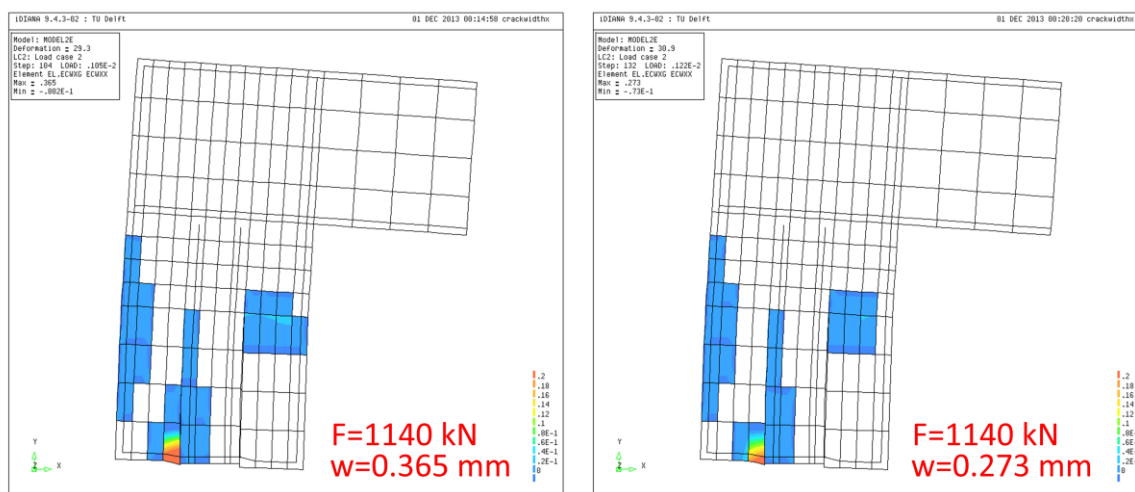


Figure 8-41 Crack width in x-direction at $F=1140$ kN for A. sub model with 2000 mm² reinforcement (max. crack width of 0.365 mm) and B. sub model with 5000 mm² reinforcement (max. crack width of 0.273 mm)

8.4.4 Model 4: Influence of cohesion and friction in a 2D FEM without horizontal reinforcement

Model 4 is developed to investigate the influence of cohesion and friction of the interfaces between the foundation pile and the surrounded concrete elements. In model 4, no reinforcement is applied in the horizontal direction. This means that the strength of the connection depends largely on the friction between the foundation pile and the surrounded concrete. In total 6 sub models are developed. These models are given in Figure 8-42:

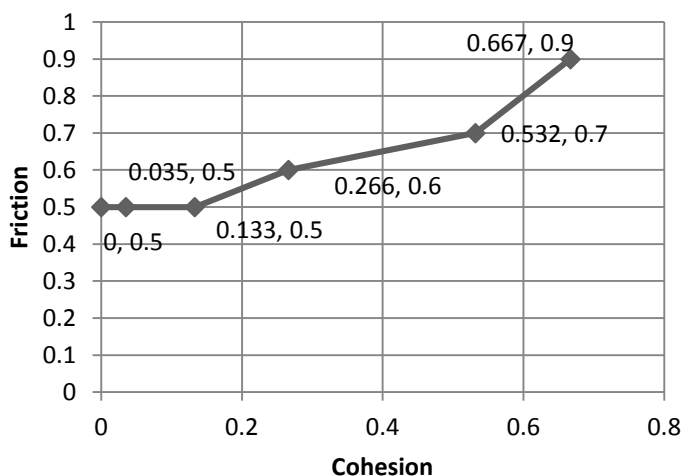


Figure 8-42 Chart of model 4 with cohesion and friction as variable (based on Table 8-4 and indirectly on the Eurocode [29])



The sub models are analysed and the results will be presented in this subsection. In the results different aspects are researched. The aspects are the strength, the structural behaviour and cracking behaviour of the connection. First the strength of the connection is presented in the force-displacement diagram of Figure 8-43. The force-displacement diagram shows that the strength of the connection improves when the friction increases. However, the improvement is small. The force-displacement diagram also shows that cohesion has no influence on the strength of the connection. The sub models with cohesion 0, 0.35 and 0.133 have the same structural behaviour according to the force-displacement diagram.

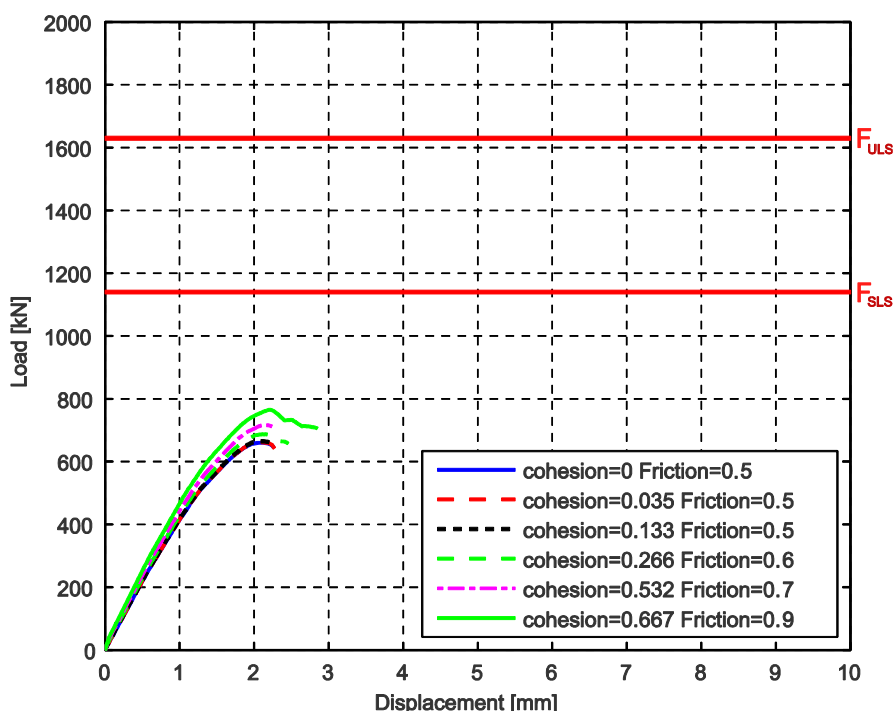


Figure 8-43 Force-displacement diagram: Cohesion and friction; without reinforcement

As showed in Figure 8-43, F_{SLS} is not reached for all sub models. Therefore, the crack width is listed as 'x' in Table 8-9. W_{ULS} is set on ∞ , because at moment of failure, the crack width on the left side of the foundation pile is relative large. Table 8-9 shows that F_{ULS} increases, when the friction coefficient increases. This that friction has a small influence on the structural strength of the connection for FEM without reinforcement.

Cohesion and Friction	W_{SLS}	W_{ULS}	F_{ULS}
c=0 and $\mu=0,5$	x	∞	660 kN
c=0,035 and $\mu=0,5$	x	∞	661 kN
c=0,133 and $\mu=0,5$	x	∞	665 kN
c=0,266 and $\mu=0,6$	x	∞	673 kN
c=0,532 and $\mu=0,7$	x	∞	716 kN
c=0,667 and $\mu=0,9$	x	∞	733 kN

Table 8-9 Critical values of Figure 8-43



The crack patterns at the moment of failure of the sub model with cohesion of 0 and friction of 0.5 and the sub model with cohesion of 0.667 and friction of 0.9 are presented in Figure 8-44. The crack patterns are similar. This means a large horizontal crack at the left of the foundation pile and a vertical at top of the foundation pile at the moment of failure. The vertical crack is important, because the development of this crack is the indicator for failure. The connection fails when the vertical crack is fully developed. The development of the vertical crack for sub models with a high friction coefficient is slower than for sub models with a low friction coefficient. Therefore, the sub models with a high friction coefficient perform better in the force-displacement diagram. However, this improvement is low.

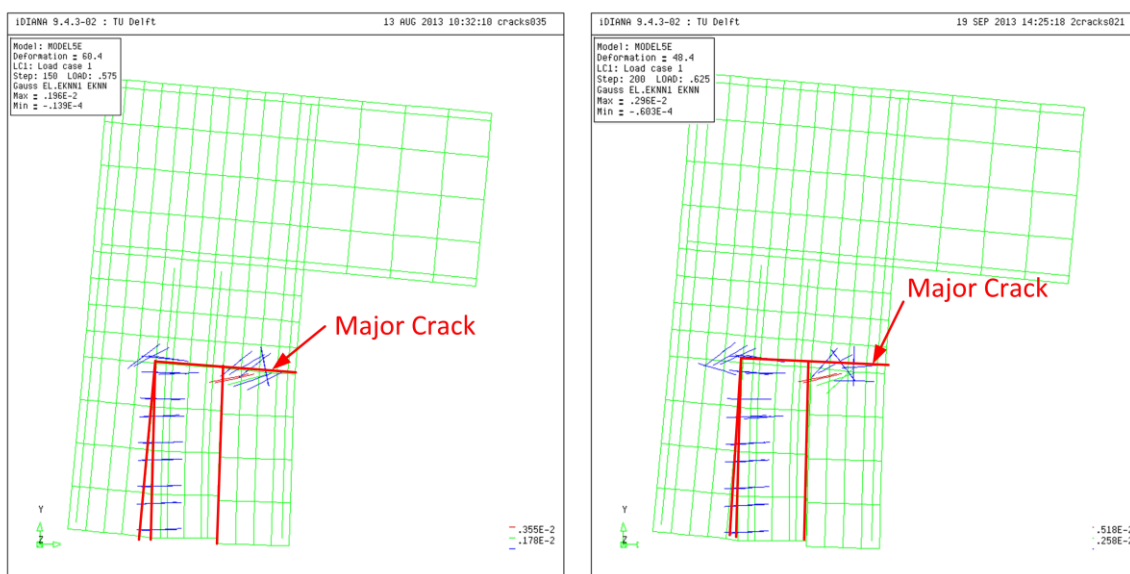


Figure 8-44 Crack patterns at moment of failure for: A. sub model with cohesion=0 and friction=0.5 and B. sub model with cohesion=0.667 and friction=0.9

8.4.5 A combination of variables

In the last subsections, the results of the influence of different variables are discussed. In this subsection, the results of different variables are combined. This is showed in Table 8-10. In total four models are compared. These are the minimum and maximum number of horizontal reinforcement bars and the minimum and maximum cohesion and friction. The other variable, the amount of reinforcement in the lowest horizontal is excluded in this subsection.

	Cohesion=0.035 and friction=0.5	Cohesion=0.667 and friction=0.9
No horizontal reinforcement bars	Model A	Model C
8 horizontal reinforcement bars	Model B	Model D

Table 8-10 A combination of two variables: the number of reinforcement bars and cohesion and friction



The force-diagram of the sub models of Table 8-10 are given in Figure 8-45. The force-displacement diagram shows that horizontal reinforcement has a major influence on the strength of the connection and on the total displacement of the connection (model B and D). Higher values for cohesion and friction lead to a small improvement of the structural behaviour (model A vs. model C), but this is low in comparison with the improvement due to horizontal reinforcement (model A vs. model B).

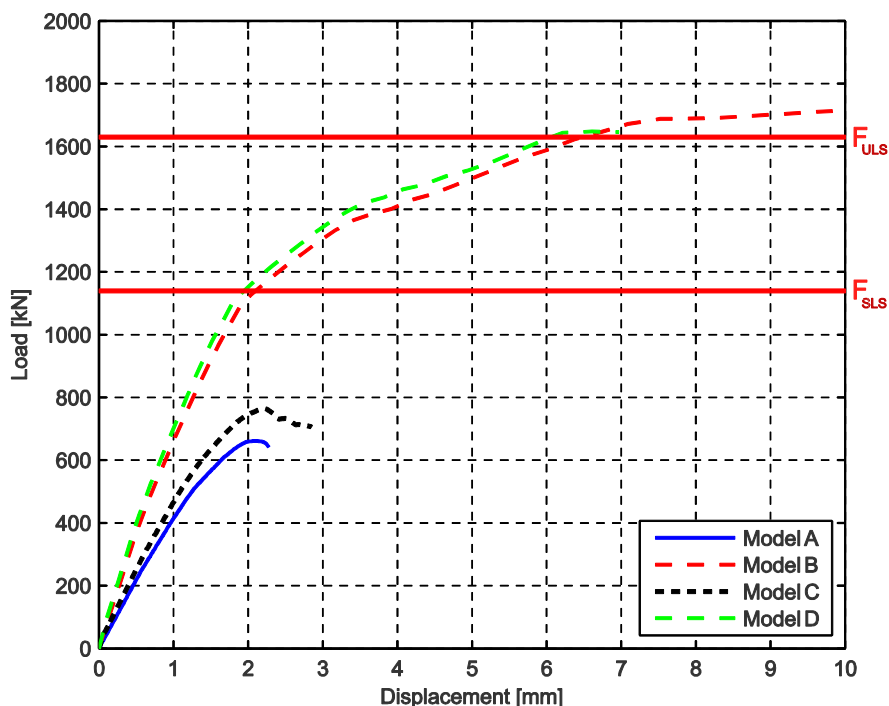


Figure 8-45 Force-displacement diagram: Combination of two variables

Figure 8-46 presents the crack patterns for the different sub models. The difference between the sub models with and without reinforcement is the cracking behaviour. For sub models without reinforcement (Figure 8-46 model A and C), a large vertical crack exist on the left side of the foundation pile. This vertical crack is only possible when the horizontal reinforcement is absent, because as showed before the tension in the x-direction is concentrated at left of the foundation pile. The sub models with horizontal reinforcement (Figure 8-46 model B and D) fail due to a horizontal crack at the top of the foundation pile. Figure 8-46 also shows that cohesion and friction have no influence on the cracking behaviour of the connection.

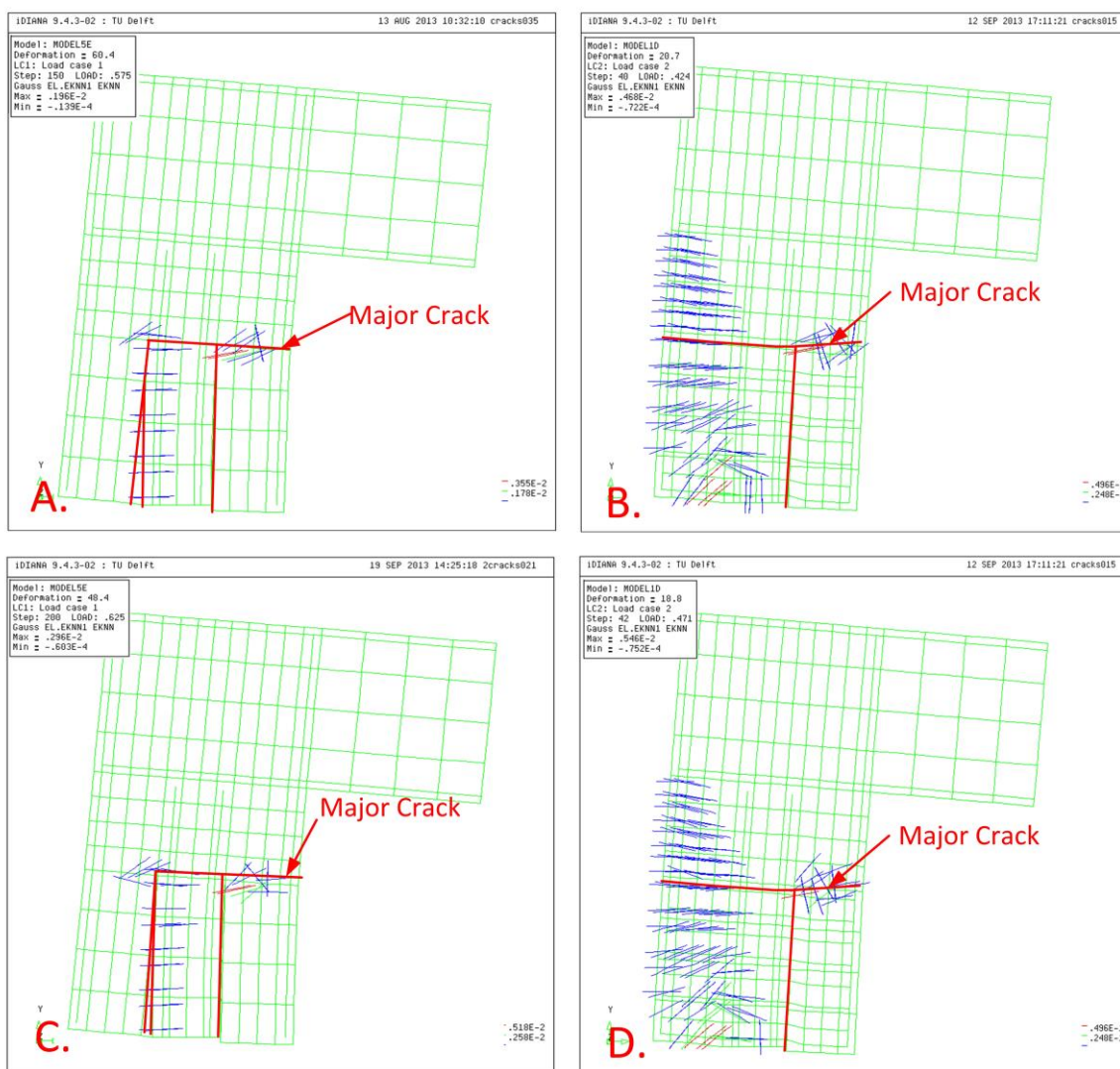


Figure 8-46 Crack patterns at moment of failure for: model A. sub model with cohesion=0.035 and friction=0.5 and without horizontal reinforcement, model B. sub model with cohesion=0.035 and friction=0.5 and 8 horizontal reinforcement bars, model C. sub model with cohesion=0.667 and friction=0.9 and without horizontal reinforcement and model D. sub model with cohesion=0.667 and friction=0.9 and 8 horizontal reinforcement bars.



8.4.6 Potential improvements

This section described, the influence of the horizontal bars and the cohesion and friction coefficients. The choice for these two parameters was based on section 7.1. Other parameters were not used for variation. In this sub section some other parameters are researched. These parameters are chosen based on the results of the subsection 8.4.1 to 8.4.4. The results showed that the FEM failed due to a horizontal crack above the foundation pile and high stresses in the foundation pile. Therefore, parameters that could have influence on this behaviour are researched. These parameters are (Figure 8-47):

1. The amount of reinforcement in the vertical bars: The amount of reinforcement in the vertical bars is modified to investigate the influence of the vertical bars on the structural behaviour of the connection.
2. An extra vertical reinforcement bar: The results of the subsection 8.4.1 to 8.4.4 showed that a horizontal crack arises on the left side of the foundation pile. Therefore, a vertical bar is added to the FEM.
3. The thickness (t) of the steel foundation pile: The thickness of the steel foundation pile is adapted to investigate the influence of the foundation pile on the structural behaviour of the connection.

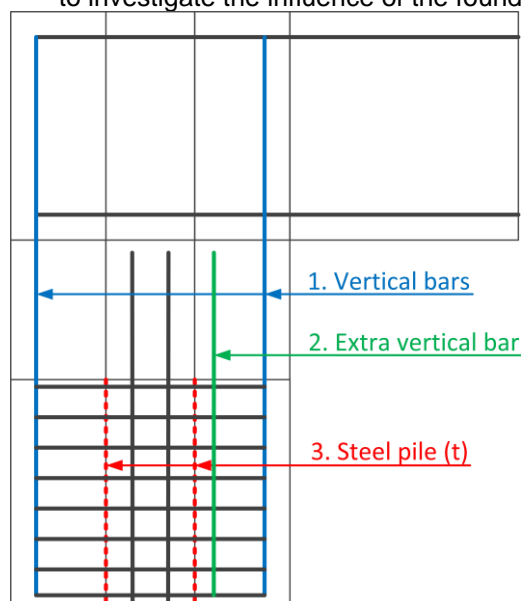


Figure 8-47 Potential improvements: 1. amount of reinforcement in the vertical bars, 2. amount of reinforcement in the extra vertical bar, 3. the thickness (t) of the steel pile

The results of the FEM could be found in Annex C. Figure C-1 and Figure C-2 show the force-displacement diagrams of the FEM with the amount of reinforcement in the vertical bar as parameter. There are two variations. The first variation is the modification of the amount of reinforcement in the right vertical bar (Figure C-1) and the second variation is the amount of reinforcement in the vertical bars on both sides (Figure C-2). The force-displacement diagram of Figure C-1 shows that a lower amount of reinforcement in the vertical bar leads to small reduction of the structural strength of the connection. However, the reduction is the same for all FEM with a lower amount of reinforcement than the standard FEM. Table C-1 shows the same result. The crack width in SLS and at $F=1643$ kN is the same for all FEM. Only, F_{ULS} is smaller for all other FEM's than the standard FEM. The force-



displacement diagram of Figure C-2 shows that a lower amount of reinforcement in both vertical bars leads to a reduction of the structural strength of the connection. This is visible for all FEM. Table C-2 shows the same result. F_{ULS} is decreasing when the reinforcement in the vertical bars is reduced. Figure C-3 shows the crack width in y-direction for the standard FEM and a FEM with a lower amount of reinforcement in both vertical bars. The crack width in y-direction is much larger for the FEM with the lower amount of reinforcement. Also, the horizontal cracks at the left side of the foundation pile are larger for the model with a lower amount of reinforcement. This is visible for all FEM with a lower amount of reinforcement in both vertical bars. The FEM with only a reduction of the reinforcement in the right vertical bar does not show larger horizontal cracks at the left side of the foundation pile. Therefore, only a reduction of the reinforcement in the left vertical bar leads to larger horizontal cracks at the left side of the foundation pile. This is logical, because the left side is loaded with tension and therefore a reduction of the reinforcement in left vertical bar leads to larger horizontal cracks.

Figure C-4 shows the force-displacement diagram for the FEM with an extra vertical reinforcement bar. The amount of reinforcement is equal to the other vertical bar at the right side of the foundation pile and therefore both vertical bars at right side are the parameter of Figure C-4. The force-displacement diagram shows that the structural behaviour of the FEM is improved, when the extra vertical bar is applied. Table C-3 shows that the crack width in ULS is lower for FEM with the extra vertical bar. F_{ULS} is similar for both FEM with and without the extra vertical bar. Figure C-5 shows that the horizontal crack is diminished due to the presence of the extra vertical bar in the connection and this lead to the improvement of the structural behaviour of the connection. An important aspect is that the extra vertical bar is added to a construction part in compression. In case of integral bridges, forces and moments are variable and could change in size and direction (see chapter 4). This could result in a change of the stresses in the construction part from compression to tension. The extra vertical bar has no improvement when the construction part is in tension.

The force-displacement diagram of the FEM with the thickness (t) of the foundation pile as variable is given in Figure C-6. The force-displacement diagram shows that a FEM with a larger thickness than the standard of 12.5 mm have a better performance in case of deformation. It is the opposite for a FEM with a smaller thickness. Table C-4 shows that w_{SLS} decreases when the thickness increases. Figure C-7 shows that the crack width decreases when thickness increases and that the displacement (u) is lower for the FEM with a larger thickness. So a larger t for the foundation pile leads to a smaller horizontal crack and less deformation. This is logical, because due to an increasing thickness the stiffness of the foundation pile increases as well and this behaviour has influence on total stiffness of the connection. Besides, the behaviour of the connection has the thickness of the foundation pile also influence on the total structure of the bridge. This means that due to a change of the stiffness of the foundation pile, the structural behaviour of the bridge changes (chapter 3 and 4). This leads to different deformations and moment.



8.5 Comparison of the results with the strut-and tie models of chapters 7

In chapter 7, strut-and-tie models are developed based on the analytical calculations. The strut-and-tie models show the flow of the forces and where compression and tension occurs. An example of a strut-and-tie model could be found in [48]. In this section, the results of the FEM are used to develop new strut-and-tie models. Also, a comparison is made between the strut-and-tie models based on the analytical calculations and the strut-and-tie models based on the results of the FEM.

The strut-and-tie models of chapter 7 (and Annex B) are showed in Figure 8-48. The two models are based on the two mechanisms for the load transfer in the foundation pile. The first strut-and-tie model shows the model where the load is transferred by friction between the foundation pile and the surrounded concrete. The second strut-and-tie model is the result of a coupling moment in the foundation. The red lines in Figure 8-48 stand for the tension in connection and the green lines are the compression. According to the first strut-and-tie model, tension occurs on the left side and at the top of the connection. The compression appears on the right side of the abutment and at the bottom of the bridge structure. The second strut-and tie model shows a more complex structural behaviour. In the abutment, the coupling is responsible for both tension and compression in the horizontal direction. Tension at top and compression at the bottom of the connection. Like the first strut-and-tie model, tension occurs at the left side and at the top of the connection and compression at the right side of the connection and at the bottom of the bridge structure. The vertical force (two times 570 kN) leads to compression in the centre of the connection.

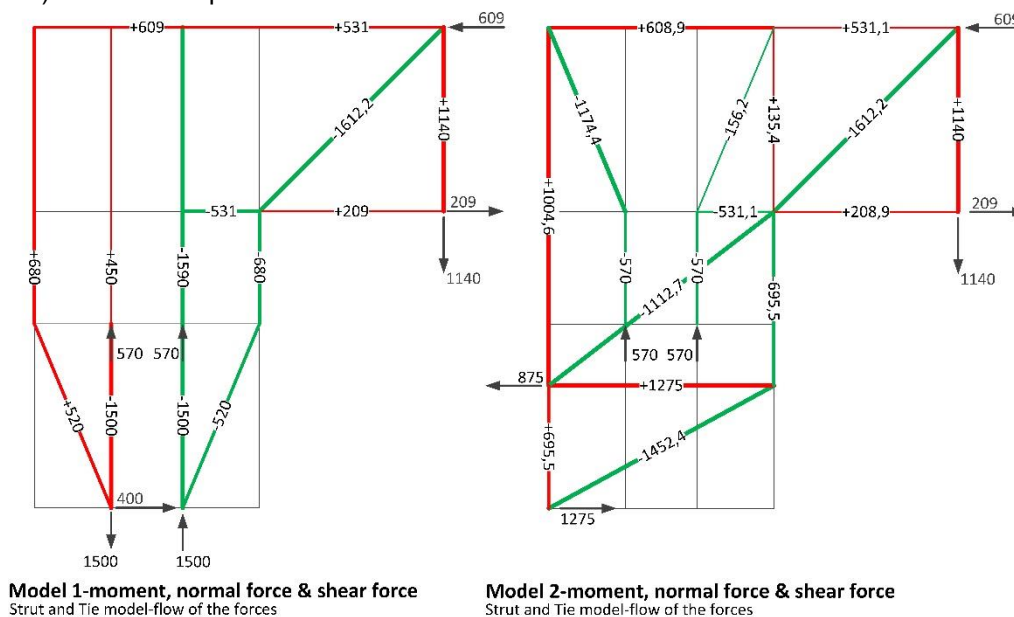


Figure 8-48 Strut-and-tie models based on the analytical calculations of chapter 7



The strut-and-tie models of Figure 8-48 will later be used for a comparison with the strut-and-tie models based on the FEM. First, the results of section 8.4 are used to construct the strut-and-tie-model based on the FEM. Figure 8-49 shows the tensile stresses in the reinforcement on the left and the principle stresses in the concrete element on the right. Both figures are the result of a standard FEM with reinforcement. The reinforcement stresses in the horizontal direction are concentrated in the left corner of the connection and the reinforcement stresses in the vertical direction are concentrated on the left side of the connection. The green and blue lines in the figure on the right are the maximum compression stresses in the concrete elements of the connection. Therefore, the maximum compression is concentrated on the right side of the connection.

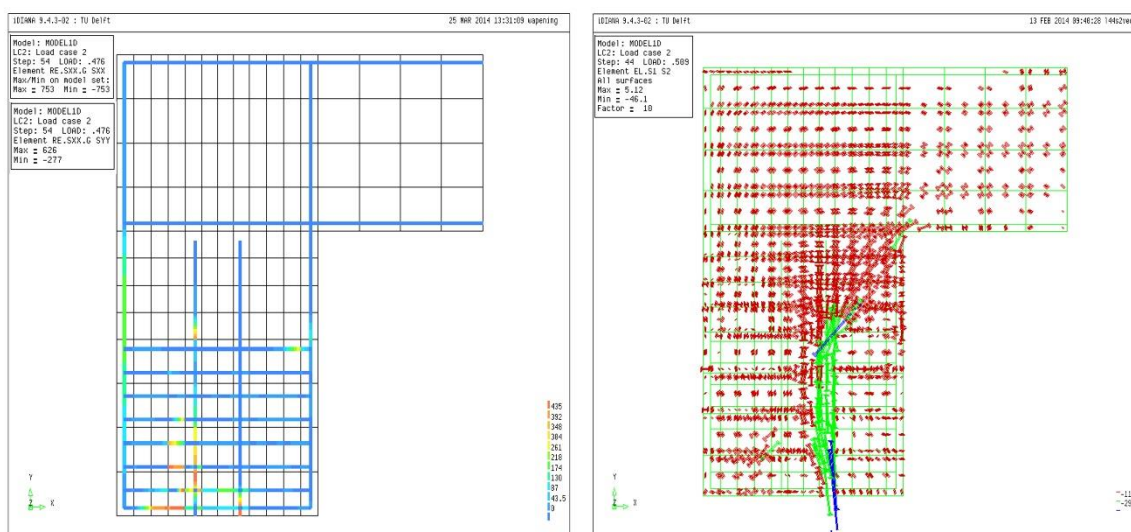


Figure 8-49 Standard FEM with reinforcement, left: Stresses in x- and y-direction in the reinforcement bars and right: the vertical principle stress σ_2

Figure 8-50 shows the principle stresses of a FEM without reinforcement in both directions (σ_1 and σ_2). The principle stresses on the left are tensile stresses in the concrete. The red lines are the maximum stresses and mainly close the cracks of the model. The green lines shows the flow of the tensile stresses and are concentrated on the left side of the foundation and on the left and top of the bridge part of the connection. The principle stresses on the right are the compression stresses. These stresses are mainly concentrated on the right of the foundation pile and on the right and the bottom of the connection.

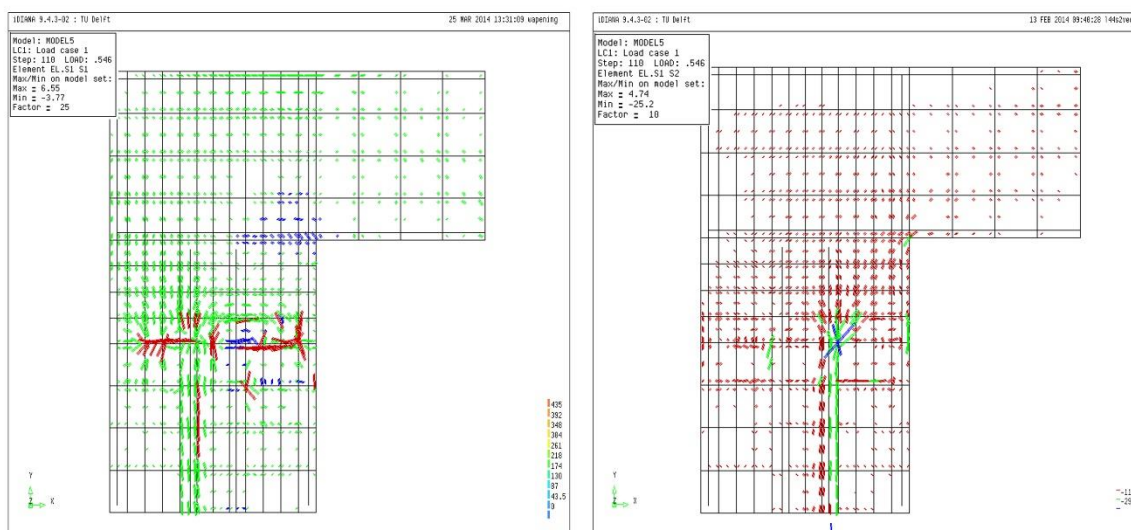
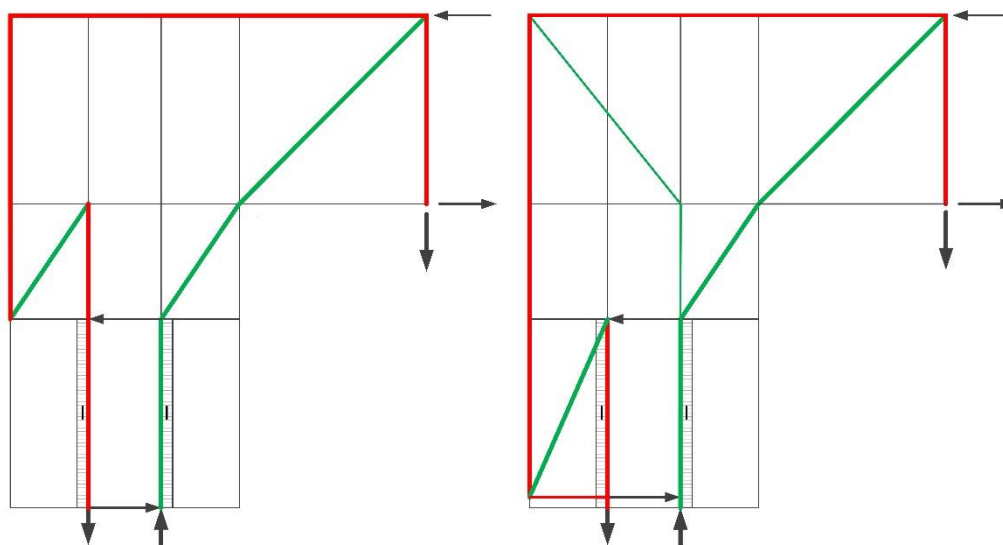


Figure 8-50 FEM without reinforcement, left: the principle stress σ_1 and right: the vertical principle stress σ_2

Figure 8-49 and Figure 8-50 could be used to construct the strut-and-tie models based on the FEM. The result is Figure 8-51. The left figure represent the strut-and-tie model based on the FEM without reinforcement (Figure 8-50). As discussed in section 8.4, the top and the left of the connection are under tension. The right and lower part of the connection are under compression. The concrete element on the left of the foundation pile is not loaded, because a vertical crack develops next to the foundation pile due to the absence of horizontal reinforcement. The foundation pile is on the left side under tension and on the right side under compression. The strut-and-tie model based on the FEM with reinforcement is presented on the right. As showed in Figure 8-51, the strut-and-tie model has mainly the same flow of the compression forces as the strut-and-tie model based on the FEM without horizontal reinforcement. The flow of the tension forces is however different. A horizontal tensile force exist in the concrete element on the left of the foundation pile due to the horizontal reinforcement. Like the strut-and-tie model based on the FEM without reinforcement, the left side of the foundation pile is under tension and the right side is under compression. According to the results of section 8.4, the forces in the strut-and-tie-model (tension and compression) are significantly larger for a strut-and-tie model based on the FEM with reinforcement than the FEM without reinforcement.



2D FEM Model without reinforcement
Strut and Tie model-flow of the forces

2D FEM Model with reinforcement
Strut and Tie model-flow of the forces

Figure 8-51 Strut-and-tie models based on the FEM

Figure 8-48 and Figure 8-51 showed both the strut-and-tie models based on the analytical calculations and the FEM. When these strut-and-tie models are compared some important aspects could be noted. These aspects are listed below:

- The analytical calculations are based on the reactive behaviour of the foundation pile on the deformations, forces and moments in the bridge deck (as discussed in chapter 7). The strut-and-tie model based on the FEM and the results of section 8.4 show that the frictional behaviour of the foundation pile has only a small effect on the structural capacity of the connection. Therefore, the strut-and-tie model based on the FEM with reinforcement has a comparable outcome as model 2 of Figure 8-48.
- Model 1 of Figure 8-48 shows similar vertical struts as the strut-and-tie models based on the FEM. These strut-and-tie models based on the FEM are however different. The forces which are presented by the vertical struts are in the foundation pile and not the concrete elements. This doesn't apply for the strut-and-tie model based on model 1. Where the forces are in the interface between the foundation pile and the concrete element. This is possible because the concrete elements and foundation pile are linear elements and therefore fully connected.
- The analytical calculations are linear calculations which lead to a full connection between the foundation pile and the concrete elements, as mentioned before. The FEM are nonlinear calculations which lead to strut-and-tie models which have no connection in tension in the horizontal direction between the concrete element and the foundation pile. Therefore, the concrete elements next to the foundation pile have no contribution to the strut-and-tie model based on the FEM without horizontal reinforcement.



8.6 Recommendations for the connection according to the results of the 2D FEM

The results of section 8.4 showed a FEM with respectively a variation in horizontal reinforcement and a variation in cohesion and friction. It can be concluded that the structural strength of the connection depends strongly on the horizontal reinforcement. Also, the crack width of the crack on the left side of the foundation pile is smaller for FEM with horizontal reinforcement in the lower part of the connection. Based on the results some recommendations can be made. This is listed below:

- Horizontal reinforcement is for a big part responsible for the strength of the connection. Especially, if the horizontal reinforcement is at the bottom part of the connection. It is therefore advisable to implement horizontal reinforcement at the bottom of the connection.
- Cohesion and friction of the foundation pile have almost no influence on the strength of the connection. Therefore, measures to improve cohesion and friction for example studs welded to the foundation pile are not recommended.
- The other part of the strength comes from the vertical reinforcement in the foundation pile and the reinforcement at the left side of the connection in combination with a compression path from the bridge deck to the right side of the foundation pile. The effects of the variation of these parameters are described in sub section 8.4.6.

The results of section 8.4 showed more findings than the conclusions described above. These findings have been researched in sub section 8.4.6 'potential improvements'. These potential improvements are the influence of the foundation pile, the influence of the vertical reinforcement and the influence of additional vertical reinforcement. The conclusions and the corresponding recommendations are listed below:

- An improvement of the foundation pile leads to lower deformations in the connection and higher rotational stiffness, but has also influence on the structural behaviour of the total bridge. In particular the elastic stiffness of the foundation pile in total. Therefore, this could have advantages, but further research is necessary.
- Vertical reinforcement plays a major role in the areas where tension occurs. A decrease of the vertical reinforcement leads to an increase of the cracks in this area and reduces the strength of the connection. The vertical reinforcement is not necessary in areas where compression occurs. It is however advisable to maintain the current reinforcement noted that the areas where compression and tension occurred could be reversed.
- A major horizontal crack occurs at the right side of the foundation pile. Vertical reinforcement in this area leads to a smaller crack but has no improvement of the strength of the connection. Besides the effect, that it is uncertain where tension and compression occurs due to variable deformations (yearly temperature cycle).



The 2D FEM showed some interesting findings. It is however not completely certain what occurs in a 3D connection beam. In a 3D connection beam, the horizontal reinforcement is concentrated in the area between the foundation piles and not distributed over the total length of the beam. This could have an effect on the crack width of the major vertical crack at left side of the foundation pile. The concentration of the horizontal reinforcement could also have an influence on the structural strength of the connection. It is therefore advisable to compose a 3D FEM of the connection.

In the next chapter, the influence of FRC composites on the 2D FEM is described. FRC composites could have influence on the cracking behaviour and the strength of the connection. The application of FRC composites in the 2D FEM is however not further detailed in this section.



9 2D FEM with FRC composites

This chapter describes the influence of FRC composites on the 2D FEM. FRC composites could have an influence on the cracking behaviour, the strength of the connection and reduce the amount of reinforcement as mentioned before in section 8.6. This influence is described in detail in section 8.1. This section shows also the design of the 2D FEM with FRC composites. In section 8.2, the mechanical properties of FRC composites are defined. These mechanical properties are based on the models of sub section 6.4.2. The results of the 2D FEM with FRC composites are explained in section 8.3.

9.1 The design of the 2D FEM with FRC composites

The results of section 8.4 showed the cracking behaviour of the 2D FEM with a standard concrete mixture. The major cracks occur vertically on the left side of the foundation and horizontally on the top of the foundation pile. The horizontal crack arises in the concrete mixture and could therefore be minimized by applying a FRC mixture. This is also applicable for the smaller cracks on the left side of the connection and in between of the reinforcement. As mentioned in section 8.5 and 8.6, a part of the strength of the connection comes from the vertical reinforcement on the left of the connection, because in this area occurs tension. Fibres improve the tension strength of a concrete mixture. There a FRC mixture in the connection could lead to an improvement of the structural strength of the connection.

In section 6.4, the potential model for a connection with FRC composites is described. This model has a FRC mixture in the lower part of the connection. That is the same area where the major cracks occur and where FRC composites could lead to an improvement of the strength of the connection. Therefore, this model will be used for the 2D FEM of chapter 8. In total two 2D FEM will be used for the analysis of the influence of FRC composites on the connection. Both 2D FEM are based on Figure 8-7. The first 2D FEM is the model with horizontal reinforcement, as showed in Figure 9-1A. The second and third 2D FEM have no horizontal reinforcement and are showed in Figure 9-1B and C. The second 2D FEM has conventional concrete inside the foundation pile and the third 2D FEM has FRC composites inside the foundation pile. Both 2D FEM of Figure 9-1B and C are researched, because in between of two foundation piles in the other direction also a concrete structure is present. By examining both limits a better understanding of the influence of FRC composites is possible. The actual solution will then lie in between these limits.

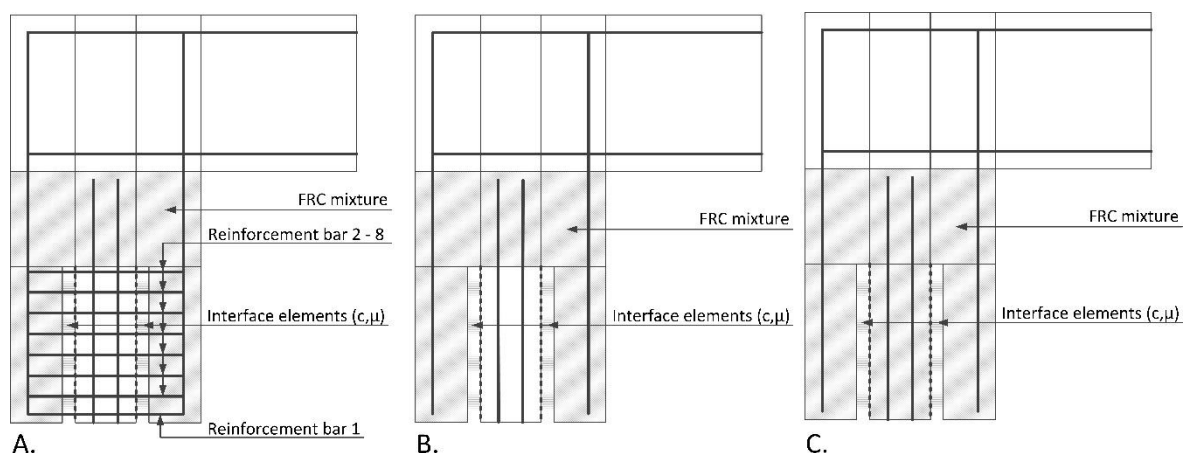


Figure 9-1 2D FEM with FRC based on Figure 8-7. A.: 2D FEM with horizontal reinforcement, B. 2D FEM without horizontal reinforcement and conventional concrete inside the foundation pile and C. 2D FEM without horizontal reinforcement and frc composites inside the foundation pile

A 2D FEM with and without horizontal reinforcement are researched. The results of section 8.4 showed that a part of the structural strength of the connection is due to the vertical reinforcement at the sides of the connection and the foundation pile. The strength of the connection could increase because of FRC composites. This could benefit for a connection with and without horizontal reinforcement.

9.2 The mechanical properties of the FRC composites used in the 2D FEM

The mechanical properties that are used for the 2D FEM are described in sub section 6.4.2. In this subsection, tensile stress-strain diagrams (Figure 6-9 and Figure 6-10) are showed which define the tensile stress-strain response of simulated FRC composites based on the research. Two different tensile stress-strain responses are characterized: 'Hardening' and 'softening'. The tensile stress-strain diagrams of Figure 6-9 and Figure 6-10 describe also different values for tension stress and strain. The tensile stress-strain diagram of Figure 9-2 is given in range with softening, hardening, tensile stress and strain as parameters. This is based on the validation grid of Figure 6-8.

The first analyses of the 2D FEM with FRC composites did not converged. This was showed in the results where only a linear phase was visible. Therefore, the stress-strain diagrams are simplified from a 'multi-linear' response to a bilinear response. These tensile stress-strain diagrams are showed in Figure 9-2 and are based on the multi-linear diagrams of Figure 6-9 and Figure 6-10.

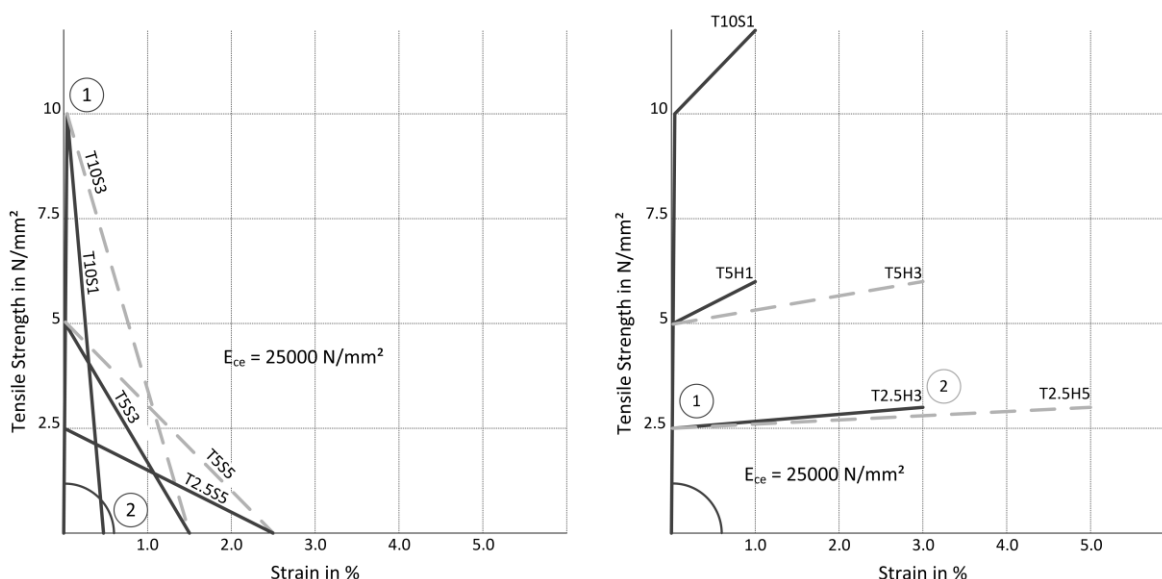


Figure 9-2 Tensile stress-strain diagrams of the proposed FRC composites. On the left: the strain-softening response and on the right: the strain-hardening response. Remark: H=hardening, Softening, T= tensile strength

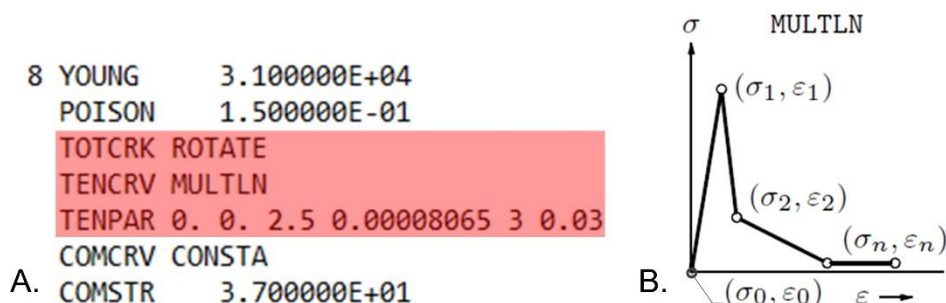
Table 9-1 shows the mechanical properties of the FRC composites used for the 2D FEM. The mechanical properties for the softening-strain response could be found on the left. These values correspond with stress-strain curve on the left of Figure 9-2. The mechanical properties of the hardening-strain response could be found on the right. These values correspond with stress-strain curve on the right of Figure 9-2.

A	$\epsilon_1(\%)$	σ_1	$\epsilon_2(\%)$	σ_2
T2.5S5	0,008065	2.5	2.5	0
T5S3	0.016129	5	1.5	0
T5S5	0.016129	5	2.5	0
T10S1	0.03226	10	0.5	0
T10S3	0.03226	10	1.5	0

B	$\epsilon_1(\%)$	σ_1	$\epsilon_2(\%)$	σ_2
T2.5H3	0,008065	2.5	3	3
T2.5H5	0,008065	5	5	6
T5H1	0.016129	5	1	6
T5H3	0.016129	10	3	12
T10H1	0.03226	10	1	12

Table 9-1 The mechanical properties of the FRC composites used for the 2D FEM. A.: softening and B.: hardening

The tensile stress – strain response is adapted to TNO Diana input file of the 2D FEM. This is presented in Figure 9-3A. The ‘highlighted part’ are the mechanical properties of the FRC composites. The ‘non-highlighted’ part are the mechanical properties that are the same as for a 2D FEM without FRC composites. These mechanical properties are compression curve, compression strength and Young’s modulus. For the TNO Diana input, the tension curve of Figure 9-3B is used. This is a multi-linear stress-strain curve.



9.3 Results

As discussed in section 9.1, there are two 2D FEM with FRC composites. The first 2D FEM is with horizontal reinforcement and the second 2D FEM has no horizontal reinforcement. In section 9.2, two tensile stress-strain responses for FRC composites are defined: softening and hardening. Therefore, in total 4 2D FEM are analysed. This is explained in the first 6 sub sections, respectively:

- Model 1: with horizontal reinforcement and hardening-strain response
- Model 2: with horizontal reinforcement and softening-strain response
- Model 3: conventional concrete inside the foundation pile, no horizontal reinforcement and hardening-strain response
- Model 4: conventional concrete inside the foundation pile, no horizontal reinforcement and softening-strain response
- Model 5: FRC composites inside the foundation pile, no horizontal reinforcement and hardening-strain response
- Model 6: FRC composites inside the foundation pile, no horizontal reinforcement and softening-strain response

The tensile stress-strain responses of Table 9-1 are used for the different 2D FEM. The left side of the table is adapted to model 2, 4 and 6 with softening-strain response and the right side is adapted to model 1, 3 and 5 with hardening-strain response. These different tensile-strain response are used for a comparison between different strains and /or tensile stresses. In addition, the 2D FEM with FRC composites are always compared with the standard 2D FEM. The standard 2D FEM has only conventional concrete in the connection.

In the last sub section, the different 2D FEM are compared. Important aspects for the comparison are the influence of hardening and softening, strain and tensile stress.

9.3.1 Model 1: with horizontal reinforcement and hardening-strain response

This subsection deals with the 2D FEM with horizontal reinforcement (Figure 9-1A) and with hardening-strain response (right figure of Figure 9-2). The different models could be found in Table 9-1B and will be used for comparison between the standard model and the model with the FRC composite. The models with a FRC composite are T2.5H3, T2.5H5 T5H1, T5H3 and T10H1.



The force-displacement diagram is given in Figure 9-4. As showed, the rotational stiffness increases for 2D FEM with a higher tensile stress. The strain has according to Figure 9-4 no influence on the structural strength of the connection. The gradient of T2.5H3 and T.25H5 is the same. This also applies for T5H1 and T5H3. The 2D FEM with T10H1 reach to a lower load than the other 2D FEM with FRC composites. The results showed that the cracking pattern is not developed and the tensile stress are not close to the critical values. Therefore, the conclusion is that the analysis of this 2D FEM diverges before failure.

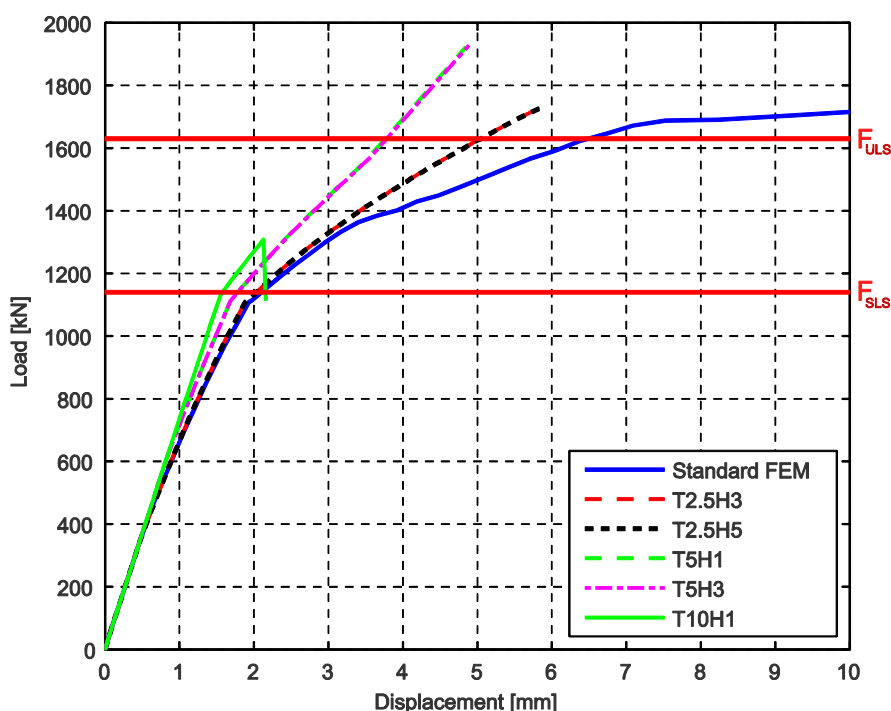


Figure 9-4 Force-displacement diagram for 2D FEM with horizontal reinforcement and hardening-strain response

Table 9-2 shows the critical values of Figure 9-4. w_{SLS} and w_{ULS} decreases when the tensile stress of the 2D FEM increases. This does not apply for the strain. w_{SLS} and w_{ULS} are the same for different strain. F_{ULS} increases for 2D FEM with a higher tensile stress, but are no improvement in comparison with the standard 2D FEM.

FRC mixture	w_{SLS}	w_{ULS} at $F_{ULS}=1308$ kN	F_{ULS}
Standard 2D FEM	0,22 mm	0,23 mm	1795 kN
T2.5H3	0,09 mm	0,12 mm	1727 kN
T2.5H5	0,09 mm	0,12 mm	1726 kN
T5H1	0,08 mm	0,10 mm	1921 kN
T5H3	0,08 mm	0,10 mm	1927 kN
T10H1	0,05 mm	0,09 mm	1308 kN

Table 9-2 Critical values of Figure 9-4

The crack patterns of the standard 2D FEM and 2D FEM with FRC composites (T5H3) at moment of failure are given in Figure 9-5. The crack pattern is fully developed for the standard 2D FEM. This is



not the case for the 2D FEM with FRC composites. The crack pattern of the 2D FEM with T5H3 is a decisive crack pattern for 2D FEM with FRC composites. The cracks are small and located in the foundation pile.

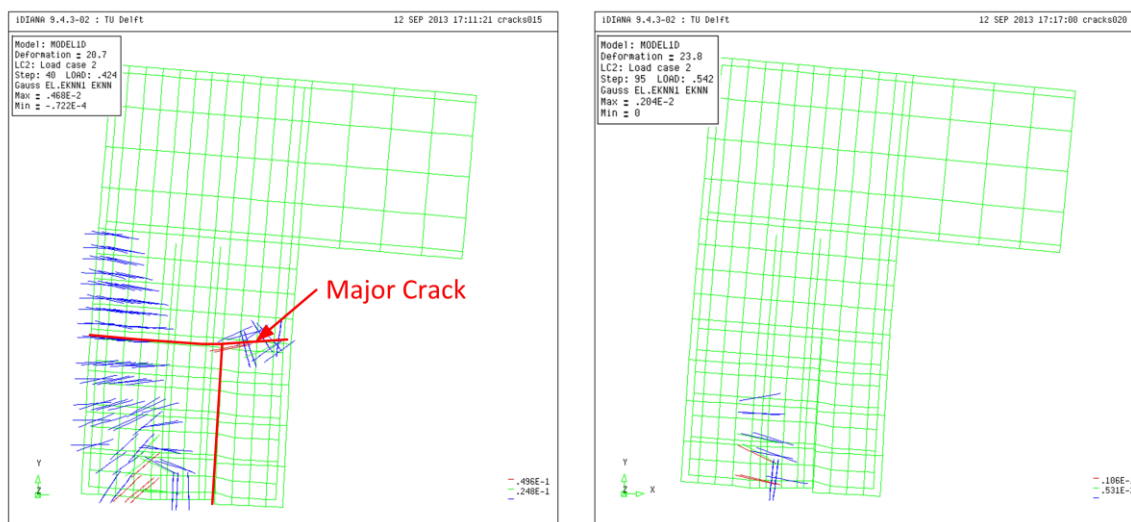


Figure 9-5 Crack pattern at moment of failure for left: standard 2D FEM and right: 2D FEM with T5H3

Figure 9-6 shows the tensile stresses in the horizontal reinforcement of the standard 2D FEM and the 2D FEM with T5H3. The tensile stresses are high for a standard 2D FEM, but low for the 2D FEM with FRC composites. The maximum is located down on the left of the foundation pile with a maximum tensile stress of approximately 200 N/mm². The tensile stresses are therefore rather low for 2D FEM with FRC composites.

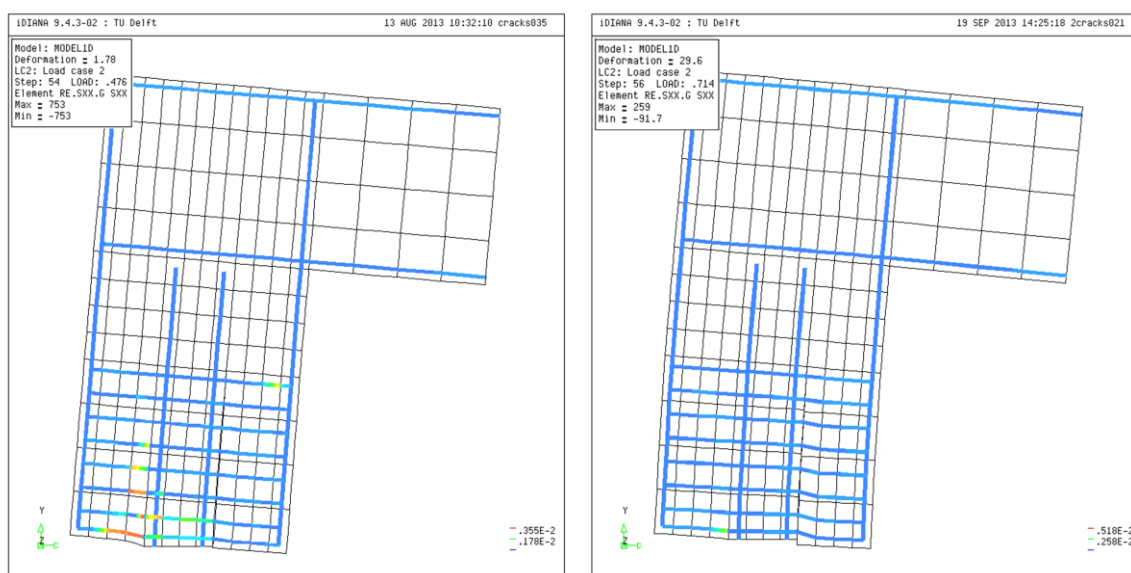


Figure 9-6 Stresses in the horizontal reinforcement for left: standard 2D FEM and right: 2D FEM with T5H3



The 2D FEM with FRC composites have a better performance in strength and stiffness of the connection than the standard 2D FEM. Also, cracks in the 2D FEM with FRC composites are smaller. Unfortunately, the analyses of these 2D FEM does not show the moment of failure, because cracks are not fully developed and also tensile stresses are lower than the maximum tensile stress in the critical areas of the connection (described in section 8.4). The force-displacement diagram of Figure 9-4 also show no horizontal branch or plastic phase for the 2D FEM with FRC composites. This indicates that the analyses of the 2D FEM with FRC composites diverges before the moment of failure. Hence, there is no difference between the 2D FEM with different strains because this is showed in the plastic phase or horizontal branch in the force-displacement diagram.

9.3.2 Model 2: with horizontal reinforcement and softening-strain response

This subsection is about the 2D FEM with horizontal reinforcement (Figure 9-1A) and with softening-strain response (left part of Figure 9-2). Table 9-1A shows the different FRC composites that are used for the comparison with the standard FEM with conventional concrete described in sub sub section 8.2.2.1. These models are T2.5S5, T5S3, T5S5, T10S1 and T10S3.

Figure 9-7 shows the force-displacement diagram for 2D FEM with horizontal reinforcement and a strain-softening response. The rotational stiffness improves when the tensile stress increases. Also a higher strain leads to a small improvement. T2.5S5 has the same gradient as the standard FEM. This is logical, because tension curve is quite similar to the standard concrete.

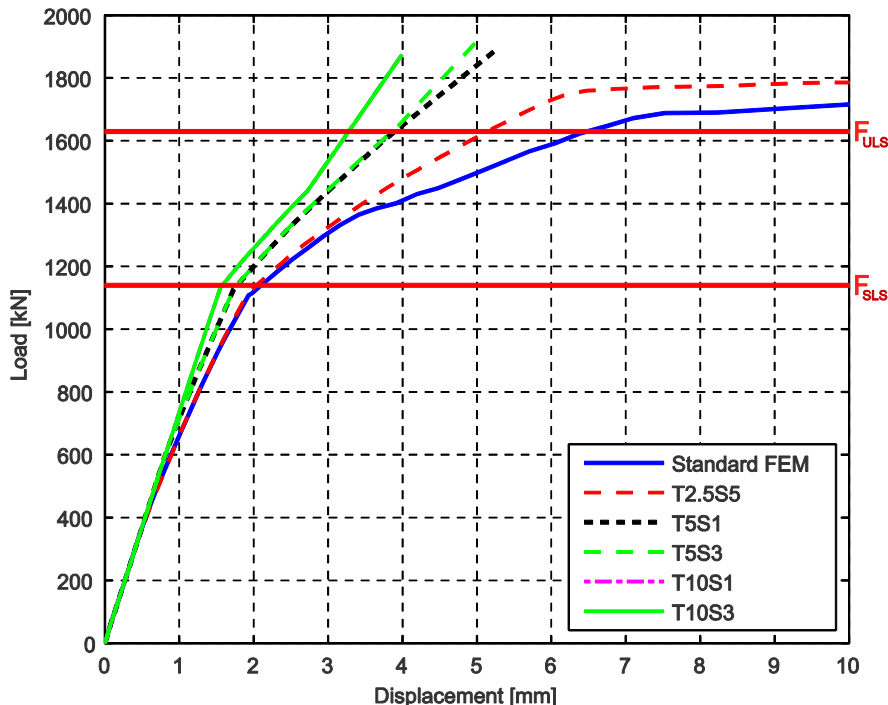


Figure 9-7 Force-displacement diagram for 2D FEM with horizontal reinforcement and softening-strain response



The critical values of Figure 9-7 are given in Table 9-3. w_{SLS} decreases for a higher tensile stress. All 2D FEM have a lower w_{SLS} than the standard FEM. The w_{ULS} is comparable for all 2D FEM. Also F_{ULS} is similar for all 2D FEM.

FRC mixture	w_{SLS}	w_{ULS} at $F_{ULS}=1439$ kN	F_{ULS}
Standard 2D FEM	0,22 mm	0,25 mm	1795 kN
T2.5S5	0,17 mm	0,33 mm	1808 kN
T5S3	0,11 mm	0,26 mm	1898 kN
T5S5	0,11 mm	0,25 mm	1923 kN
T10S1	0,04 mm	0,20 mm	1874 kN
T10S3	0,04 mm	0,20 mm	1874 kN

Table 9-3 Critical values of Figure 9-7

Figure 9-8 shows the crack pattern for a standard 2D FEM and 2D FEM with T10S1. The standard 2D FEM has a developed crack pattern at the moment of failure. This is not case for the 2D FEM with T10S1, where the cracks are insignificantly small. The 2D FEM with T10S1 is normative for all 2D FEM with FRC composites except for the 2D FEM with T2.5S5. The crack pattern and the horizontal reinforcement for the 2D FEM with T2.5S5 are given in Figure 9-9. These figures of Figure 9-9 show a similar behaviour for 2D FEM with T2.5S5 as the standard 2D FEM. Besides, the 2D FEM with T2.5S5 is the only 2D FEM with FRC composites with a plastic branch according to the force-displacement diagram of Figure 9-7. This implies that the 2D FEM with T2.5S5 reach the moment of failure.

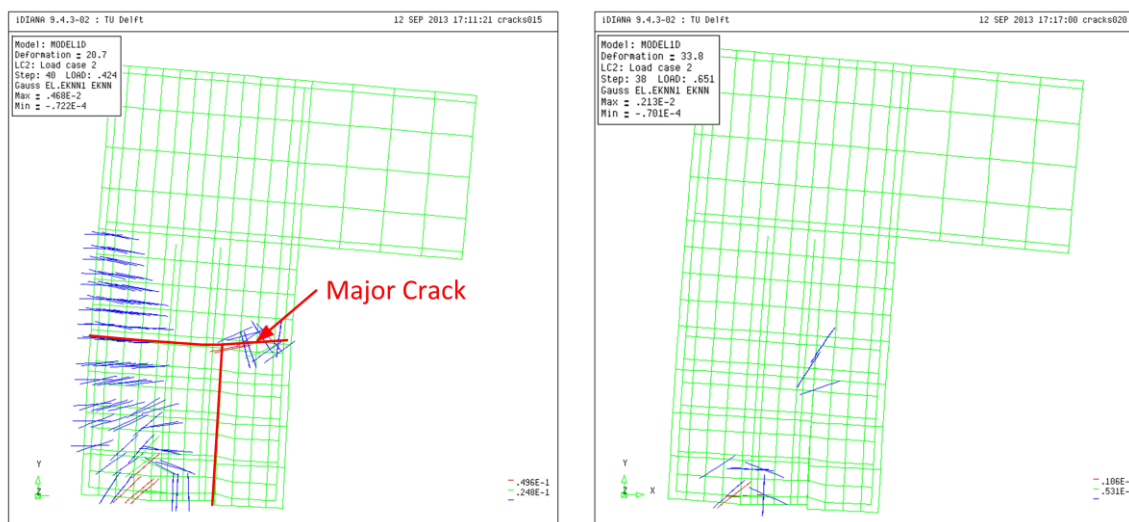


Figure 9-8 Crack pattern at moment of failure for left: standard 2D FEM and right: 2D FEM with T10S1

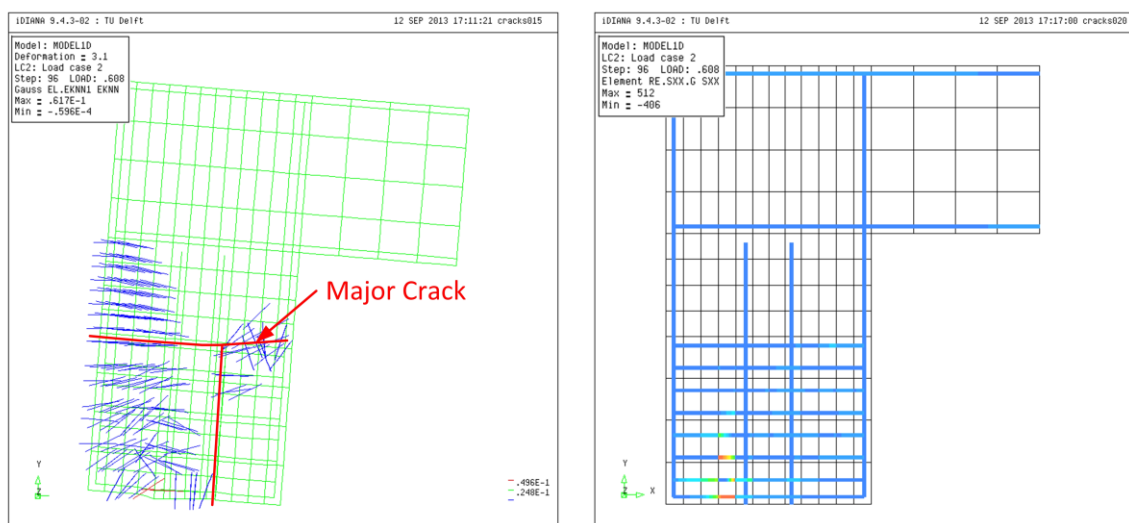


Figure 9-9 2D FEM with T2.5S5 with left: the crack pattern and right: the stresses in the horizontal reinforcement

Figure 9-6 which shows the tensile stresses in the horizontal reinforcement for a 2D FEM with strain hardening response is also applicable for the 2D FEM with strain softening response. This means that also for the 2D FEM with strain softening response, the tensile stresses in the horizontal reinforcement are rather low. This shows together with an undeveloped crack pattern and the absence of a plastic/horizontal branch in the force-displacement diagram that the 2D FEM with FRC composites do not reach the moment of failure in the presented results. Except for the 2D FEM with T2.5S5. The reason why only this 2D FEM with FRC composites reach the moment of failure is that the tensile stress-strain behaviour of the material is of all FRC composites the closest to the stress-strain behaviour of the standard concrete mixture.

9.3.3 Model 3: No FRC composites inside the foundation pile, no horizontal reinforcement and hardening-strain response

The 2D FEM that is analysed in this sub section has no horizontal reinforcement and no FRC composites inside the foundation pile as showed in Figure 9-1B and the hardening-strain response as displayed on the right of Figure 9-2. In Table 9-1B, the different models could be found that are compared with each other. These models are the standard FEM with conventional concrete described in sub sub section 8.2.2.1, T2.5H3, T2.5H5 T5H1, T5H3 and T10H1.

The force-displacement diagram of Figure 9-10 shows the effect of a hardening-strain response on a 2D FEM without horizontal reinforcement. As showed, the structural strength of the connection improves when the tensile stress of the FRC composite increases. A higher strain does not lead to an improvement of the structural strength of the connection.

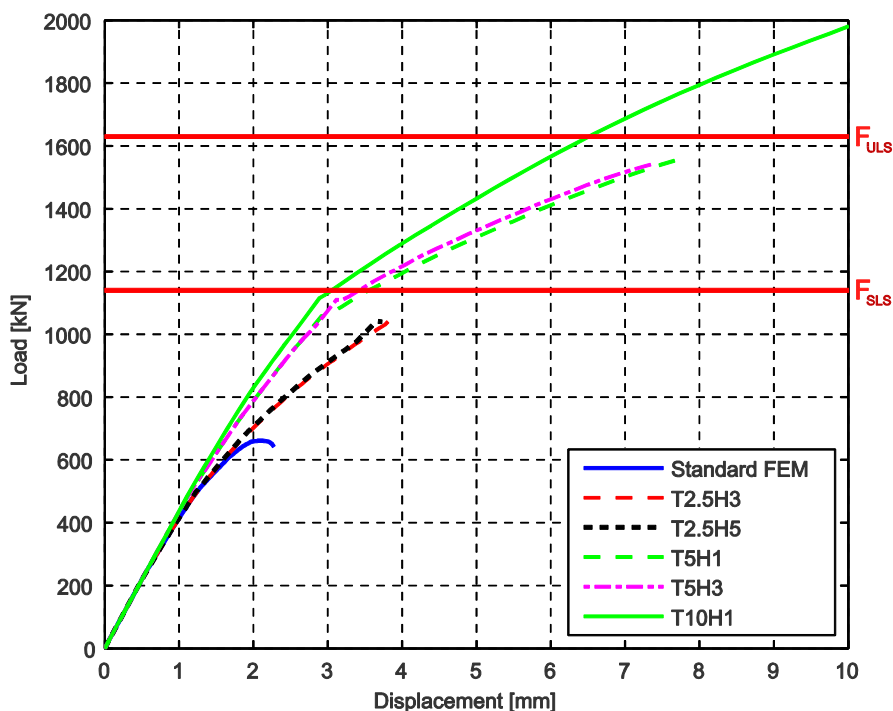


Figure 9-10 Force-displacement diagram for 2D FEM without horizontal reinforcement and hardening-strain response

Table 9-4 shows the critical values of Figure 9-10. The F_{ULS} is greater for 2D FEM with a higher tensile stress. The F_{ULS} for 2D FEMs with the same tensile stress, but a different strain is equal. This means the influence of the strain is minimal. W_{SLS} and w_{ULS} are not visible for 2D FEM without horizontal reinforcement.

FRC mixture	w_{SLS}	w_{ULS}	F_{ULS}
Standard 2D FEM	x	∞	661 kN
T2.5H3	x	∞	1065kN
T2.5H5	x	∞	1042 kN
T5H3	x	∞	1562 kN
T5H3	x	∞	1544 kN
T10H1	x	∞	2090 kN

Table 9-4 Critical values of Figure 9-10

The crack patterns for a standard 2D FEM and 2D FEM with T2.5H3 are given in Figure 9-11. The cracks for a 2D FEM with T2.5H3 are small in comparison with the standard 2D FEM. Also, the major horizontal crack on the right side of the foundation pile does not occur for 2D FEM with T2.5H3. The major vertical crack on the left side of the foundation pile in the standard 2D FEM is also present in the 2D FEM with T2.5H3. Therefore, the 2D FEM with T2.5H3 also fails due to failure between the connection and the foundation pile. The crack pattern of the 2D FEM with T2.5H3 is representative for all 2D FEM with FRC composites except the 2D FEM with T10H1.

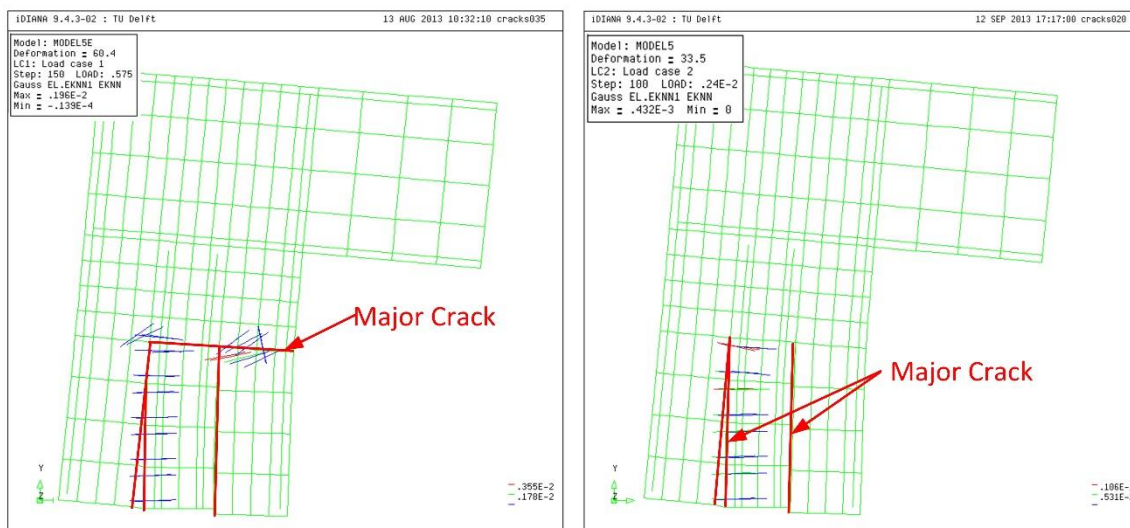


Figure 9-11 Crack pattern at moment of failure for left: standard 2D FEM and right: 2D FEM with T2.5H3

Figure 9-12 shows the crack pattern and stresses in the vertical reinforcement of a 2D FEM with T10H1. The stresses in the vertical reinforcement of the foundation pile has reach the maximum tensile strength of reinforcement. Also, the cracks mostly occur inside the foundation pile. This means that the 2D FEM with T10H1 fails due to failure of the foundation pile.

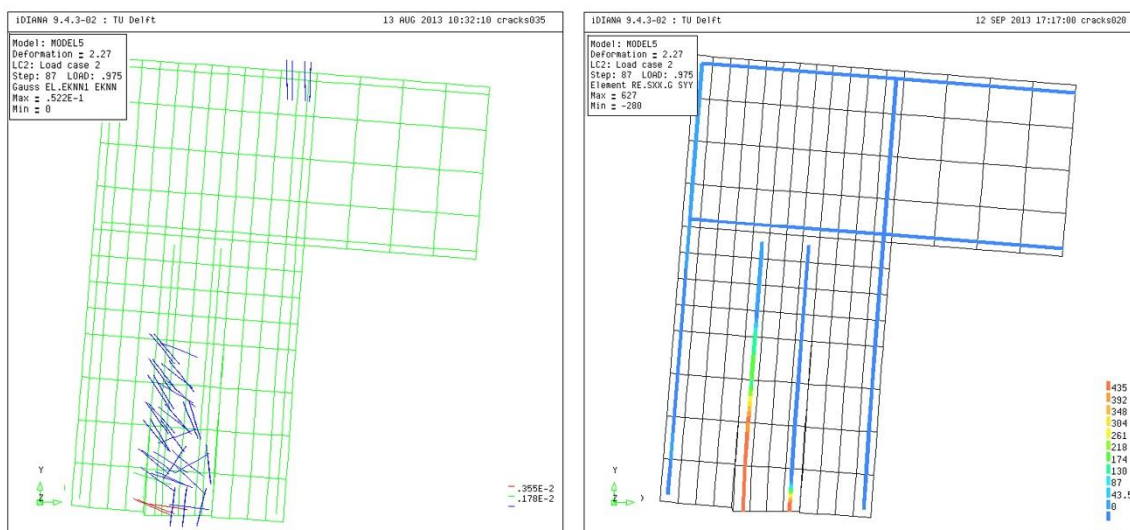


Figure 9-12 2D FEM with T10H1 with left: the crack pattern and right: the stresses in the vertical reinforcement

The force-displacement diagram and the figures with the crack patterns show that a higher tensile strength of the concrete leads to an increasing structural strength of the connection. This is not case for a higher strain, which has almost no influence on the structural strength of the connection. Further, the crack patterns show that the connection can be seen as a 'mortise and Tenon joint'. The standard 2D FEM fails due to failure of the mortise and the 2D FEM with T10H1 fails because of failure of the tenon.



9.3.4 *Model 4: No FRC composites inside the foundation pile, no horizontal reinforcement and softening-strain response*

In this subsection, the 2D FEM without reinforcement and FRC composites inside the foundation pile (Figure 9-1B) and the softening-strain response (right part of Figure 9-2) is researched. Table 9-1A shows the models that are used for the comparison between the different models with strain-softening response. These models are the standard 2D FEM with conventional concrete described in sub sub section 8.2.2.1, T2.5S5, T5S3, T5S5, T10S1 and T10S3.

The influence of strain-softening response on the 2D FEM without horizontal reinforcement is given in the force-displacement diagram of Figure 9-13. The structural strength of the connection improves when the tensile stress of the FRC composite increases. This is also applied for the strain of the FRC composite. When the strain of the FRC composite increases, also the structural strength improves.

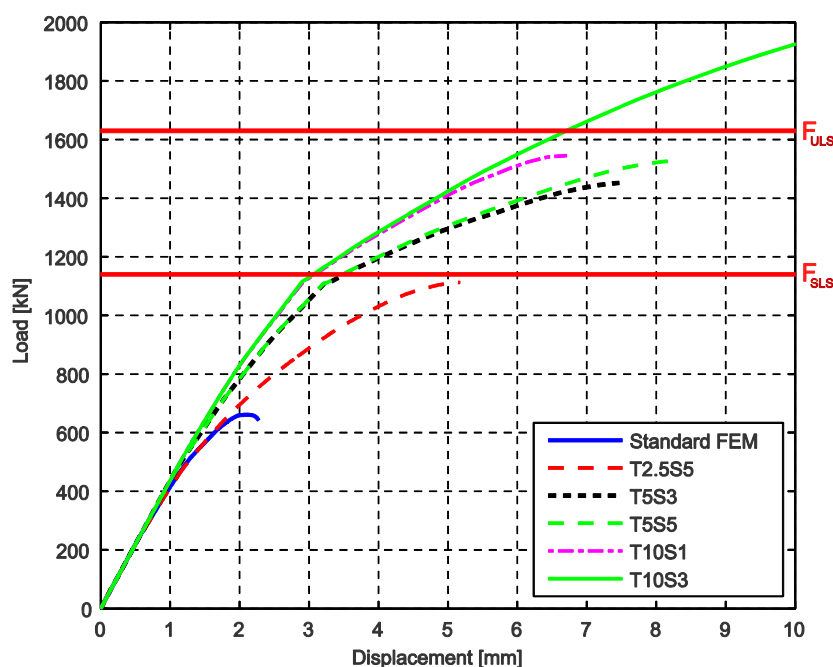


Figure 9-13 Force-displacement diagram for 2D FEM without horizontal reinforcement and softening-strain response

The critical values of Figure 9-13 are showed in Table 9-5. F_{ULS} increases for 2D FEM with a higher tensile stress. The critical values also show that F_{ULS} increases when the strain increases. W_{SLS} and W_{ULS} are not visible for 2D FEM without horizontal reinforcement.

FRC mixture	W_{SLS}	W_{ULS}	F_{ULS}
Standard 2D FEM	x	∞	661 kN
T2.5S5	x	∞	1113 kN
T5S3	x	∞	1452 kN
T5S5	x	∞	1529 kN
T10S1	x	∞	1546 kN
T10S3	x	∞	2124 kN

Table 9-5 Critical values of Figure 9-13



Figure 9-14 shows the crack patterns for a standard 2D FEM and a 2D FEM with T2.5S5. As showed, both 2D FEM fail due to failure between the connection and the foundation pile. The major difference between the 2D FEM is that more small cracks are present in the 2D FEM with T2.5S5. This is also the case for the other 2D FEM with FRC composites. Only the 2D FEM with T10S3 reach the maximum tensile strength of the reinforcement. This is showed in the figure on the right of Figure 9-15. This does however not lead to failure. The 2D FEM with T10S3 fails also due to failure between the connection and the foundation pile.

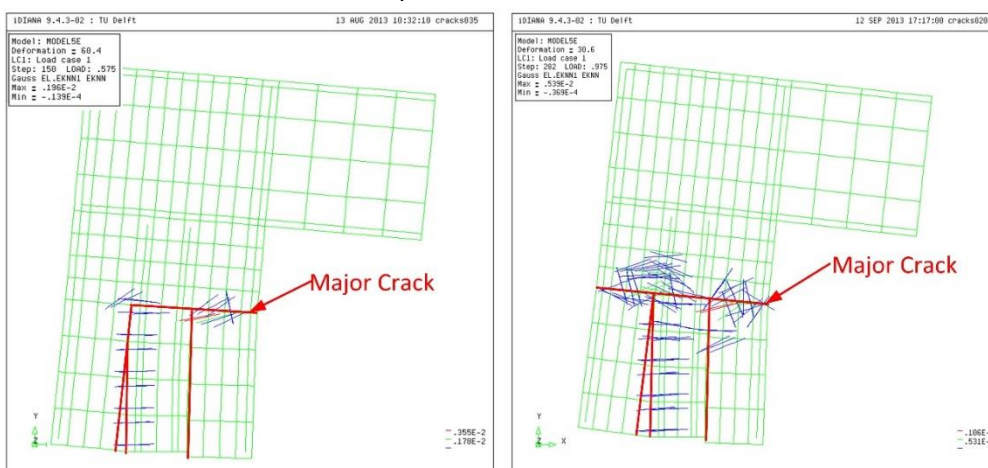


Figure 9-14 Crack pattern at moment of failure for left: standard 2D FEM and right: 2D FEM with T2.5S5

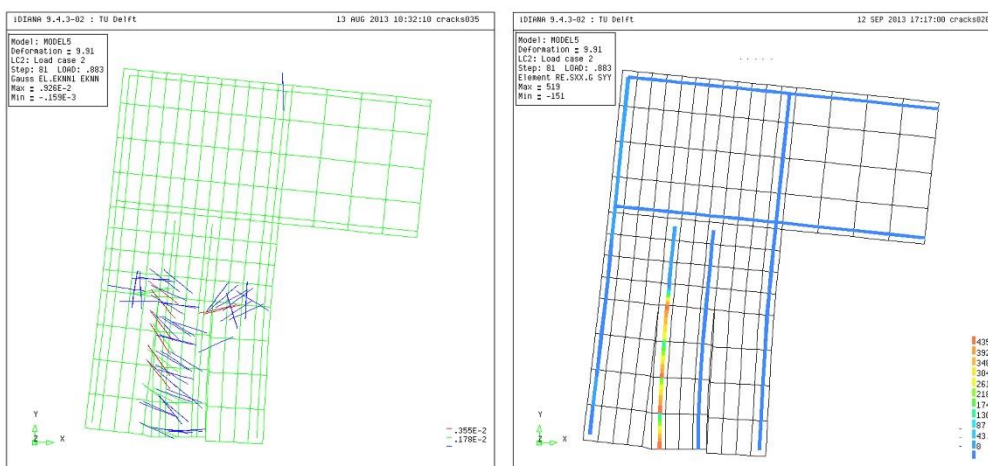


Figure 9-15 2D FEM with T10S3 with left: the crack pattern and right: the stresses in the vertical reinforcement

9.3.5 Model 5: FRC composites inside the foundation pile, no horizontal reinforcement and hardening-strain response

This sub section describes the 2D FEM (Figure 9-1C) without horizontal reinforcement, FRC composites inside the foundation pile and hardening-strain response (Figure 9-2A). The different models could be found in Table 9-1B and will be used for comparison between the standard 2D FEM with conventional concrete and the 2D FEM with the FRC composites. The 2D FEM with a FRC composites are T2.5H3, T2.5H5 T5H1, T5H3 and T10H1.



Figure 9-16 shows the force-displacement diagram of the 2D without horizontal reinforcement, FRC composites inside the foundation pile and strain-hardening response. This figure shows that a higher tensile strength leads to a higher structural strength of the connection. This does not apply for a higher strain. The 2D FEM with the same tensile strength, but a different strain have the same line in the force-displacement diagram.

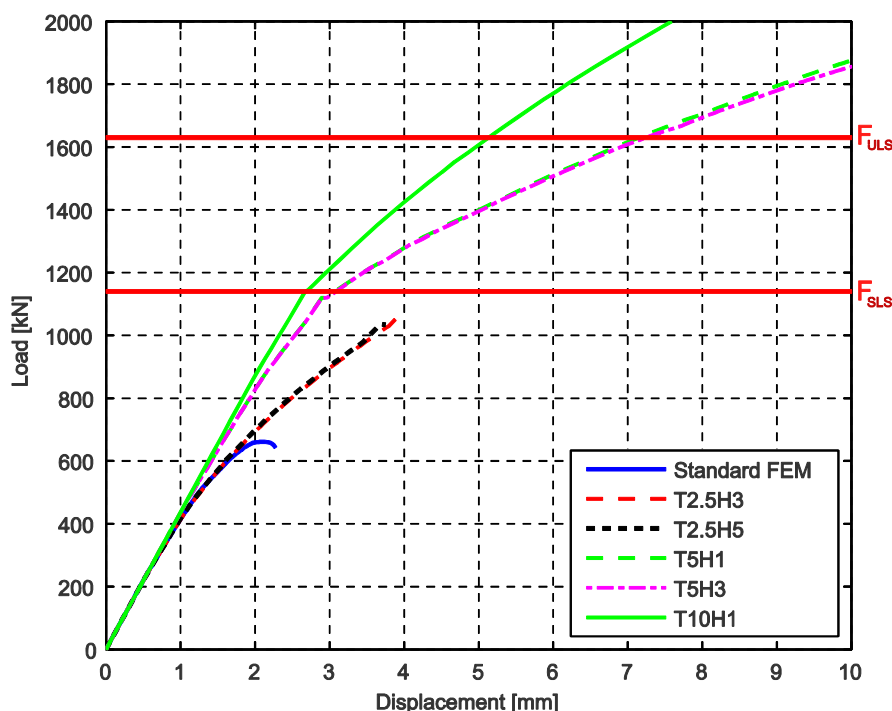


Figure 9-16 Force-displacement diagram for 2D FEM without horizontal reinforcement and hardening-strain response

The critical values of the force-displacement diagram (Figure 9-16) are given in Table 9-6. This table shows that the values are higher for 2D FEM with a higher tensile strength. This is not applicable for the strain. The strain has according this table no influence. This corresponds with the observations described before.

FRC mixture	w_{SLS}	w_{ULS}	F_{ULS}
Standard 2D FEM	x	∞	661 kN
T2.5H3	x	∞	1061kN
T2.5H5	x	∞	1034 kN
T5H3	x	∞	2210 kN
T5H3	x	∞	2199 kN
T10H1	x	∞	2793 kN

Table 9-6 Critical values of Figure 9-16

Figure 9-17 presents the crack pattern of the standard 2D FEM on the left and vertical stresses of the 2D FEM with T2.5H3. It was not possible to display the crack pattern of the 2D FEM with T2.5H3, because the analysis of this model did not configure one. Therefore, the vertical stresses are showed.



Figure 9-17 shows that a major vertical crack next to the foundation pile leads to failure of the connection. The cracking pattern of the standard 2D FEM also shows that horizontal cracks occur at top of the foundation pile. This is not present in the 2D FEM with FRC composites.

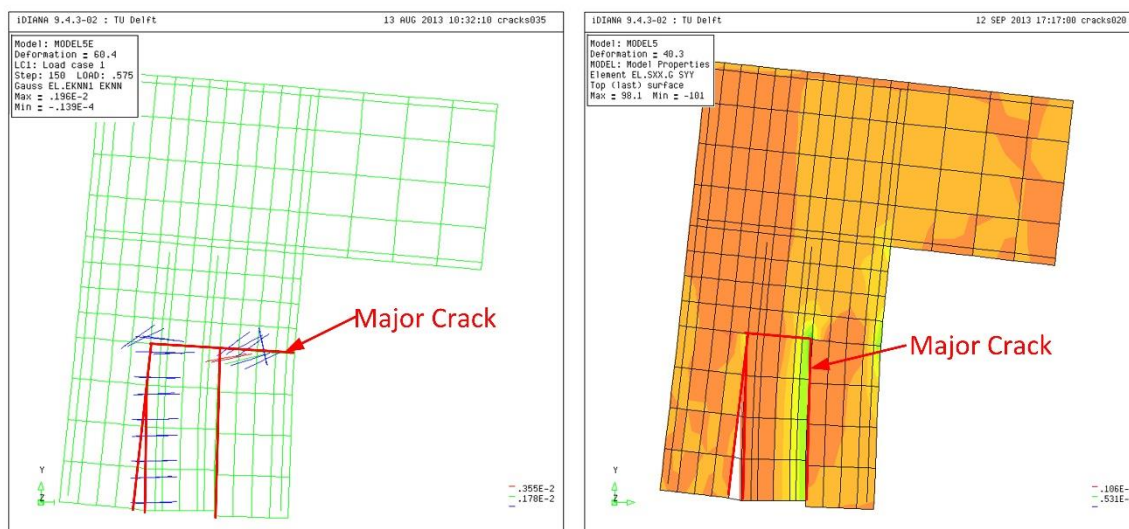


Figure 9-17 Left: Crack pattern at moment of failure for the standard 2D FEM, right: stresses in the vertical direction at moment of failure for the 2D FEM with T2.5H3

The crack pattern and the stresses in the vertical reinforcement of the 2D FEM with T10S3 at moment of failure are showed in Figure 9-18. The crack pattern shows that small cracks occur at the top of the connection. This does however not lead to failure of the connection. The figure on the right shows that the maximum tensile stresses in the vertical reinforcement occur at the bottom of the connection. These tensile stresses are exceeding the tensile strength, which could indicate that the connection fails at this location. This is however not clear, because the major vertical cracks around the foundation pile could also be the failure mechanism.

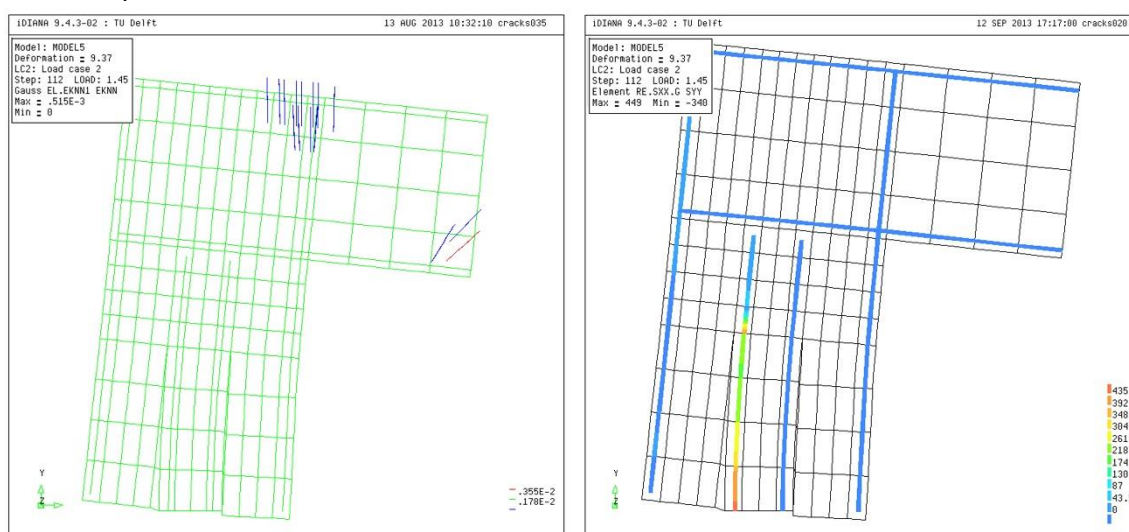


Figure 9-18 2D FEM with T10H1 at moment of failure, left crack pattern and right: stresses in the vertical reinforcement



9.3.6 Model 6: FRC composites inside the foundation pile, no horizontal reinforcement and softening-strain response

This sub section is about the 2D FEM with FRC composites inside the foundation pile (Figure 9-1C), without the horizontal reinforcement and softening strain-response (Figure 9-2B). In Table 9-1B, the different models could be found that are compared with each other. These models are the standard FEM with conventional concrete described in sub sub section 8.2.2.1, T2.5H3, T2.5H5 T5H1, T5H3 and T10H1.

The force-displacement diagram of Figure 9-19 shows the 2D FEM with FRC composites inside the foundation pile, without horizontal reinforcement and softening-strain response. A higher tensile strength of the 2D FEM leads to an increase of the structural strength of the connection. This is in lesser extent also applicable for the strain. A higher strain leads also to a small increase of the structural strength. This is shown when respectively the 2D FEM with T5S3 and T10S and the 2D FEM with T10S1 and T10S3 are compared.

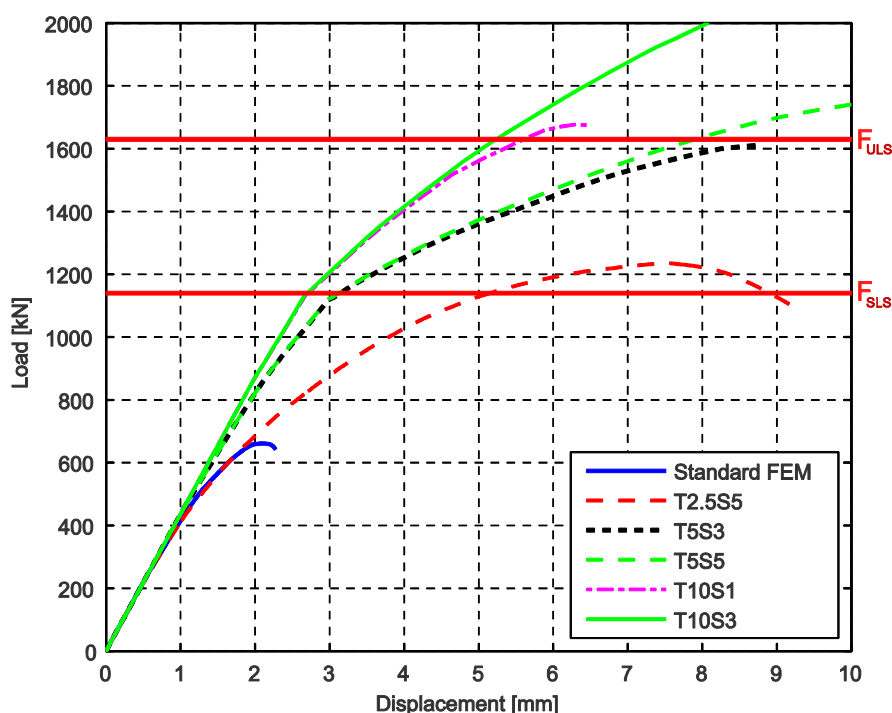


Figure 9-19 Force-displacement diagram for 2D FEM without horizontal reinforcement and softening-strain response

Table 9-7 shows that a higher tensile strength and a higher strength leads to an increase of the structural strength for 2D FEM with strain-softening response. This corresponds with the analysis as described before.



FRC mixture	W_{SLS}	W_{ULS}	F_{ULS}
Standard 2D FEM	x	∞	661 kN
T2.5S5	x	∞	1236 kN
T5S3	x	∞	1611 kN
T5S5	x	∞	1743 kN
T10S1	x	∞	1674 kN
T10S3	x	∞	2318 kN

Table 9-7 Critical values of Figure 9-19

The crack patterns for a standard 2D FEM and 2D FEM with T2.5S5 are showed in Figure 9-20. Both 2D FEM fail due to a major vertical and horizontal crack around the foundation pile, as showed in the figure. The main difference is that more small cracks develop in the 2DFEM with T2.5S5. The failure mechanism of the major crack is applicable for all 2D FEM with FRC composites. The smaller cracks are however less present in the 2D FEM with FRC composites with a higher tensile strength.

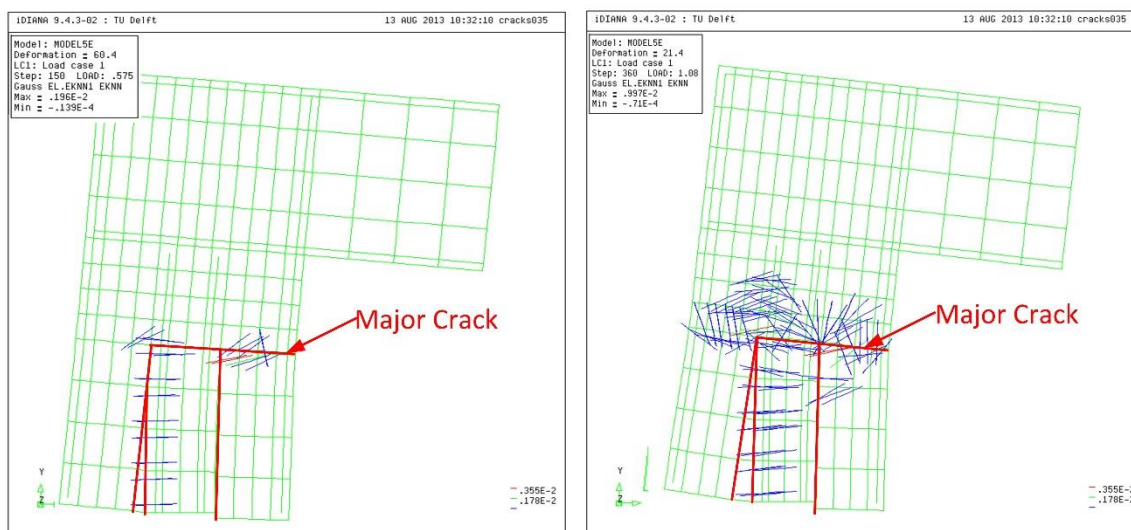


Figure 9-20 Crack pattern at moment of failure for left: the standard 2D FEM and right: the 2D FEM with T2.5S5



Figure 9-21 shows the crack pattern and the stresses in the vertical reinforcement of the 2D FEM with T10S3 at moment of failure. The crack pattern shows the same major cracks as showed in Figure 9-20. Only, small cracks at top of the connection are also present in this figure. The high tensile stresses in the vertical reinforcement are concentrated on top of the foundation pile. Inside the foundation pile, the tensile stresses are lower than the tensile strength.

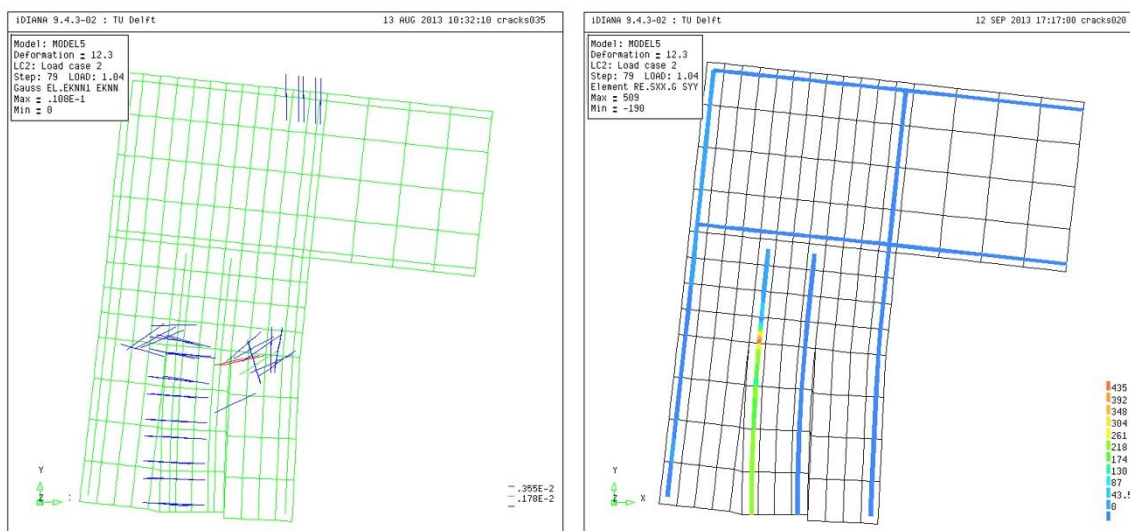


Figure 9-21 2D FEM with T10S3 at moment of failure, left: Crack pattern and right: stresses in the vertical reinforcement



9.3.7 Comparison between the different 2D FEM with FRC composites

The influence of FRC composites on the 2D FEM with and without reinforcement is described in the last sub sections. In this sub section, a comparison between different 2D FEM with FRC composites is made. In total three different comparisons are discussed. These are the influence of hardening versus softening, difference between 2D FEM with and without reinforcement and influence of FRC composites inside the foundation pile. The first two comparisons, 'hardening versus softening' and 'with or without reinforcement', use 2D FEM without FRC composites inside the foundation pile.

9.3.7.1 Comparison between 2D FEM with and without reinforcement

The force-displacement diagram of the 2D FEM with and without reinforcement is given in Figure 9-22. The FRC composites used in this comparison are the T2.5S5 and the T10S3. These are the minimum and maximum tensile strength of Table 9-1. The force-displacement diagram shows that a higher tensile strength for 2D FEM without reinforcement leads to a higher structural strength and 2D FEM with reinforcement have an improved rotational stiffness when the tensile strength is higher. In addition, the 2D FEM with no reinforcement and T10S3 has a comparable structural strength as the 2D FEM with reinforcement. Even though it shows that a higher tensile strength also lead to an improvement of the rotational stiffness for 2D FEM without reinforcement. It is however less than the 2D FEM with reinforcement.

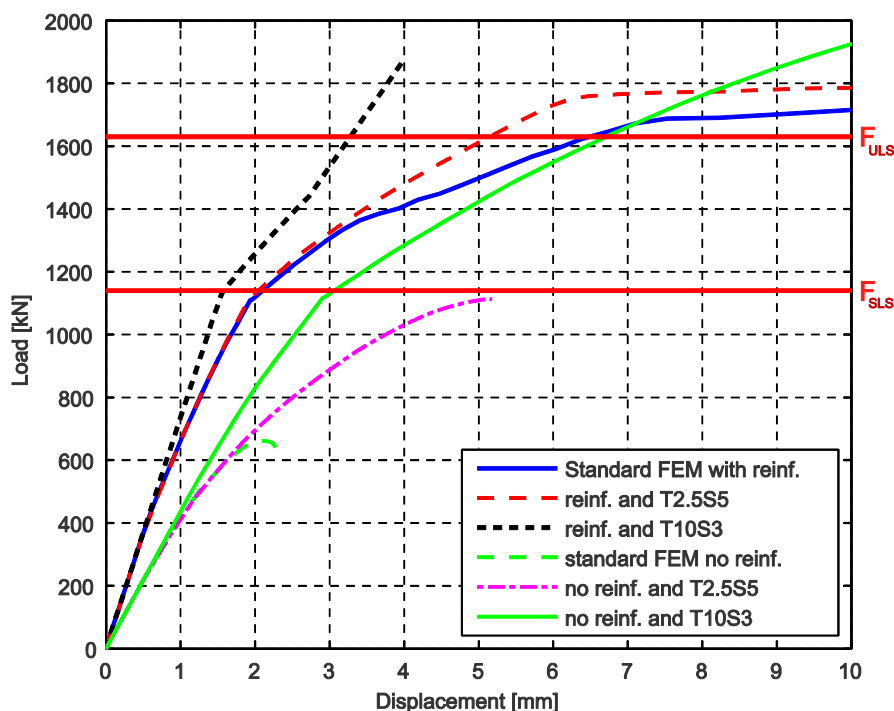


Figure 9-22 Force-displacement diagram of 2D FEM with and without reinforcement. 2D FEM are with FRC composites Reinf. = reinforcement



9.3.7.2 Hardening versus softening

The comparison between hardening and softening response is made in this sub subsection. Two force-displacement diagrams are analysed: The first diagram is without reinforcement and the second is with reinforcement. The FRC composites with hardening response are T2.5H3, T5H1 and T10H1 and with softening response are T2.5S5, T5S5 and T10S3.

The force-displacement diagram of Figure 9-23 shows the 2D FEM without reinforcement and hardening versus softening. The 2D FEM with hardening response have a slightly better performance in structural strength than the 2D FEM with softening response. This applies for all 2D FEM with hardening response in this research. This is however small for 2D FEM without reinforcement.

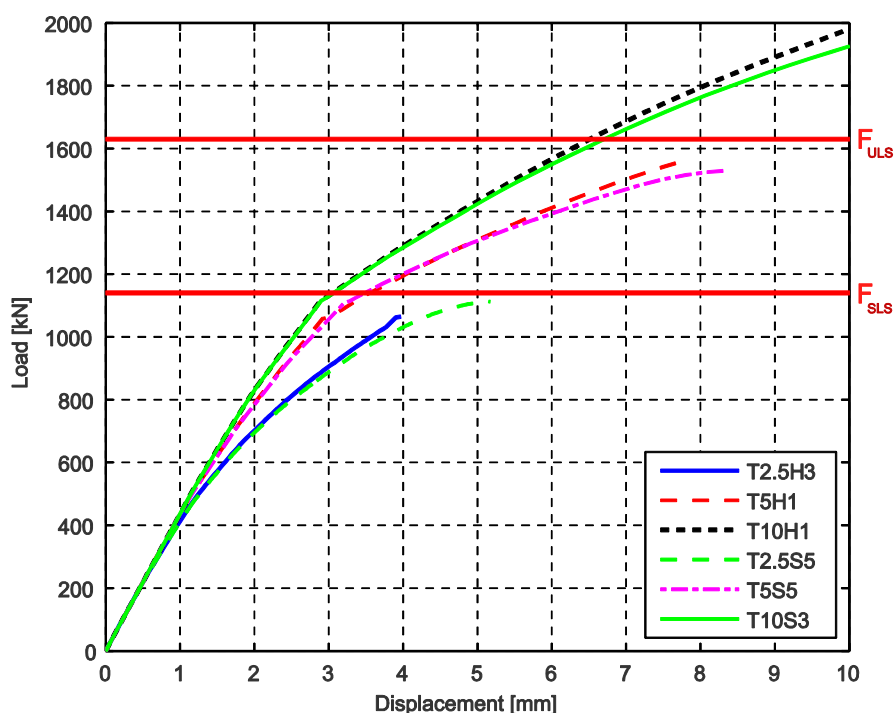


Figure 9-23 Force-displacement diagram of 2D FEM with reinforcement. 2D FEM without hardening and softening are compared.



The force-displacement diagram of Figure 9-24 presents the 2D FEM with reinforcement and hardening versus softening. The 2D FEM with hardening response have a higher structural strength than the 2D FEM with softening response. The difference is however small. This force-displacement diagram also shows that the analysis of the 2D FEM with hardening response are more unstable. This means that the maximum structural strength of the 2D FEM is not reach. For example, the 2D FEM with T10H1 which fails before the moment of failure is reached. This is also discussed in sub section 9.3.1.

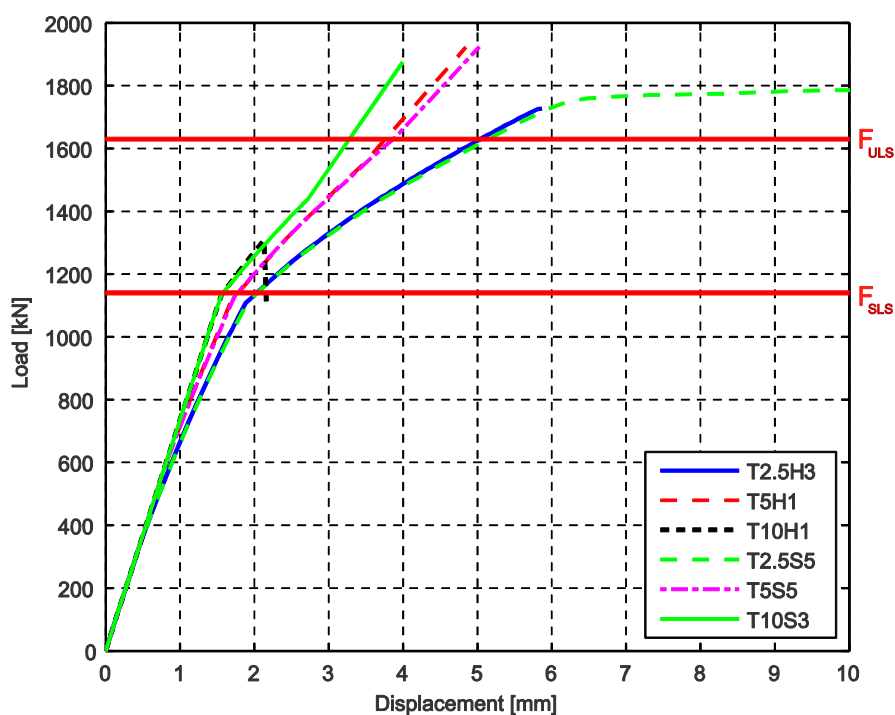


Figure 9-24 Force-displacement diagram of 2D FEM with reinforcement. 2D FEM with hardening and softening are compared.



9.3.7.3 Comparison between 2D FEM with and without FRC composites inside the foundation pile

The sub section deals with the comparison between 2D FEM with and without FRC composites inside the foundation pile. The comparison consists of the 2D FEM with T2.5H3, T10H1, T2.5S5 and T10S3. These 2D FEM are lowest and the highest tensile strength and both strain-softening and -hardening response. All 2D FEM do not have horizontal reinforcement in the foundation pile area.

The force-displacement diagram of Figure 9-25 shows the comparison between 2D FEM with and without FRC composites inside the foundation pile. The 2D FEM with FRC composites have a better performance in rotational stiffness in the connection. Also, the 2DFEM with a low tensile strength show that the 2D FEM with FRC composites inside the foundation pile have a higher structural strength of the connection. This is not visible for the 2D FEM with a high tensile strength, because it is outside the range of the graph, but also the 2D FEM with a high tensile strength and FRC composites have a higher structural strength.

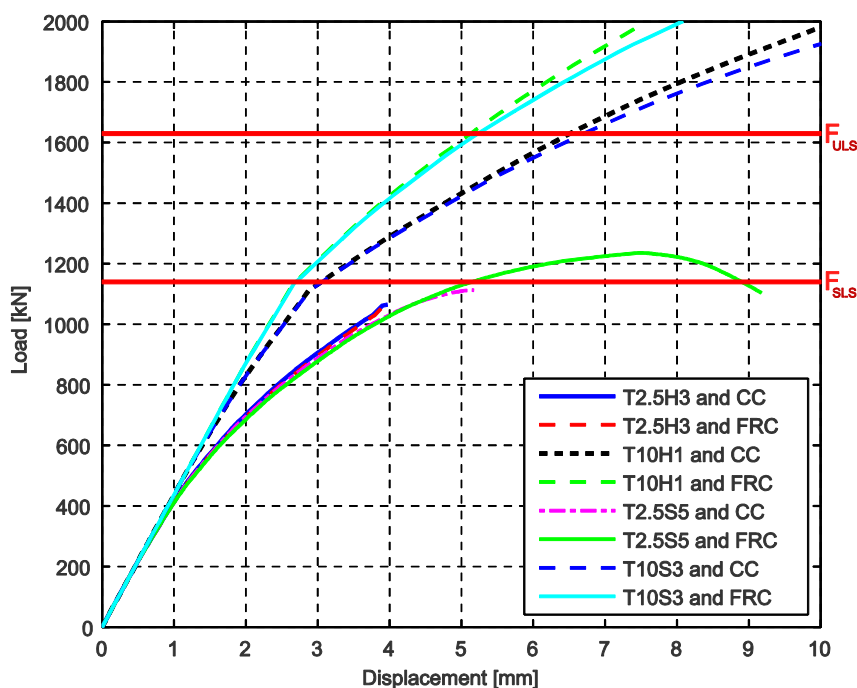


Figure 9-25 Force-displacement diagram of 2D FEM with and without FRC composites inside the foundation pile. CC= conventional concrete inside the foundation pile and FRC = FRC composites inside the foundation pile



Figure 9-26 shows the crack patterns of the 2D FEM with T10H1. On the left, the 2D FEM without FRC composites inside the foundation pile could be found and on the right, the 2D with FRC composites inside the foundation pile. The figure shows that FRC composites inside the foundation pile leads to less cracks in this area. Besides, it ensures a lower tensile stress in the foundation pile reinforcement and to more elastic foundation pile. The shape of the foundation pile is more parabolic. This is in total leads to a higher structural strength of the whole connection.

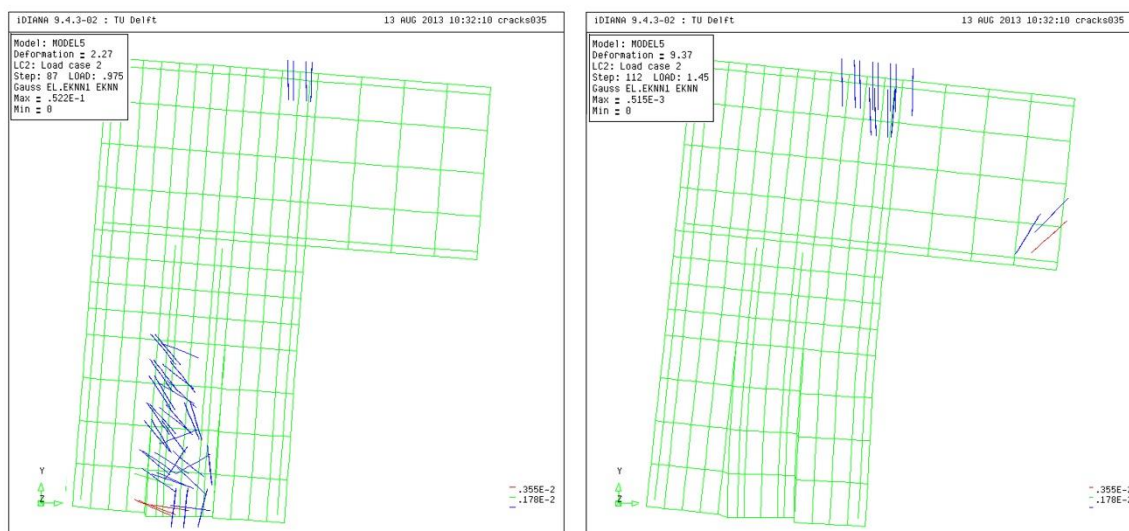


Figure 9-26 Crack pattern of 2D FEM with T10H1, left: without FRC composites inside the foundation pile and right: with FRC composites inside the foundation pile



9.4 Recommendations and Conclusions

In a short summary, section 9.3 shows the results of the 2D FEM with FRC composites. The FRC composites are mixtures with strain hardening or strain softening response and a variation in tensile strength and strain. The 2D FEM used in the analysis are with and without reinforcement. In the last sub section a comparison is made between the different 2D FEM with FRC composites. Based on the results of the 2D FEM with FRC composites, a number of conclusions can be drawn. These are listed below:

- A higher tensile strength for 2D FEM with horizontal reinforcement leads to an improvement of the rotational stiffness, but not to an increase of the structural strength.
- A higher tensile strength for 2D FEM without reinforcement leads to an increase of the structural strength of the connection.
- FRC composites inside the foundation pile of a 2D FEM improves the structural strength and the rotational stiffness of the connection
- A higher tensile strength for 2D FEM with horizontal reinforcement leads to an improvement of the rotational stiffness, but not to an increase of the structural strength.
- An improvement of the 2D FEM due to a higher strain is not visible in the results. It does not lead to an improvement of the structural strength or the rotational stiffness.
- The difference in the results between strain hardening and straining softening response is negligible. Therefore, strain hardening response is in case of a bridge connection not an improvement.

The conclusions show that 2D FEM without horizontal reinforcement and with a high tensile strength have a comparable structural strength as a 2D FEM with horizontal reinforcement and a normal tensile strength. Therefore on basis of this 2D FEM, it is possible to replace conventional concrete for FRC composites with a high tensile strength and to reduce the horizontal reinforcement in the connection at the same time. It is needed to mention that the rotational stiffness is lower for a connection without horizontal reinforcement and FRC composites. However, this is not necessary a problem when the total structure of the integral bridge is taken into account.

Further, FRC composites could be used in a connection with horizontal reinforcement as well. Then FRC composites are added to the connection to improve the rotational stiffness and to reduce the crack width. This is however not possible for the large horizontal crack next to foundation pile. This crack depends on the interaction between the foundation pile and the surrounding concrete. An improvement of the rotational stiffness is only beneficial, when the total structure of the integral bridge demands an increase of the connection rigidity. This depends on the specifications of the structure of the integral bridge.



10 Conclusion and recommendations

At the start of this thesis a 'plan of approach' (plan van aanpak) is drafted. In this document, a problem definition is formulated together with an approach to tackle the problem. This problem definition at start of the thesis was:

Problem definition

A lot of reinforcement is needed in the connections and joints of integral bridges. This makes the embedding of reinforcement in the connection rather complex. This one of the reasons for not applying integral bridges, because it is uncertain if this amount of reinforcement is needed and if it is still executable.

At the start, the solution for this problem definition was sought in the direction of 'fibre reinforced concrete (FRC)'. This was formulated in the following goal:

Goal

The goal is to research if FRC composites are a useful application for monolithic connections of integral bridges. This applies for connections between super- and substructure and connections between the bridge decks.

In addition to the goal, a question was formulated. This is showed below:

Is engineered cementitious composite/ fibre reinforced concrete suitable to be applied in monolithic connections of integral bridges?

In this chapter, it is attempted to give answer to this question. In addition, it is tried to present a conclusion after this report. During the process, the focus of the thesis is changed to a more general view about the connections of current integral bridges and the reinforcement applied in these connections. Therefore, not only the question of this thesis is answered, but also the results of the research to connections in current integral bridges is included.



10.1 Conclusion

An integral bridge is a durable structure due to the absence of expansion joints and bearings. However, without expansion joints and bearings the bridge deforms into the soil due to the deformation of the bridge deck. Important is that a bridge deck can be deform that certain problems related to deformation do not occur or are kept under control. These problems are the settlement of the soil, damaging to pavement, foundation, wing walls and abutment and early age cracking. By taking these problems into consideration, integral bridges are good alternative to conventional bridges.

Fibre reinforced cementitious composites could be distinguished from conventional concrete due to the application of fibres. The application of fibres leads to some interesting properties, for example nstrength, ductility, toughness, durability, stiffness and thermal resistance. ECC in particular has an increase of tensile strain and a huge reduction of the crack width. It could be said that the possibilities of FRC composites are not fully exploited on basis of this research.

The conclusions in regarding to the connection of the integral bridge are based on the results of the calculations. The calculations both analytical and FEM showed the structural behaviour of the connection under a loading combination of forces and moment. This presented information about the design of the connection and which parts are important for the strength of the connection.

First, the analytical calculations of chapter 7 show that a coupling force in the foundation pile is the decisive structural behaviour for the connection (see section 7.5). This was confirmed by the 2D FEM of chapter 8, where the influence of the reinforcement and cohesion and friction between the foundation pile and the surrounding concrete is researched. The results of the 2D FEM showed further that the structural strength of the connection depends strongly on the horizontal reinforcement, which crosses the foundation pile in this model (see section 8.4, 8.5 and 8.6). Also, the crack width of the crack on the left side of the foundation pile is smaller for FEM with horizontal reinforcement in the lower part of the connection, which shows the importance of the horizontal reinforcement.

The 2D FEM of chapter 8 is used to research the influence of FRC composites in a connection of an integral bridge. The FRC composites are mixtures with strain hardening or strain softening response and a variation in tensile strength and strain. The 2D FEM used in the analysis are with and without reinforcement. The results show that the use of FRC composites lead to an improvement of the rotational stiffness and for 2D FEM without the horizontal reinforcement also to a higher structural strength. The difference in the results between strain hardening and straining softening response is negligible. Therefore, it can be concluded on basis of the 2D FEM that FRC composites could be used as replacement of a part of the reinforcement. The high tensile strength of the FRC composites lead to a connection with a similar structural strength as as connection with horizontal reinforcement. It is needed to mention that the rotational stiffness is lower for a connection without horizontal reinforcement and FRC composites. However, this is not necessary a problem when the total structure of the integral bridge is taken into account.



10.2 Recommendations

On basis of this thesis, certain recommendations could be made. These recommendations are split in recommendations for the connection of integral bridges, for FRC composites and for integral bridges in general.

The connection of integral bridges

- The 2D FEM showed that cohesion and friction have almost no influence on the structural strength of the connection. It is therefore not advisable to invest in dowels on the foundation pile.
- The research shows that the horizontal reinforcement at the bottom of the connection is more efficient than the horizontal reinforcement more to the top. Therefore, it is advisable to concentrate the horizontal reinforcement at the bottom of the connection.
- The results of the 3D FEM were insufficient. More research is needed to understand the behaviour of the connection in the extra direction. This applies for the cracking behaviour of the bridge connection.
- FRC composites could replace reinforcement inside the connection on basis of the research. This lead to less complex construction of the connection.

Integral bridges

- The study showed that the interaction between the integral bridge and the soil still uncertain. More research is needed before integral bridges are commonly applied in the Netherlands.
- The study also shows that structure of integral bridges is rather complex in comparison with conventional bridges. Yet, the benefits of integral bridges, like lower maintenance are clear. More experience of structural engineers with integral bridges could ensure that integral bridges are more applied.

FRC composites

- FRC composites have certain benefits relative to normal concrete. Examples are the higher tensile strength and higher strain. The search for good applications of this material could lead to an increase of the use of FRC composites. Another possible application could be a joint between the bridge decks of both conventional and integral bridges. This is previously proposed in the study.
- Standardisation or 'strength and strain classes could also be beneficial for the use FRC composites.
- Research that is aligned to practice or in cooperation with engineering companies could also boost the use of FRC composites.



References

- [1] A. Laaksonen, "Structural behaviour of long concrete bridges," Tampere University of technology, 2011.
- [2] A. Paraschos and A. M. Amde, "A survey on the status of use, problems and costs of associated with integral abutment bridges," New York City Department of Transportation.
- [3] Dr.ir. C. van der Veen, *lecture material of concrete bridges CIE5127*, Delft University of Technology, 2012.
- [4] fib taskgroup 6.4, "precast concrete bridges," fib, 2004.
- [5] Spanbeton, "Bruggen\liggers," [Online]. Available: www.spanbeton.nl. [Accessed 2012].
- [6] dr.ir.drs. C.R. Braam and prof.dr.ir. J.C. Walraven, *Prestressed Concrete*, Delft: Delft University of Technology, 2011.
- [7] "section 10 inspection and evaluation of substructures," infrasture engineers inc., 2013. [Online]. Available: <http://www.infrastructureengineers.com/KnowledgeLibrary2011/PDFs/>.
- [8] Wisconsin Department of Transportation, "WisDOT bridge manual," 2012.
- [9] S. v. d. Voorde, "Abraham Lipski en de uitvinding van de preflex-balk," *Cement*, no. 6, pp. 26-29, 2008.
- [10] M. P. Burke Jr., *Integral and Semi-integralbridges*, Wiley-Blackwell, 2009.
- [11] J. Kunin and S. Alampalli, "Integral Abutment Bridges: Current practice in the US and Canada," New York Department of Transportation, 1999.
- [12] A. Maijenburg, "Integraalbruggen - Stand van zaken," Rijkswaterstaat/Delft University of Technology, 2000.
- [13] ir. P. van der Sanden, "Integraal kunstwerken met verrassingen," *Cement*, pp. 44-49, 2 2009.
- [14] ir. J.M.J.F. Thijs, "Integraalviaducten met voegloze overgangen in de A73-zuid," *Cement*, pp. 26-30, 6 2006.
- [15] S. Arsoy, R. M. Barker Ph.D. and M. J. Duncan Ph.D., "The Behaviour of Integral Abutment Bridges," Virginia Department of Transportation and the University of Virginia, 1999.
- [16] The Highways agency, "BA 92/46 The design of integral bridges," The Highways agency;, 2003.
- [17] K. F. Dunker and D. Liu, "Foundations for integral abutments," *practice periodical on structural design and construction (asce)*, vol. 12, pp. 22-30, 2007.
- [18] H. White 2nd, "integral abutment bridges: comparison of current practice between European countries and United States of America," New York Department of Transportation, 2007.
- [19] R. E. Abendroth and L. F. Greimann, "Field testing of integral abutments," Iowa State University, 2005.
- [20] R. F. Maruri and S. H. Petro, "Integral Abutments and Jointless Bridges (IAJB) 2004 Survey Summary," in *THE 2005 – FHWA CONFERENCE*, 2005.



- [21] R. E. Abendroth and L. F. Greimann, "an integral abutment bridge with precast concrete piles," Iowa State University, 2007.
- [22] E. Yandzio, "Design guide for steel sheet pile bridge abutments," The steel construction institute, 1998.
- [23] J. S. Horvath, "Integral-Abutment Bridges: Problems and Innovative Solutions Using EPS Geofoam and Other Geosynthetics," Manhattan College, 2000.
- [24] G. L. England, N. C. Tsang and D. I. Bush, Integral bridges - A fundamental approach to the time-temperature loading problem, Imperial College, Highways agency, 2000.
- [25] M. Dicleli and S. M. Albhaisi, "Effect of cyclic thermal loading on the performance of steel H-piles in integral bridges with stub abutments," *Journal of Constructional Steel Research*, vol. 60, pp. 161-182, 2004.
- [26] R. Hällmark, P. Collin, H. Pétursson and B. Johansson, "Simulation of Low-cycle Fatigue in Integral Abutment Piles," Luleå University of Technology, 2007.
- [27] C. Lan, "On the performance of super long integral abutment bridges: parametric analyses and design optimization," University of Trento, 2012.
- [28] NEN-EN 1991-1-5 Eurocode 1: Belastingen op constructies -Deel 1-5: Algemene belastingen - Thermische belasting, Nederlands Normalisatie instituut, 2007.
- [29] NEN-EN 1992-1-1 Eurocode 2: Ontwerp en berekening van betonconstructies - Deel 1-1: Algemene regels voor gebouwen, Nederlands Normalisatie Instituut, 2011.
- [30] E.-I. Tazawa, Autogenous Shrinkage of Concrete, Japan Concrete Institute (JCI), 1999.
- [31] M. Sivakumar and M. Arockiasamy, "Effects of Restraint Moments in Integral Abutment bridges," in *THE 2005 – FHWA CONFERENCE Integral Abutment and Jointless Bridges (IAJB)*, 2005.
- [32] R. M. Barker et al, "Manual for design of bridge foundations," Transportation Research Board, Washington, 1991.
- [33] A. M. Wolde-Tinsae and L. Greimann , "design model for piles in jointless bridges," *Journal of Structural Engineering*, vol. 1988, no. 6, pp. 1354-1371, 1987.
- [34] J. C. Walraven, "High performance fiber reinforced concrete: progress in knowledge and design codes," *Materials and Structures*, no. 42, p. 1247–1260, 2009.
- [35] Prof. K. Rokugo et al., "Recommendations for design and construction of Fiber reinforced cement composites with multiple fine cracks (HPFRCC)," Japan society of civil engineers, 2008.
- [36] A. E. Naaman and H. W. Reinhardt, "Proposed classification of HPFRC composites based on their tensile response," *Material and structures*, vol. 39, p. 547–555, 2006.
- [37] E. S. Lappa, "High Strength Fibre Reinforced Concrete: Static and fatigue behaviour in bending," Delft University of Technology, Delft, 2007.
- [38] I. Markovic, "High-Performance Hybrid-Fibre Concrete: Development and Utilisation," Delft University of Technology, Delft, 2006.



- [39] V. Li and T. Kanda, "Engineered Cementitious Composites for Structural Applications," in *ASCE Forum*, 1998.
- [40] V. C. Li, "On Engineered Cementitious Composites (ECC): A Review of the Material and Its Applications," *Journal of Advanced Concrete Technology (Japan Concrete Institute)*, no. 3, pp. 215-230, 2003.
- [41] M. Sahmaran and V. C. Li, "Durability of mechanically loaded engineered cementitious composites under highly alkaline environments," *Cement & Concrete Composites*, no. 30, pp. 72-81, 2008.
- [42] Y. Zhu, Y. Yang and Y. Yao, "Use of slag to improve mechanical properties of engineered cementitious composites (ECCs) with high volumes of fly ash," *Construction and building materials*, no. 36, p. 1076–1081, 2012.
- [43] J. ZHOU, "Performance of Engineered Cementitious Composites for Concrete Repairs," Delft University of Technology, 2011.
- [44] M. Fujishiro, K. Suda and Y. Nagata, "Voegloos voorgespannen betonviaduct met ECC," *Cement*, no. 4, pp. 24-25, 2008.
- [45] V.C. Li et al., "On the Shear Behavior of Engineered Cementitious Composites," University of Michigan; Institute of Technology, Shimizu Corporation.
- [46] C. K. Leung, Y. N. Cheung and J. Zhang, "Fatigue enhancement of concrete beam with ECC layer," *Cement and Concrete Research*, no. 37, p. 743–750, 2007.
- [47] "Stringer Panel Method," Tu Delft, 1999. [Online]. Available: <http://homepage.tudelft.nl/p3r3s/spancad/index.html>.
- [48] prof.dr.ir. J. Blauwendraad, "Ontwerpen van betonconstructies met een staaf-paneel model [Dutch]," *Cement*, vol. 5, pp. 48-58, 1994.
- [49] ir. P.C.J. Hoogenboom, "Validatie van het staaf-paneel model [Dutch]," *Cement*, vol. 6, pp. 20-27, 1994.
- [50] prof.dr.ir.J. Blauwendraad, "Staven, panelen en elementen," *Cement*, vol. 7, pp. 80-85, 2012.
- [51] *TNO Diana version: 9.4.3, release date: July 1, 15:44:13, 2011.*
- [52] *NEN 6770 Staalconstructies TGB 1990 Basiseisen en basisrekenregels voor overwegend statisch belaste constructies*, 1997.
- [53] Rijkswaterstaat, "Richtlijnen ontwerp kunstwerken (ROK 1.0)," RWS Dienst Infrastructuur, 2011.
- [54] M. Dicleli and S. Erhan, "Effect of soil-bridge interaction on the magnitude of internal forces in integral abutment bridge components due to live load effects," *Engineering Structures*, pp. 129-145, 32 2010.



Appendix A: Strut-and-tie and shear-panel models

1.1 Shear panel models, strut-and-tie models and stresses of method 1

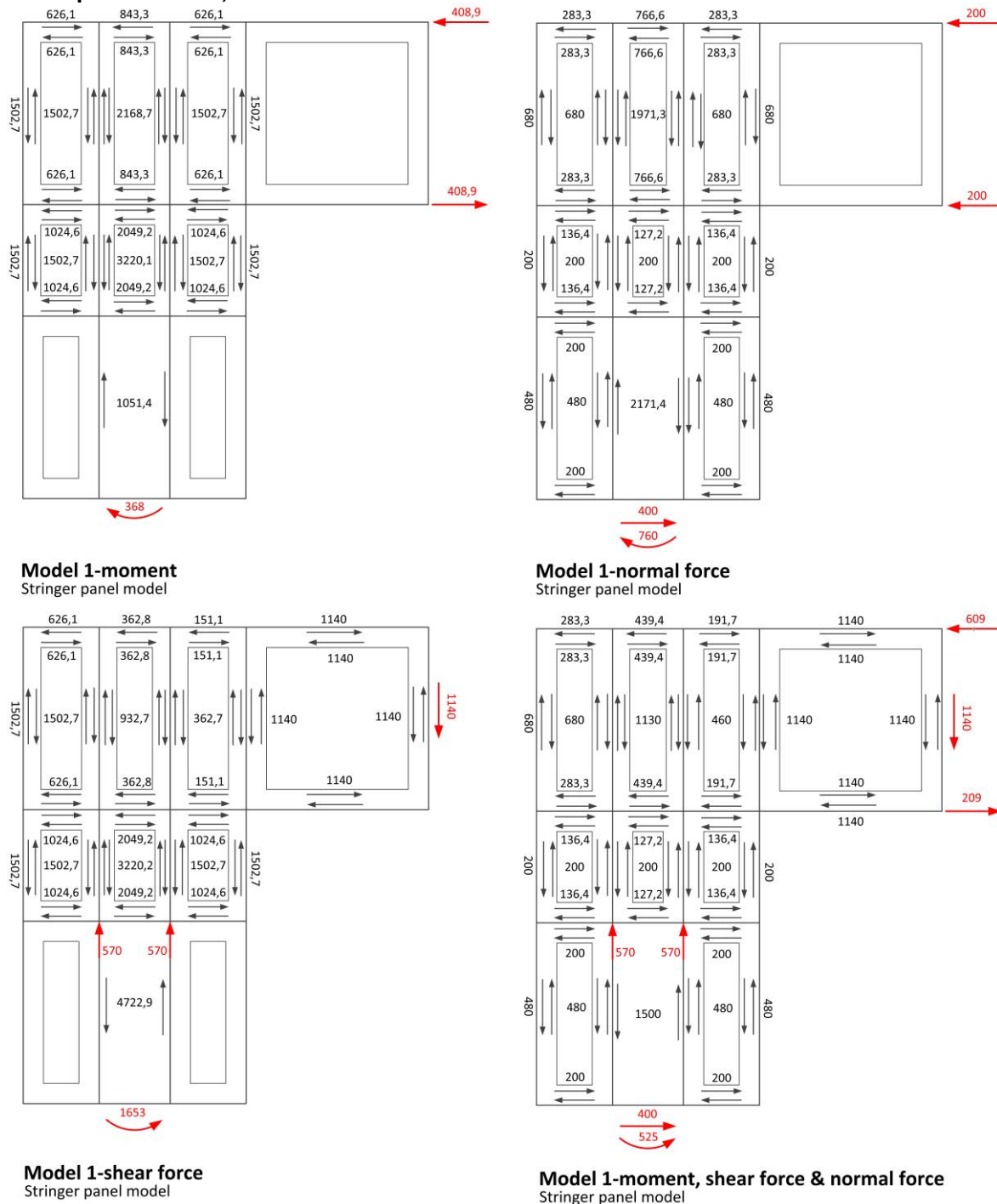
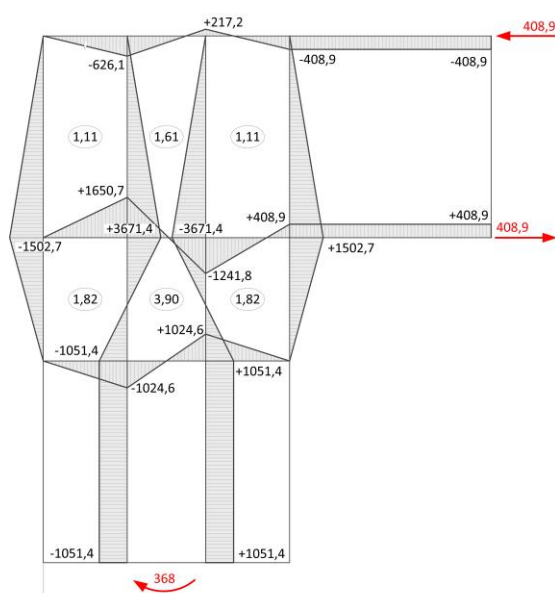
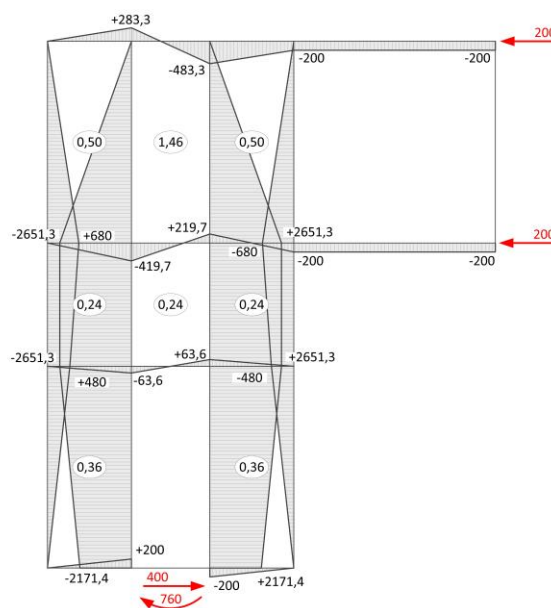


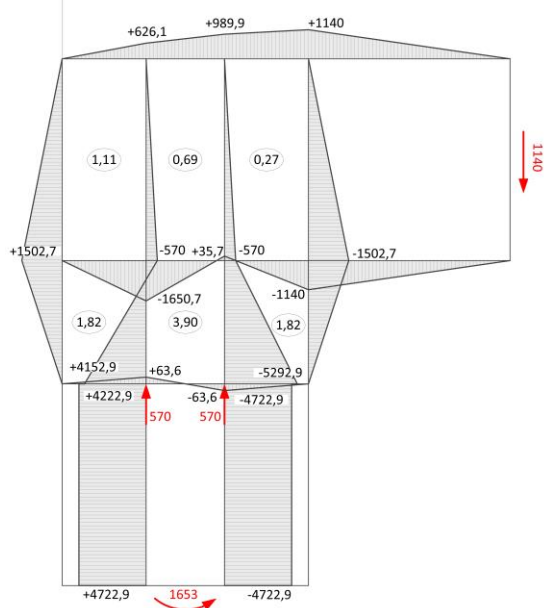
Figure 1 Shear panel models of method 1



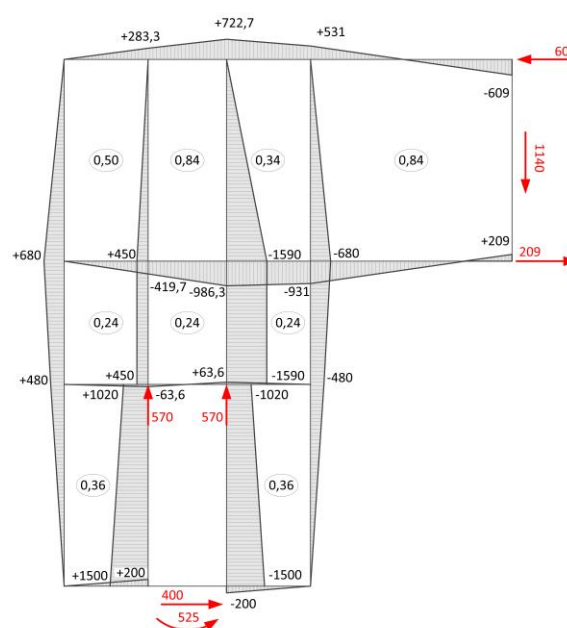
Model 1-moment
SPM normal forces & shear stresses



Model 1-normal force
SPM normal forces & shear stresses

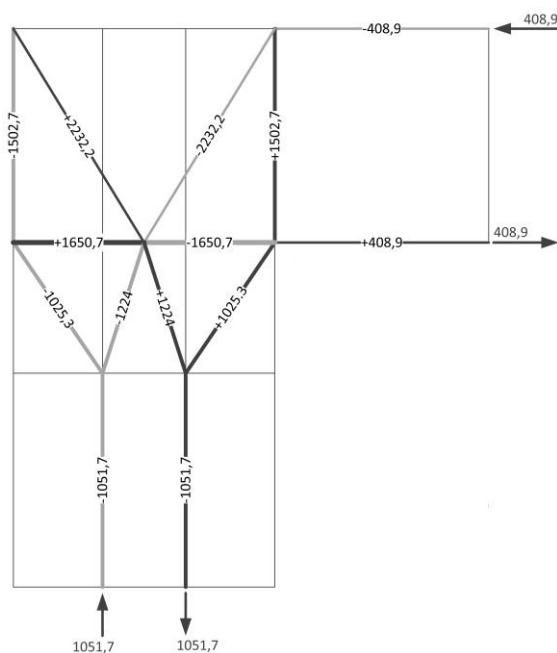


Model 1-shear force
SPM normal forces & shear stresses

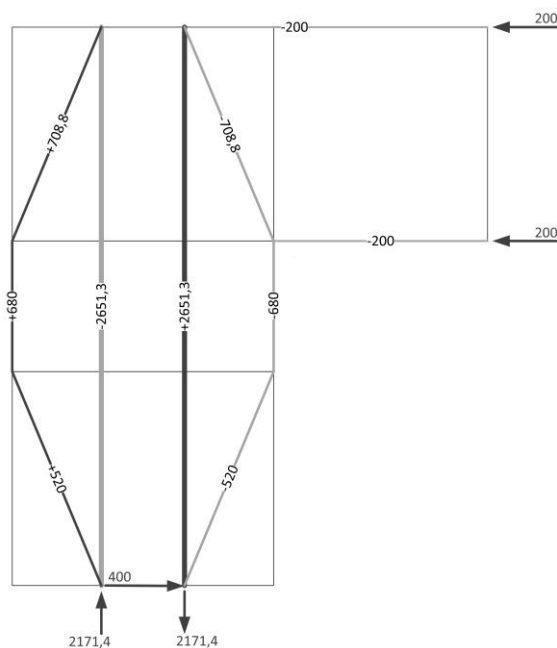


Model 1-moment, shear force & normal force
SPM normal forces & shear stresses

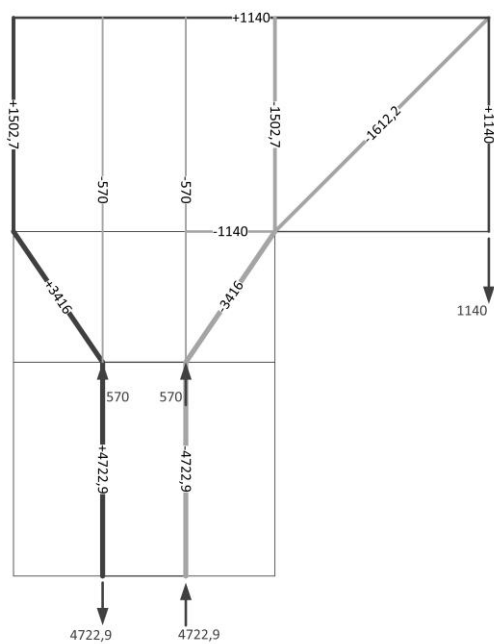
Figure 2 Normal and shear stresses of method 1



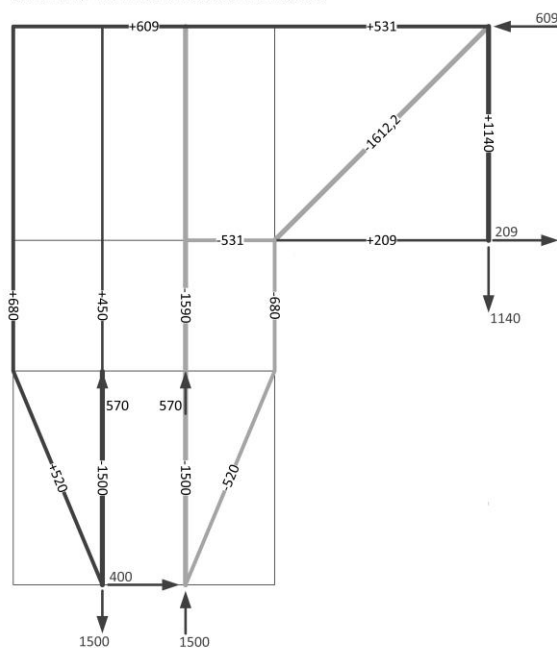
Model 1-moment
Strut and Tie model-flow of the forces



Model 1-normal force
Strut and Tie model-flow of the forces



Model 1-shear force
Strut and Tie model-flow of the forces

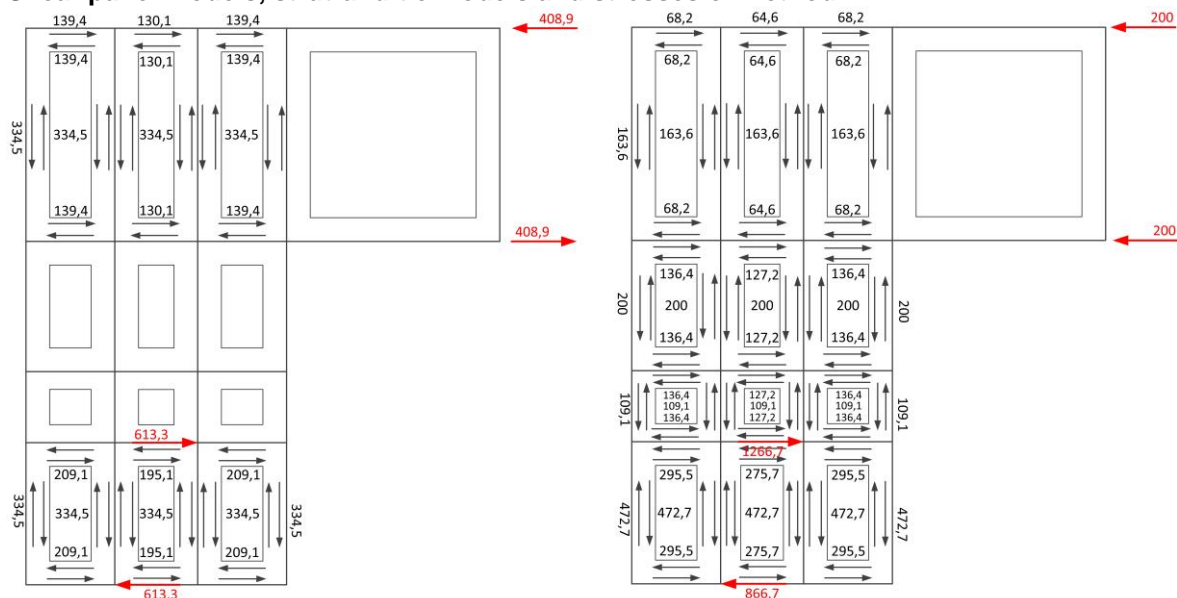


Model 1-moment, normal force & shear force
Strut and Tie model-flow of the forces

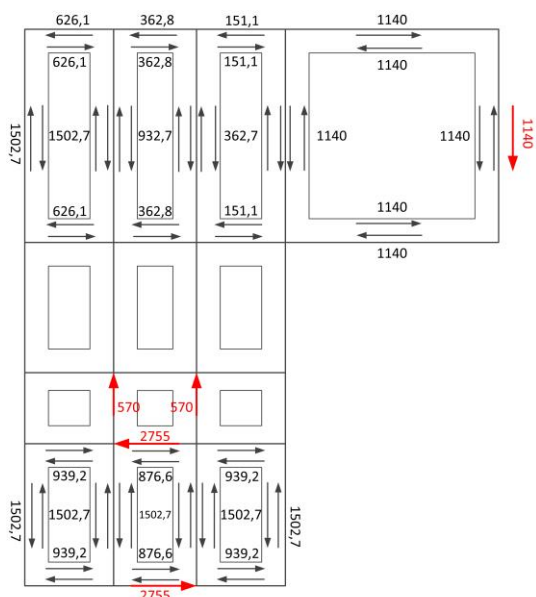
Figure 3 Strut-and-tie models of method 1



1.2 Shear panel models, strut-and-tie models and stresses of method 2



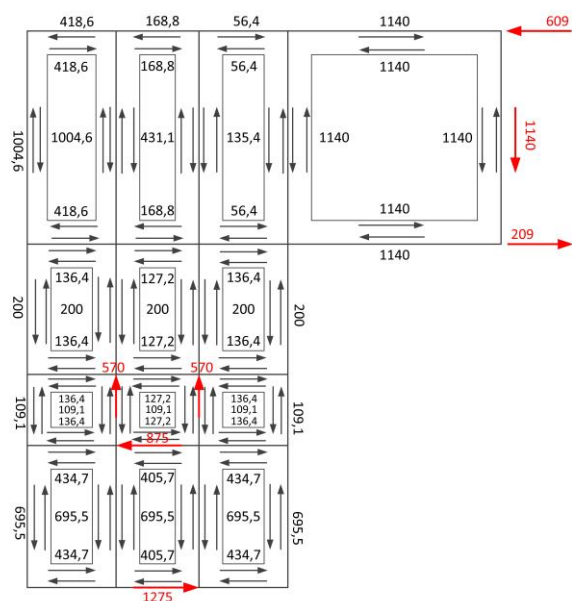
Model 2-moment
Stringer panel model



Model 2-shear force
Stringer panel model

Figure 4 Shear panel models of method 2

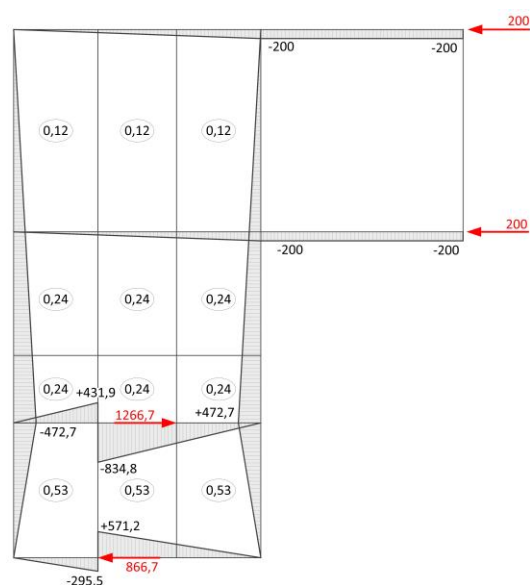
Model 2-normal force
Stringer panel model



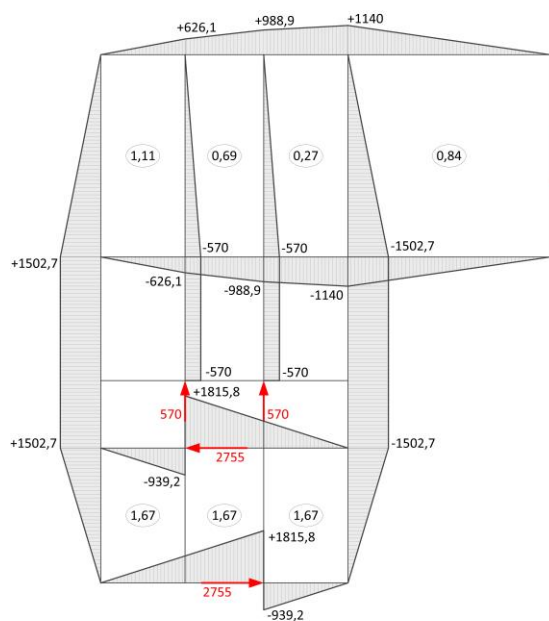
Model 2-moment, shear force & normal force
Stringer panel model



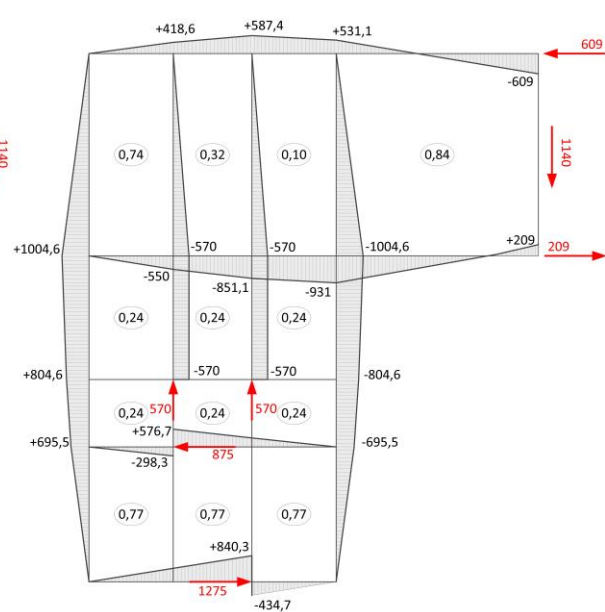
Model 2-moment
SPM normal forces & shear stresses



Model 2-normal force
SPM normal forces & shear stresses

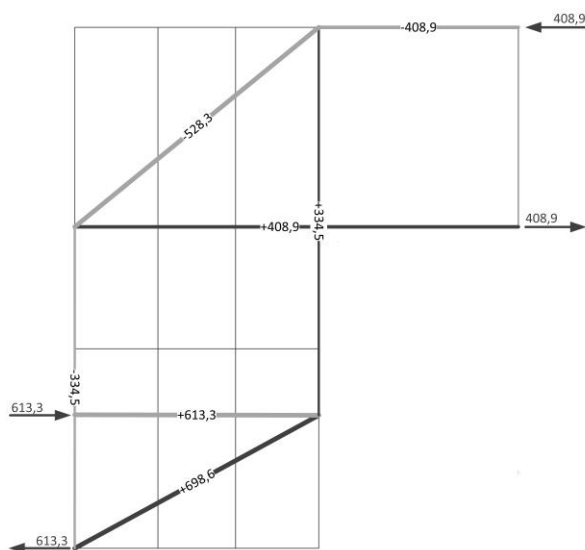


Model 2-shear force
SPM normal forces & shear stresses

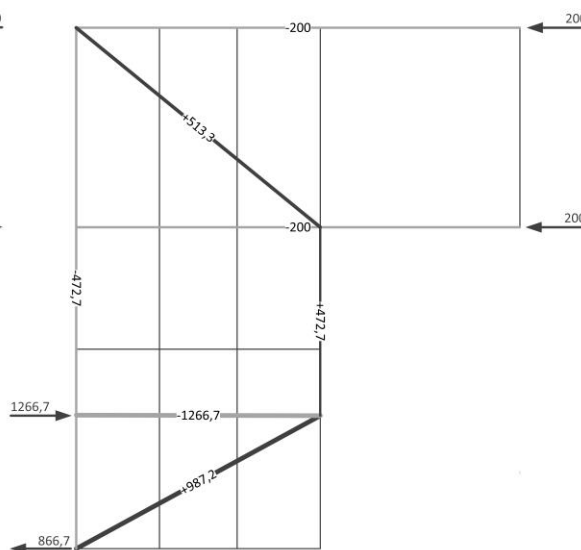


Model 2-moment, shear force & normal force
SPM normal forces & shear stresses

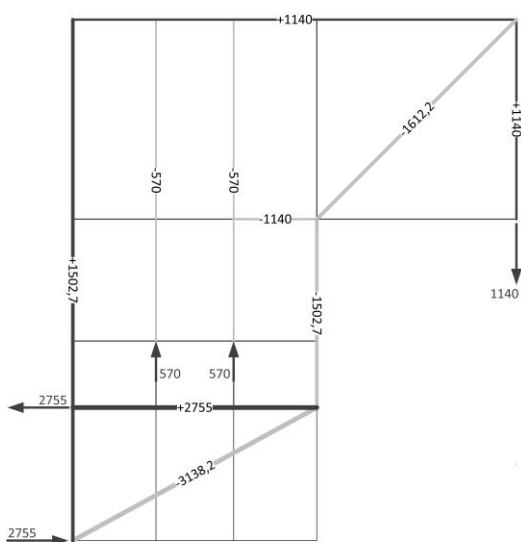
Figure 5 Normal and shear stresses of method 2



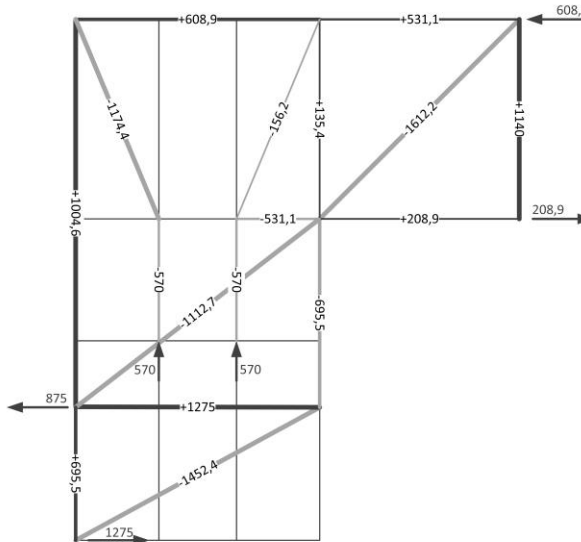
Model 2-moment
Strut and Tie model-flow of the forces



Model 2-normal force
Strut and Tie model-flow of the forces



Model 2-shear force
Strut and Tie model-flow of the forces



Model 2-moment, normal force & shear force
Strut and Tie model-flow of the forces

Figure 6 Strut-and-tie models of method 2



Appendix B: Data input and dcf-file in TNO DIANA

1.1 Data-input TNO DIANA

Parts of the DAT-file for a standard 2D FEM with horizontal reinforcement are showed below. This is representative for all 2D FEM in chapter 8 and 9.

'REINFORCEMENTS'

LOCATI

```
7 BAR
  LINE    0.400000E+02  0.400000E+02  0.000000E+00
          0.400000E+02  0.231000E+04  0.000000E+00
8 BAR
  LINE    0.106000E+04  0.400000E+02  0.000000E+00
          0.106000E+04  0.231000E+04  0.000000E+00
9 BAR
  LINE    0.400000E+02  0.231000E+04  0.000000E+00
          0.200000E+04  0.231000E+04  0.000000E+00
10 BAR
  LINE    0.400000E+02  0.149000E+04  0.000000E+00
          0.200000E+04  0.149000E+04  0.000000E+00
11 BAR
  LINE    0.427500E+03  0.000000E+00  0.000000E+00
          0.427500E+03  0.140000E+04  0.000000E+00
12 BAR
  LINE    0.672500E+03  0.000000E+00  0.000000E+00
          0.672500E+03  0.140000E+04  0.000000E+00
14 BAR
  LINE    0.400000E+02  0.400000E+02  0.000000E+00
          0.106000E+04  0.400000E+02  0.000000E+00
16 BAR
  LINE    0.400000E+02  0.850000E+03  0.000000E+00
          0.106000E+04  0.850000E+03  0.000000E+00
18 BAR
  LINE    0.400000E+02  0.730000E+03  0.000000E+00
          0.106000E+04  0.730000E+03  0.000000E+00
20 BAR
  LINE    0.400000E+02  0.610000E+03  0.000000E+00
          0.106000E+04  0.610000E+03  0.000000E+00
22 BAR
  LINE    0.400000E+02  0.490000E+03  0.000000E+00
          0.106000E+04  0.490000E+03  0.000000E+00
24 BAR
  LINE    0.400000E+02  0.370000E+03  0.000000E+00
          0.106000E+04  0.370000E+03  0.000000E+00
26 BAR
  LINE    0.400000E+02  0.250000E+03  0.000000E+00
          0.106000E+04  0.250000E+03  0.000000E+00
28 BAR
  LINE    0.400000E+02  0.130000E+03  0.000000E+00
          0.106000E+04  0.130000E+03  0.000000E+00
```



```
MATERIALS
/ 7-12 14 16 18 20 22 24 26 28 /      7
GEOMETRY
/ 9 10 /      3
/ 7 8 /      4
/ 11 12 /     5
/ 14 /      7
/ 16 18 20 22 24 26 28 /      9
'MATERIALS'
  1 YOUNG      3.100000E+04
    POISON    1.500000E-01
    TOTCRK ROTATE
    TENCRCV LINEAR
    TENSTR     2.900000E+00
    EPSULT     2.175000E-03
    COMCRV CONSTA
    COMSTR     3.700000E+01
  2 YOUNG      3.850000E+04
    POISON    1.500000E-01
    TOTCRK ROTATE
    TENCRCV LINEAR
    TENSTR     4.200000E+00
    EPSULT     2.175000E-03
    COMCRV CONSTA
    COMSTR     6.700000E+01
  3 YOUNG      2.100000E+05
    POISON    3.000000E-01
    YIELD VMISES
    HARDIA 415. 0.002175 415. 0.15 0. 0.1501 0. 100.
    HARDEN WORK
  4 DSTIF      3.100000E+04      1.347800E+04
    FRICTI
    FRCVAL     3.500000E-02      5.000000E-01      1.000000E-05
    GAP|
    GAPVAL     1.000000E-05
    MODE2 0
  5 DSTIF      3.100000E+04      1.347800E+04
  6 DSTIF      3.850000E+04      1.673900E+04
  7 YOUNG      2.100000E+05
    YIELD VMISES
    HARDEN WORK
    HARDIA 435. 0.002175 470. 0.045 0. 0.0451 0. 100.
```



```
'GEOMETRY'
  1 THICK      1.500000E+03
  2 THICK      1.500000E+03
  CONFIG MEMBRA
  3 CROSSE     3.016000E+03
  4 CROSSE     7.363000E+03
  5 CROSSE     1.250000E+03
  7 CROSSE     3.436000E+03
  8 RECTAN     1.250000E+01   4.100000E+02
  9 CROSSE     1.963000E+03

'SUPPORTS'
/ 1 10 88 93 98 103 108 117 126 135 144 / TR 1
/ 1 10 88 93 98 103 108 117 126 135 144 / TR 2

'LOADS'
CASE 1
ELEMEN
/ 153 157 161 165 /
EDGE KSI1
FORCE -0.444444E+03
DIRECT 1
/ 153 157 161 165 /
EDGE KSI1
FORCE -0.126667E+04
DIRECT 2
/ 153 /
EDGE KSI1
FORCE 0.136296E+04 0.204445E+04 0.272593E+04
DIRECT 1
/ 157 /
EDGE KSI1
FORCE 0.000000E+00 0.681482E+03 0.136296E+04
DIRECT 1
/ 161 /
EDGE KSI1
FORCE -0.136296E+04 -0.681482E+03 0.000000E+00
DIRECT 1
/ 165 /
EDGE KSI1
FORCE -0.272593E+04 -0.204445E+04 -0.136296E+04
DIRECT 1
CASE 2
ELEMEN
/ 153 157 161 165 /
EDGE KSI1
FORCE -0.126667E+04
DIRECT 2
/ 153 /
EDGE KSI1
FORCE 0.136296E+04 0.204445E+04 0.272593E+04
DIRECT 1
/ 157 /
EDGE KSI1
FORCE 0.000000E+00 0.681482E+03 0.136296E+04
DIRECT 1
/ 161 /
EDGE KSI1
FORCE -0.136296E+04 -0.681482E+03 0.000000E+00
DIRECT 1
/ 165 /
EDGE KSI1
FORCE -0.272593E+04 -0.204445E+04 -0.136296E+04
DIRECT 1
```



1.2 Dcf-file in TNO DIANA

There are two different dcf-files used: The first dcf-file has only one step with iterative steps with moment, shear force and normal force till failure. The second dcf-file has automatic steps with 1.0 x moment, shear force and normal force and the second step is with iterative steps and only moment and shear force till failure.

1.2.1 *Dcf-file in TNO Diana with only iterative steps*

```
*FILOS
  INITIA
*INPUT
  READ FILE "mode15A.dat"
*END
*NONLIN
  BEGIN EVALUA
    REINFO INTERF
  END EVALUA
  BEGIN EXECUT
    BEGIN LOAD
      LOADNR 1
      BEGIN STEPS
        BEGIN ITERAT
          ARCLEN
          INISIZE=0.01
          MAXSIZ=0.005
          NSTEPS=1000
        END ITERAT
        SAVE
      END STEPS
    END LOAD
  END EXECUT
  BEGIN OUTPUT FEMVIE
    FILE "mode15E"
    DISPLA TOTAL TRANSL GLOBAL
    FORCE REACTI TRANSL GLOBAL
    FORCE EXTERN TRANSL GLOBAL
    STRAIN CRACK GREEN
    STRAIN CRKWDT GREEN GLOBAL
    STRAIN PLASTI GREEN GLOBAL
    STRESS TOTAL CAUCHY GLOBAL
  END OUTPUT
  BEGIN OUTPUT TABULA
    BEGIN SELECT
      NODES 550 554 558 562 566 574 582 590 598
    END SELECT
    FORCE EXTERN TRANSL GLOBAL
    DISPLA TOTAL TRANSL GLOBAL
  BEGIN LAYOUT
    LINPAG 15000
  END LAYOUT
  END OUTPUT
*END
```



1.2.2 *Dcf-file in TNO Diana with automatic and iterative steps*

```
*FILOS
INITIA
*INPUT
  READ FILE "mode12d.dat"
*END
*NONLIN
BEGIN EVALUA
  REINFO INTERF
END EVALUA
BEGIN EXECUT
  BEGIN LOAD
    LOADNR 1
    BEGIN STEPS
      BEGIN AUTOMA
        ARCLEN
        SIZE=1
        MAXSIZE=0.03
      END AUTOMA
      SAVE
    END STEPS
  END LOAD
END EXECUTE
BEGIN EXECUT
  BEGIN LOAD
    LOADNR 2
    BEGIN STEPS
      BEGIN ITERAT
        ARCLEN
        INISIZE=0.01
        MAXSIZ=0.002
        NSTEPS=2000
      END ITERAT
      SAVE
    END STEPS
  END LOAD
END EXECUT
```



```
BEGIN OUTPUT FEMVIE
  FILE "mode12d"
  DISPLA TOTAL  TRANSL GLOBAL
  FORCE  REACTI  TRANSL GLOBAL
  FORCE  EXTERN  TRANSL GLOBAL
  STRAIN CRACK  GREEN
  STRAIN CRKWDT GREEN GLOBAL
  STRAIN PLASTI GREEN GLOBAL
  STRESS TOTAL  CAUCHY GLOBAL
END OUTPUT
BEGIN OUTPUT TABULA
  BEGIN SELECT
    NODES 550 554 558 562 566 574 582 590 598
  END SELECT
  FORCE  EXTERN  TRANSL GLOBAL
  DISPLA TOTAL  TRANSL GLOBAL
  BEGIN LAYOUT
    LINPAG 15000
  END LAYOUT
END OUTPUT
*END
```



Appendix C: Potential improvements

1.1 Influence of the vertical reinforcement bars

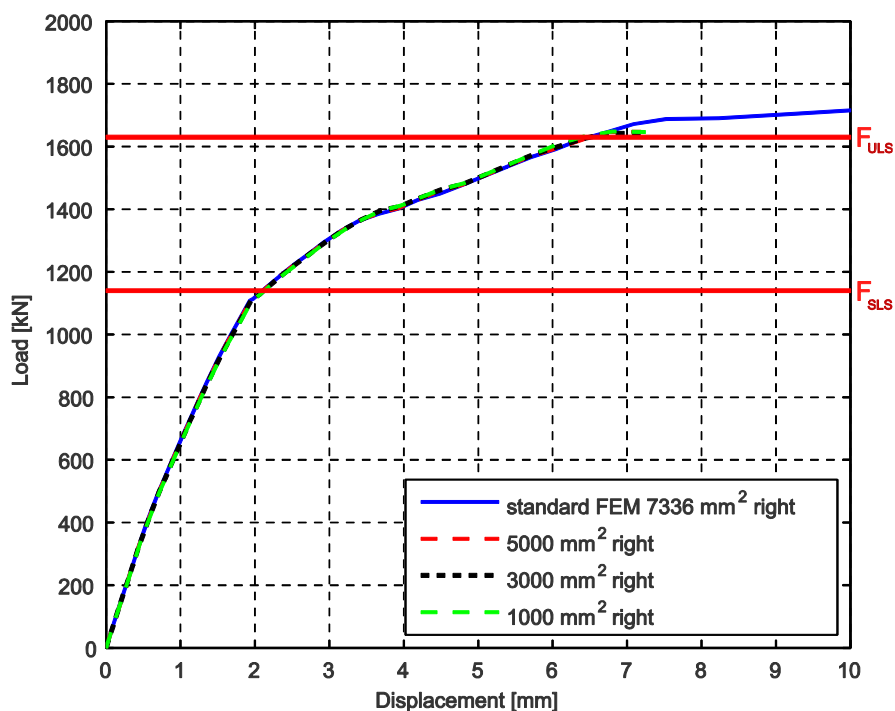


Figure 1 Force-displacement diagram: Influence of the right vertical reinforcement bar

Vertical bar	w_{SLS}	w_{ULS} at $F=1643$ kN	F_{ULS}
Standard FEM 7336 mm² both	0,22 mm	0,41 mm	1795 kN
5000 mm² right	0,22 mm	0,41 mm	1648 kN
3000 mm² right	0,22 mm	0,47 mm	1643 kN
1000 mm² right	0,22 mm	0,41 mm	1648 kN

Table 1 Crack width and force in SLS and ULS

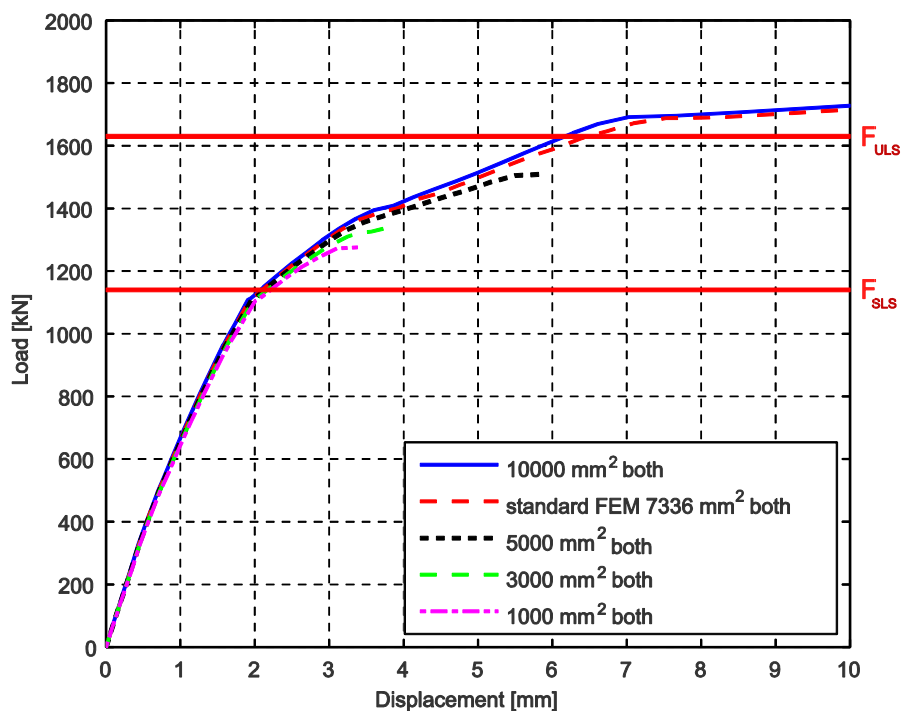


Figure 2 Force-displacement diagram: Influence of both vertical reinforcement bars

Vertical bar	w_{SLS}	w_{ULS} at $F=1276$ kN	F_{ULS}
10000 mm² both	0,22 mm	0,32 mm	1795 kN
Standard FEM 7336 mm² both	0,22 mm	0,32 mm	1795 kN
5000 mm² both	0,21 mm	0,32 mm	1509 kN
3000 mm² both	0,21 mm	0,31 mm	1335 kN
1000 mm² both	0,21 mm	0,30 mm	1276 kN

Table 2 Crack width and force in SLS and ULS

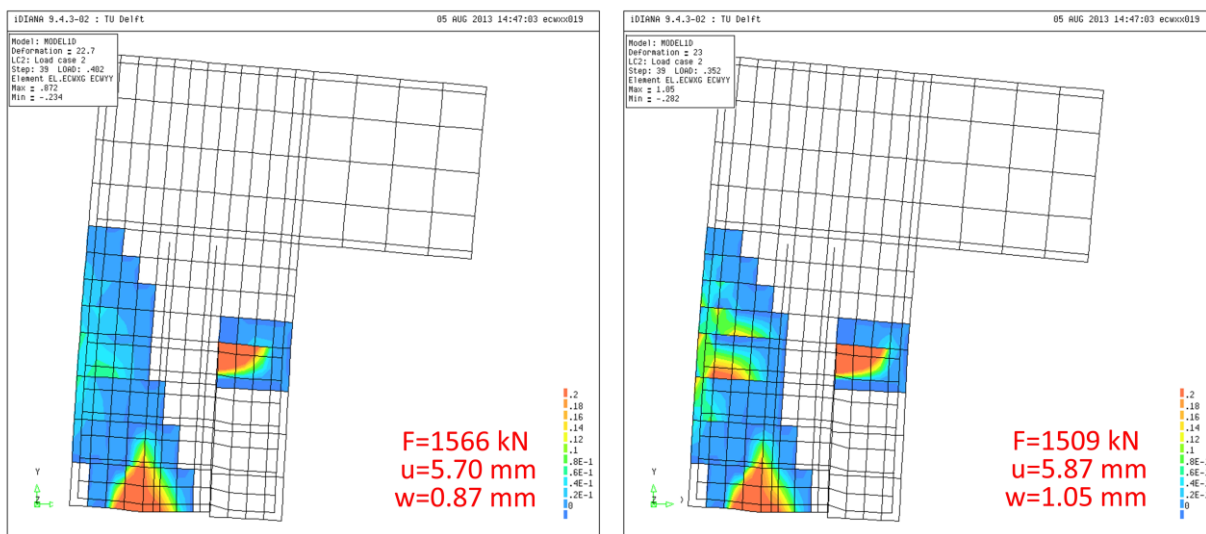


Figure 3 Crack width in y-direction left: standard model and right: model with 5000 mm² both

1.2 Influence of the extra vertical bar

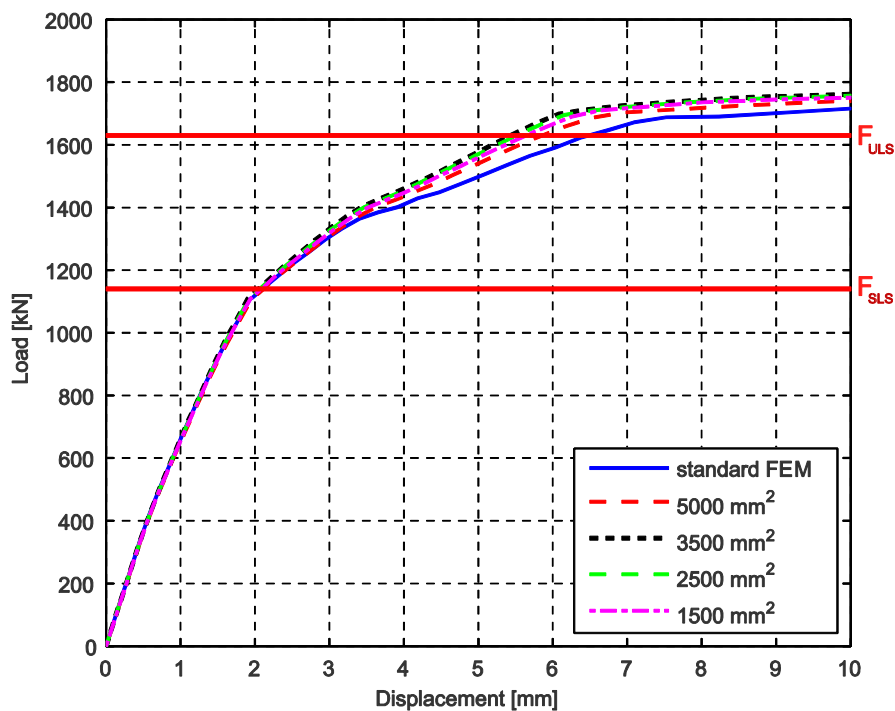


Figure 4 Force-displacement diagram: Influence of the extra vertical bar



Extra vertical bar	w_{SLS}	w_{ULS} at $F=1700$ kN	F_{ULS}
Standard FEM	0,22 mm	0,52 mm	1795 kN
5000 mm²	0,22 mm	0,39 mm	1790 kN
3500 mm²	0,21 mm	0,39 mm	1804 kN
2500 mm²	0,21 mm	0,39 mm	1813 kN
1500 mm²	0,21 mm	0,40 mm	1816 kN

Table 3 Crack width and force in SLS and ULS

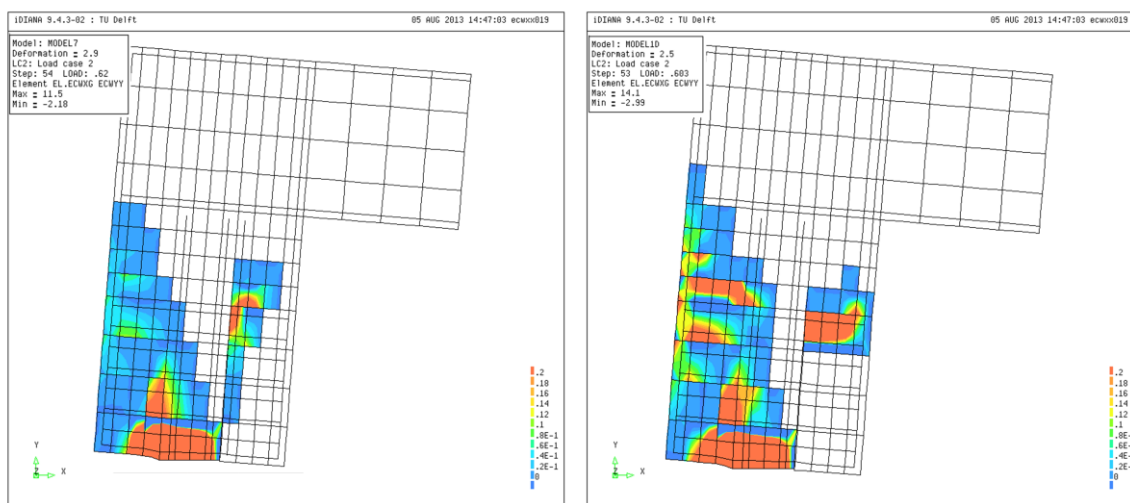


Figure 5 Crack width in y-direction at moment of failure, left: FEM with 3500 mm² in the vertical bars on the right side and right: standard FEM without extra vertical bar



1.3 Influence of the steel foundation pile

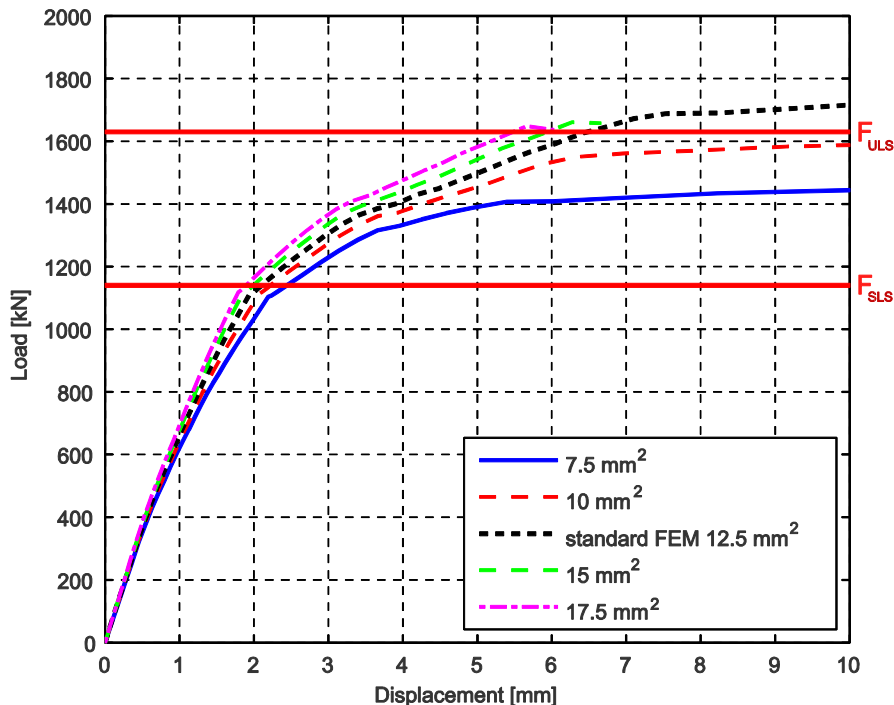


Figure 6 Force-displacement diagram: Influence of the steel foundation pile

Thickness of the pile	w_{SLS}	w_{ULT} at $F=1390$ kN	F_{ULT}
7,5 mm	0,26 mm	0,33 mm	1482 kN
10 mm	0,22 mm	0,31 mm	1643 kN
Standard (12,5 mm)	0,21 mm	0,31 mm	1795 kN
15 mm	0,20 mm	0,31 mm	1661 kN
17,5 mm	0,18 mm	0,31 mm	1648 kN

Table 4 Crack width and force in SLS and ULS

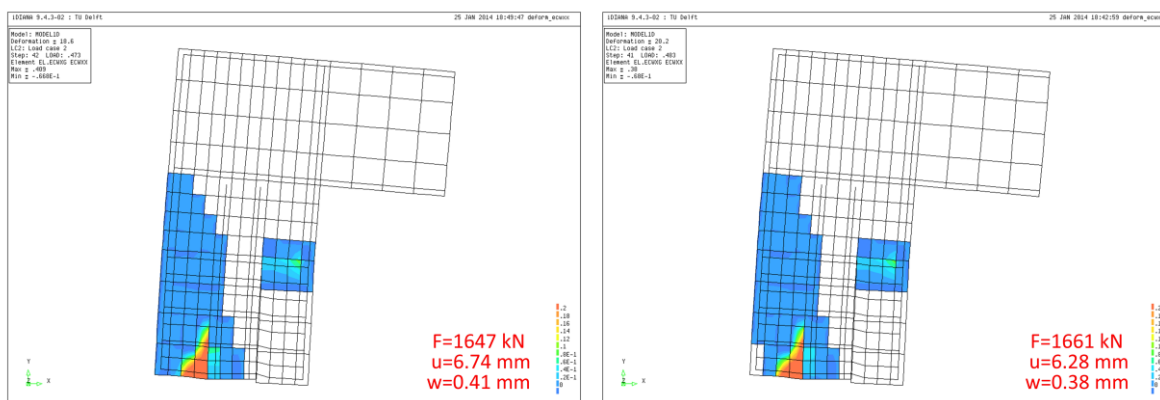


Figure 7 Crack width in x-direction left: standard model and right: model with $t=15$ mm



Appendix D: 3D FEM of the bridge connection

This appendix shows the 3D FEM of the bridge connection (Figure 1). The 3D FEM is developed to give a better understanding of the forces, cracks and stresses in the extra direction. For example, cracks could be concentrated next to the foundation pile where no horizontal reinforcement is present. This is not the case for the 2D FEM where reinforcement and the foundation pile are in the same layer.

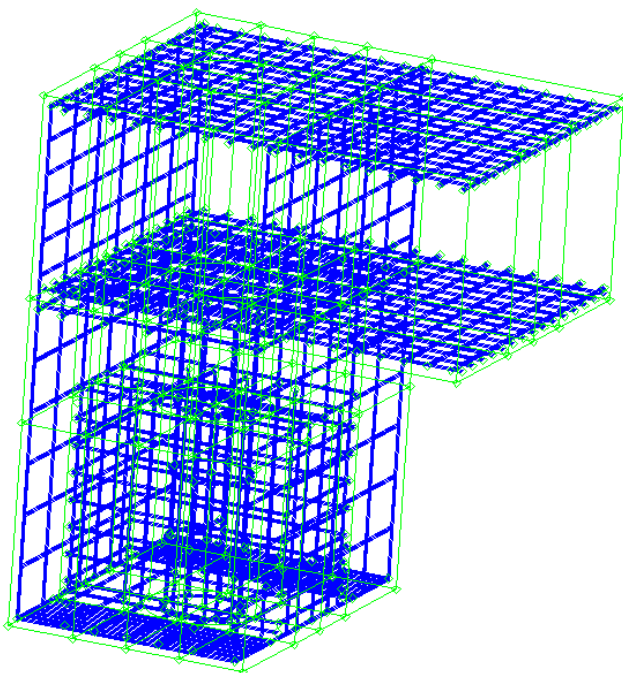


Figure 1 3D FEM of the bridge connection

The 3D FEM is not present in the main report, because the results of the analysis were not sufficient. All the analyses had no convergence before failure of the 3D FEM. Therefore only the input of the 3D FEM is presented in this chapter. The results of the analyses are summarily.

1.1 Input Data-file of the standard 3D FEM

This section deals with the input data of the 3D FEM. The first subsection covers the physical structure. Then, the material properties are presented. The last two subsections deal with the elements and mesh and the boundary conditions and loads.

1.1.1 Physical structure

This subsection discusses the dimensions of the 3D FEM and focuses on the reinforcement used for the 3D FEM. The dimensions of the 3D FEM are shown in Figure 2. The 'external dimensions' are the same as the 2D FEM. The only difference are the dimensions of the foundation pile.

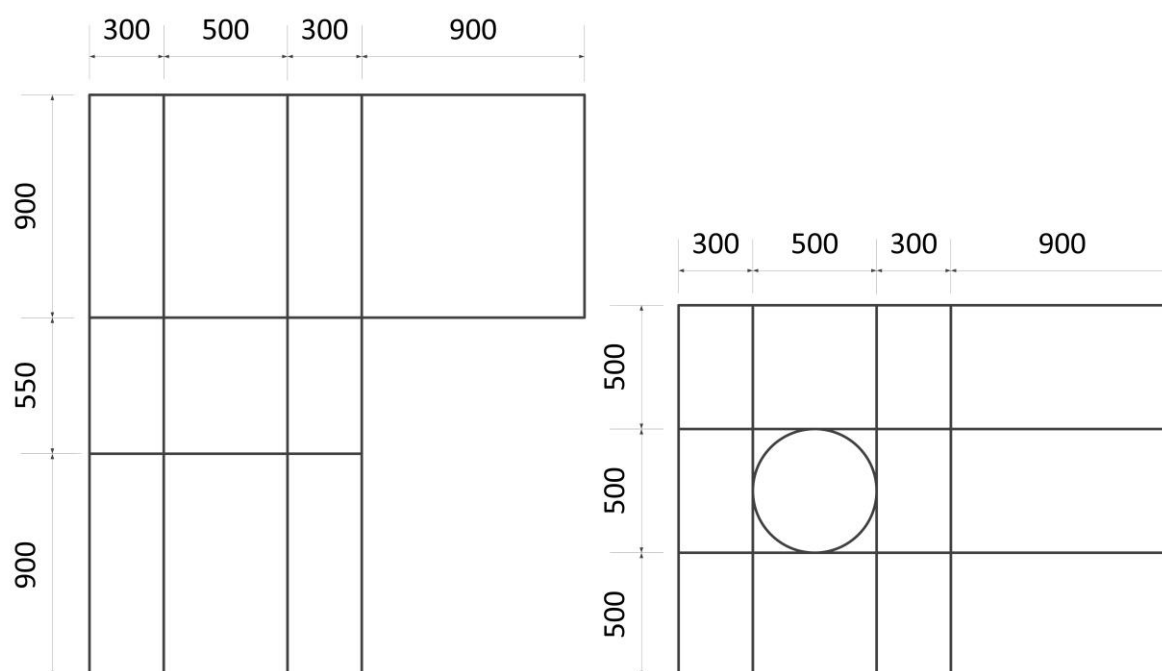


Figure 2 the basic physical structure of the 3D FEM with on the left the cross section and on the right the top

Figure 3 shows an overview of the reinforcement used in the 3D FEM. This is divided in 3 colours, which will be further discussed in detail. First, the reinforcement on the edges (red) are examined. Then, the reinforcement inside the foundation pile (green) and finally, the reinforcement around the foundation pile.

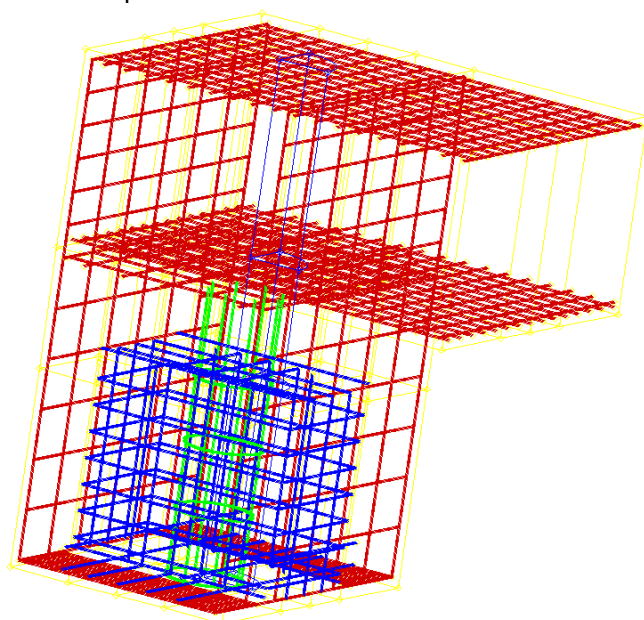


Figure 3 the reinforcement of the 3D FEM: Red: Reinforcement on the edge, blue: Reinforcement around the foundation pile and green: Reinforcement inside the foundation pile



The reinforcement on the edges is given in Figure 4. The applied reinforcement are grids which are named 'RE1', 'RE2' and 'RE3'. A more detailed information is present in Table 1.

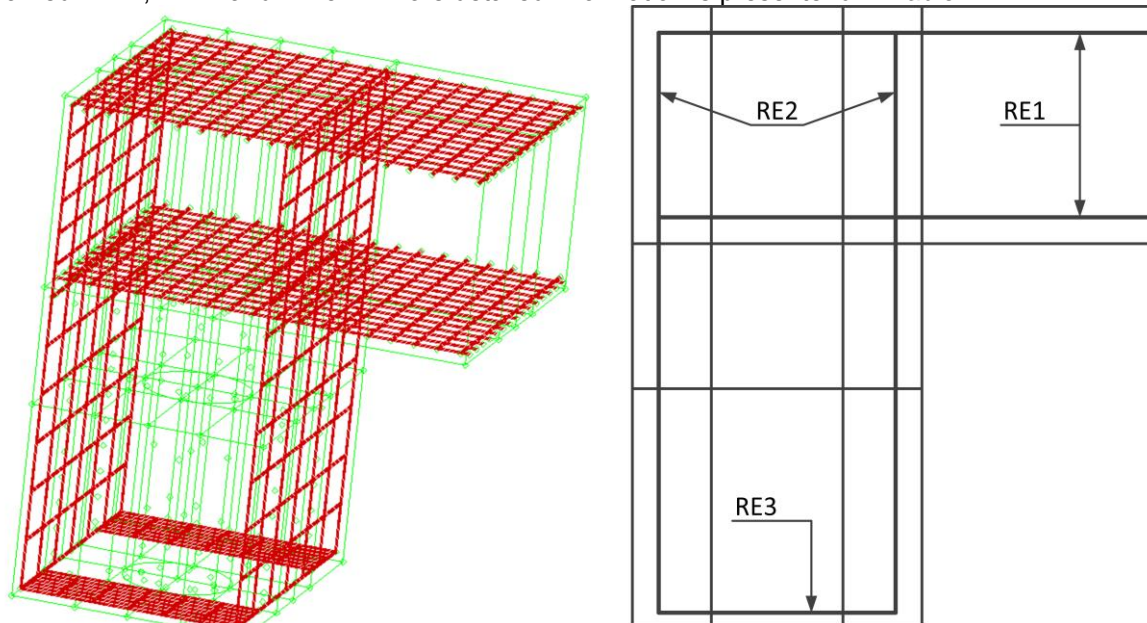


Figure 4 Reinforcement on the edges. Left: overview of the reinforcement and right: cross-section of the reinforcement

Figure 5 shows the reinforcement inside the foundation pile. The foundation pile reinforcement consist of reinforcement loops 'RE5' and reinforcement bars 'RE4'.

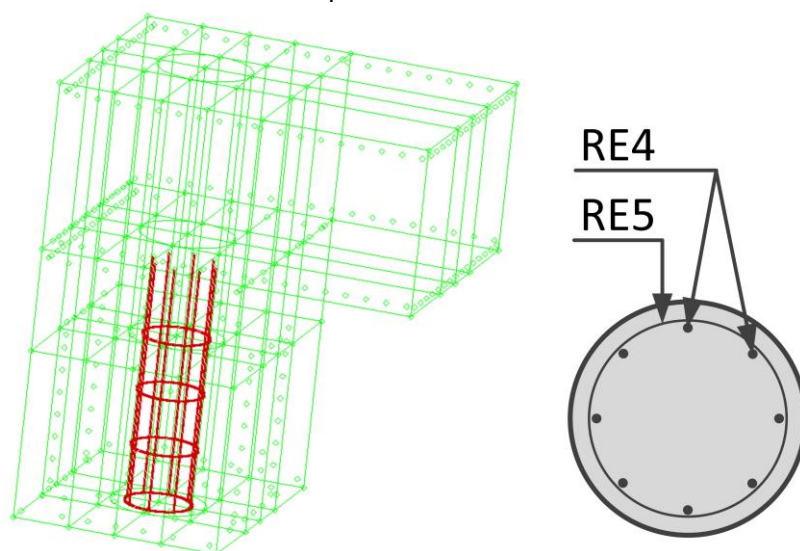


Figure 5 Reinforcement inside the foundation pile. Left: overview of the reinforcement and right cross-section of the foundation pile

Figure 6 shows the reinforcement around the foundation pile. RE6 are reinforcement loops, which are blue in Figure 6. RE7 and RE8 are the pink reinforcement loops over the foundation pile. RE9, RE10 and RE11 are reinforcement bars, which are located next to the foundation pile.

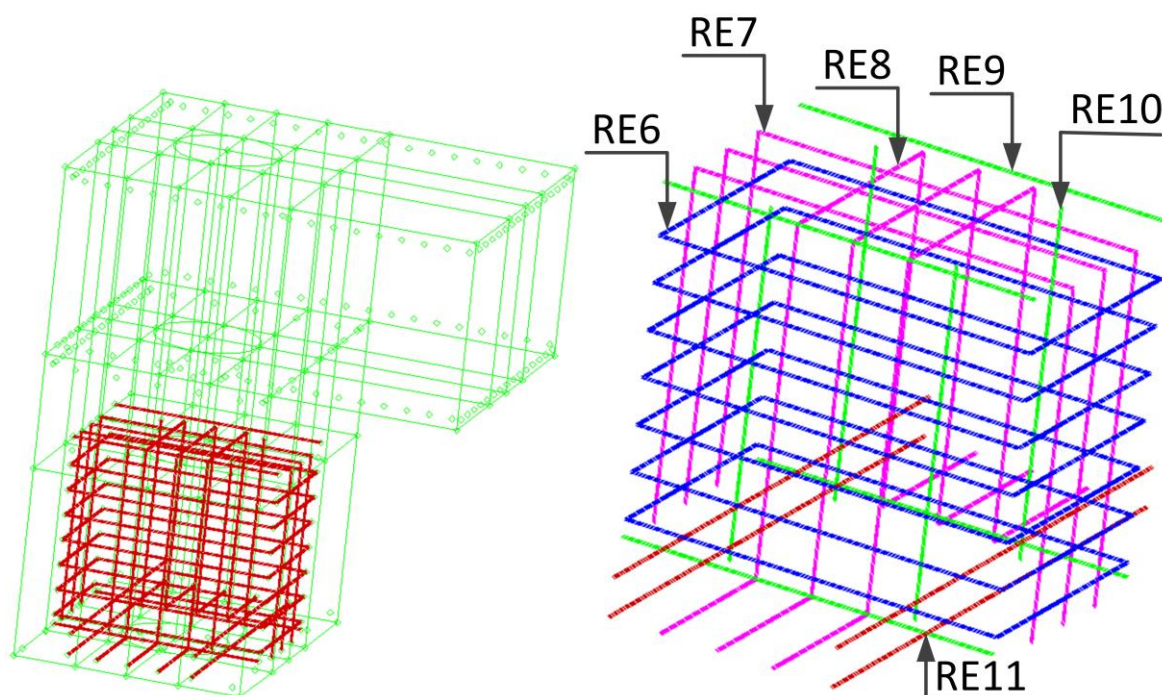


Figure 6 Reinforcement around the foundation pile. Left: Overview of the reinforcement and right: Zoomed in on the reinforcement

More details about the reinforcement are presented in Table 1. The letters 'A' and 'B' stand for respectively parallel and perpendicular.

Reinforcement name	Amount(A)	Length bar l(L)	Amount(B)	Length bar(L)
RE1	Ø16-100	1950 mm	Ø25-100	1500 mm
RE2	Ø25-100	2250 mm	Ø20-200	1500 mm
RE3	Ø25-100	1000 mm	x	x
RE4	8 Ø20	1300 mm		
RE5	4 Ø12	n/a		
RE6	7 Ø25	n/a		
RE7	3 Ø20	n/a		
RE8			3 Ø20	n/a
RE9	4 Ø16	1000 mm		
RE10	4 Ø16	800 mm		
RE11			4 Ø25	1500 mm

Table 1 Reinforcement in the 3D FEM. A=parallel and B=Perpendicular



1.1.2 Material properties

Figure 7 shows the input data of the material properties of the 3D FEM. This input data is the same as for the 2D FEM. Therefore, for an explanation of the material properties see subsection 8.2.2 of the main report.

```
'MATERIALS'  
1 YOUNG      3.100000E+04  
  POISON     1.500000E-01  
  TOTCRK    ROTATE  
  TENCVR    LINEAR  
  TENSTR     2.900000E+00  
  EPSULT     2.175000E-03  
  COMCRV    CONSTA  
  COMSTR     3.700000E+01  
2 YOUNG      3.850000E+04  
  POISON     1.500000E-01  
  TOTCRK    ROTATE  
  TENCVR    LINEAR  
  TENSTR     4.200000E+00  
  EPSULT     2.175000E-03  
  COMCRV    CONSTA  
  COMSTR     6.700000E+01  
4 YOUNG      2.100000E+05  
  YIELD     VMISES|  
  HARDEN    WORK  
  HARDIA    435. 0.002175 470. 0.045 0. 0.0451 0. 100.  
6 YOUNG      2.100000E+05  
  POISON     3.000000E-01  
  YIELD     VMISES  
  HARDIA    415. 0.002175 415. 0.15 0. 0.1501 0. 100.  
  HARDEN    WORK  
7 DSTIF     3.100000E+04      1.347800E+04      1.347800E+04  
  FRICTI  
  FRCVAL     3.500000E-02      5.000000E-01      1.000000E-05  
  GAP  
  GAPVAL     1.000000E-05  
  MODE2     0  
8 DSTIF     3.100000E+04      1.347800E+04      1.347800E+04
```

Figure 7 Input data of the material properties of the 3D FEM



1.1.3 Elements and mesh

A variety of elements are used for the construction of the 3D FEM. The elements for the connection are mostly the rectangular 3D elements CHX60 which are showed in Figure 8A. The foundation pile and its surrounding are more complex (Figure 8B). The 3D elements in the foundation pile are the triangular elements CTP45. The thin elements in Figure 8B are the interface elements CQ48I and the flat elements CQ40S.

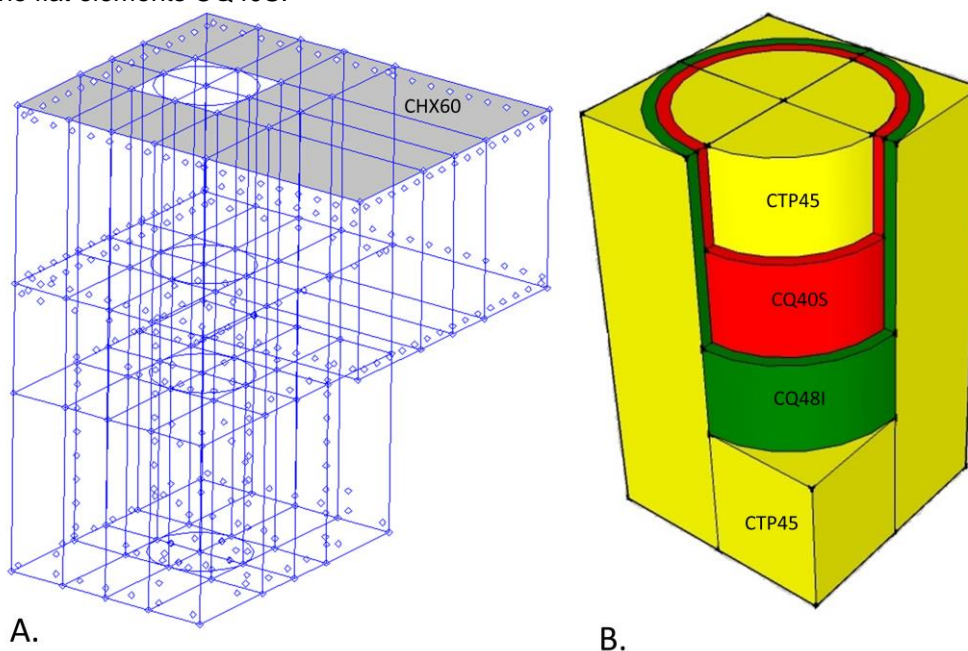


Figure 8 A. geometry of the 3D FEM with in grey the rectangular elements CHX60. B. A close up of the elements of the foundation pile with elements CTP45, CQ48I and CQ40S

The 3D elements CH60X and CTP45 are respectevily a 20 nodes brick and a 15 node wedge. The integration scheme is set on the standard settings with gauss integration and quadratic interpolation. The elements are showed in Figure 9.

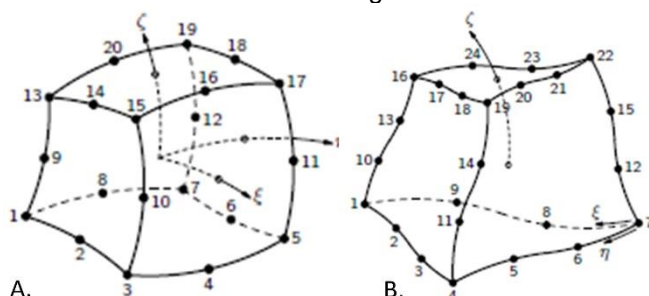


Figure 9 A. rectangular 3D element CHX60 and B. triangular 3D element CTP45



The flat element CQ40S and the interface element CQ48I are showed in Figure 10. The flat element is an 8-node element which represent the steel tube of the foundation pile. The frictional behaviour between the foundation pile and the surrounding concrete is simulated by the interface element of CQ48I. The settings for these elements are also standard with gauss integration and quadratic interpolation.

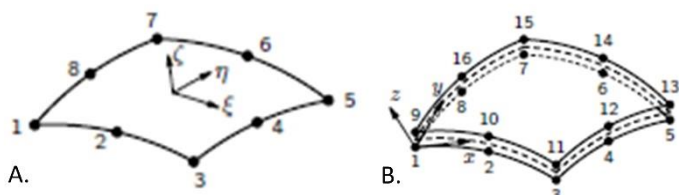


Figure 10 A. Flat element CQ40S and B. interface element CQ48I

Fiofaj shows the top of 3D FEM with the mesh. The mesh for the rectangular elements is divided in 4x4x4 scheme. Therefore, the elements in the foundation pile are smaller and not evenly distributed. This was with the complex structure not possible to create a better distributed mesh.

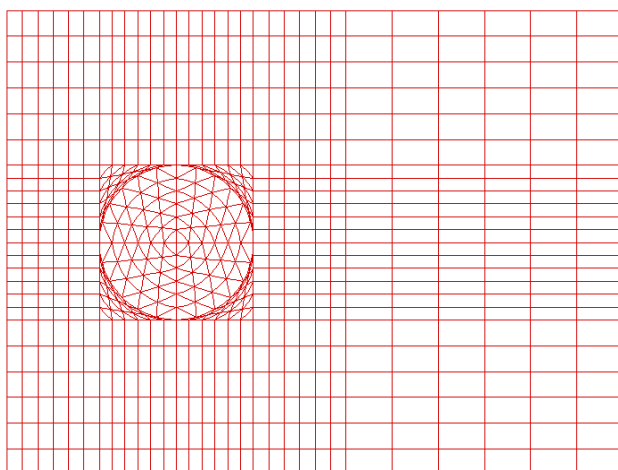


Figure 11 top of the mesh of the 3D FEM



1.1.4 *Boundary conditions and loads*

The boundary conditions are set to avoid instability of the 3D FEM. The location of the b.c.'s are showed in the left figure of Figure 12. The displacement is zero for the direction perpendicular to the plane and for the direction parallel to plane. The right figure of Figure 12 shows the location of the forces and moments. The forces and moments are the same as for the stringer-panel models of chapter 7 and the 2D FEM of chapter 8. This means 1140 kN (\downarrow) in the vertical direction, 400 kN in the horizontal direction (\leftarrow) and a moment of 368 kNm (counter-clockwise). The moments and forces are equally divided over the plane.

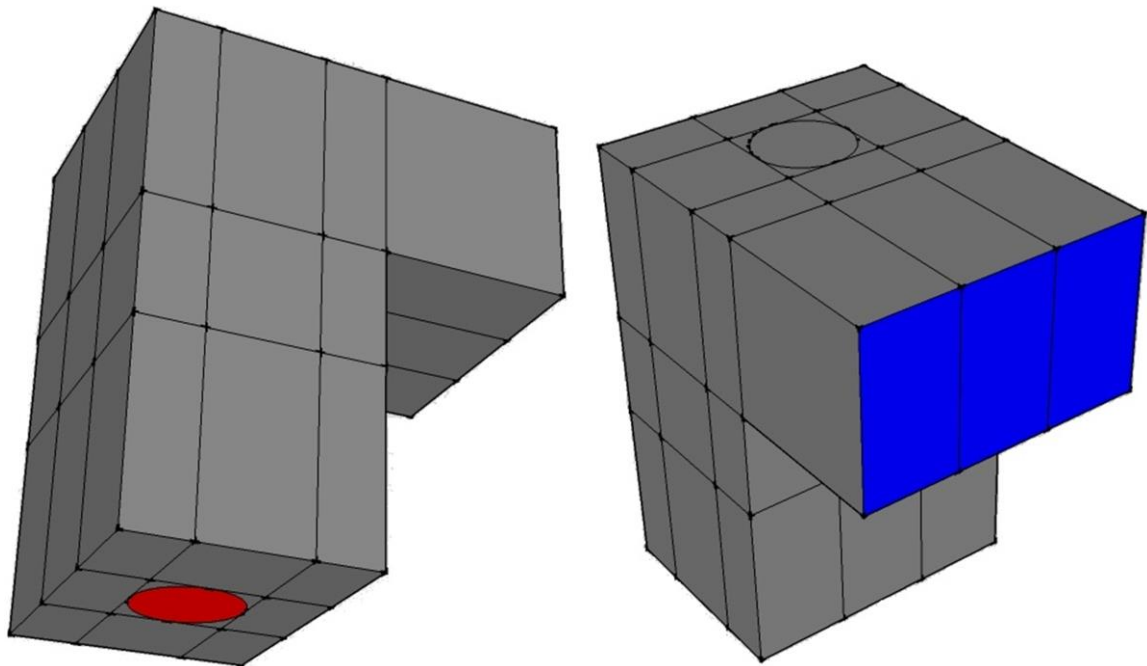


Figure 12 3D FEM with left: location of the boundary conditions in red and right: location of the forces.



1.2 Results of the 3D FEM

The analyses of the 3D FEM did diverge most of the times before the moment of failure of the connection was reached. Therefore, the research to the 3D FEM is not attached to the main report but to the appendices. This section will show some of the results of the 3D FEM.

The force-displacement diagram of **Error! Reference source not found.** shows the results of the standard 2D FEM and two analyses of the standard 3D FEM. The standard 3D FEM has horizontal reinforcement and the standard values for cohesion and friction ($c=0,5$ and $\mu=0,035$). The 3D FEM with iterative and automatic steps fails after the first branch and does not show the plastic phase. This analysis is representative for most of the analyses with the 3D FEM. The results of this 3D FEM also show no sign of cracks or high stresses. This is different for the 3D FEM with arc length control. This 3D FEM is showed in the force-displacement diagram too. The gradient of the 3D FEM is lower than the standard 2D FEM, but the maximum force is higher. A lower gradient means that the rotational stiffness of the 3D FEM is less than the standard 2D FEM. The 3D FEM with iterative and automatic steps confirms this. A higher maximum force does not necessarily mean that the structural capacity of the 3D FEM is larger than the standard 2D FEM. The use of arc length control could lead to a higher force than an analysis procedure with iterative and automatic steps which is used for all 2D FEM. Arc length control is also called indirect displacement control and adapts the loading during iterations in one load step. The arc length control is a more stable procedure, but shows a different force-displacement behaviour than the iterative and standard load control.

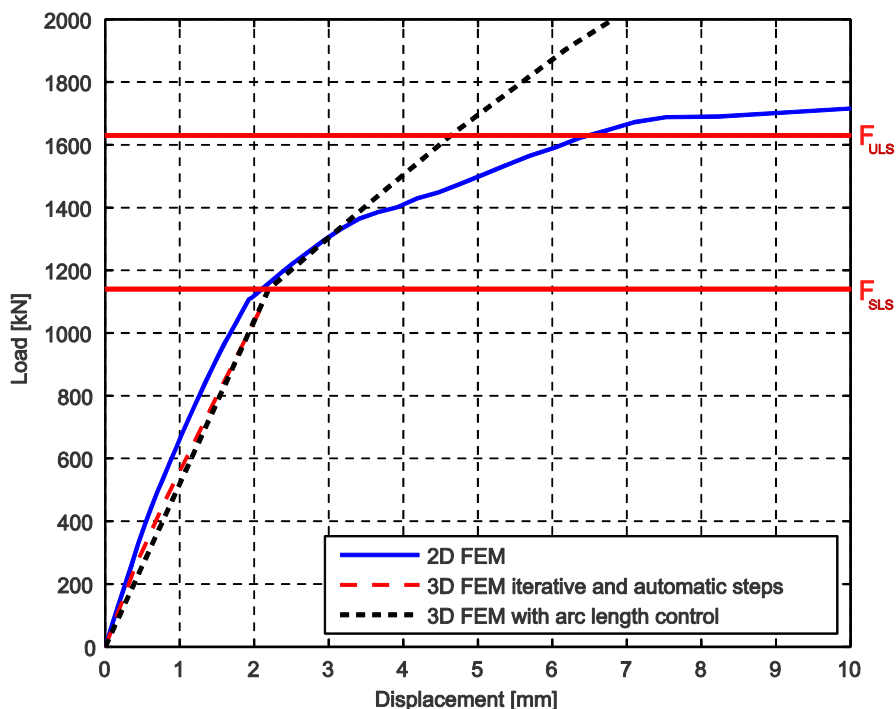


Figure 13 Force-displacement diagram with standard 2D FEM and 3D FEM with horizontal reinforcement



Figure 14 shows the crack width of 3D FEM with arc length control. The figure on the left shows a cross-section in x-z plane which crosses the foundation pile in the centre. The figure on the right crosses the 3D FEM just above the bottom of the foundation pile and is taken in the x-y plane. The left figure shows the crack width in z-direction at moment of failure. The largest cracks occur at the same location as happens for the cracks in the 2D FEM. This means a major crack above the foundation pile and concentration of cracks inside the foundation pile. The right figure shows the cracks in y-direction. Two major diagonal cracks on both sides of the foundation pile occur. This gives a good view of the effective width in the 3D FEM.

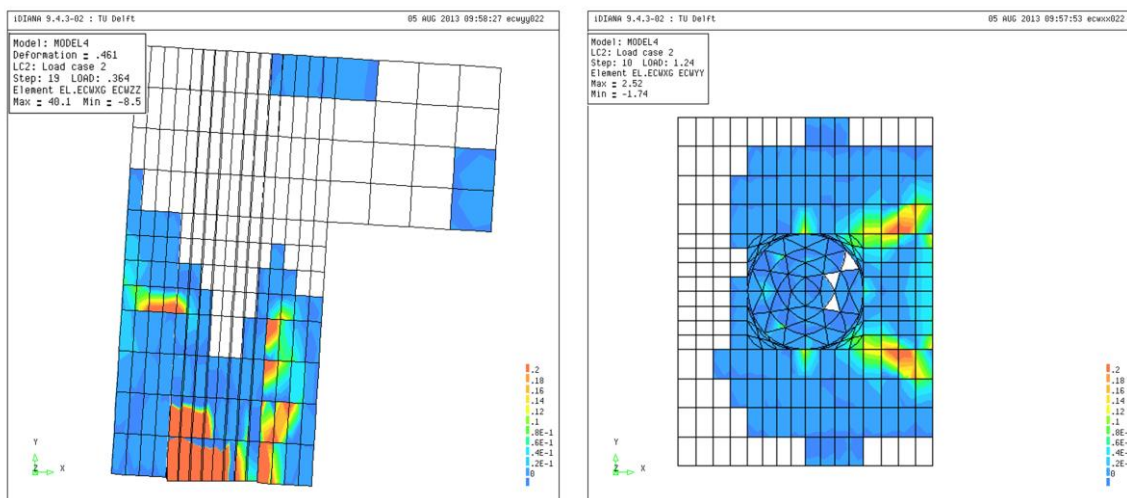


Figure 14 3D FEM with arc length control, left: crack width in z-direction and right crack width in y-direction

In summary, the results of the 3D FEM are similar to the results of the 2D FEM. The maximum structural capacity cannot be determined on basis of these results. Also, the influence of the horizontal reinforcement and friction and cohesion in the 3D FEM is not clear due to the incomplete analyses.